U.F.R.S.T.M.P
Groupe de Formation Doctorale
des Sciences de la Terre

THESE

présentée pour l'obtention du grade de
Docteur de l'Université Henri-Poincaré Nancy I
en Science du Sol, avec le Label Européen

par

Sonia CZARNES

ADHESION SOL : RACINE ET BIOPHYSIQUE DE LA RHIZOSPHERE DU MAÏS

le 1 Juillet 1998

Membres du jury :

J. DEXHEIMER,	Professeur à l'Université de Nancy I	Président
C. CHENU,	Directeur de recherche INRA, Versailles	Rapporteur
B. JAILLARD,	Directeur de recherche INRA, Montpellier	Rapporteur
F. BARTOLI,	Directeur de Recherche CNRS, Nancy	Directeur de thèse
A.R. DEXTER,	Professeur, S. R. I., Royaume Uni	Examinateur
C. DOUSSAN,	Chargé de recherche INRA, Avignon	Invité
P. HINSINGER,	Chargé de recherche INRA, Montpellier	Invité

CENTRE NATIONAL DE LA RECHERCHE SCIENTIFIQUE

Centre de Pédologie Biologique
UPR 6831 - 54501 Vandœuvre-les-Nancy

Silsoe Research Institute
MK45 4HS Bedford, Royaume Uni

A ma famille,

A ma mère et
Bernard,

A Christophe.

REMERCIEMENTS

Cette thèse a été realisée au Centre de Pédologie Biologique du CNRS de Nancy dans l'équipe Agrégation des Sols dirigée par **F. Bartoli**, en collaboration avec le Silsoe Research Institute dans le groupe Science du Sol dirigé par **A. R. Dexter**. J'ai bénéficié de l'aide et du soutien de nombreuses personnes à qui je voudrais ici présenter tous mes remerciements.

Monsieur J. Dexheimer, Professeur à l'Université de Nancy I, qui m'a fait l'honneur de présider ce jury.

Madame C. Chenu, Directeur de Recherche à l'INRA de Versailles et **Monsieur B. Jaillard**, Directeur de recherche à l'INRA de Montpellier, pour avoir accepté la lourde tâche d'être les rapporteurs de ce travail.

Monsieur J. Guerif, Directeur de Recherche à l'INRA de Laon, pour la discussion que nous avons eu au Silsoe Research Institute. Je le remercie pour l'honneur qu'il m'a fait d'accepter d'évaluer ce travail et de faire partie de ce jury.

Monsieur C. Doussan, Chargé de Recherche à l'INRA d'Avignon et **Monsieur P. Hinsinger**, Chargé de Recherche à l'INRA de Montpellier, membres invités de ce jury, pour l'intérêt qu'ils portent à mon travail et pour notre discussion au dernier colloque "rhizosphère" à Aix, qui m'a beaucoup encouragée.

J'adresse tous mes remerciements à **A. R. Dexter**, Professeur, pour m'avoir accueilli dans son laboratoire de Science du Sol au Silsoe Research Institute (Royaume Uni), pour sa disponibilité, pour ses grandes compétences, ses conseils avisés, ses encouragements et surtout, pour m'avoir initiée aux concepts et aux dispositifs expérimentaux de la mécanique des sols, qui forment la trame de fond de mon mémoire de thèse. Sa contribution à la réalisation de ce travail a été déterminante et je le remercie du fond du coeur. J'y associe particulièrement l'un de ses collaborateurs, **S. Hiller**, pour sa participation, également déterminante, à l'étude de l'adhésion sol:racines par l'approche rhéologique.

Je tiens à remercier très chaleureusement **F. Bartoli**, mon directeur de thèse, pour m'avoir initiée et formée à la recherche depuis mon DEA jusqu'à ce jour, pour sa disponibilité, ses grandes compétences, sa rigueur, ses conseils scientifiques. Il a été durant mes années de thèse un guide constant et nos discussions sur de nombreux sujets ont été pour moi très importantes.

Mes remerciements vont également à tous mes compagnons de l'équipe Agrégation des Sols: **G. Burtin, M. Doirisse** et **R. Phillipy**. Je remercie G. Burtin pour les analyses granulométriques, la mise au point de la rupture du sol adhérant aux racines par ultrasonication modérée et les mesures en porosimétrie de mercure et R. Philippy pour les courbes de rétention d'eau en conditions quasi-statiques. Les photos du dispositif de culture en chambre de culture ont été réalisées par M. Doirisse. Je n'oublie pas leur soutien moral et leur bonne humeur ce qui m'a beaucoup aidé pour mener à bien cette thèse.

Au cours de ma thèse, j'ai eu l'opportunité et la chance de passer 9 mois au Silsoe Research Institute, grâce à une bourse de 6 mois du British Council et au programme Alliance, qui a permis à l'équipe Agrégation des Sols du CPB et au groupe de Science du Sol du Silsoe Research Institute de collaborer de façon fructueuse. Je remercie ici toutes les personnes qui ont contribué à rendre mes séjours très agréables et enrichissants: **N. Bird, P. Bruneau, P. Hallett, S. Hiller, D. Longstaff, R. Whalley** et **C. Watts**. J'ai aussi beaucoup apprécié l'aide scientifique et technique de **P. Hallett, D. Longstaff, C. Watts** de l'équipe Science du Sol ainsi que **G. Davies** et **D. Bruce** de l'équipe biomécanique au Silsoe Research Institute. Je remercie **D. Bruce** pour m'avoir permis l'utilisation des équipements de son équipe avec notamment la machine universelle de mesure de force.

Je remercie **B. Gerard, M. Bloin**, du CPB et **S. Niquet**, du CIRIL, pour leur aide en matière d'analyse organique élémentaire, de mise au point du dispositif de culture et d'analyse d'image, respectivement. Merci aussi à **M. Mercier** pour son soin et sa gentillesse dans la réalisation des photographies des systèmes sol adhérent:racines ainsi que des planches photos et le service Reprographie du CRPG pour son aide efficace et souriante.

Mes remerciements vont également à toutes les **personnes du CPB** qui, en m'accordant leur précieuses amitié, m'ont beaucoup aidée pour réaliser cette thèse dans une ambiance très sympathique et qui se reconnaîtront.

Je tiens à remercier **Gisèle, Jean-Pierre** et **Virginie** pour leur gentillesse et leur amitié, pour leurs encouragements pendant les moments difficiles de la rédaction de thèse. J'ai l'impression de devenir un peu lorraine grâce à eux!

Je remercie mes voisins **Mme et Mr Flosse** sur lesquels j'ai toujours pu compter.

Une pensée toute particulière est adressée à mon amie **Christelle**. Il me tarde de la retrouver dans notre petit bistro parisien pour poursuivre nos longues discussions et confidences. Notre amitié, très précieuse à mes yeux, m'a énormement aidée pendant ces années de thèse.

Je n'oublie pas pour autant de remercier **ma famille** qui m'a soutenue et encouragée pendant cette thèse. Je remercie tout particulièrement **ma mère** qui m'a été d'un grand soutien financier et qui, même à distance, a toujours trouvé les mots justes pour me remonter le moral. Je lui suis très reconnaissante pour cela.

Enfin, je remercie **Christophe** pour son aide et son soutien et, pour la curiosité qu'il a porté à mes travaux. Mes deux dernières années de thèse sont pour moi inoubliables...

SOMMAIRE

SOMMAIRE

INTRODUCTION

INTRODUCTION

Après avoir défini quelques termes comme la rhizosphère, le sol adhérant aux racines, le rhizoplan et l'interface sol:racine, nous identifierons les interactions biologiques et physiques se produisant à l'interface sol:racine et à son voisinage.

1. Notions de rhizosphère, de sol adhérant aux racines, de rhizoplan, d'interface sol : racine et de poils racinaires

La rhizosphère

La *rhizosphère* (Hiltner, 1904) est l'étroite zone volumique de sol soumise à l'influence des racines vivantes, se manifestant notamment par l'exsudation de substances polysaccharides stimulant l'activité microbienne. La rhizosphère peut aussi être définie plus simplement comme étant le volume de sol au sein duquel on peut observer des interactions entre le système racinaire d'une plante et son environnement immédiat. La rhizosphère est parfois divisée en deux régions: (1) l'*endorhizosphère*, comprenant la région interne de la racine (la stèle avec les éléments conducteurs: le xylème et le phloème, l'épiderme, le cortex et l'endoderme) et le *rhizoplan*, qui est la surface externe racinaire, et (2) l'*ectorhizosphère* comprenant la région externe de la racine (mucigel bactérien et racinaire, poils racinaires, mucilage racinaire et cellules détachées de l'extremité racinaire).

Par opposition à la rhizosphère, le *sol dit "non rhizosphérique"* (bulk soil) peut être défini comme étant situé en dehors de la rhizosphère et étant peu influencé par le système racinaire.

La rhizosphère est un réacteur multi-agents d'une grande complexité dont l'équilibre est régi par une multitude de mécanismes biologiques, physiques et physico-chimiques, interagissant fortement les uns avec les autres (figure 1).

L'importance de cette zone d'influence est variable selon le sol, la plante et le stade de développement de cette plante.

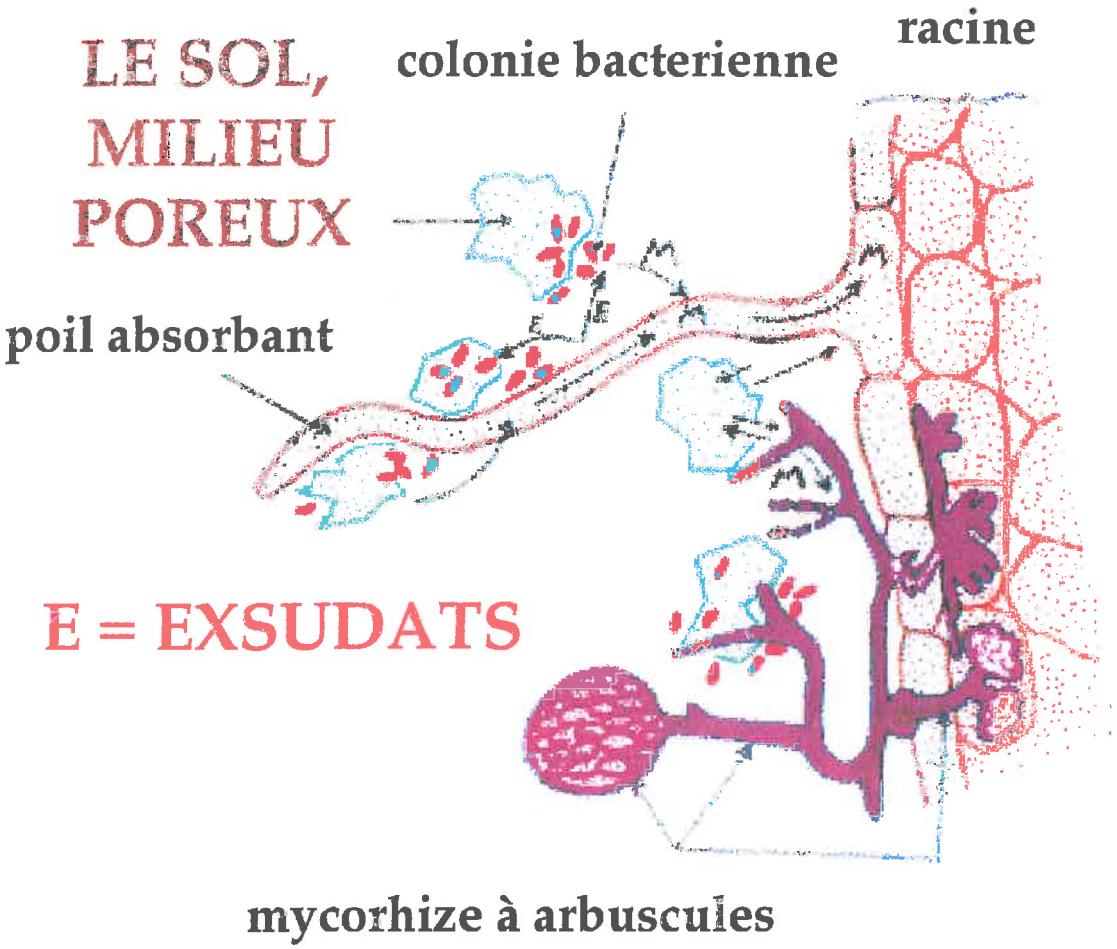

Figure 1. La rhizosphère: interactions racines - microorganismes - sol.

Au niveau des flux de carbone organique et d'éléments minéraux, la rhizosphère est au centre d'échanges importants: flux de carbone organique (exsudats) (Groleau - Renaud, 1998) et flux de protons (Haynes, 1990; Jaillard *et al.*, 1996) sortant des zones racinaires apicales, flux d'eau et d'éléments minéraux, du sol aux racines (figure 1). Les exsudats racinaires, riches en polysaccharides, stabilisent les aggrégats directement ou indirectement, en fournissant une source d'énergie pour les microorganismes rhizosphériques qui, à leur tour, secrètent des polysaccharides agrégeants (Gückert, 1973; Tisdall et Oades, 1979; Oades, 1989; Van Noordwick *et al.*, 1993; Gouzou *et al.*, 1993; Amellal, 1996; Amellal *et al.*, 1998 $_{a,b}$).

Au niveau physique, l'*"effet rhizosphère"* se manifeste par une modification de la structure du sol, soit par agrégation (Haynes et Francis, 1993) soit par fragmentation (Tri, 1968; Materechera *et al.*, 1992, 1994). La biomasse microbienne et la taille des agrégats rhizosphériques dépendent de la densité racinaire. C'est ainsi que, pour un sol limoneux, l'effet rhizosphère est le plus marqué pour les céréales à très fortes biomasses racinaires (Haynes et Francis, 1993). La biomasse microbienne et la taille des agrégats sont alors plus élevées dans la rhizosphère que dans le sol non rhizosphérique.

Le rhizoplan et l'interface sol : racine.

•***Le rhizoplan***

Le *rhizoplan* correspond à la surface externe racinaire. C'est une zone privilégiée pour les microorganismes qui y adhèrent et en font le point de départ de leur colonisation dans la rhizosphère (Amellal, 1996). La nature et les caractéristiques de cette surface racinaire varie en fonction de l'âge de la plante.

•***L'interface sol : racine.***

L'*interface sol:racine* est la surface de contact entre la racine et le sol. Cette interface est essentielle, tant pour l'alimentation en eau et en éléments nutritifs de la plante (aspect physique et chimique de l'interface sol:racine) que pour la secretion par les racines de composés biologiques comme les exsudats, les mucilages et les lysats qui sont des substrats pour les microorganismes favorisant ainsi leur colonisation de la plante au sol (aspect biologique de l'interface sol:racine).

Au niveau biologique, les principales composants de l'interface sont les parois des cellules rhizodermiques ainsi que les poils racinaires avec tous les composés biologiques précédemment cités qui vont cimenter les particules de sol en aggregats et renforcer la force de liaison entre la racine et les particules de sol.

Au niveau physique, un film d'eau est toujours présent à la surface des racines et des poils racinaires, permettant le continuum racine - eau - sol. Le contact sol:racine est souvent discontinu et il va être amelioré ou non suivant la densité du sol environnant la racine (Van Noordwich *et al.*, 1992). Il peut être

réduit soit par différents processus tel que (i) l'élargissement du diamètre des cavités occupées par les racines lorsque celles-ci poussent dans un sol contenant une quantité relativement importante d'argiles gonflantes (smectites), dû à la rétraction du sol adhérant aux racines lorsque l'humidité de ce sol diminue (Mackay et Barber, 1984, 1985, 1987; Meisner et Karnok, 1991) et (ii) la diminution du diamètre racinaire, lors du séchage diurne (Huck *et al.*, 1970_b).

A l'opposé, le contact sol:racine peut être augmenté grâce à l'activité du cambium qui augmente progressivement le diamètre racinaire dans le cas des dicotylédones. Les monocotylédones, ne possédant pas de cambium, n'ont pas cette possibilité d'augmenter leurs diamètres racinaires qui, par contre, diminuent avec l'âge du fait d'une dégénérescence du cortex par l'invasion de microorganismes ou du déssèchement.

Un mauvais contact sol:racine tend à être compensé par différents mécanismes d'origine biologique comme le développement des poils racinaires qui varie suivant le type de sol et l'humidité du sol, avec notamment une augmentation de la densité et de la longueur des poils racinaires lorsque l'humidité du sol diminue (Mackay et Barber, 1984, 1985, 1987; Meisner et Karnok, 1991).

Les poils racinaires

Les poils racinaires, composants biologiques importants de l'interface sol:racine, sont des expansions tubulaires des cellules rhizodermiques qui ont comme origine des cellules protodermiques simples ou des cellules protodermiques spécialisées appelées trichoblastes. Le développement des poils racinaires est acropète. Les premiers apparaissent à proximité immédiate de l'apex racinaire. La majorité des observations morphologiques sur les poils racinaires, qui ont comme materiel d'étude de très jeunes racines, ont révélé un développement acropète suivent un gradient uniforme de longueur de ces poils racinaires, de la partie apicale à la partie basale de la racine (Cormack, 1949). Jaunin et Hofer ont définit trois zones pilifères le long de très jeunes racines de maïs cultivé en boîte de Pétri: une partie apicale, sans poils racinaire, une partie centrale qui est la zone des poils racinaires proprement dite et une partie basale, sans poils racinaires. La longueur maximale des poils racinaires se situe au niveau de la région basale de la zone pilifère (partie centrale) confirmant le développement acropète de ces poils racinaires.

Les poils racinaires ont été relativement peu étudiés. De ce fait, leurs différentes fonctions sont de nos jours encore très controversées. Le volume de sol exploré par la racine l'est de façon beaucoup plus efficace grâce aux poils racinaires qui sont donc impliqués dans l'absorption d'eau et de nutriments (Barley, 1970; Ewens et Leigh, 1985; Mira *et al.*, 1988). Cailloux (1972) a observé que seule l'extrémité des poils racinaires est réellement impliquée dans l'absorption ou l'excretion d'eau. Par ailleurs, Jones *et al.* (1983) ont démontré que les valeurs de conductivités hydrauliques des poils racinaires, des cellules rhizodermiques (sans poils racinaires) et des cellules corticales de racines de blé n'étaient pas significativement différentes, prouvant ainsi que les membranes des poils racinaires ne sont pas particulièrement perméables. Parallèlement aux études sur le rôle possible des poils racinaires dans l'absorption d'ions, d'autres ont été entreprises sur l'effet de différent éléments minéraux sur le développement et le fonctionnement des poils racinairess. Par exemple, dans le cas du phosphore, Ewens et Leigh (1985) ont montré que la concentration de phophore en solution n'avait pas d'influence sur la longueur des poils racinaires de blé.

Les poils racinaires sont influencés par les conditions environnementales de différentes façons. Parmi les facteurs externes, l'humidité a été le facteur le plus étudié et une relation étroite entre l'humidité et la production de poils racinaires a été largement mise en évidence. Les racines de la plupart des plantes produisent ainsi beaucoup plus de poils racinaires dans l'air humide que dans l'eau. Ceci est particulièrement bien visible pour le maïs dont les racines ont une apparence laineuse dans l'air humide alors qu'elles deviennent parfaitement lisses lorsqu'on les transfère dans l'eau (Cormack, 1949). De même, Reid et Bowen (1979) ont observé une diminution significative du diamètre racinaire de *Medicago truncatula* et une augmentation significative de la longueur de ses poils racinaires, lorsque la teneur en eau du sol diminuait. Les racines étaient même exemptes de poils racinaires lorsque le sol était saturé d'eau.

D'autres facteurs peuvent interagir avec l'humidité du sol. Ainsi, Mackay et Barber (1985) ont établi que (i) la croissance des poils racinaires augmente lorsque l'humidité du sol et la quantité de phosphore du sol diminuent et que (ii) l'humidité du sol est le facteur dominant.

Concernant l'effet du type de sol sur la production de poils racinaires, une contreverse existe, établie sur de rares résultats. Mackay et Barber (1987) ont utilisé trois sols différents qui n'ont pas eu d'influence spécifique sur le degré de croissance des poils racinaires de racines de maïs.

A l'opposé, Meisner et Karnok (1991) ont montré que des racines cultivées dans un sol limono-sableux, un melange sable/argile dans les proportions 4:1 et un sol sablo-limoneux étaient recouvertes par des poils racinaires selon des taux de 47, 17 et 14%, respectivement.

Enfin, le rôle important joué par les poils racinaires pour l'ancrage des jeunes racines dans le sol (Ennos, 1989) et le maintient du contact sol:racines est maintenant admis. Ceci nous conduit à faire le point de l'état des connaissances en matière d'adhésion sol:racines.

Le sol adhérant aux racines et l'adhésion sol:racines

• Le sol adhérant aux racines

C'est la gaine ou le manchon de sol entourant les racines ("rhizosheath") et y adhérant assez fortement. La distribution spatiale de ce sol adhérant aux racines a déja été décrite, dès 1882, par Sachs, dans le cas du blé (figure 2).

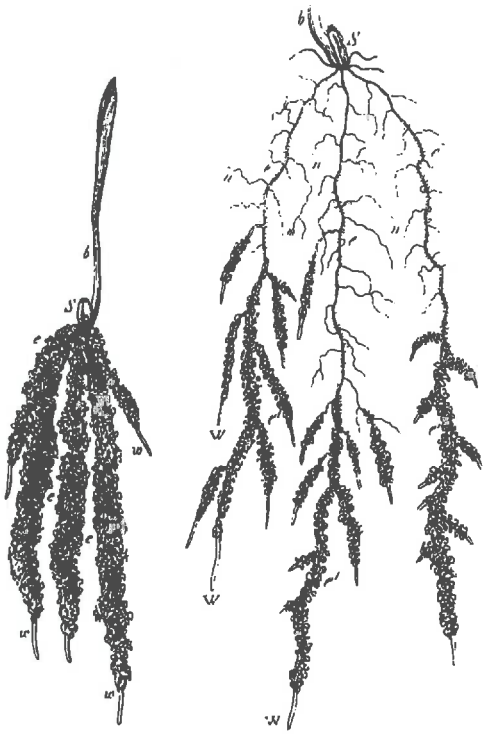

Figure 2. Dessin de plantes de blé montrant le sol adhérant aux racines (d'après Sachs, 1882).

Des études morphologiques, notamment celle de McCully et Canny (1988), ont permis de caractériser le sol adhérant aux racines. Il est composé de particules de sol, de microorganismes, de substances mucilagineuses. Les poils racinaires sont bien souvent enchevêtrés dans ce sol adhérent (figure 3).

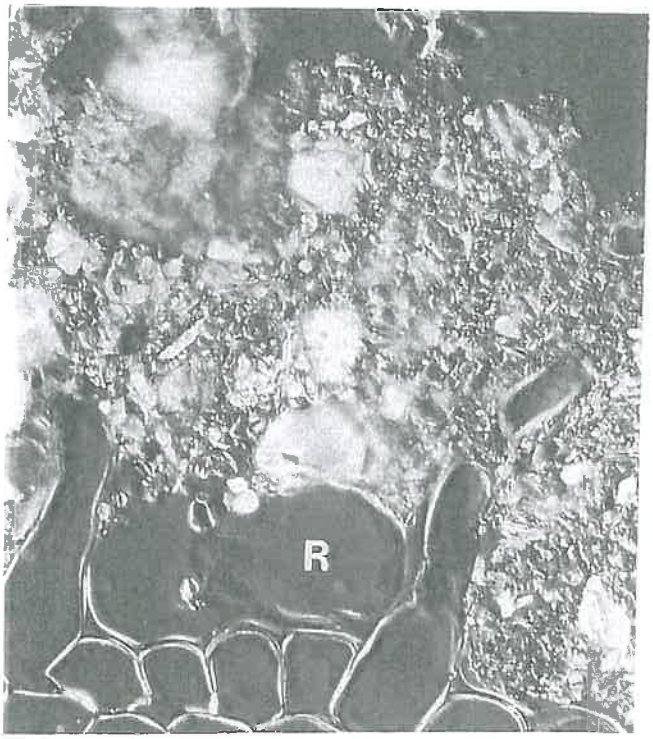

***Figure** 3. Coupe transversale d'une jeune racine nodale de maïs montrant la surface racinaire et la zone de sol adhérant à la racine. Cette coupe passe à travers deux poils absorbants et une cellule détachée qui provient de l'extrémité racinaire. Grossissement: 5 580 (d'après McCully et Canny, 1988).*

La première étude quantitative sur le sol adhérant aux racines a été réalisée par Sprent en 1975, dans le cas du pois cultivés dans du sable, à différentes conditions hydriques. La quantité de sol adhérant aux racines diminue en fonction de la teneur en eau du sable.

La quantité du sol fermement adhérant aux racines dépend du type de sol, de sa teneur en eau, de l'age de la plante mais aussi, de l'énergie utilisée pour secouer le système racinaire afin d'éliminer le sol faiblement adhérant. Ainsi, le sol adhérant aux racines a pu être subdivisé en sol fortement adhérant et faiblement adhérant au système racinaire (Parke et al., 1990). De ce fait, une

définition pratique du sol adhérant aux racines utilisée peut être la suivante: le sol adhérant aux racines est le sol qui reste fixé aux racines après avoir secoué les systèmes sol:racines, de façon standardisée (Gouzou, 1992; Czarnes, 1994, Amellal, 1996).

Watt *et al.* (1994) ont pu mettre en évidence de façon plus complète trois fractions de sol adhérent, de plus en plus fermement liée aux racines de maïs, grâce à trois traitements successifs des racines: sonication puis eau chaude et finalement, brossage des racines. De plus, ils ont montré que la culture d'une plante de maïs dans un sol à faible teneur en eau accroît le développement de la gaine de sol adhérant aux racines, augmente la force d'adhésion de celle-ci aux racines, et stimule la production de poils absorbants.

La distinction entre sol fortement ou faiblement adhérant au système racinaire nous amène maintenant à définir une notion nouvelle, celle de l'adhésion sol:racines.

•***Adhésion sol : racines***

L'adhésion ou, l'action d'adhérer peut être expliqué de la façon simplifiée et générale suivante : deux objets adhèrent en vertu de la force d'adhésion, et leur union qui en résulte est l'adhérence. Si on considère l'un des deux objets, ce dernier va tenir fortement par un contact étroit de la totalité ou de la plus grande partie de la surface de l'autre objet. Par ailleurs, ces deux objets ont entre eux peu ou beaucoup d'adhérence et si on veut les disjoindre, il faut une force assez grande pour surmonter la force d'adhésion qui les tient unies.

Des études sur l'adhésion de particules solides ont été realisées montrant notamment l'importance de l'état de la surface de contact entre ces particules sur la force d'adhésion entre elles. Fuller et Tabor ont étudié, en 1975, l'adhésion entre des billes de verre lisses et une surface plane de plexiglass tout d'abord lisse puis, de rugosité de plus en plus importante. Ils ont montré que, par rapport à un état lisse de la surface pour lequel l'adhésion est maximale, une rugosité relativement faible de la surface était suffisante pour faire diminuer fortement la force d'adhésion.

Dans le cas de systèmes biologiques et physiques comme le système sol:racines, l'adhésion sol:racines est beaucoup plus complexe et donc plus difficile à définir. Ceci nécessite notamment de bien identifier et caractériser l'interface sol:racines (ou le contact sol:racines) grâce à des approches micromorphologiques microscopiques comme celles réalisées par Van Noordwich *et al.* (1992). Il est aussi necessaire de mesurer des forces d'adhésion sol:racines grâce aux approches rhéologiques (technique de "pelage"), ce que personne n'a encore réalisé : Cela constitue l'un des objectifs de ma thèse.

2. Biophysique de la rhizosphère

Comme nous l'avons déjà évoqué lors des définitions des concepts de rhizosphère et d'interface sol:racine, de sol adhérant aux racines, les interactions biologiques et physiques entre le système racinaire et le sol sont fondamentales. Cette biophysique de la rhizosphère dépend beaucoup du stade de développement de la plante, et tout particulièrement de celui de son système racinaire.

Croissance racinaire

Une bonne connaissance de la structure du système racinaire (par ex. Pagès et Pellerin, 1994) est donc essentielle pour comprendre le fonctionnement d'une plante et les interactions racines - microorganismes - sol se produisant dans la rhizosphère (figure 1). La distribution du système racinaire dans le sol permet une prospection accrue de l'eau et des éléments nutritifs du sol, favorisant une meilleure croissance de l'ensemble de la plante. Cette distribution est hétérogène dans le cas des systèmes racinaires fasciculés comme celui du maïs. A cette hétérogénéité spatiale se surimpose une hétérogénéité temporelle du système racinaire, lorsque des racines explorent de nouvelles portions de sol et que d'autres meurent.

L'hétérogénéité spatiale du système racinaire peut être induite par des changements de conditions édaphiques. C'est ainsi qu'une augmentation de *contrainte mécanique,* que l'on peut observer lorsqu'on passe d'un sol poreux à un sol plus compact, induit une augmentation du diamètre racinaire et une diminution de la longueur racinaire et du rapport biomasse racinaire/biomasse

totale (par ex. Bengough *et al.*, 1997; Grégory *et al.*, 1997). Bengough *et al.* (1997) ont ainsi montré que le diamètre racinaire d'une racine ne subissant pas de contrainte mécanique était relativement constant, sauf à une distance d'un centimètre de l'apex, alors que le diamètre d'une racine subissant une contrainte mécanique augmente faiblement depuis l'apex jusqu'à une distance nettement supèrieure à la précédente. Bengough *et al.* (1997) ont aussi démontré que la résistance maximale d'un sol à laquelle une racine peut s'opposer, lors de sa pénétration dans le sol, est déterminée par la pression de turgescence maximale, générée dans la zone d'élongation racinaire, et par la forme et les caractéristiques de friction de l'extrémité racinaire.

Si la morphologie racinaire est aussi modifiée par la contrainte mécanique, cette dernière a aussi un effet positif sur l'exsudation racinaire (Groleau - Renaud, 1998) qui, à son tour, favorise la pénétration de la racine dans le sol, et donc la croissance racinaire. Bengough *et al.* (1997) ont ainsi établi que l'exsudation du mucilage et la desquamation de cellules de l'extrémité racinaire pouvaient jouer un rôle dans la diminution de la résistance de friction à la surface racinaire lorsque cette racine est soumise à une contrainte mécanique.

La croissance du système racinaire dépend également de la *contrainte hydrique*. Les résultats obtenus, pour une culture de maïs sur un sol limoneux, par MacKay et Barber (1985) peuvent servir d'exemple: l'augmentation du potentiel hydrique de - 173 kPa à - 728 kPa a un effet positif très net sur la longueur racinaire totale, la densité de poils racinaires et la surface racinaire dûe aux poils racinaires. De façon analogue, Gregory *et al.* (1997) ont montré, au cours de leur revue, que le rapport biomasse racinaire/biomasse totale du blé augmentait, quelque soit le stade de développement de la plante, lorsque le sol sableux, utilisé pour la culture, était drainé et partiellement séché.

Exsudation racinaire

Les exsudats, pris au sens large, peuvent être subdivisés en trois familles de composés: (i) les exsudats, composés solubles de faible poids moléculaire (des sucres, des acides aminés et des acides organiques) et libérés de façon passive dans le sol, (ii) les mucilages, composés non diffusibles de fort poids moléculaire (essentiellement des polysaccharides), et libérés selon des processus métaboliques (sécrétions par l'appareil de Golgi de la zone de la coiffe racinaire et par les

cellules rhizodermiques), (iii) les lysats, composés libérés par autolyse des cellules épidermiques en dégénérescence. Nous n'évoquerons ici que les mucilages racinaires, en particulier ceux du maïs, très abondants par rapport à ceux d'autres espèces végétales (Chaboud, 1983; Groleau - Renaud, 1998).

Le mucilage du maïs est composé d'acides uroniques, de galactose, d'arabinose, de xylose et de fucose, selon des rapports moléculaire de 3 : 7 : 8 : 5 : 11. Du glucose et du fructose sont aussi présents (Oades, 1978).

Des observations microscopiques du mucilage ont mis en évidence sa nature hétérogène, ce dernier pouvant se subdiviser en deux couches emboîtées, une couche interne de texture fibreuse, et une couche externe granulaire (Gückert *et al.*, 1975). Selon Foster (1982), la première couche proviendrait de sécrétions des cellules épidermiques alors que la seconde proviendrait de la coiffe racinaire.

L'extrémité racinaire (zone apicale) est le site privilégié de l'exsudation. Les sites d'exsudation peuvent s'étendre de l'extrémité racinaire jusqu'à la zone d'élongation dans la région des poils racinaires. Du mucilage a aussi été observé sur les poils absorbants (Greaves et Darbyshire, 1972).

Au fur et à mesure de la croissance racinaire, le matériel mucilagineux reste associé avec le rhizoderme, produisant une gaine de mucilage perméable, qui peut ou non être complétée par la production de mucilage provenant de la coiffe racinaire et par la desquamation de cellules rhizodermiques (Oades, 1978).

Les facteurs susceptibles de modifier qualitativement ou quantitativement l'exsudation racinaire sont nombreux. Ils y a notamment les facteurs du milieu comme le stress hydrique, la présence des microorganismes, la température, l'intensité lumineuse, etc, ainsi que les facteurs intrinsèques de la plante, dont son stade de développement (Groleau - Renaud, 1998). Matsumoto *et al.* (1979) ont ainsi montré, pour le maïs, que le maximum d'exsudation racinaire se situait très nettement entre 5 et 15 jours alors que le maximum de croissance (biomasse aérienne) avait lieu après, entre 15 et 30 jours de culture (figure 4).

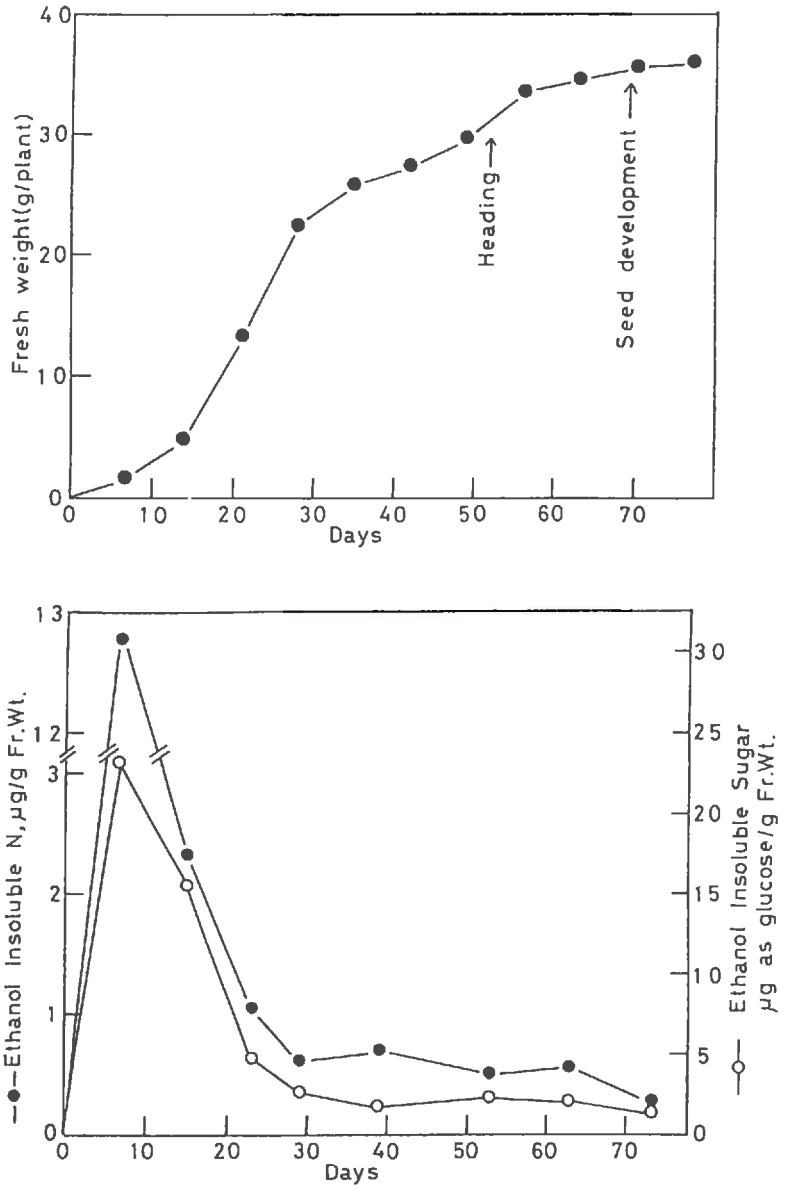

Figure 4. Relation entre la croissance du maïs (biomasse aérienne) (a) et l'excrétion de sucres insolubles (éthanol) (b) (d'après Matsumoto et al., 1979).

Les fonctions du mucilage vis à vis des racines sont très importantes. Il y a en particulier le rôle de protection des racines contre les infections, la dessiccation de l'extrémité racinaire ou les blessures mécaniques causées par les particules de sol.

Le mucilage est aussi un échangeur de cations grâce aux groupements carboxyliques de ses acides polyuroniques. Ces groupements COO^- peuvent ainsi se lier aux cations en position échangeable au sein des fractions argileuses du sol (Greaves et Darbyshire, 1972), ce qui expliquerait largement les propriétés agrégeantes des exsudats (adhésion sol:racines, macro-agrégation et stabilisation des agrégats de la rhizosphère) (Oades, 1989,1993; Chenu, 1993). Le mucilage est également une source d'énergie très stimulante pour les micro-organismes de la rhizosphère qui vont, à leur tour, produire des exo-polysaccharides.

Activité microbienne dans la rhizosphère

Le mucilage racinaire stimule très nettement l'activité des micro-organismes de la rhizosphère. D'un point de vue microbiologique, l'"*effet rhizosphère*" se caractérise ainsi par un rapport R/S élevé, de l'ordre de 50 à 200, où R est le nombre de microorganismes dans la rhizosphère et S celui dans le sol à plus de 8 cm de la surface racinaire. Ce rapport diminue très rapidement, de façon exponentielle, depuis la surface racinaire vers le sol non-rhizosphérique (Rovira et Davey, 1974; Haynes et Francis, 1993; Amellal, 1996; Amellal *et al.*, 1998_b). De nombreux micro-organismes de la rhizosphère produisent des exopolysaccharides agrégeants (Gouzou, 1992; Gouzou *et al.*, 1993; Amellal, 1996).

L'effet agrégeant et stabilisant de ces polysaccharides d'origine microbienne varie suivant les souches bactériennes, la quantité et la nature de leurs polysaccharides (conformation, poids moléculaire, propriétés de surface) (Chapman et Lynch, 1985), la nature et les conditions hydriques du sol (Gouzou *et al.*, 1993; Amellal, 1996; Amellal *et al.*, $1998_{a,b}$). Des études ultrastructurales ont par ailleurs montré que l'adhésion des microorganismes à la surface des colloides minéraux ou organo-minéraux est très marqué, et qu'elle s'effectue par l'intermédiaire de leurs exopolysaccharides (Guckert *et al.*, 1975; Chenu *et al.*, 1987; Dorioz *et al.*, 1987, 1993; Villemin et Toutain, 1987; Chenu, 1993; Amellal, 1996; Amellal *et al.*, $1998_{a,b}$).

Le rôle spécifique des mucilages des microorganismes rhizosphériques par rapport à celui des mucilages racinaires n'a pu être étudié, dans la rhizosphère du blé, que grâce à la comparaison de rhizosphères inoculées ou non (témoins) (Gouzou *et al.*, 1993; Amellal *et al.*, $1998_{a,b}$).

Impact de la croissance racinaire sur la structure du sol adhérant aux racines et l'ancrage des racines dans le sol

Lorsqu'une racine pénètre dans les pores du sol, elle exerce une pression radiale et axiale dans ce sol (Misra *et al.*, 1986), rendant plus compact le sol situé juste autour de la racine et devant l'extrémité racinaire en croissance. C'est ainsi que Greacen *et al.* (1968) ont observé, par rayon X, une baisse exponentielle de la densité du sol en fonction de la distance radiale à une racine de 1 mm de diamètre. Cette compaction différentielle a la même variabilité spatiale lorsqu'un pénétromètre arrondi, de diamètre analogue, remplace la racine pour pénétrer dans le sol (figure 5).

Greacen *et al.* (1968) et Dexter (1987) ont développé un modèle permettant de prédire cette diminution exponentielle de la densité du sol en fonction de l'éloignement de l'interface sol:racine, en prenant le cas d'une racine progressant dans un sol de structure homogène. Récemment, Bruand *et al.* (1996), en étudiant les changements de porosité autour des racines du maïs à partir de lames minces d'un sol limoneux, ont pu valider le modèle de Dexter (1987). La tomographie par rayon X a aussi récemment permis d'identifier, en trois dimensions, une zone plus foncée à l'interface sol:racine, attribuable à la compaction du sol dans cette zone de contact (Zwiggelaar *et al.*, 1997).

L'architecture du système racinaire et son mode d'adhésion au sol assure aussi un ancrage de la plante dans le sol. Cet ancrage évolue notamment en fonction de l'espèce végétale et de son stade de développement.

Une indication de la distribution spatiale des points d'ancrage et des forces d'ancrage le long de la racine a été obtenue par des mesures de la force nécessaire pour détacher des racines du sol (Ennos, 1989, 1990, 1993).

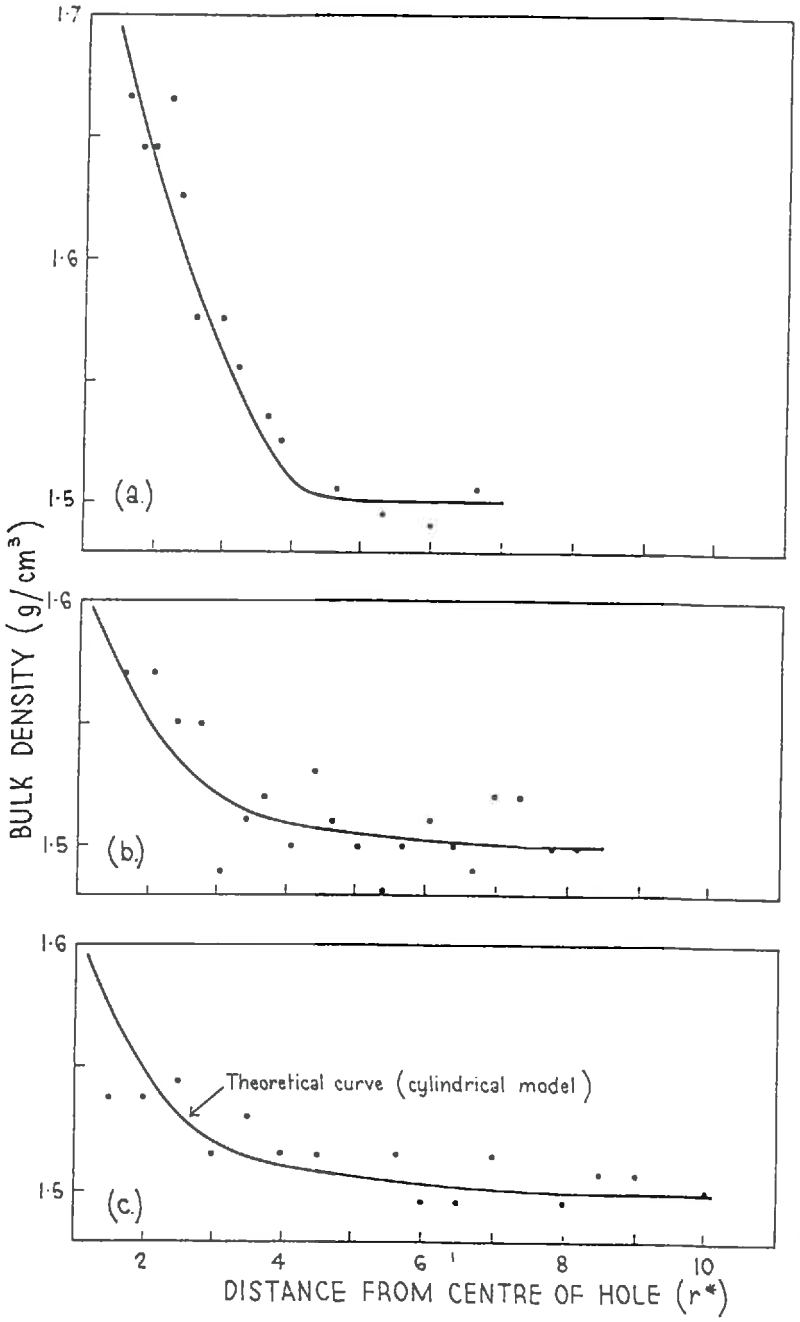

Figure 5. *Evolution de la densité apparente d'un sol limoneux, préparé à une densité apparente de 1.5 g/cm3 et à une suction de 30 kPa, en fonction de la distance radiale à une racine d'1 mm de diamètre (c) ou à un pénétromètre de 3 mm de diamètre arrondi (a = 30°) (b) ou pointu (a = 5°) (a) (d'après Greacen et al., 1968).*

Transferts hydriques dans la rhizosphère jusqu'à l'interface sol : racine

L'absorption d'eau du sol par la plante est déterminée par (1) le potentiel foliaire et le taux de transpiration et (2) par les résistances aux flux d'eau du sol à la racine.

Le cycle jour - nuit du potentiel foliaire module les transferts d'eau de la plante à l'atmosphère. Pendant la journée, le taux d'évapotranspiration, bien souvent supérieur à l'absorption d'eau, entraine une diminution de l'eau de stokage et une déshydratation des tissus de la plante. L'inverse se produit pendant la nuit (Huck, 1984; Lafolie *et al.*, 1991; Jensen *et al.*, 1993). De plus, Herkelrath *et al.* (1977) ont établi que la variation cyclique du potentiel foliaire était quasi-constante mais que le potentiel foliaire diminuait lorsqu'une culture de maïs était soumise à une dessiccation.

Par ailleurs, depuis l'analyse classique de Gardner (1960) du flux radial d'eau vers une "simple" racine, des études plus récentes ont démontré la présence d'une résistance interfaciale sol:racine, dûe probablement à un faible contact entre les racines et le sol (Herkelrath *et al.*, 1977; Bristow *et al.*, 1984; Barataud *et al.*, 1995; Stirzaker *et al.*, 1996). Il a été clairement établi que la zone de contact entre le sol adhérant au système racinaire et les racines est fonction de la teneur en eau du sol et que le transfert d'eau, du sol à la plante, ne pouvait se modéliser qu'en prenant en compte cette zone de contact (Herkelrath *et al.*, 1977; Veen *et al.*, 1992; Barataud et al., 1995).

Si l'on considère l'ensemble du système racinaire, la variation spatiale de l'absorption d'eau à partir de différentes régions du sol a été également bien décrite. Cette variation spatiale dépend de la géométrie du système racinaire ainsi que de la distribution de l'eau dans le profil de sol ou dans le pot de culture (Taylor et Klepper, 1978; Barataud *et al.*, 1995, Stirzaker *et al.*,1996; Clothier et Green, 1997; Doussan *et al.*, 1998). L'inter-relation existant entre les distributions spatiales de l'eau et des racines varie au cours de la culture de la plante.

L'hétérogénéité de l'absorption d'eau à l'intérieur d'une racine dépend aussi du stade de dévelopement des vaisseaux conducteurs du xylème, comme l'on montré Mc Cully et Canny (1989) et Doussan *et al.* ($1998_{a,b}$).

3. Contexte, objectifs et plan de cette étude

Contexte et objectifs de l'étude

Ce sujet de recherche porte sur l'adhésion sol:racines ainsi que sur les interactions biophysiques existant entre le sol et les racines de maïs. Il complète une série de travaux de recherche entrepris conjointement par l'équipe d'écologie microbienne de la rhizosphère et l'équipe d'agrégation des sols du CPB (Gouzou, 1992; Czarnes, 1994; Amellal, 1996) et portant sur l'agrégation de la rhizosphère de blé provoquée par l'inoculation de bactéries productrices d'exopolysaccharides.

Ces travaux de recherche ont révélé (1) que l'activité microbienne agrégeante de ces bactéries productrices d'exopolysaccharides dépendait fortement des caractéristiques hydriques de la rhizosphère (Amellal, 1996; Amellal *et al.*, $1998_{a,b}$) et (2) que l'état d'adhésion sol:racines, caractérisé par le rapport entre la masse de sol adhérant aux racines et la biomasse racinaire, variait de façon analogue. Les stocks d'eau que peut emmagasiner le sol adhérant aux racines sont donc des paramètres importants à prendre en considération pour le fonctionnement biologique du sol rhizosphérique. Une meilleure analyse du sol adhérant aux racines permettrait aussi de mieux appréhender les études sur la colonisation et l'activité microbienne de la rhizosphère.

De façon complémentaire, comme nous l'avons noté au cours de cette revue bibliographique, la zone de contact sol:racines est capitale pour les transferts d'eau et d'éléments nutritifs du sol à la plante. Aussi, dans ce sujet de recherche, une attention toute particulière est portée à cette zone de contact sol:racines, première interface de résistance au flux hydrique, la seconde étant l'interface feuille:atmosphère au niveau des stomates.

Ce contact sol-racines dépendrait de l'état d'adhésion sol:racines ainsi que de certaines propriétés mécaniques et géométriques des racines et du sol. Ceci est notre hypothèse.

La principale question que nous nous sommes posée est la suivante:
quel est l'impact du type de sol et de sa teneur en eau, sur l'état d'adhésion sol:racines?

La plante que nous avons choisi pour cette étude est le maïs. En Lorraine, région d'élevage par excellence, le maïs d'ensilage est très utilisé pour la nourriture des animaux. Sa culture s'effectue le plus souvent sur des sols

argileux (pélosols), mais aussi sur des sols limoneux (sols bruns lessivés). Du fait de ses racines puissantes ("têtes de rotation"), le maïs présente également l'avantage de pouvoir pousser sur des sols sableux, notamment grâce à une irrigation intensive. Le maïs est également une plante très étudiée, tant pour la géométrie de son système racinaire (ex: Pagès et Pellerin, 1994) que pour son exceptionnelle exsudation racinaire (Groleau - Renaud, 1998).

L'aptitude de différents sols à adhérer aux racines de maïs sera quantifiée, en fonction de leur potentiel hydrique. Trois sols (horizons de surface) à textures sableuse, limoneuse et limono-argileuse ont été ainsi choisis pour cette étude. Les points de repère physique seront les courbes de rétention d'eau (drainage) de chacun de ces sols, à l'équilibre ou lors d'une cinétique de séchage (sol avec ou sans plante).

L'étude des modes d'adhésion sol:racines a été réalisée à l'aide de deux approches complémentaires :

(1) - cinétique globale de rupture du sol adhérant aux racines, à l'échelle de l'ensemble du système racinaire, à l'aide d'agitation mécanique à l'air ou d'immersion dans de l'eau et d'ultra-sonication du système sol:racines.

Une étude préalable des cinétiques de séchage et des cycles contrôlés d'humectation et de dessiccation, a été réalisée dans la rhizosphère de maïs, de 11 jours de culture, ainsi que dans le sol témoin, sans plante. L'effet de ces séchages plus ou moins prononcés, et des cycles d'humectation et de dessiccation associés, sur les propriétés mécaniques du sol a été ensuite abordé, à la fois à l'échelle de l'ensemble du système racinaire et à celle l'agrégat.

La géométrie du système racinaire, les propriétés intrinsèques des sols, l'imprégnation du sol adhérent par les exsudats racinaires seront particulièrement pris en compte pour expliquer nos données, quelles soient hydriques ou mécaniques.

(2) - approche rhéologique à l'échelle centimétrique, à l'aide d'un dispositif spécifique de croissance de jeunes plantules de maïs et de mesures de forces de séparation sol:racines, permettant de calculer des énergies de rupture sol:racines.

A cette occasion, nous avons élaboré une théorie de l'adhésion sol:racines qui pourrait s'appliquer à l'analyse rhéologique d'autres systèmes complexes adhérents entre eux.

Plan de ce mémoire

Le mémoire est divisé en trois chapitres comprenant chacun un ou deux articles soumis, écrits en anglais.

Il commence tout d'abord par une présentation des matériaux utilisés où sont décrits l'origine, les caractéristiques et les préparations des sols et des semences de maïs (chapitre I). Dans ce cadre, une étude plus approfondie des propriétés mécaniques de deux boules de sol adhérentes sera entreprise afin de mieux aborder l'étude de l'adhésion sol:racines par l'approche rhéologique. Pour clore ce premier chapitre, un résumé des méthodes et des objets d'étude utilisés sera présenté sous forme de tableau synthétique.

Nous aborderons ensuite l'étude des interactions sol:racines à l'échelle du système racinaire avec, tout d'abord, l'analyse des cinétiques de séchage, et des cycles contrôlés d'humectation et de dessication associés, dans la rhizosphère de maïs et dans le sol témoin sans plante, puis l'étude de l'impact de ces modes de séchage sur les propriétés mécaniques du sol adhérant aux racines (chapitre II).

Nous présenterons ensuite l'étude de l'adhésion sol:racines que nous avons abordé, à l'échelle centimétrique, à l'aide de l'approche rhéologique (chapitre III).

Tous ces résultats seront résumés et synthétisés au cours de la conclusion générale, résumé des acquis et les limites de notre travail, qui nous amènera à suggérer quelques perspectives de recherches ultèrieures.

Pour des raisons d'identification, les numéros des légendes, des tableaux et des figures de ces trois chapitres sont précédés du chiffre romain correspondant, que le tableau ou la figure provienne ou non d'une (ou de deux) publication. Le seul inconvénient est que cela se traduit par des couples de figures I. 1 à I. 3, et II. 1 à II. 9 ainsi que par des couples de tableaux I. 1 et II. 1.

CHAPITRE I

MATERIELS ET METHODES

Ce chapitre comprend un article soumis à la revue Soil & Tillage Research (partie II.).

Czarnes S., Dexter A.R. and Bartoli F. Mechanics of two adherent centimetric remoulded soil balls : a preliminary examination

MATERIELS ET METHODES

I.- Matériels: Origines, caractéristiques et préparations

A.- Sols

1.- Origines et échantillonnage

Trois types d'horizons de surface ont été choisis pour cette étude. Ils se différencient par leur texture sableuse, limoneuse et limono-argileuse.

Le *sol sableux de Bordeaux* appartient aux sols podzoliques de la région des Landes (Sud-ouest de la France), qui se sont développés sur des matériaux alluviaux et sableux marins du Miocène et du Quaternaire. Depuis 20 ans, les plantations de pin du 19 ème siècle sont de plus en plus remplacées par la culture du maïs avec irriguation intensive, dans des régions spécifiques où ces sols podzoliques sont humides et plus organiques (podzols humiques hydromorphes selon Duchaufour, 1977). Le sol de Bordeaux était cultivé en maïs depuis 4 ans. Il a été échantillonné en Avril 1995 par D. Plenet de la station d'Agronomie de l'INRA de Bordeaux.

Le *sol limoneux d'Orgeval* appartient aux sols bruns lessivés glossiques (Duchaufour, 1977) du Bassin Parisien, qui se sont développés à partir des matériaux limoneux éoliens quaternaires. La région du bassin versant de l'Orgeval (CEMAGREF), situé à 80 km à l' Est de Paris, est une région dont la culture intensive du blé existe depuis 40 ans. Le sol brun lessivé glossique qui se développe au sein de sa couverture limoneuse est organisé suivant une toposéquence, du plateau au rû de Mélarchez, composée de trois unités pédologiques se différenciant les unes des autres grâce à leurs horizons de surface (unités de plateau, de mi-versant et de bas de versant, colluvionné). Le sol d'Orgeval échantillonné en novembre 1994 (culture en blé d'hiver) appartient à l'unité colluvionnée de bas de versant de la toposéquence étudiée par Bartoli *et al.* (1995) et Gomendy (1996).

Le *sol limono-argileux* de la ferme expérimentale ENSAIA de *La Bouzule*, située à 12 km au Nord-Est de Nancy, appartient à une unité mixte de versant sur lequel les sols bruns lessivés de plateau ont été pour partie érodés, laissant alors affleurer les pélosols de l'Est de la France qui se sont développés à partir des argiles sédimentaires liasiques. Ce sol est sous culture intensive de blé et de maïs depuis 20 ans. Il a été échantillonné en Avril 1997.

2.- Agrégats et sols remaniés

Les trois horizons de surface ont été séchés à l'air puis tamisés à 4 mm. Ils ont ensuite été utilisés sous cette forme d'*agrégats (ou de particules)*, pour l'étude des interactions sol:racines à l'échelle du système racinaire (chapitre II) ou sous forme de *sol remanié*, plus ou moins compact.

La préparation de sols remaniés pour l'étude mécanique de cylindres de sol de diamètre 25 mm et de hauteur 50 mm, et de boules de sol adhérentes de diamètre de 25 à 30 mm (paragraphe propriétés mécaniques) a été effectué de la façon suivante. Chaque échantillon de sol tamisé a été malaxé à la main avec un excès d'eau distillée avant d'être mis en équilibre avec un potentiel hydrique de - 5 kPa (table à succion), pendant 3 jours. Certains de ces sols remaniés, préparés à - 5 kPa, ont alors subi des séchages plus prononcés, à différents potentiels hydriques, afin d'étudier l'effet de l'intensité du séchage sur leurs propriétés mécaniques.

La préparation de boîtes de sols remaniés pour l'étude de l'adhésion sol:racines, à l'échelle de la très jeune plantule de 4 jours (chapitre III), a été moins drastique (sols remaniés plus poreux). Le sol tamisé a été doucement mélangé, à la main et dans des sacs plastiques, avec une certaine quantité d'eau distillée, déterminée à partir des courbes de rétention d'eau de chaque sol (voir propriétés hydro-physiques). Après cette préparation, les sacs de sol remanié, plus ou moins humide, ont été placés dans une chambre thermostatée à environ 10 °C, pendant 4 à 7 jours de façon à faciliter l'équilibre de la rétention d'eau dans le sol.

3.- Granulométrie et propriétés de surface

Les résultats d'analyses de granulométrie ainsi que celles des propriétés de surface, effectuées sur les sols tamisés à 4 mm, sont présentés dans le tableau I. 1.

L'*analyse granulométrique*, sans destruction préalable des matières organiques, a été réalisée par tamisage et par sédimentation, selon la méthode de la pipette de Robinson, effectuée après dispersion du sol par des résines sulfonates Na échangeuses de cations (Rouiller *et al.*, 1972).

Les trois sols sont notamment caractérisés par des teneurs très différentes en fraction < 2 µm : argiles organo-minérales de 1.9 %, 16.4 % et 33.1 % pour les sols de Bordeaux, d'Orgeval et de La Bouzule, respectivement (tableau I. 1.), qui seront dénommés sol sableux, limoneux et argileux tout au long de cette étude, afin de mieux les différencier (le sol "argileux" est en fait un sol limono-argileux).

	Granulométrie (%)						
Sites	sables grossiers >200 µm	sables fins 50-200 µm	limons grossiers 20-50 µm	limons fins 2-20 µm	argiles < 2 µm	S_{BET} (m^2/g)	$S_\mu/S_{t\text{-}plot}$ (%)
Bordeaux	85.7	8.1	0.9	3.6	1.9	0.3	10
Orgeval	1.3	2.7	44.6	29.8	16.4	13.6	34.4
Bouzule	11.5	4.2	19.6	27.3	33.1	40.8	24.9

Tableau I. 1. *Granulométrie et propriétés de surface des sols étudiés (horizons de surface)*

Des isothermes d'absorption d'azote gazeux à la température de l'azote liquide (77 °K) ont été obtenus sur les sols tamisés à 4 mm, préalablement dégazés pendant 22 heures, à l'aide d'un appareil volumétrique équipé d'une gauge de pression 0 - 1000 Tor.

Les *surfaces spécifiques* ont été calculées selon la méthode classique utilisant l'équation BET et selon la méthode dite du t-plot (Gregg et Singh, 1967), qui consiste à utiliser une surface alumineuse non poreuse de référence, afin de décomposer la surface spécifique totale en une surface due au micropores, de quelques dizaines d'angströms de diamètre, et une surface due aux macropores.

La surface spécifique totale augmente en fonction de la teneur en argiles (tableau I. 1.) comme cela a été établi sur différentes gammes de sols par Petersen *et al.* (1996). Nous verrons au cours du chapitre III que la surface spécifique d'un sol est un paramètre physique qu'il faut largement prendre en compte pour expliquer les mesures d'énergie de rupture sol:racines. La proportion de la surface spécifique due aux micropores représente 10 %, 34.4 % et 24.9 % pour les sols de Bordeaux, d'Orgeval et de La Bouzule, respectivement (tableau I. 1.). C'est en

quelque sorte une surface peu accessible (réseau de micropores) qui serait associée aux micro-domaines argileux des agrégats qui ont été par ailleurs observés en microscopie électronique à transmission sur des coupes ultra-fines, dans le cas du sol d'Orgeval (Gomendy, 1996; Bartoli *et al.*, 1998).

4.- Fractions argileuses organo-minérales

Les résultats d'analyses minéralogiques et organiques des fractions argileuses organo-minérales sont présentés dans le tableau I. 2.

L'ultra-fractionnement des argiles dispersées aux résines Na, a été réalisé l'aide de l'ultracentrifugeuse Sharpless dont on peut régler la force de centrifugation et le débit d'arrivée des suspensions (Rouiller *et al.*, 1984). La *caractérisation minéralogique* de la fraction argile totale (pour le sol de Bordeaux) et des sous-fractions argileuses (pour les sols d'Orgeval et de La Bouzule) a été réalisée par diffraction X (diffractomètre à anticathode au cobalt) sur lames d'argiles orientées (traitements : saturation en K, ethylène glycol et chauffage à 550 °C).

Pour le sol de Bordeaux, les smectites, minéraux argileux prédominants, n'ont pu être mises en évidence qu'après destruction préalable des matières organiques par une solution de NaOCl. La kaolinite est aussi présente, de façon secondaire, et l'illite et le quartz ont été détectés à l'état de traces. La fraction argileuse du sol d'Orgeval est composée de 35 % de smectites (< 0.1 µm) et de 15 % d'intertrastifiés illite-smectite (0.1 à 0.5 µm), et de 50 % d'illite, de vermiculite et de kaolinite, dont les proportions sont égales (Bartoli *et al.*, 1995; Gomendy, 1996). La fraction argileuse du sol de la Bouzule a une composition minéralogique assez proche de celle du sol d'Orgeval (tableau I. 2.).

Ces fractions argileuses organo-minérales sont extrêmement riches en matières organiques dans le cas du sol sableux podzolique de Bordeaux (27.6 % de carbone organique) alors qu'elles sont pauvres en matières organiques dans le cas des deux autres sols, avec des teneurs en carbone organique égales à 3.5 et 2.3 % pour les sols d'Orgeval et de La Bouzule, respectivement (tableau I. 2.). Cette opposition se retrouve au niveau de la nature de ces matières organiques, observée par spectrométrie infra-rouge (voir en annexe), poly-aromatiques et hydrophobes pour le sol de Bordeaux (C/N = 23.6), riche en polysaccharides et en protéines et hydrophiles pour les sols d'Orgeval et de La Bouzule (C/N = 8.4 et 9.9, respectivement) (tableau I. 2.).

Sites	smectites et illite-smectite (%)	illite, vermiculite et kaolinite (%)	C org (% fraction)	Corg (% C total)	C/N
Bordeaux	prédominance de smectites		27.6	32	23.6
Orgeval	50	40	3.5	72	8.4
Bouzule	40	60	2.3	45	9.9

Tableau I. 2. Nature des argiles et carbone organique de la fraction argileuse $< 2\mu m$

5.- Capacités d'échange cationiques et acidités

Le *pH* a été mesuré à l'eau (pH $_{H2O}$) et au NH_4Cl 0.5 N (pH NH_4Cl). Les cations échangeables ont été déplacés par une solution de NH4Cl 0.5 N : 4 g de sol ont été mélangés à 80 ml de NH4Cl 0.5 N puis centrifugés. Les cations, principalement calcium, magnésium et potassium du surnageant ont été dosés par absorption atomique, à l'aide d'un spectromètre ICP AES JY 32.

Tous les sols étudiés sont saturés, notamment en calcium, du fait du chaulage. Corrélativement, ils sont proches de la neutralité, hormis le sol sableux de Bordeaux, légèrement acide (tableau I. 3.) La *capacité d'échange* de ces sols (tableau I. 3.) augmente avec la teneur en argiles (tableau I. 1.), ce qui est classique (Duchaufour, 1977; Scheffer et Schachtschabel, 1976). Le sol sableux est ainsi pauvre en éléments nutritifs potentiellement disponibles pour la plante.

Sites		Capacité d'échange au NH4Cl 0.5 N (meq / 100g)						
	pH $_{H2O}$	pH $_{NH4Cl}$	Ca^{2+}	Mg^{2+}	K^+	S	T	S/T (%)
Bordeaux	5.6	4.46	4.68	1.88	0.02	6.6	6.8	97.3
Orgeval	6.8	5.96	19.5	0.79	0.08	20.4	20.5	99.3
Bouzule	7.0	5.74	25.7	2.63	0.37	28.8	29.0	99.1

Tableau I. 3. pH et capacités d'échange cationiques.
S = somme des "bases échangeables", T = somme des cations échangeables, S/T = taux de saturation.

6.- Propriétés hydro-physiques

a.- Rétention d'eau

Les courbes de rétention d'eau par drainage ont été obtenues à partir de petits cylindres PVC de 5.6 cm^3 remplis de sol tamisé à 4 mm que l'on a saturé d'eau par capillarité, dans une enceinte fermée (cloche en verre), avant de les mettre en équilibre avec un potentiel hydrique déterminé, à l'aide d'une presse à membranes de Richards. Les temps d'équilibre ont été de 3 à 5 jours, selon la pression choisie. Ces courbes de rétention d'eau nous ont servi de références au cours de toute cette étude, pour choisir des potentiels matriciels lors de l'analyse de l'adhésion sol:racines (chapitre III) et des propriétés mécaniques du sol adhérant aux racines (chapitreII). Elle nous ont également servi de références pour étudier les cinétiques successives de séchage se déroulant dans la rhizosphère de maïs lors des cycles de séchage et d'irrigation contrôlés (chapitre II).

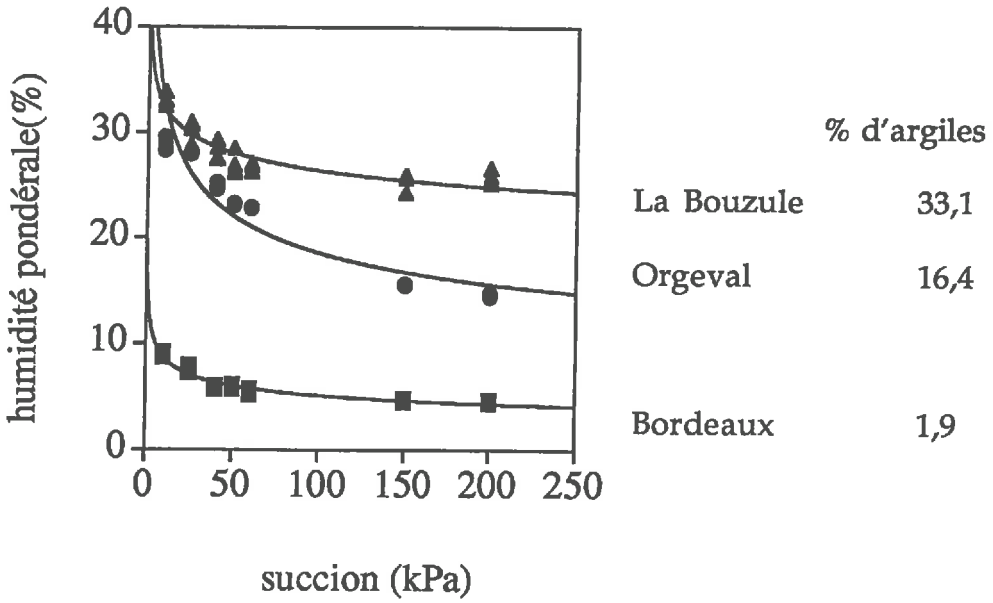

Figure I. 1. Courbes de rétention d'eau de cylindres de sol tamisé à 4 mm (drainage)

Il faut tout d'abord noter que la teneur en eau gravimétrique des sols drainés à 250 kPa est fonction de la teneur en argiles (fig. I. 1. et tableau I. 4.), ce qui est classique (Scheffer et Schachtschabel, 1976).

De plus, la teneur en eau à saturation du sol sableux est très faible, du fait que la majorité de ses pores ont des tailles relativement élevées, supérieures à 100 µm (porosité de transfert localisée entre les particules de sables grossiers).

A l'opposé, cette teneur en eau à saturation des sols d'Orgeval et de La Bouzule est relativement élevée du fait de l'importance de leurs méso- et micro-porosités inter-agrégats, observées par MEB et MET sur des lames minces et des coupes ultra-fines, dans le cas du sol d'Orgeval (Gomendy, 1996; Bartoli *et al.*, 1998).

Le sol limoneux d'Orgeval est drainant ce qui est attribué à la fois à sa faible rugosité d'interface solide:pores et à sa forte connectivité de pores (Gomendy, 1996; Bartoli *et al.*, 1998; Gomendy *et al.*, 1998). A l'opposé, les deux autres sols ont du mal à sécher (fig. I. 1.). Ceci serait attribuable à la teneur en argiles relativement élevée dans le cas du sol de La Bouzule, ce qui diminuerait la connectivité des pores pouvant retenir l'eau, comme l'ont recemment montré Bartoli *et al.* (1998) pour une gamme de sols limoneux à teneur en argiles variant de 15 à 30 %. Par contre, la séchage relativement difficile du sol sableux podzolique de Bordeaux, par rapport à la plupart des sols sableux, plus drainant, serait attribuable au caractère hydrophobe de ses matières organiques.

b.- Limites d'Atterberg

La limite de plasticité est la teneur en eau pour laquelle le sol passe d'un état plastique à un état friable. En pratique, la mesure de la limite de plasticité est réalisée suivant la méthode standardisée suivante: un petit cylindre de sol de diamètre 3 mm est roulé à la main jusqu'à ce qu'il commence à se fissurer un peu. La limite de liquidité est la teneur en eau pour laquelle le système sol:eau passe d'un état liquide à un état plastique. Elle a été déterminée par la technique drop-cone (BS 1377, 1975). L'indice de plasticité est la différence entre les limites de liquidité et de plasticité.

Les limites d'Atterberg dépendent à la fois de la teneur en argile et de leur minéralogie. Le calcul de l'activité (rapport indice de plasticité/teneur en argiles) permet de différencier l'influence de ces deux facteurs.

L'augmentation des limites d'Atterberg de liquidité et d'indice de plasticité en fonction de la teneur en argiles (tableau I. 4.) est classique (par ex. Mitchell, 1993). Elle est plus prononcée pour les valeurs de limites de liquidité (tableau I.4.). Dans le cas du sol de Bordeaux, très sableux, la mesure de la limite de plasticité n'a pas été possible car ce sol est trop friable.

Les limites d'Atterberg et notamment, les propriétés de plasticité des sols, permettent de mieux comprendre leurs propriétés mécaniques (fin de ce chapitre) dont nous avons également étudié l'influence sur l'état d'adhésion sol:racines (chapitre III).

Sites	argiles < 2 µm (%)	teneur en eau du sol saturé (%) P = 10 KPa	teneur en eau du sol drainé (%) P = 200 KPa	limites d'Atterberg (%)			Activité = Indice de plasticité / argiles
				limite de liquidité	limite de plasticité	Indice de plasticité	
Bordeaux	1.9	9	5	24.5	n m	n m	n m
Orgeval	16.4	28	15	34.4	23.4	11	0.67
Bouzule	33.1	31	25	48.2	26.9	21.3	0.64

nm: non mesurable (sol non plastique)

Tableau I. 4. *Propriétés hydro-physiques*

B.- Maïs

1.- Choix, prégermination et sélection des semences

Les semences de maïs (*Zea mays*) utilisées appartiennent au cultivar DEA. Elles nous ont été fournies par la société Pioneer France Maïs de Toulouse qui leur a fait subir un traitement antifongique.

Un calibrage des semences à l'état sec à été effectué sur une population de 107 semences et la distribution des masses de semences obtenue a permis de sélectionner, au début de chaque expérience, des semences dont les masses sont comprises entre 0.234 et 0.270 g (zone médiane de la distribution des masses de semence dans laquelle se situe 50 % de la population). Les semences sont mises à prégermer à l'obscurité en boite de Petri sur un filtre humidifié, dans une étuve à 28 °C, pendant environ trois jours. Une observation des semences prégermées est alors réalisée, et seules les semences dont les radicules sont semblables et rectilignes ont été sélectionnées. Les deux autres critères de sélection ont été une masse proche de 0.40 g ainsi qu'une longueur de radicule comprise entre 14 et 20 mm.

2.- Cultures du maïs

Ces semences sélectionnées ont été utilisées de deux façons.

La première a consisté à faire pousser le maïs pendant 11 jours (stade du développement végétatif où l'exsudation est maximale) dans un des sols afin d'étudier les interactions sol:racines à l'échelle de l'ensemble du système racinaire (chapitre II). La culture du maïs est réalisée dans des pots cylindriques en PVC noir, utilisés en horticulture, de 4 cm de diamètre et de 20 cm de hauteur. Ces pots ont la particularité d'avoir une forme semi-conique à leur base (diminution du diamètre de 4 à 2 cm). Les pots sont remplis de sol séché à l'air et tamisé à 4 mm. La porosité est de 0.58 et 0.50 $cm^3 . cm^{-3}$ pour les sols limoneux et sableux, respectivement, le volume du pot rempli de sol étant mesuré en le remplissant d'eau et la densité des particules étant considérée comme égale à 2.65 $g . cm^{-3}$. Une semence prégermée est alors déposée à la surface du sol. Les pots sont alors placés en chambre de culture (phytotron), dont les paramètres climatiques sont les suivants:

- température de jour (17 heures) de 24°C et de nuit (7 heures) de 20°C,
- éclairement de 37 à 54 mmoles de photons $. m^{-2} . s^{-1}$ à la surface des pots, en fonction de la position à l'intérieur de la chambre de culture, assurant un photopériodisme de 17 heures,
- humidité de l'air : 60 ± 10 %.

La chambre phytotronique est équipée d'un dispositif de mesure du potentiel hydrique (micro-tensiomètres) et d'un système d'irriguation progressive, goutte à goutte (perfuseurs médicaux), qui a une position fixe.

L' irrigation progressive est effectuée au cours de la période nocturne jusqu'à l'obtention du potentiel matriciel minimum que l'on s'est fixé. Le premier article du chapitre II fournit plus de détails sur le dispositif expérimental factoriel ainsi que sur l'étude des cycles d'humectation et de dessication dans la rhizosphère du maïs.

La récolte est effectuée après 11 jours de culture, après une dernière période de séchage de 17 heures. Un contrôle de la croissance des plantes au moment de la récolte est réalisé en excisant les jeunes plantules et en pesant leurs biomasses aériennes.

La deuxième utilisation des semences prégermées à été effectuée dans le cadre de l'étude de l'adhésion sol:racines, à l'échelle de la très jeune plantule de maïs agée de 4 jours (chapitre III). Pour cette étude, un dispositif spécifique de croissance des semences prégermées à la surface d'un sol a été mis au point afin de pouvoir séparer progressivement, de la surface du sol, la graine puis la racine de chaque plantule (fig. I. 2.). Le protocole de culture est le suivant. Chaque semence prégermée et sélectionnée est transférée à la surface d'un sol contenu dans une boîte cylindrique en PVC, opaque, de 60 mm de diamètre et de 40 mm de haut. Un fil de pêche est attaché autour de la graine. C'est par ce fil de pêche que la graine, puis la racine, seront séparées de la surface du sol. Une petite membrane en latex est placée juste en-dessous de la graine de façon à limiter le contact sol:graine. La jeune plantule est alors positionnée à la surface du sol avec la graine proche d'un des côtés de la boîte pour permettre à la racine de croître jusqu'à l'autre coté de la boîte, ce qui correspond à une élongation racinaire maximale de 55 mm environ. Une autre membrane en latex, de même diamètre que celui de la boite, est placée au-dessus de la jeune plantule. Enfin, la boîte est fermée par un couvercle en PVC, après avoir complété le volume de la boîte non rempli de sol par un "bouchon" en polystyrène. La boîte est alors pivotée de 90 ° pour orienter la racine verticalement et ainsi permettre sa croissance gravitropique. L'expérimentation consistant à mesurer la force qui lie le sol à la racine commence après une croissance racinaire d'un jour effectuée dans ce dispositif de croissance, dans une chambre thermostatée à 25 °C.

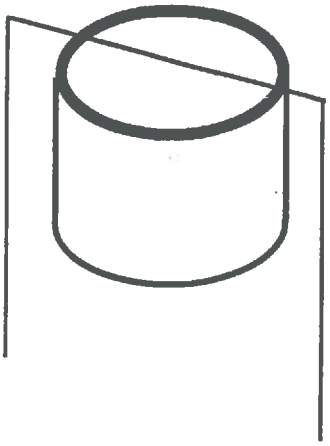

Boîte de culture cylindrique en PVC opaque

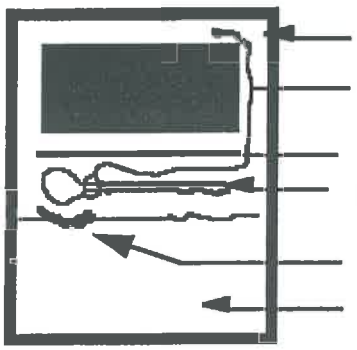

Boîte en PVC opaque
Fil de pêche
Membrane circulaire en latex
Semence prégermée
Petite membrane en latex
Sol

(a) préparation de la boîte de culture

(b) rotation de 90 °
(croissance racinaire gravitropique)

(c) début du test de séparation sol : racine après 24 heures de culture dans une chambre thermostaté à 25 °C

Figure I. 2. *Dispositif spécifique de croissance des jeunes plantules de maïs avec les trois étapes principales depuis la préparation de la boîte de culture (a) jusqu'au début du test de séparation sol:racine (c).*

II. - Propriétés mécaniques de deux boules adhérentes de sol remanié

article soumis pour la revue Soil & Tillage Research

Czarnes S., Dexter A.R. and Bartoli F. Mechanics of two adherent centimetric remoulded soil balls : a preliminary examination

Lors de ces expériences, les deux boules de sol remanié ont été compressées progressivement ensemble (fig. I. 3., publication soumise ci-jointe). De façon inverse, elles ont été séparées progressivement l'une de l'autre. Grâce à la mesure de la force nécessaire pour les séparer, nous avons pu calculer l'énergie d'adhésion entre ces deux boules de sol. Ceci sera exposé au cours du chapitre III.

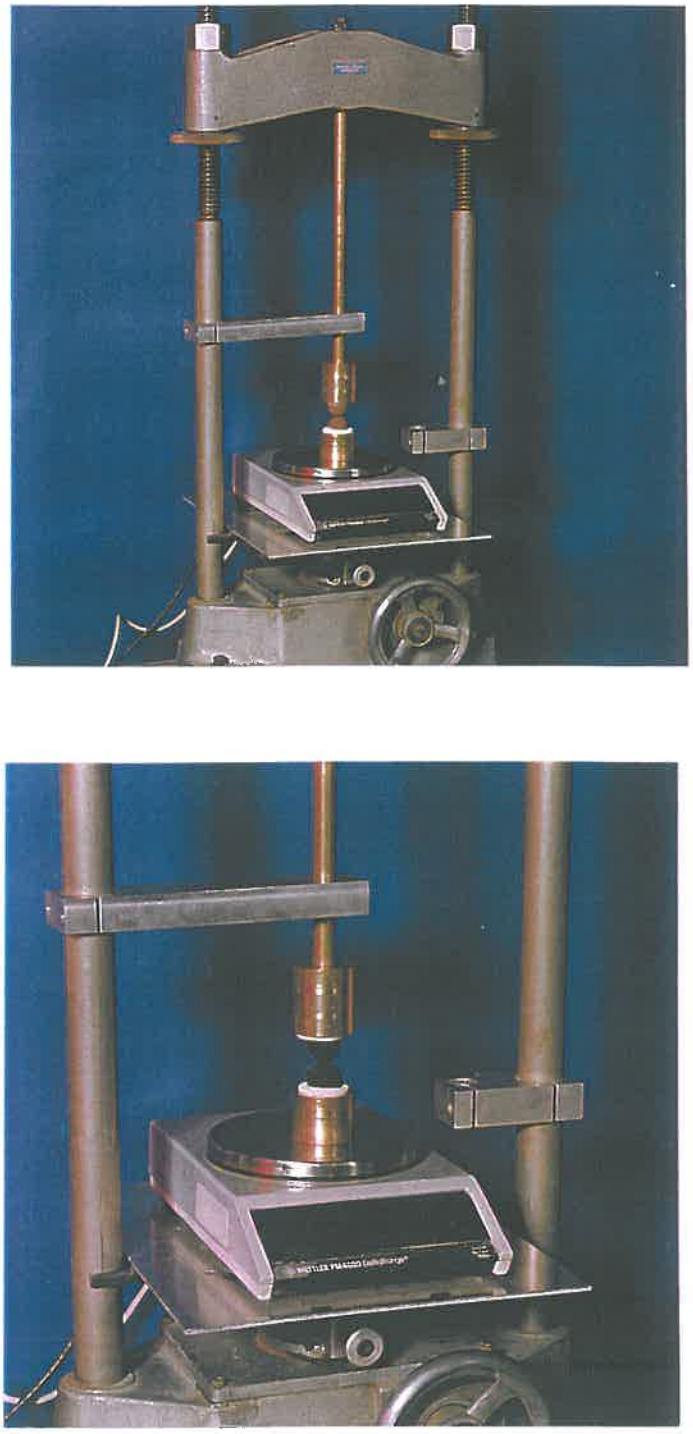

Figure I. 3. *Dispositif de mesure de la compression entre deux boules adhérentes de sol remanié. Vue générale (a) et détail (b).*

Mechanics of two adherent centimetric remoulded soil balls : a preliminary examination

S. CZARNES[a, b], A.R. DEXTER[a, c*] and F. BARTOLI[b]

[a] *Silsoe Research Institute, Wrest Park, Silsoe, Bedford MK45 4HS, United Kingdom*

[b] *Centre de Pédologie Biologique UPR 6831 du CNRS associé à l'Université Henri Poincaré - Nancy I, BP 5, 54501 Vandoeuvre-les-Nancy, France*

[c] *present address: Instytut Uprawy Nawozenia i Gleboznawstwa, ul. Czartoryskich 8, 24 - 100 Pulawy, Poland*

[*] Corresponding author tonyd@iung.pulawy.pl

Key words: remoulded soils balls, granular and clayey soils, stress:strain relationships, modelling.

Résumé

Les propriétés mécaniques de deux boules centimétriques, adhérentes, de sol remanié ont été étudiées en fonction de leur teneurs en argiles et en eau.

La courbe pression de compression:déformation d'applatissement a été modelisée à l'aide d'une loi puissance, dont le coefficient est négatif pour les courbes de forme convexe des sols argileux plastiques, ou positif pour les courbes de forme concave des sols granulaires friables. Une modélisation physique de la relation pression:déformation a été réalisée, grâce au concept de pression effective, puis discutée.

Summary

The mechanics of two adherent centimetric remoulded soil balls has been studied as a function of both soil clay and water contents.

The relationship between the compression stress and the flattening strain was fitted with a power law equation, with either a negative or a positive power law coefficient for either the convex stress:strain curve of the plastic clayey soils or the concave stress:strain curve of the friable granular soils, respectively. Modelling of the stress:strain relationship using the concept of effective stress have also been investigated and discussed.

Introduction

Fragmentation of temperate topsoils by ploughing occurs either after harvest in the autumn or in the spring when the soil is at a suitable water content. This lead to macro-pore volume discontinuity and embedded multi-scaled soil structure. At the macro-scale, soil fragments or clods are in contacts, with rounded macro-pores between them. At the micro-scale, micro-aggregates and particles of approximately 20 µm to 250 µm diameter, and their pore network complements, can be observed e. g. by using SEM micrographs of soil thin sections (e. g. Fiès & Bruand, 1990; Gomendy, 1996; Bartoli *et al.*, 1998).

Classical concepts of mechanics applied to continuous materials can not be directly used for tilled topsoils with such hierarchical structures (Dexter, 1991). Macro-pore volume discontinuity, scale laws and clod:clod adhesion should be taken into account as well as the fact that stresses applied on clods are heterogeneous. It is the reason why we are proposing a new simplified method for characterizing the mechanics of tilled topsoils.

We first prepare remoulded centimetric soil balls in order to homogenise the soil structure (e.g. Monnier *et al.*, 1973) by greatly increasing the number of contacts between particles and micro-aggregates (e. g. Dexter *et al.*, $1984_{a, b}$; Mitchell, 1993; Attou, 1996). We measure the flattening strain of the interfaces of two adherent remoulded topsoil balls as a function of axial compressive stress, in order to simulate, in a very simplified way, the mechanics of adherent topsoil clods as occur after cultivation.

This paper describes preliminary application of this new methodology to both granular or plastic topsoils of a wide range of clay content. The aim of this study is also modelling of the strain:stress relationships using either (i) a common mathematical curve-fitting approach for both granular and plastic remoulded topsoils or (ii) the concept of effective stress which has been developed by Terzaghi (e. g. *in* Mitchell, 1993) by studying the effect of matric water potential on the relationships between the axial compressive stress and the flattening strain ratio for two adherent granular remoulded topsoil balls.

Materials and methods

* Topsoils and modelling clay

Two granular sandy and silty topsoils were selected for this study: Bordeaux and Orgeval, with organo-mineral clay contents of 1.9 % and 16.4 %, respectively (table 1), and, with BET surface area values of 0.28 $m^2.g^{-1}$ and 13.6 $m^2.g^{-1}$, respectively. Two plastic clayey topsoils were also selected: Foggathorpe and Fladbury, with clay contents of 59 % and 79 %, respectively (table 1). A proprietary brand of modelling clay ("Plasticine") has also been used as a reference. Although this is not soil, it has a similar plastic cohesive consistency.

The Bordeaux granular topsoil belongs to the podzolic South-Western french soils of the Landes area which are developed in Miocene and quaternary sandy marine and alluvial materials. Over the previous 20 years, nineteenth-century pine plantations had been progressively replaced by maize culture, with intensive irrigation, in specific areas where the podzolic soils are wet and more organic. The sandy topsoil was collected in April 1995, at 0 to 0.25 m depth, and had been under maize for 4 years. The Orgeval granular topsoil belongs to the silty leached brown soils of the Parisian Basin which are developed in quaternary silty eolian materials. In this area there had been intensive continuous wheat agriculture for the previous 40 years. The silty topsoil was collected in November 1994, at 0 to 0.25 m depth, under winter wheat and within the downslope colluvial topsoil unit of the soil toposequence which has been previously described by Bartoli *et al.* (1995). The Foggathorpe clayey topsoil belongs to the alluvial brown soils of the Foggathorpe series which are developed in quaternary lacustrine alluvium deposits (Furness & King, 1978) whereas the Fladbury clayey soil topsoil belongs to the alluvial vertic soils of the Fladbury series which are developed in quaternary river alluvium deposits (Reeve, 1978). These two clayey topsoils were collected at 0.5 m depth.

The sandy granular topsoil was characterized by a predominant 0.2 mm to 2 mm coarse sand fraction (85.7 %) (table 1), composed of coated quartz grains, with some internal cracks (X-ray diffraction data of the sand fractions and Backscattered Electron Scanning Images (BESI) of soil thin sections are not shown). The value of the ratio between the 50 µm to 20 µm coarse silt fraction and the 2 µm to 20 µm fine silt fraction was 1.5 for the silty granular topsoil (table 1). It is a representative ratio value for such North-Eastern french silty soils (Walter *et al.*, 1997). The BESI of soil thin sections showed that the silt quartz

particles are mostly white, angular and coated grains, which interact with grey clay plasma coatings (Gomendy, 1996; Bartoli *et al.*, 1998). Coated quartz grains were either in contact or separated from each other by pore necks, with radii equal to or less than 4 µm. Interconnected pores, 5 µm to 20 µm pore average radii, delimited packings of 3 to 6 quartz grains surrounded by clay coatings. Mean total porosity value of the silty granular topsoil was 0.5 cm^3. cm^{-3}, with a predominant microporosity occurring on BESI of soil thin sections (Gomendy, 1996; Bartoli *et al.*, 1998).

Smectites were the predominant clay minerals for the sandy granular topsoil (Bordeaux), with kaolinite as a secondary clay mineral, and illite and quartz as trace minerals whereas the clay fraction of the silty granular topsoil (Orgeval) was composed of 35 % of < 0.1 mm smectites (0.17 nm XRD peak after the ethylene-glycol pre-treatment) and of 65 % of 0.1-2 mm illite-smectite interstratified clay, illite, vermiculite and kaolinite whose proportions are rather equal (Bartoli *et al.*, 1995; Gomendy, 1996). Predominant clays were illite and interstratified illite-smectite, and smectites for the Foggathorpe and the Fladbury clayey plastic topsoils (Reeve, 1978; Furness & King, 1978).

The studied silty and clayey long-term tilled topsoils were also poor in organic carbon (less than 1 %) whereas the Bordeaux sandy short-term topsoil was rich, with 2.2 % organic carbon. Conversely, topsoil organic matter was rich both in nitrogen and in oxygenated functional groups for the silty granular topsoil (C/N ratio value of 8.4), and probably for the non-analysed clayey plastic topsoils, whereas it was polyaromatic for the sandy granular topsoil (C/N ratio value of 23.6).

Finally, all the topsoils studied were neutral and mostly calcium saturated, but without calcium carbonates, with pH values of soil suspensions in water of 6.8 to 7.9 (Reeve, 1978; Furness & King, 1978; Gomendy, 1996), except for the sandy organic topsoil which was relatively acid (pH value of 5.6).

topsoil samples	soil types	Particle-size distribution (%)					Atterberg limits (%)			Activity = Plastic Index/clay ratio
		coarse sand >200 µm	fine sand 50-200 µm	coarse silt 20-50 µm	fine silt 2-20 µm	clay < 2 µm	Liquid limit	Plastic limit	Plastic Index	
Bordeaux	podzolic	85.7	8.1	0.9	3.6	1.9	24.5	nm	nm	nm
Orgeval	leached brown	1.3	2.7	44.6	29.8	16.4	34.4	23.4	11	0.67
Foggathorpe	alluvial brown	4		37		59	75.9	29.3	46.6	0.79
Fladbury	alluvial vertic	6		22		72	110.6	41.9	68.7	0.95

nm: Measure not possible

Table I. 1. Main textural and plastic characteristics of the studied topsoils.

*** Atterberg limits and soil activity**

Soil swelling and shrinkage as well as stress:strain relationships are closely linked to soil plasticity properties such as the Atterberg limits (Mitchell, 1993). The plastic limit (or lower plastic limit) is determined as the soil water content at which the soil stiffens from a plastic to a semi-rigid friable state. In practice it was defined as the water content at which a sample of soil can just be rolled into a thread of 3 mm diameter without breaking (Sowers, 1965). The liquid limit (or upper plastic limit) is defined as the soil water content at which the soil:water system changes from a viscous liquid to a plastic body. It was determined by the drop-cone technique (BS 1377, 1975). The plasticity index was computed as the difference between the liquid limit and the plastic limit.

Both the type and amount of clay in a soil influences the values of the Atterberg limits. To separate them, the ratio of the plasticity index (%) to the clay fraction (%), termed the soil activity (Skempton, 1953 *in* Mitchell, 1993) has also been used in this study.

*** Preparation of remoulded topsoil cylinders or balls**

The experiments required either cylindrical remoulded topsoil samples of initial diameter D_C value of 25 mm, with a height:diameter ratio value of 2, or pairs of remoulded topsoil balls of initial diameter D_b values of 20 mm to 38 mm, or 25 mm to 30 mm for either "Plasticine" or remoulded topsoils, respectively. Both remoulded topsoil cylinders and balls were prepared by hand-rolling batch of wet aggregates of < 4 mm.

The two sandy and silty granular topsoils were first wetted by hand mixing water and soil, with an excess of water. They were then dried at a matric water potential of - 5 kPa for three days on a sand table. Some of them were further dried at matric water potential values of - 10 kPa or - 50 kPa for one week using pressure plates (Klute, 1986). In contrast, matric water potential of the studied clayey plastic topsoils has not been controlled. Their remoulded soil balls were prepared at different water contents occuring within their plastic domains (fig. 2): 29.9 % and 33.7 %, or 57.3 % and 63.5 % for the Foggathorpe and Fladbury remoulded topsoil balls, respectively.

Mean bulk density and water content values have been determined on the studied remoulded topsoils and mean soil porosity and volumetric water content value counterparts have been calculated, assuming particle density values of 2.65 $g.cm^{-3}$ or 2.7 $g.cm^{-3}$ for the granular or the clayey plastic topsoils,

respectively.

*** Unconfined compressive test**

The major principal compression stress (axial stress) has been determined on the two remoulded granular topsoils using the unconfined compression test (e.g. Watts & Dexter, 1993). Each cylindrical sample of material was loaded axially at a rate of 4.5 mm min^{-1} using a loading frame of the type used for triaxial testing of soil core samples. The axial applied force, F_a, recorded as a function of percentage axial strain using a load cell which was calibrated with known weights. The output from the load cell was recorded with a signal analyser (Advantest model R9211B) for subsequent analysis. By definition, the cylindrical compression axial stress, σ_C, is the ratio between the applied axial force, F_a, and the surface area, $\pi D_C^2/4$, of the cylinder disc plane characterized by its diameter, D_C:

$$\sigma_C = 4F_a/\pi D_C^2 = F_a/S \qquad (1)$$

The dimensionless axial strain, R_a, is the ratio between the axial strain (mm) and the initial height (mm) of the cylinder of remoulded topsoil. In this study, both F_a and σ_C values have been recorded at a R_a value of 0.2 as usual (Watts & Dexter, 1993) or at failure for the sandy granular topsoil where the maximum compressive stress did not readily reach a maximum value; failure was deemed to have occurred when a certain R_a value (typically 0.2) was reached.

*** Flattening between pairs of balls of remoulded topsoil**

Two sets of mechanical experiments have been carried out: (i) the step by step record of the dimensionless strain flattening ratio R_f as a function of the compression stress or (ii) the record of the compression axial stress when a standardized R_f value of 0.47 has been reached during continuous compression of the two adherent topsoil balls. These two methods are described as follows.

- Step by step increasing compressive stress method (cyclic loads)

For the two remoulded granular topsoils, four or five replicates with a - 10 kPa matric potential were chosen, whereas two gravimetric water content

values have been used for the remoulded plastic topsoils: 29.9 % and 33.6 %, or 57.3 % and 63.5 % for the Foggathorpe or Fladbury remoulded topsoil balls, respectively.

For each pair of either "Plasticine" or remoulded topsoil balls, different successive levels of force were applied and their strain flattening ratios were determined as follows. At the beginning of the experiment, the two remoulded topsoils balls, characterized by either their initial water content or matric water potential were put in Cling Film to keep them moist. Then, each mould was poured with liquid plaster of Paris (calcium sulphate with water). Each remoulded topsoil ball was pressed into the mould until about half of the sphere was inside the plaster of Paris and so inside the mould (fig. 1). Few second after, when the plaster of Paris was firm, the upper mould was attached to the cross-beam of the apparatus and the lower mould was placed on a digital balance below it (fig. 1). The step by step compression method was ready to start when the two soil balls were in contact. The preparation of the experiment occured very quickly and so, the water content of each remolded soil ball was assumed to be constant in particularly in the contact zone between the two balls which was not inside the plaster of Paris.

The pairs of balls of remoulded topsoil were pressed together axially at a rate of 4.5 mm min^{-1}, in the loading-frame. When each increasing level of applied axial force had been reached, each pair of spheres was pulled apart and the diameter, D_f, of the flat interface which had developed between them (fig. 1) was measured with digital calipers, with a length resolution value of 10^{-2} mm. This enabled the dimensionless strain flattening ratio, $R_f = D_f/D_b$ to be determined. The experiment was stopped when the flattening diameter reached about one-half of the initial ball's diameter.

In axial soil cylinder mechanics (unconfined compressive test), the axial stress corresponding to an applied axial force is constant because the surface area on which this force is applied is almost constant ($\pi D_c^2/4$: see above). In contrast, in the mechanics of two adherent soil balls, the value of the axial compressive stress decreases significantly from a maximal stress value ($\sigma_{b\text{-}max}$) to a minimal one ($\sigma_{b\text{-}min}$) when the axial force is applied from the two circular flattening surface areas of diameter D_f to the two largest surface areas of diameter D_b, respectively:

$$\sigma_{b\text{-}max} = 4F_a/\pi D_f^2 \qquad (2)$$

$$\sigma_{b\text{-}min} = 4F_a/\pi D_b^2 = R_f^2 \sigma_{b\text{-}max} \qquad (3)$$

The strain was essentially homogeneous in the tests on cylindrical soil samples (unconfined compressive test) whereas it was mainly a surface deformation in axial mechanics of two adherent soil balls, at least for R_f values less than 0.5.

In this study, the minimal compression axial stress $\sigma_{b\text{-}min}$ values so determined on each pair of adherent balls of remoulded topsoil were also compared to the cylinder axial compressive stress σ_c value determined on each remoulded topsoil cylinder counterpart. For that, trigonometric calculations lead to the following power-law relationship between the dimensionless strain flattening ratio R_f and its axial dimensionless strain ratio R_a:

$$R_f = 1.87 R_a^{0.487} \qquad (4)$$

where R_f value was 0.8 for a R_a value counterpart of 0.2 (unconfined compressive test).

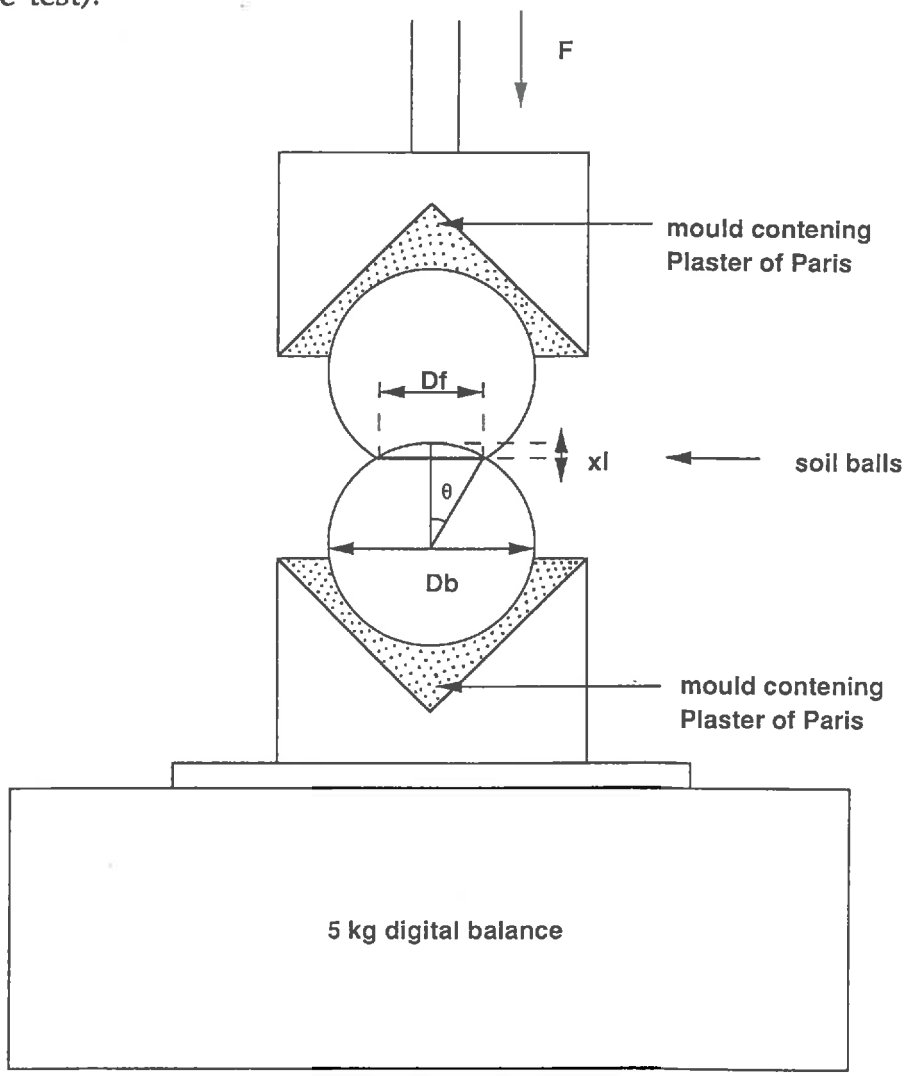

Figure I. 1. Experimental procedure and main geometrical characteristics of the pairs of flattening remoulded topsoil balls. F = axial compressive force, D_b and D_f = ball and flattening cicle area diameters , x_l = axial strain length.

- Flattening test

Only the two remoulded granular topsoils have been used in this last set of experiments. Here, the pairs of balls of remoulded topsoil were pressed together continuously until their flat interfaces reached about half the initial diameter Db (Rf value of 0.47), using only one load and not successive increasing loads as previously. The applied axial force was then noted and the maximal and minimal stresses were computed as above.

*** Concept and theory used**

In this paper, we combined the classical Coulomb - Mohr theory of soil strength with the concept of effective stress developed by Terzaghi (e. g. *in* Mitchell, 1993) to characterize the stress:surface deformation by compression between two spherical soil samples.

According to the Coulomb - Mohr theory of strength, shear failure occurs in a material when some critical shear stress τ is exceeded, where τ may be expressed as:

$$\tau = c + \sigma \tan \phi \qquad (5)$$

where σ is the normal stress on the plane of the failure and c and ϕ, the cohesion and angle of friction, are two constants which characterize the material. Following the reviews of Mullins & Panayiotopoulos (1984) and of Mitchell (1993), when a saturated porous material is subject to external stress, the pore water, having no shear strength is ineffective in mobilizing shear resistance. Thus, ignoring any possible effects due to trapped air, the effective stress σ' is dependent on both the applied normal stress σ and the pore water pressure u, as follows:

$$\sigma' = \sigma - u \qquad (6)$$

Similarly, when the pore water is under a tension ψ (matric water potential), the tension supplements any external applied stress so that, in a saturated soil:

$$\sigma' = \sigma + \psi \qquad (7)$$

In an unsaturated soil, assuming that the air in soil pores is at atmospheric pressure, the effective stress is given by:

$$\sigma' = \sigma + \chi\psi \qquad (8)$$

where χ is a function of the degree of saturation ranging from 0 in a dry soil to 1 in a saturated soil (e. g. Mullins & Panayiotopoulos, 1984; Young & Mullins, 1991; Mitchell, 1993). The soil strength characteristic is the relation between soil strength and either matric water potential or water content. It varies with soil

type and soil management (e. g. Davies, 1985; Young & Mullins, 1991 and Watts & Dexter, 1993). In granular soils in which the long-range interparticle attractions and repulsions are both small, the effective stress corresponds to the true intergranular pressure (Mitchell, 1993).

Results and discussion

* Atterberg limits

The values of the Atterberg limits of the remoulded topsoils (table 1) have been plotted as a function of their clay contents, deliminating a plastic domain (dotted area of figure 2). In this study, the water contents of the studied remoulded topsoils were within this plastic domain. On the other hand, measurement of the plastic limit for the sandy topsoil was not possible. Similar observations have been previously observed on quartz which did not develop plastic mixtures with water, even when ground to sizes less than 2 mm (Casagrande, 1932 *in* Mitchell, 1993).

As usually observed, the increase of the Atterberg limits as a function of clay content was much more pronounced for the liquid limit than for the plastic limit (fig. 2). This leads to a large increase of the plasticity index as a function of clay content (table 1) (e. g. Smith *et al.*, 1985; Mitchell, 1993). In this study, the increase of each Atterberg limit as a function of clay content was also non-linear (fig. 2). This can be attributed to the increase, from the sandy topsoil to the clayey ones, of smectite content within the clay fraction. Soil activity effectively increased as a function of clay content (table 1). Smith *et al.* (1985) have also demonstrated that both Atterberg limits are more closely related to specific surface area, hygroscopic water content and cationic exchange capacity than to clay content, indicating that the clay mineralogy must be taken into account in these Atterberg limits correlations.

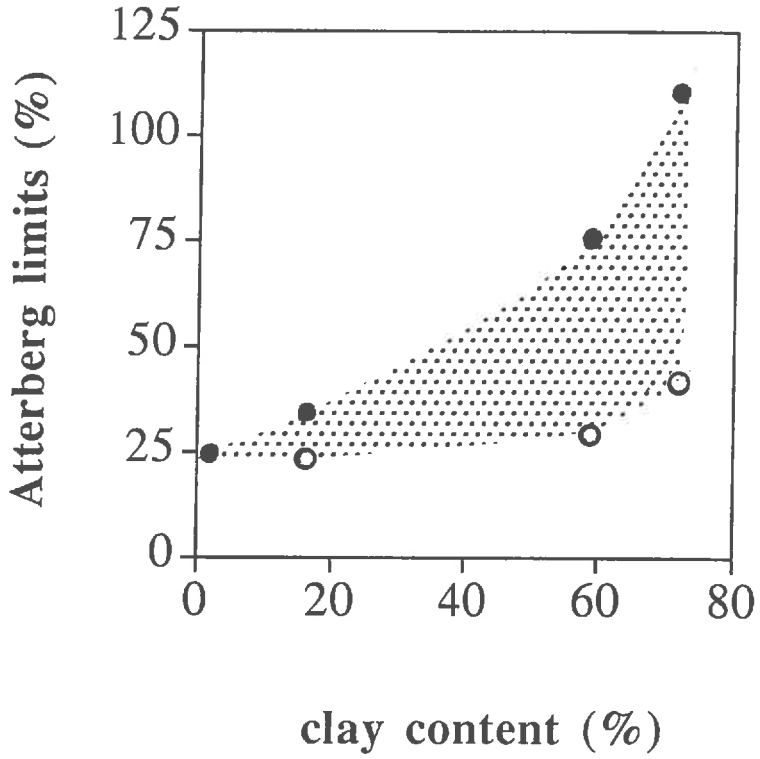

Figure I. 2. Atterberg limits of the studied remoulded topsoils as a function of their clay content. Open and filled circles correspond to the plastic and liquid limits, respectively. The dotted area deliminated the plastic domain of the studied topsoils.

*** Porosity of centimetric remoulded soil balls**

The mean porosities of the remoulded granular topsoil balls were 0.36 ± 0.01 cm^3. cm^{-3} and 0.37 ± 0.01 cm^3. cm^{-3} for the sandy and silty remoulded topsoil balls, respectively, and these porosities were water-saturated for both granular remoulded topsoils equilibrated at matric water potential values of - 5 kPa. Similar porosity values of 0.34 to 0.39 cm^3. cm^{-3} have been reported by Panayiotopoulos & Mullins (1985) and by Chretien (1986) for a range of compacted sands and sandy soils characterized by quartz grains with rounded sharpes similar to those of the two studied granular topsoils.

The mean porosity value of 0.36 to 0.37 cm^3. cm^{-3} for the two studied granular remoulded topsoil balls corresponds to the porosity value of 0.367 cm^3. cm^{-3} of a random heap of equal spheres, in dense packing (Finney, 1970). This is

intermediate between that of simple cubic arrays (0.476 cm^3. cm^{-3}) and those of close-packed hexagonal or face-centred cubic arrays (0.259 cm^3. cm^{-3}) (e. g. Chretien, 1986; Mitchell, 1993). Therefore, for many purposes, a random array of spheres can be considered to be composed of a mixture of regular cubic and close-packed arrays (Smith *et al.*, 1929 *in* Mitchell, 1993). In such microscopic structural models, the observed porosity value of 0.36 to 0.37 cm^3. cm^{-3} corresponds to a mean number of contacts between soil particles and micro-aggregates of 8 (Hartge, 1994). On the other hand, as previously suggested by Mitchell (1993), smaller soil particles can occupy pore spaces between larger particles, leading to lower porosity values than for uniform spheres but irregular particle shapes also result in a tendancy toward higher porosity values. The net result is that the range of porosity values in remoulded soils, with probable single-grain fabrics, is not much different from that for uniform spheres. This is why, in this study, the random packing of uniform spheres has been taken into account for microscopic modelling of the strain:stress relationships for two adherent balls of granular remoulded topsoil.

In contrast, the porosity values of the two studied remoulded clayey topsoil balls were relatively high: (i) 0.43 and 0.45 cm^3. cm^{-3} for the Foggathorpe remoulded plastic topsoil prepared at water contents of 29.9 and 33.6 %, respectively; with water saturation ratios of 105 and 110 %, respectively, and (ii) 0.56 and 0.64 cm^3. cm^{-3} for the Fladbury remoulded plastic topsoil prepared at water content values of 57.3 and 63.5 %, respectively, with corresponding water saturation ratios of 118 and 93 %, respectively. These relatively high porosity values should be attributed to either the easy hand-rolling of these plastic clayey topsoils or to the shrinkage which occurs during air-drying of the studied remoulded clayey soil balls, leading to growth of intra-balls crack.

*** Stress : strain relationships for two adherent remoulded topsoil balls**

In this section, we consider the relationship between the maximal axial compression stress, $\sigma_{b\text{-}max}$, and the dimensionless flattening ratio, R_f, for two adherent balls of either modelling clay or remoulded clayey or granular topsoils.

- Stress:strain relationships for two adherent modelling clay balls

The maximal stress:strain relationship appeared to be almost linear, with no ball diameter effect, for modelling clay balls of diameter 24 to 38 mm whereas the smallest balls of diameter of 20 mm tend to have larger surface deformations within the same range of stress values (fig. 3). In the light of these preliminary results, we therefore decided to prepare remoulded topsoil balls with diameters of 25 - 30 mm.

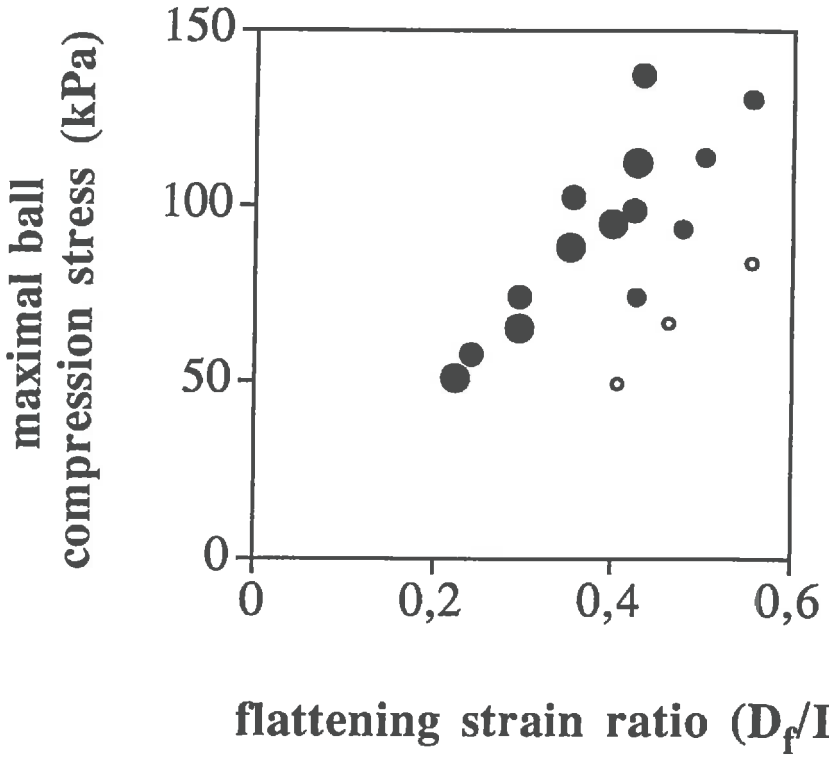

Figure I. 3. Relationships between the maximal axial compressive stress and the flattening strain ratio for two pairs of adherent plasticine balls of different diameters: 20 mm (open circles), and 24 mm, 32 mm and 38 mm (filled circles, from the smallest to the largest ones, respectively).

- Stress:strain relationships for two adherent clayey remoulded topsoil balls

For the studied plastic topsoils, non linear convex stress:strain relationships have been observed (fig. 4). Such ductile deformations have been widely described for similar clayey soils (e. g. Tripodi *et al.*, 1992; Mitchell, 1993).

Non-linear increase of the axial compressive stress as a function of the flattening ratio leads to an asymptote value of the stress:strain curve which was about approximately one-half for the Fladbury remoulded topsoil balls (79 % clay) than that for the Foggathorpe ones (59 % clay) (fig. 4). For each studied plastic remoulded topsoil, the asymptote value of the stress:strain curve also decreased as a function of its water content (figs. 4a and 4b).

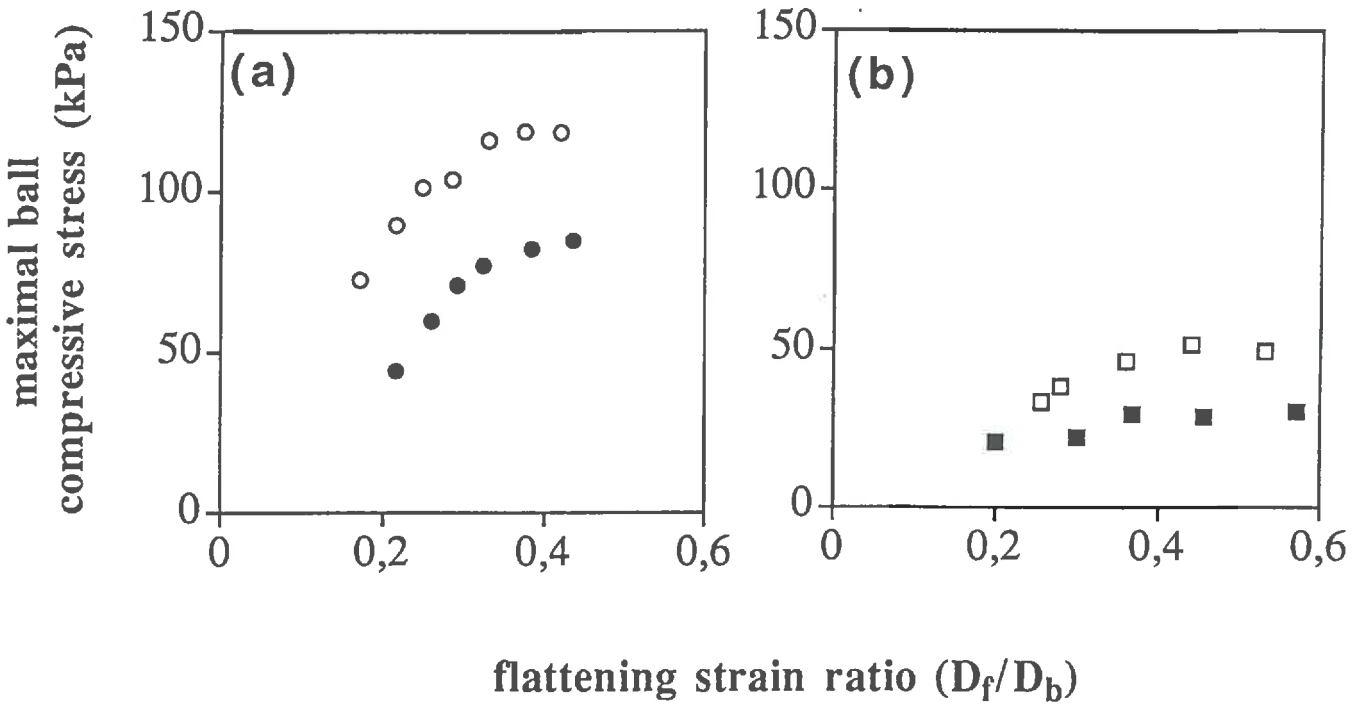

Figure I. 4. Relationships between the maximal axial compressive stress and the flattening strain ratio for two adherent clayey remoulded topsoil balls, either Foggathorpe (a) or Fladbury (b) remoulded topsoils, with 59 % or 72 % clay, respectively. Open and filled circles correspond to wet and very wet samples, respectively, which were characterized by water contents of 29.9 % and 33.7 % for the Foggathorpe remoulded topsoil, and of 57.3 % and 63.5 % for the Fladbury one.

The first result confirms the fact that compressibility increases as a function of clay content and the proportion of smectites and interstratified illite-smectites. It is mainly attributed to an increase of clay swelling leading to an increase of both plasticity and creep rate (e. g. Tripodi *et al.*, 1992; Mitchell, 1993). In this study, increase of both clay content and proportion of smectites within the clay fraction and, conversely, of both the plasticity index and the soil activity value, has been reported above from the Foggathorpe topsoil to the Fladbury one. Similarly, the second result confirms that the wetter is a clayey soil, the more plastic it is and, conversely, the more compressible and the less consolidated it is (Mitchell, 1993).

- Stress:strain relationships for two adherent granular remoulded topsoil balls

Each studied granular remoulded topsoil has been characterized by an important variability of their stress:strain replicate graphs (figs 5a and 5b). It could be attributed to the artisanal way of hand-rolling the replicates and also, to different types of stress:strain behaviours.

The first one was common to the two studied granular remoulded topsoils and was characterized by a rapid increase of the stress leading to non-linear concave stress:strain relationships with the exception of one linear stress:strain relationship obtained with the silty topsoil (open symbols of figures 5a and 5b). Similar non-linear concave either void ratio change:strain or stress:strain relationships have been previously reported by Mitchell (1993) for granular soils when subjected to cyclic loads.

The second type of failure stress:strain behaviour is the brittle one (Mitchell, 1993) which occurred for two sets of experiments carried out on the Bordeaux remoulded topsoil balls (filled symbols of fig. 5a). The stress rises rapidly to a peak value, with increasing deformation, where-upon failure occurs and the stress level drops substantially to a residual value. Conversely, we have reported within the Atterberg limits section that it was impossible to measure the plastic limit of this sandy topsoil (table 1).

An intermediary stress:strain relation between the two first type of failure is obtained with the sandy topsoil (dotted symbols of fig. 5a).

A third type of stress:strain relation is shown on figure 5b (filled symbols) with a very low increase of the axial compressive stress followed by a rapid increase thereafter. It could be attributed to a metastable fabric as previously suggested by Mitchell (1993). In this study, residual micro-aggregates would still have existed within some remoulded silty topsoil balls. Micro-aggregates are separated by larger pores than those occurring between quartz grains and their clay coatings (Gomendy, 1996; Bartoli *et al.*, 1998). Disruption of these micro-aggregates when subjected to the cyclic loads should lead to a reduction of the effective axial compressive stress because of the tendency for the volume to decrease, and the strength is less.

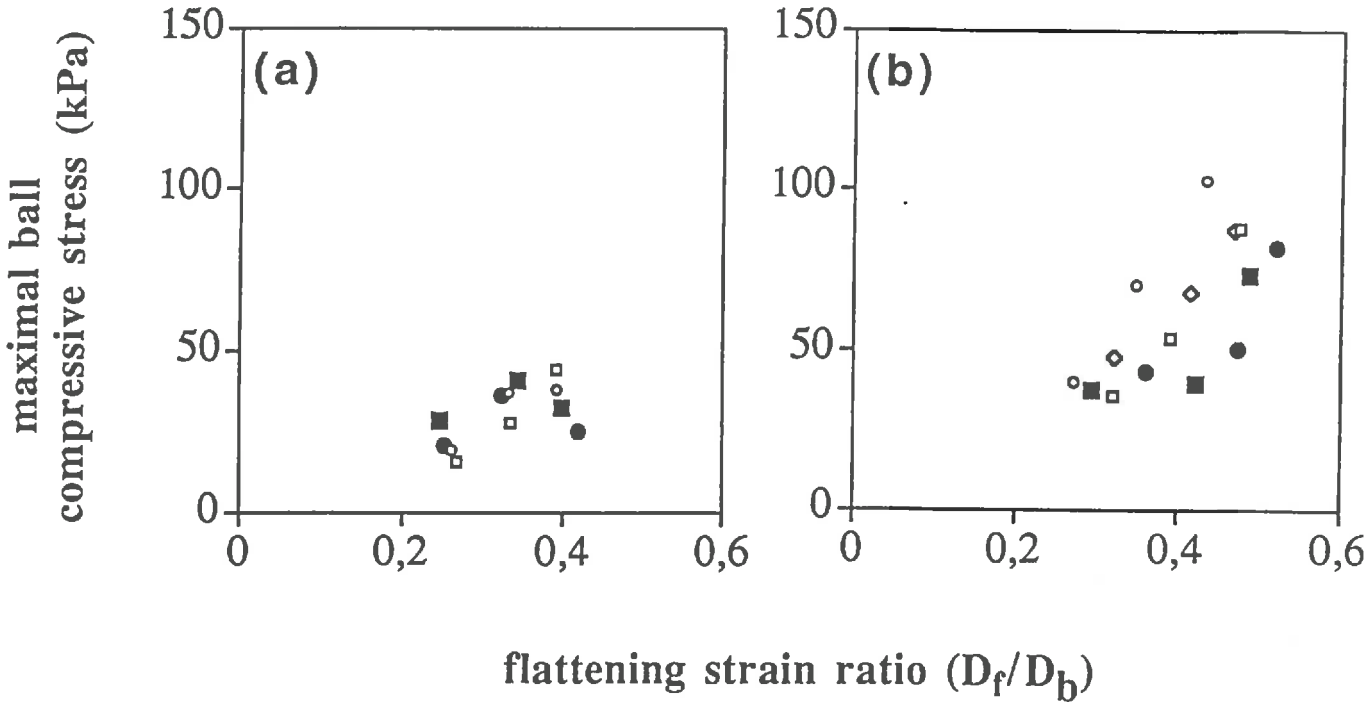

Figure I. 5. Relationships between the maximal axial compressive stress and the flattening strain ratio for two adherent granular remoulded topsoil balls which were prepared at a soil water suction value of 10 kPa, either Bordeaux (1.9 % clay) (a) or Orgeval (16.4 % clay) (b) topsoils. Each symbol corrresponds to an experimental set. Filled symbols correspond to two sets of experiments which characterize either a brittle behavior (a) or a special stress:strain behaviors which could be attributed to a metastable fabric (b).

When granular soils are compressed, quartz grains are repositioned into more efficient packings leading to a diminution of both the diameter of water-filled pore diameter and the porosity, and, conversely, to an increase of both the water suction and the soil strength (e. g. Mitchell, 1993; Horn *et al.*, 1994). Let us now first consider the possible effect of this type of increase of apparent cohesion for the two adherent granular remoulded topsoil balls because we have better geometrical information on them than on their clayey remoulded topsoil ball counterparts. Assuming a random compact array of equal spheres, the pore diameter:particle diameter ratio could be of 0.284 which leads to mean pore diameter of 4.3 µm and of 43 µm for the silty and the sandy remoulded topsoil balls, respectively, characterized by mean particle diameter of 30 µm and of 300 µm, respectively. The use of the Washburn equation (1921), where the pore is

considered to be cylindrical (parallel capillary tubes) (e. g. *in* van Brackel, 1975; Bruce & Luxmoore, 1986), further leads to mean capillary pressure values of 35 kPa and of 3.5 kPa for the silty and the sandy remoulded topsoil balls, respectively. We may now assume that the structural rearrangment of the particles into more efficient packings could occur from a random compact array of equal spheres to a much more compact regular close-packed hexagonal or face-centred cubic array of the same equal spheres which could tend to be regularly aligned for producing macroscopic flattened surface areas. The mean water-filled pore diameter:mean particle diameter ratio was also computed from the experimental results of Panayiotopoulos & Mullins (1985) on packing of sands. This ratio varies from 0.13 to 0.22, with an average value of 0.179 which is rather similar to the theoretical pore diameter:particle diameter ratio of 0.155 for compact close-packed hexagonal or face-centred cubic array of equal spheres (porosity value of 0.26 cm^3. cm^{-3}) which is assumed here to be the final particles rearrangement occuring near the flattening strain area. The mean final pore diameter should be then of 2.3 µm and of 23 µm, and their capillary pressure value counterparts of 65 kPa and of 6.5 kPa for the silty and the sandy remoulded topsoil balls, respectively. The increase of the capillary pressure, and therefore of possible part of the compressive stress value, should be then of 30 kPa and of 3 kPa for the silty and the sandy remoulded topsoil balls, respectively.

Such theoretical differences in increase of capillary pressure could partly explain the fact that, for the same flattening strain ratio, the axial compressive stress was often larger for the two adherent silty remoulded topsoil balls than for their sandy topsoil counterparts (fig. 5b). But the observed increase of maximal compressive stress (up to 80 kPa or 40 kPa for the silty or the sandy remoulded topsoil balls, respectively: fig. 5) was much more important than this theoretical increase of capillary pressure (30 kPa and of 3 kPa for the silty and the sandy remoulded topsoil balls, respectively). This discrepency increased as a function of the particle diameter and could be attributed to strong resistances due to interlocking rough surfaces of compact particles and to possible grain abrasion (e. g. Panayiotopoulos & Mullins, 1985; Mitchell, 1993).

*** Modelling of the stress:strain relationship for two adherent remoulded topsoil balls**

- Mathematical modelling of the stress:strain relationship for two adherent remoulded topsoil balls

A common power law curve fitting approach for both granular and plastic remoulded topsoils has been succesfully used (figs 6 and 7; table 2). It is shown clearly that the power law coefficients b of the relations between the maximal stress and the flattening strain ratio characterize the convexity ($b < 1$) or the concavity ($b > 1$) of the non-linear stress:strain curves of either the clayey plastic remoulded topsoils or the granular remoulded topsoils, respectively (fig. 6; table 2). The stress:strain relationship was linear for the plasticine with a power law coefficient of 0.977 (fig. 6a; table 2). Conversely, the constant A of the power law equation $y = Ax^b$, which corresponds to the axial compressive stress at the flattening strain ratio of 1, increased as a function of this power law coefficient b (table 2).

In summary, three types of mechanical behaviours have been characterized using the power-law fitting approach as a common modelling framework: plastic (power law coefficient b of 0.4), intermediate but always plastic (power law coefficient b of 0.9 to 1), and granular (power law coefficient b of 1.6) for the Fladbury clayey remoulded topsoil (72 % clay), the Foggathorpe clayey remoulded topsoil (59 % clay) and the plasticine, and the two granular remoulded toposoils (1.9 and 16.4 % clay), respectively (table 2). These three types of mathematical models may correspond to the sliding regime (shear residual angle of friction of less than 10°), the transitional regime (residual angle of friction of 10° to 25°) and the rolling shear regime (residual angle of friction of 25° to 30°), respectively, which have been previously described and reviewed by Mitchell (1993) for clayey soils (more than 55 % clay), intermediate soils (25 to 55 % clay) and granular soils (less than 25 % clay), respectively.

On the other hand, all the relations between the minimal axial compressive stress for two adherent balls and the flattening strain ratio were characterized by very concave power law curves (power law coefficient $b > 2$: table 2) and, conversely, by very low minimal stress values for flattening strain ratios less than 0.4 (fig. 7). These results confirm that the strain was mainly a surface deformation in axial mechanics of two adherent soil balls, at least for Rf values less than 0.4.

The minimal and maximal axial compressive stress can be expressed as:

$$\sigma_{b\text{-}max} = A \cdot R_f^{\,bmax} \qquad (9)$$

$$\sigma_{b\text{-}min} = A \cdot R_f^{\,bmin} \qquad (10)$$

With the equation (3) the maximal and minimal relation can be expressed now as:

$$\sigma_{b\text{-}min}/\sigma_{b\text{-}max} = R_f^{\,2} = R_f^{\,bmin - bmax}$$

and so, the relation between the two power low coefficients is (table 2):

$$bmin - bmax = 2$$

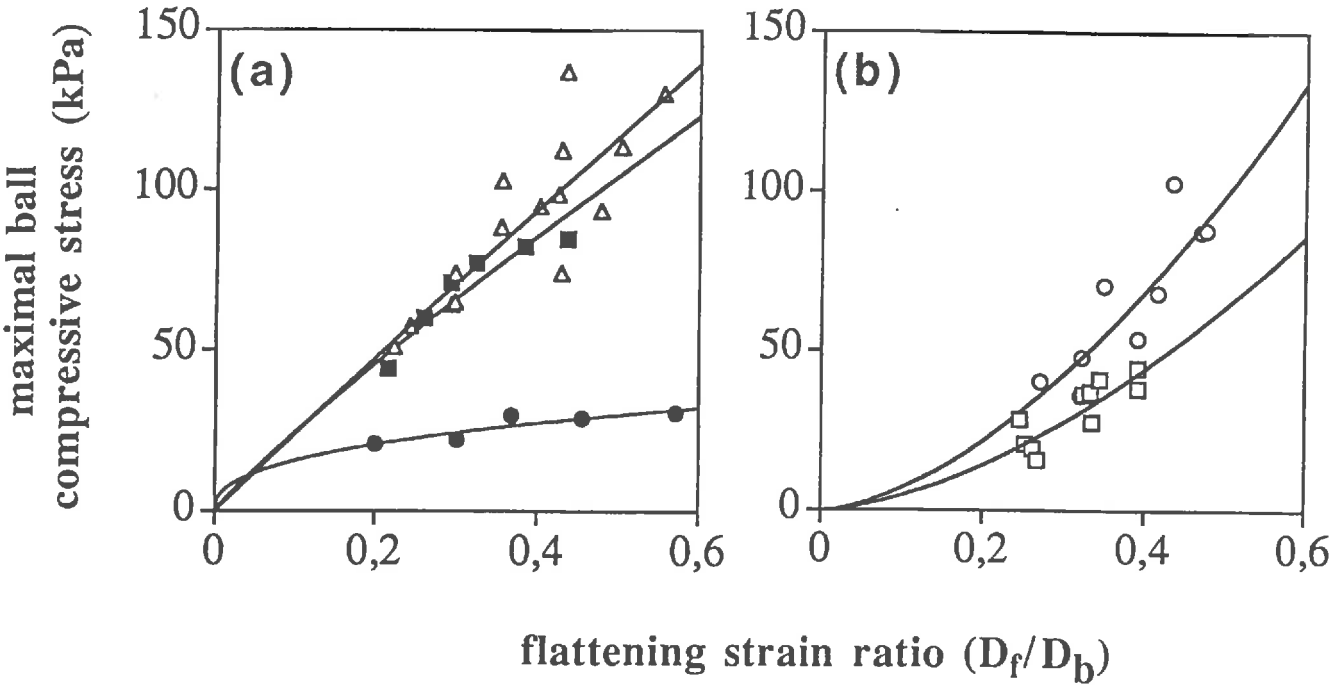

Figure I. 6. Mathematical modelling of the relations between the maximal axial compressive stress (y) and the flattening strain ratio (x) for two adherent remoulded topsoil balls: (i) plasticine (open triangles), Foggathorpe (filled squares) or Fladbury (filled circles) clayey remoulded topsoils which were prepared at 33.7 % and 63.5 % water content, respectively (figure 6a) and (ii) Bordeaux (open squares) or Orgeval (open circles) granular remoulded topsoils which were both prepared at a suction value of 10 kPa (figure 6b). The corresponding power-law equations are reported on table 2.

Soil sample	Behaviour	Maximal stress				Minimal stress			
		b max	A	r	P	b min	A	r	P
Fladbury at 63,5 % water content	Plastic	0.40	39.2	0.907	< 0.05	2.40	39.2	0.997	< 0.001
Plasticine	Intermediate but always plastic	0.98	229.5	0.876	< 0.001				
Foggathorpe at 37,7 % water content		0.90	194.9	0.940	< 0.01	2.90	194.9	0.994	< 0.001
Orgeval at 10 kPa	Granular	1.65	312.8	0.862	< 0.01	3.65	312.8	0.966	< 0.001
Bordeaux at 10 kPa		1.64	198.6	0.808	< 0.01	3.63	198.6	0.950	< 0.001

Table I. 2. Mathematical modelling of the stress:strain relationships for two adherent remoulded topsoil balls. Statistics (correlation coefficient r and probability P) and parameters b and A of the fitting power law equations $y = Ax^b$, where y is the either maximal or minimal axial compressive stress and x is the flattening strain ratio.

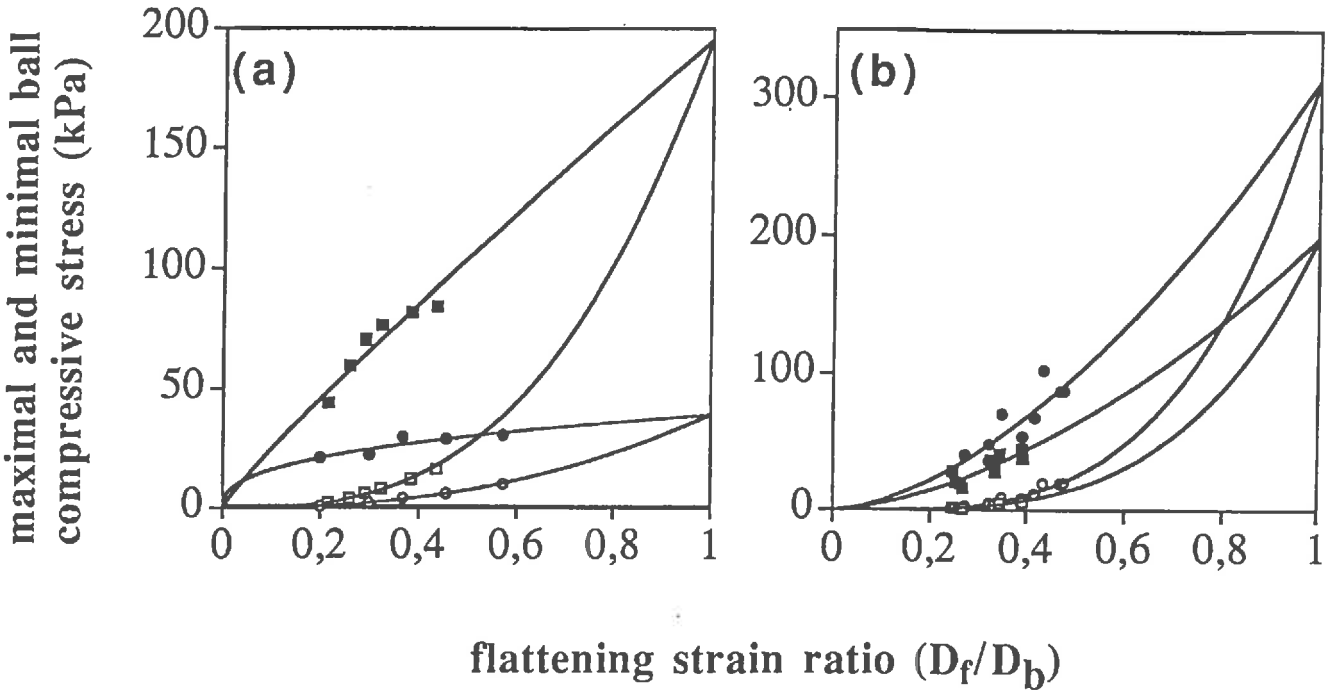

Figure I. 7. Mathematical modelling of the relations between the maximal (filled symbols) or the minimal (open symbols) axial compressive stress and the flattening strain ratio for two adherent remoulded topsoil balls: (i) Foggathorpe or Fladburry clayey remoulded topsoils which were prepared at 33.7 % and 63.5 % water content, respectively (figure 7a) and (ii) Bordeaux (open squares) or Orgeval (open circles) granular remoulded topsoils which were both prepared at a suction value of 10 kPa (figure 7b). The corresponding power-law equations were reported on table 2. The filled and the open symbols correspond to the maximal and to the minimal axial compressive stress, respectively.

- Effect of soil water suction on the stress:strain relationship for two adherent granular remoulded topsoil balls

The minimal axial compressive stress corresponding to the flattening test for two adherent remoulded topsoil balls increased as a function of the initial water suction value and the increase was much more pronounced for the silty topsoil than for the sandy one (fig. 8a). Conversely, the axial compressive stress corresponding to the unconfined compressive test for remoulded topsoil cylinders also increased as a function of the initial soil water suction value, also with lower stress values for the sandy topsoil than for the silty one (fig. 8b). Similar relationships between the shear strength and either the soil water suction or the water content have been previously reported by Spoor & Godwin (1979), Davies (1985), Young & Mullins (1991) and Watts & Dexter (1993). Drying tends to pull the particles together, thus functioning as a cohesive force. So, for a similar flattening ratio, the stress necessary to compress the two remoulded soil balls is higher for the drier samples than the wetter ones, as required by equation (8).

Although only two sets of experiments have been carried out for soil water suction values lower than 10 kPa, in both remoulded topsoil adherent balls and cylinders mechanical tests, the relation between the stress and the suction could at first be linear up to a soil water suction of 10 kPa (saturated remoulded topsoils) as required within a short matric water potential domain by equation (8). We could so use the intercepts of the straight stress:suction lines with the stress axis in order to know the value of the external axial compressive stress which was necessary to apply either on the diameter areas of adherent remoulded topsoil balls for producing a flattening dimensionless strain of 0.47 or on similar diameter area values of remoulded topsoil cylinders for producing a volumetric dimensionless strain of 0.2. This applied stress value was of 2.2 kPa and of 1.2 kPa, for the silty and the sandy remoulded topsoil, respectively, using the flattening test (fig. 8a) and of 12.6 kPa and 9 kPa, for the silty and the sandy remoulded topsoil, respectively, using the unconfined compressive test (fig. 8b).

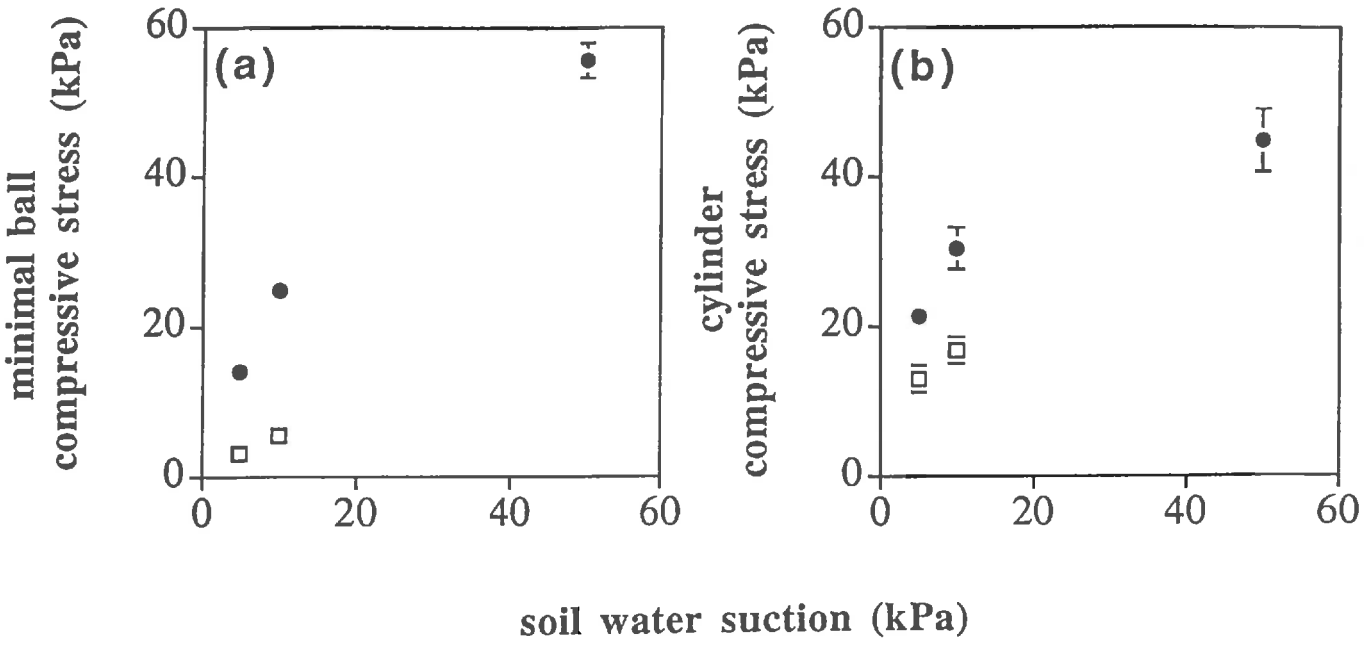

Figure I. 8. Effects of the suction value on either the minimal axial compressive stress at a flattening strain ratio of 0.47 for two adherent granular remoulded topsoil balls (a) or the axial compressive stress at an axial strain ratio of 0.2 for their cylinder counterparts (b). Open squares and filled circles correspond to the Bordeaux (1.9 % clay) or to the Orgeval (16.4 % clay) remoulded topsoils.

Firstly, it leads to the fact that the value of the applied axial compressive stress was 5.7 to 7.5 times greater on the remoulded topsoil cylinders than on their adherent ball counterparts, confirming that volumetric deformation is very low, quite negligible, for the balls after the flattening test whereas it is rather important (20 % of the initial cylinder volume) for the cylinders after the unconfined compressive test.

Secondly, the ratio between the calculated applied stress for the silty remoulded topsoil and that for its sandy remoulded topsoil counterpart was of 1.8 and 1.4 for the flattening test and the unconfined compressive test, respectively, confirming that the soil strength characteristic varies with soil type (e. g. Davies, 1985; Young & Mullins, 1991 and Watts & Dexter, 1993). This internal soil strength could be mainly attributed to resistances due to interlocking of the rough surfaces of compact particles and to possible grain abrasion (e. g. Panayiotopoulos & Mullins, 1985; Mitchell, 1993).

For the silty topsoil, and for both the flattening and the unconfined compressive tests, a decrease of the stress:suction slope value has been also observed from the 5 kPa to 10 kPa saturated domain to the 10 kPa to 50 kPa drained one (fig. 8). This observation could be attributed to the fact that the silty

remoulded topsoil was partly drained at a suction value of 50 kPa leading to a value of the χ coefficient (equation (8)) less than 1 whereas this χ coefficient value could be equal to 1 (equation (7)) for the near-saturated topsoil which was prepared at soil water suction values of 5 kPa and of 10 kPa. For the silty remoulded topsoil, the suction had also a stronger effect on the stress for the flattening test than for the uncompressive test. This could be attributed to the fact that stronger structural rearrangment of the particles into more efficient packings could have locally occured for producing flattening surface areas than those occurring during the 20% volume reduction of the soil cylinder.

Finally, the relation between the minimal axial compressive stress for two adherent remoulded topsoil balls at a flattening strain ratio of 0.47 increased non-linearly as a function of the axial compressive stress for its cylinder counterpart at a volumetric axial ratio of 0.2 (fig. 9). The more dry and more cohesive is the soil, the less plastic is the soil that is to say more difficult is the geometrical macroscopic change from a spherical shape to a flattening surface area. The flattening test therefore appears to be a useful tool for characterizing soil plasticity within discontinuous porous media such as adherent tilled topsoil clods.

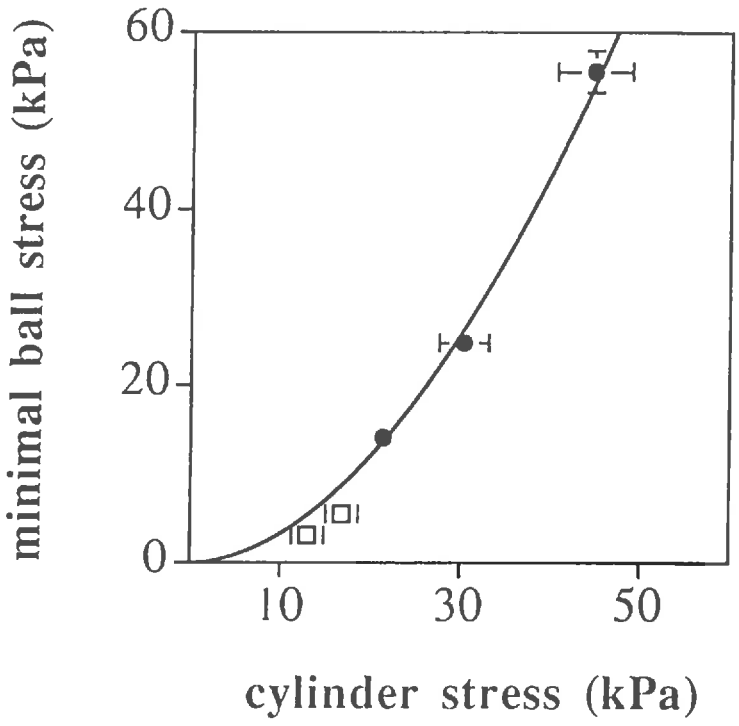

Figure I. 9. Relationship between the minimal axial compressive stress for two adherent granular remoulded topsoil balls and the axial compressive stress for their cylinder counterparts both at an axial strain ratio of 0.2. Open squares and filled circles correspond to the Bordeaux (1.9 % clay) or to the Orgeval (16.4 % clay) remoulded topsoils.

Conclusion

This study was aimed at improving our understanding of mechanics of tilled topsoils which are characterized by discontinuities between adherent soil clods. A device for simulating cyclic or progressive loading on adherent soil clods was designed using two adherent remoulded topsoil balls with similar diameters. The main results were:

1. A non-linear convex relationship between the axial maximal compression stress and the flattening strain ratio has been observed for the clayey remoulded topsoils and the results showed that the higher is the clay content and the wetter is the clayey soil, the more plastic it is.

2. In contrast, a non-linear concave stress:strain relationship, with failure or metastable fabric behaviour, occurred for the granular remoulded topsoils.

3. The compression stress:flattening strain curve was fitted with a power law equation, with either a <1 or >1 power law coefficient for either the convex stress:strain curve of the plastic clayey soils or the concave stress:strain curve of the friable granular soils, respectively.

4. The minimal axial compressive stress corresponding to the flattening test for two adherent remoulded topsoil balls increased as a function of the initial soil water suction value, as required by the concept of effective stress, and this increase was much more pronounced for the silty topsoil than for the sandy one.

5. The relation between the minimal axial compressive stress for two adherent remoulded topsoil balls at a flattening strain ratio of 0.47 increased non-linearly as a function of the axial compressive stress for its cylinder counterpart at a volumetric axial ratio of 0.2. The drier and the more cohesive is the soil, the more difficult is the geometrical macroscopic change from a spherical shape to a flattened surface area.

As a conclusion, the flattening test appears to be a useful tool for characterizing soil plasticity within in discontinuous porous media such as adherent tilled topsoil clods. It is also a promising tool for further studies on clod:clod adhesion in which two adherent soil balls are pulled apart.

Acknowledgements

Sonia Czarnes would like to thank the British Council for providing a Fellowship which enabled this work to be done at the Silsoe Research Institute. The authors would also like to thank Professor G. Spoor of Silsoe College of Cranfield University, England for his help with the Fladbury and Foggothorpe soils.

References

Attou, F. Etude expérimentale d'assemblages squelette-argile. Apport à la compréhension du comportement physique des sols. Université d'Orléans, thèse.

Bartoli, F., Bird, N., Gomendy, V. and Vivier, H., 1998. The relationship between silty soil structures and their mercury porosimetry curve counterparts. Fractals and percolation. *European Journal of Soil Science* (accepted with revisions).

Bartoli, F., Burtin, G., Royer, J.J., Gury, M., Gomendy V., Philippy, R., Leviandier, T. and R. Gaffrej R., 1995. Spatial variability of topsoil characteristics within one silty soil type. Effects on clay migration. *Geoderma*, **68**: 279-300.

Bruce, R.R. & Luxmoore, R.J., 1986. Water retention : field methods. *In : Methods of Soil Analysis. Part I. Physical and Mineralogical Methods.* Agronomy Monograph n°9 (2nd edition). American Society of Agronomy - Soil Science Society of America, Madison, pp. 663-686.

BS1377. 1975. *Methods of Test for Soils for Civil Engineering Purposes.* British Standards Institution, London.

Chrétien, J., 1986. Rôle du squelette dans l'organisation des sols. Université de Dijon, thèse d'état française.

Davies, P., 1985. Influence of organic matter content, moisture status and time after reworking on soil shear strength. *Journal of Soil Science*, **36**, 299-306.

Dexter, A.R., 1991. Amelioration of soil by natural processes. *Soil &Tillage Research*, **20**, 87-100.

Dexter A.R., Kroesbergen B. & Kuipers, H., 1984$_a$. Some mechanical properties of aggregates of top soils from the IJsselmeer polders. 1. Undisturbed soil aggregates. *Netherlands Journal of Agricultural Science*, **32**, 205-214.

Dexter A.R., Kroesbergen B. & Kuipers, H., 1984$_b$. Some mechanical properties of aggregates of top soils from the IJsselmeer polders. 2. Remoulded soil aggregates and the effects of wetting and drying cycles. *Netherlands Journal of Agricultural Science* **32**, 215-227.

Fiès, J.C. & Bruand, A., 1990. Textural porosity analysis of a silty clay soil using pore volum balance estimation, mercury porosimetry and quantified backscattered electron scanning image (BESI). *Geoderma* **47**, 209-219.

Finney, J.L. 1970. Random packings and the structure of simple liquids: 1. The geometry of random close packing. *Proceedings of the Royal Society*, **A319**, 479-493.

Furness, R. R. & King, S. J., 1978 Soils in North Yorkshire IV. *Soil Survey Record n° 56. Harpenden.*

Gomendy, V., 1996. Variabilités spatiale et temporelle des propriétés structurales et hydriques des horizons de surface de la couverture limoneuse du bassin versant d'Orgeval (Brie). *Nancy University pHD thesis.*

Hartge, K. H., 1994. Soil structure, its development and its implications for properties and processes in soils - a synopsis based on recent research in Germany. *Z. Pflanzenernähr. Bodenk.* **157**, 159-164.

Horn, R., Taubner, H., Wuttke, M. & Baumgartl, T. 1994. Soil physical properties related to soil structure. *Soil & Tillage Research*, **30**, 187-216.

Klute, A., 1986. Water retention : laboratory methods. *In* Methods of Soil Analysis, part 1 : Physical and mineralogical methods. *Soil Science Society of America, Agronomy Monograph* n° **9**, pp.635-662

Mitchell, J.K., 1993. *Fundamentals of soil behavior, second edition*. John Wiley & Sons, New York.

Monnier, G., Stengel, P. & Fiès, J.C., 1973. Une méthode de mesure de la densité apparente de petits agglomérats terreux. Application à l'analyse des systèmes de porosité du sol. *Annales agronomiques*, **24**, 533-545.

Mullins, C.E. & Panayiotopoulos, K.P. 1984. The strength of unsaturated mixture of sand and kaolin and the concept of effective stress. *Journal of Soil Sciences*, **35**, 459-468.

Panayiotopoulos, K. P. & Mullins, C. E., 1985. Packing of sands. *Journal of Soil Science*, **36**, 129-139.

Reeve, M. J., 1978. Soils in Northamptonshire 1. *Soil Survey Record n° 54. Harpenden.*

Smith C W, Hadas A, Dan J and Koyumdjisky H 1985 Shrinkage and Atterberg limits in relation to other properties of principal soil types in Israel. Geoderma 35, 47-65.

Smith, W.O., Foote, P.D. & Busang, P.F. 1929. Packing of homogeneous spheres. *Physical Review*, **34**, 1271-1274.

Sowers, G.F. 1965. Consistency. In: *Methods of Soil Analysis* (eds. C.A. Black, D.D. Evans, J.L. White, L.E. Ensminger & F.E. Clark) Agronomy **9**, pp 391-399, American Society of Agronomy, Madison.

Spoor, G. & Godwin, R. J., 1979. Soil deformation and shear strength characteristics of some clay soils at different moisture contents. *Journal of Soil Science*, **30**, 493-498.

Tripodi, M. A., Puri, V. M. , Manbeck, H. B. & Messing G. L; 1992. Constitutive Models for cohesive particulate materials. *J. agric. Engng Res.*, **53**, 1-21.

van Brackel, J., 1975. Pore space models for transport phenomena in porous media. *Powder Technology*, **11**, 205-236.

Walter, C., Schvartz, C., Claudot, B., Bouedo, T. and Aurousseau, P., 1997. Synthèse nationale des analyses de terre réalisées entre 1990 et 1994. *Etude et Gestion des Sols*, **4**, 205-219.

Watts, C.W. & Dexter, A.R. 1993. A Hand-held Instrument for the In situ Measurement of soil shear strength in the puddled layer of paddy fields. J. agric. Engng Res., **54**, 329-337.

Young, I.M.& Mullins, C.E. 1991. Factors affecting the strength of undisturbed cores from soils with low structural stability. *Journal of Soil Science*, **42**, 205-217.

III.- Méthodes utilisées et objets d'étude

Le tableau I. 4. fait l'inventaire des méthodes utilisées, en fonction de nos objets d'étude, que l'on peut classer comme étant "multiagents" lorsqu'il s'agit des systèmes sol:plante, ou aussi "agent", lorsque seul, le sol, ou la plante, est étudié.

Nous avons ainsi classé ces méthodes en 5 rubriques: propriétés structurales, observations morphologiques et analyse d'image, propriétés hydriques, propriétés mécaniques, adhésion:l'approche rhéologique. Certaines de ces méthodes ont été plus utilisées au cours de certains chapitres, ce que nous avons également mentionné sur le tableau I. 4.

Toutes ces méthodes seront détaillées au cours de ces différents chapitres, constitués essentiellement de publications en préparation ou soumises.

	Sol			Plante	système sol:plante	sol adhérant (SA) ou non aux racines
		sol remanié				
	agrégats	cylindre	2 boules adhérentes			
propriétés structurales		porosité totale (densité apparente)				porosimétrie mercure
observations morphologiques et analyse d'images				racine sur boite de Pétri *ch III.*	- architecture du système racinaire après une série de cycles H et D - racine à la surface du sol *ch III.*	distribution spatiale du SA au cours de la cinétique d'agitation mécanique du système SA:racines ch II. 2.
propriétés hydriques	- rétention d'eau à l'équilibre P-H_2O *ce chapitre et ch II. 1.* - rétention d'eau après une série de cycles H et D *ch II. 1.*				rétention d'eau in situ après une série de cycles H et D (micro-tensiométres et irriguations à l'aide de perfuseurs médicaux) *ch II. 1.*	teneur en eau après une série de cycles H et D *ch II. 2.*
propriétés mécaniques	résistance en traction et friabilité *ch II. 2*	résistance au cisaillement	résistance à la compression *ce chapitre*	Elasticité et courbure *ch III.*	agitation mécanique et sonication *ch II. 2.*	résistance en traction et friabilité *ch II. 2*
adhésion : approche rhéologique			energie de rupture *ch III.*		interface sol:racine: test de séparation (energie du rupture) et analyse vidéo. *ch III.*	

Tableau I. 4. *Méthodes utilisées et objets d'étude en fonction du type de sol (sableux, limoneux et argileux) et du potentiel hydrique. Cycles H et D = cycles d'humectation et de dessication*

CHAPITRE II

INTERACTIONS SOL:RACINES A L'ECHELLE DU SYSTEME RACINAIRE

Ce chapitre comprend une série de deux articles soumis à la revue Plant and Soil.

I. - Cycles contrôlés d'humectation - dessiccation dans la rhizosphère du maïs en chambre phytotronique : effet du type de sol et de l'intensité du séchage

Czarnes S. and Bartoli F. Wetting and drying cycles in the maïze rhizosphere under controlled conditions. I. Soil and daily minimum soil water suction effects

II. - Cycles contrôlés d'humectation - dessiccation dans la rhizosphère du maïs en chambre phytotronique : conséquences sur les propriétés mécaniques du sol adhérant aux racines

Czarnes S. Dexter A.R. and Bartoli F. Wetting and drying cycles in the maïze rhizosphere under controlled conditions. II. Mechanics of the root-adhering soil

INTERACTIONS SOL:RACINES A L'ECHELLE DU SYSTEME RACINAIRE

Présentation de l'étude des interactions sol : racines à l'échelle du système racinaire

Pour essayer de répondre à la question posée dans l'introduction, "quel est l'impact du type de sol et de sa teneur en eau sur l'état d'adhésion sol:racines?", une première étape de recherche a consisté à bien contrôler les conditions hydriques de la rhizosphère, et leurs dynamiques, pendant la période de culture du maïs.

Les variations spatiales de l'absorption de l'eau par les racines des plantes ont été relativement bien décrites et modélisées en fonction de l'architecture racinaire et de la distribution spatiale de l'eau dans le sol. Cela n'est pas le cas de la variabilité temporelle de l'absorption de l'eau par les racines, pourtant aussi essentielle. C'est la raison pour laquelle nous avons caractérisé, dans le cadre de la première publication, les cinétiques de séchage, plus ou moins marquées, et les cycles contrôlés d'humectation et de dessication se produisant dans la rhizosphère de maïs et dans le sol témoin de référence, sans plante. Pour cette étude, nous avons utilisé (1) des micro-tensiomètres pour suivre l'évolution du potentiel hydrique de la rhizosphère et de son sol témoin associé et (2) des perfuseurs médicaux afin d'irriguer ces sols de façon très progressive, au goutte à goutte, pendant la période nocturne de la chambre de culture, afin d'atteindre la valeur minimale journalière de potentiel hydrique que l'on s'est fixé.

L'effet du type de sol et de l'intensité du séchage (valeur minimale journalière de potentiel hydrique) sur les propriétés hydriques, et leurs dynamiques, a été étudié dans la rhizosphère de maïs, par référence au sol témoin, soumis aux mêmes conditions expérimentales.

Un des résultats essentiels de ce travail a été de révéler un effet rhizosphère marqué dans le cas du sol sableux, ce qui a été attribué à la fois à sa très faible capacité à alimenter la plante en eau et à un processus de compensation biologique qui a permis à la plante d'élaborer une architecture du système racinaire très favorable à l'absorption de l'eau par les racines. Une hypothèse

forte sur les vitesses de flux d'eau dans la rhizosphère sableuse de maïs a été évoquée afin d'expliquer le phénomène d'hystérésis observé entre la courbe de rétention d'eau de la rhizosphère et celle de son sol témoin, obtenues dans des conditions dynamiques analogues.

Le contrôle de ces cycles d'humectation - dessiccation a été aussi réalisé afin de mieux appréhender l'étude des interactions sol:racines à l'échelle du système racinaire et notamment, l'étude de l'impact de l'intensité du séchage et des cycles d'humectation - dessication sur les propriétés mécaniques des agrégats et des particules adhérants aux racines d'une jeune plantule de maïs agé de 11 jours. Ce stade de développement a été choisi car il correspond à la période d'exsudation racinaire maximale (Matsumoto *et al.*, 1979). Cette étude fait l'objet de la seconde publication.

Immédiatement après la récolte des plantules de maïs, de façon à éviter le séchage des échantillons, des cinétiques de rupture du sol adhérant au système racinaire ont été réalisées suivant deux méthodes indépendantes: agitation mécanique à l'air et ultrasonication ménagée dans de l'eau du système sol:racines. Des informations sur l'instabilité, ou inversement sur la stabilité, de ce sol adhérant aux racines ont ainsi pu être obtenues. Elles ont été reliées au type de sol ainsi qu'à ses propriétés hydriques, générées par des conditions dynamiques de drainage.

Des analyses d'image complémentaires nous ont permis de montrer que les agrégats adhérant à la zone apicale étaient très stables, ce qui est attribuable aux exsudats racinaires.

A l'échelle du système racinaire, la cohésion du sol adhérant aux racines est relativement difficile à interpréter car elle dépend à la fois de la force de cohésion à l'intérieur de chaque agrégat de sol adhérent (résistance intra-agrégat) et de la force de cohésion entre ces agrégats (résistance inter-agrégat). Ainsi, dans ce système, différentes forces, à différentes échelles, interagissent. De façon à mieux comprendre nos résultats, une étude complémentaire des propriétés mécaniques (résistance en traction, friabilité) du sol adhérant aux racines a été entreprise à l'échelle de l'agrégat, dans le cas du sol limoneux.

Les agrégats adhérant aux racines de la rhizosphère se sont avérés être plus stables que ceux du sol témoin, ce qui a été clairement relié à la quantité d'exsudats racinaires et microbiens les imprégnant, d'autant plus importante que le potentiel hydrique est élevé. Le rôle très probable des poils racinaires sur la stabilité de ces agrégats sera mis en évidence dans le chapitre III.

Wetting and drying cycles in the maize rhizosphere under controlled conditions. I. Soil and daily minimum soil water suction effects

S. CZARNES and F. BARTOLI[*]

Centre de Pédologie Biologique UPR 6831 du CNRS associé à l'Université Henri Poincaré - Nancy I, BP 5, 54501 Vandoeuvre-les-Nancy, France

Key words: culture chamber, maize rhizosphere, soil texture, soil drying, soil water suction, wetting and drying cycles

[*] Corresponding author. Present address: Centre de Pedologie Biologique UPR 6831 du CNRS associé à l'Université Henri Poincaré - Nancy I, BP 5, 54501 Vandoeuvre-lès-Nancy, France

Tel: (33) 3 83 51 08 60 Fax: (33) 3 83 57 65 23 e-mail: bartoli@cpb.cnrs-nancy.fr

Abstract

Water cycle in the soil:plant:air system leads to specific hydraulic properties of the rhizosphere, e. g., soil water potential, and its dynamics, and soil water retention. Although these soil hydraulic properties are crucial for the plant, particularly under hydric stress, few information is available on the effects of environmental factors such as soil type and initial soil water potential on these soil properties.

In this study, our objectives were (i) to measure soil water potential using a micro-tensiometer in two contrasting soils with and without maize (*Zea maiys* L.) roots, during nighttime irrigation and daytime drying controlled cycles, with four daily minium soil water potential values, and (ii) to compare, at the end of the maize culture, the soil water retention curves of the rhizosphere and of the control soil for both soils.

A clear plant effect on both the preliminary soil drying and the wetting and drying controlled cycles was found for the sandy topsoil whereas it was moderate for the silty topsoil. The rhizosphere silty soil dried much more than its control countrepart but the soil water retention curves of the rhizosphere silty soil and of the control silty soil were similar. In contrast, a a soil water hysteresis effect was observed between the soil water retention curves of the rhizosphere sandy topsoil and of the control sandy topsoil. This hysteresis effect could be attributed to significant slower water flow speed in the control sandy soil as compared with the rhizosphere sandy soil.

In conclusion, recording and analysing experimental soil water retention data in the rhizosphere and in its control soil counterpart appears to be important for a better knowledge of the water cycle in the in the soil:plant:air system.

Introduction

In the rhizosphere, water transport has been described using the soil:plant:air continuum theory (Philip, 1966) which is based on an electrical analogue. Water moves along water potential gradients through a series of resistances connected with capacitances that simulate water storages (Huck, 1984).

Since the classical analysis by Gardner (1960) of the radial water transport from soil to roots, severals studies have identified different water resistances as functions of root environmental conditions. A simple hydraulic resistance in the root coupled to a viscous flow in the soil was proposed by Reicosky and Ritchie (1976) and Passioura (1980). Usually, a large soil:root interfacial resistance was attributed to a poor soil:root contact (Herkelrath et *al.*, 1977; Faiz and Weatheley, 1978; Bristow et *al.*, 1984; Veen *et al.*, 1992; Stirzaker and Passioura, 1996). It could explain why the sum of the resistances in the plant and the soil was often too small to account for the fall in water pressure between the leaf xylem and the soil, especially when plants were growing in sandy soils, which were prone to dry rapidly. The relative importance of all these resistances may vary as a function of soil texture, structure and hydraulic conditions.

The transpiration flow, which is continuously balanced by the flow from root water uptake and from water storage, is at a maximum during daytime and at a minimum during the night, leading to regular duirnal cycles of leaf water potential. During daytime, transpiration often exceeds water uptake causing negative storage flow and tissue dehydratation; the reverse often occurs during nighttime (Huck, 1984; Lafolie *et al.*, 1991; Jensen *et al.*, 1993). Herkelrath *et al.* (1977) have showed that, as a soil dried, (i) both the daytime minimum and the nighttime maximum leaf water potential fell linearly with time, with a roughly constant difference between successive maxima and minima and (ii) the decrease in potential during the drying cycle was lower for the leaf than for the soil.

The topic is complex and it is not straightforward to measure and to marry water potential of the soil, of the roots, of the leaves and of the atmosphere. Here we only measure soil matric potential using a micro-tensiometer in two contrasting soils with and without maize roots, during nighttime irrigation and daytime drying cycles. We also measure soil water content at the end of the experiments. Our aims are modest but nevertheless an important first step in recording and analysing experimental data. This is interesting by itself, because

no one, in our knowledge, has presented such microscale information for maize submitted to daily irrigation and drying cycles.

This study was also designed to give some useful information on the biological and physical interactions occurring in the maize rhizosphere. In this study, maize plants 11 day-old were chosen because that time corresponds to an optimal maximum for maize root exudation (Matsumoto *et al.*, 1979). We so tried to indirectly measure exudation from the roots and to study its effects, combined to the effects of soil drying in the rhizosphère, on the root-adhering soil strength (second part of this series of papers). In this paper, our main objective was to study the effects of soil type and daily minimum soil water potential on controlled wetting and drying cycles occurring in the maize rhizosphere and its control soil counterpart.

Materials and methods

Soils

Selected properties of the two topsoil samples are listed in Table 1. The first studied soil was a sandy podzolic soil (Podsols, FAO) developed in Miocene and Quaternary marine and alluvial sandy materials. It was located near Bordeaux, in the Landes area, South-Western France and had been under pine forest for one century and under maize for 4 years. The topsoil was kindly supplied by D. Plenet, INRA Bordeaux. The second studied soil was a silty leached brown soil (Luvisols, FAO) developed in the Quaternary silty materials of the Parisian Basin. It was located 80 km east of Paris, in the Orgeval catchment and had been under intensive wheat agriculture for the past 40 years. Each topsoil sample was air-dried and sieved to < 4 mm.

	Particle-size distribution (%)					BET			
Topsoil samples	coarse sand >200 µm	fine sand 50-200 µm	coarse silt 20-50 µm	fine silt 2-20 µm	clay < 2 µm	Specific surface area (m2/g)	pH H_2O	0.5 M NH_4Cl CEC (mg/100g)	Organic carbon content (%)
Sandy	85.7	8.1	0.9	3.6	1.9	0.3	5.6	6.8	1.7
Silty	1.3	2.7	44.6	29.8	16.4	13.6	6.8	20.5	0.8

Table 1: Main soil characteristics.

Organo-mineral clay fractions were poor in organic carbon (OC) for the long-term cultivated silty topsoil, with OC value of 3.5 % whereas they were rich for the short-term cultivated sandy topsoil, with an OC value of 27.6 %. Conversely, organic matter of the clay fraction was rich in both nitrogen and oxygenated functional groups for the silty topsoil whereas it was polyaromatic and rich in aliphatic functional groups for the sandy one (C/N ratio and IR spectroscopy data, not shown). Details on the two studied topsoils have been reported elsewhere (Czarnes *et al.*, 1998).

Soil water retention by drainage

Soil air-dried aggregates were gently packed into 5.6 cm^3 PVC cylinders of 2.7 cm internal diameter. Then, the soil-filled cylinders were water-saturated by capillarity within a closed volume at room temperature for 48 hours and desaturated at a constant soil water suction thereafter, using the classical Richards membrane method (Klute, 1986). Water can only drained from the packed aggregates to the outside by the top and the bottom of the soil-filled cylinders. Five replicates of gravimetric water content by soil water suction value (10, 20, 40, 50 and 60 kPa) were carried out and the time for pressure:drainage equilibrium varied from 3 to 5 days.

Cylinders of soil aggregates: preparation and characteristics

Each air-dried and sieved to < 4 mm topsoil sample was divided into 8 equivalent sub-samples of 250 to 300 g using a Fritsch laborette 27 rotary divider linked to a Fritsch laborette 24 sampling vibratory feeder. Then, 230 g (silty topsoil) or 270 g (sandy topsoil) of each of these sub-samples was gently packed into an horticultural PVC pot of 4 cm internal diameter and 20 cm height. Each pot was cylindrical in the top 15 cm and partly conical in the bottom 5 cm, with a progressive decrease of the cylinder diameter from 4 to 2 cm. The mean porosity value was of 0.58 $cm^3\ cm^{-3}$ for the silty topsoil whereas it was 0.50 $cm^3\ cm^{-3}$ for the sandy topsoil, measuring the soil-filled volume of the pot with water and assuming particle density value of 2.65 $cm^3\ cm^{-3}$. Then, each soil sample was progressively wetted by capillarity, to near saturation.

A preliminary study of the macro-structure of the silty soil in the pots (Czarnes, 1994) showed that (i) soil structural units were of 4 to 20 mm size,

(ii) the macro:total porosity ratio was of nearly 70 %, (iii) no statistical difference of macro-porosity as a function of the pot depth was observed.

Factorial design

A 2 * 2 * 4 factorial design with three replications was used. The factors were: soil type (the silty and the sandy topsoil packed aggregates), soil with or without maize culture (non-planted control) and four soil water suction values (10, 20, 40 and 50 kPa) which were obtained by drying the nearly water-saturated soils in the culture chamber. For each topsoil and each water suction value we therefore used six pots filled with nearly water-saturated packed soil aggregates, with one half for plant culture and the other half for control (three replicates by treatment). Both control and maize soil-filled pots were separately transferred into the culture chamber some hours after soil water saturation and sowing of maize.

Maize seedlings: growth, selection and sowing

The maize seeds which were used for this study belong to the *Zea mays L.* cultivar DEA. They were submitted to an antifungal treatment by Pioneer France Maïs, Toulouse, France, which kindly supplied us with the seeds. Batches of seeds were germinated on filter papers in Petri dishes for about three days. The selected seedlings were characterized by similar radicle features. They were flat and straight, their weights were close to 0.40 g and their lengths were in the range 14 to 20 mm. Then, on one side of each soil-filled pot, each 3 day-old seedling was sown 1 cm below the surface of the nearly water-saturated soil.

Culture chamber conditions and soil water characteristics

The control and maize soil-filled pots, with nearly water-saturated packed soil aggregates, were separately transferred to a constant environment growth chamber with temperature controlled at 24 °C ± 1 °C for the daytime period and 20 °C ± 1 °C for the nighttime period, humidity 60 % ± 10 % and lighting photon intensity 37 to 54 µmol m^{-2} s^{-1}, as a function of the position inside the growth

chamber. The fluorescent lights were switched on for 17 hours and off for 7 hours each day.

A view of the growth chamber shows our device with one micro-tensiometer in the surface centre of each soil-filled pot, one maize plant on the one side and one solution administration set (perfupack) on the opposite side (Figs. 1 and 2). It is important to note that the micro-tensiometer ceramic was located in the middle of the soil volume which may correspond to the maximum maize root water uptake as a function of the maize growth (Fig. 2) (Doussan *et al.*, 1998; Doussan and Pagès, 1998).

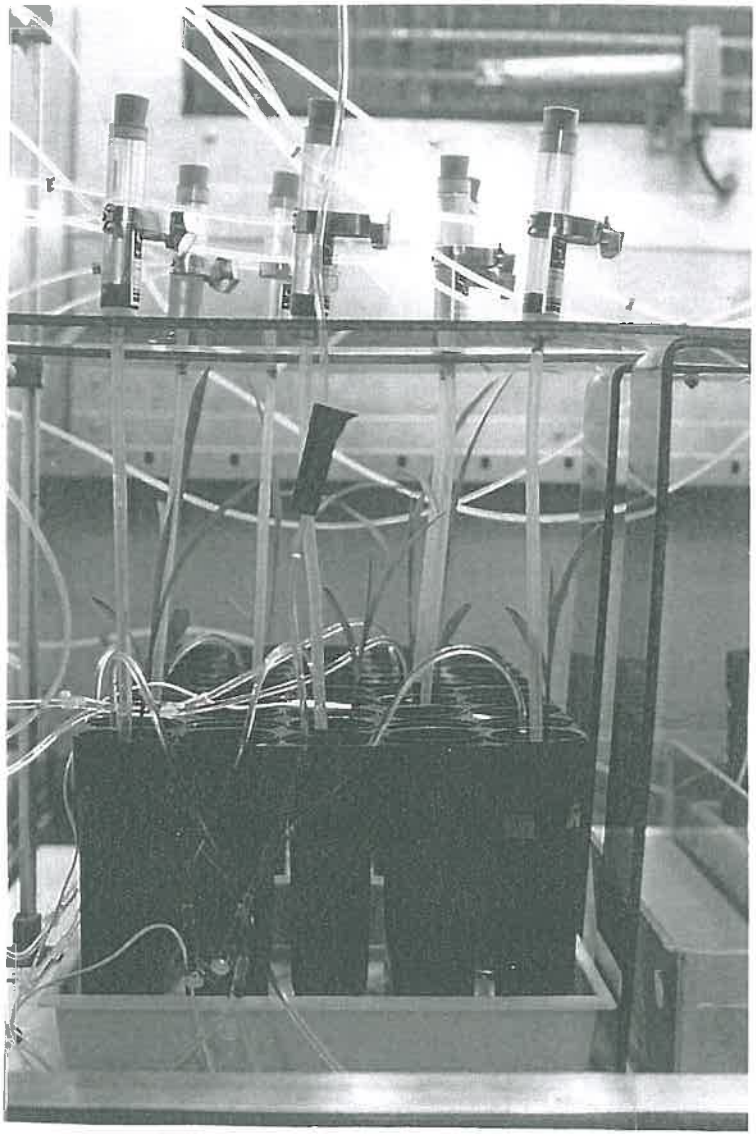

Figure II. 1. *General overview of the growth chamber with the micro-tensiometers.*

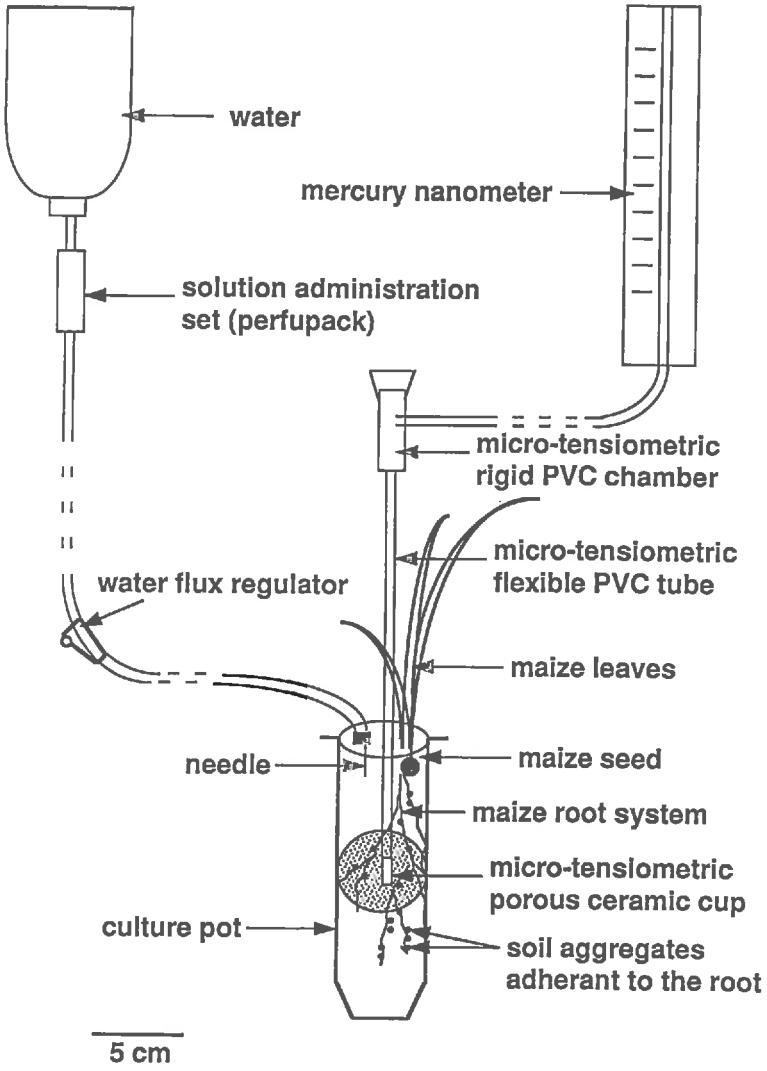

Figure II. 2. Schematic representation of a maize soil-filled pot with (i) one micro-tensiometer in the centre for soil water suction measurments and (ii) one solution administrative set for drop by drop irigation during the daytime period.

In this study, 12 STM 2030S micro-tensiometers, made by SDEC, 19 rue Edouard Vaillant, 37 000 Tours, France, were used for measurments of soil water suction within the 0 to 70 kPa range. Each micro-tensiometer had a micro-porous ceramic cup of 7.5 mm diameter and 30 mm length. The effective outside cup surface area was of 4.8 cm^2. The ceramic cup was connected with a flexible PVC tube linked to a rigid PVC chamber of 21.5 mm diameter which is, in its turn, linked to a capillary flexible tube connected, in its final length, to a mercury manometer used to read the mercury heigth values. The ceramic was previously saturated with distilled degased water for 24 hours.

In the centre of each soil surface, we dug a hole of 6 mm diameter and 90 mm length with a metallic cylinder (Fig. 2). A sample of nearly liquid mud soil was introduced in the hole, where the micro-tensiometer was placed immediately thereafter, leading to good water contact between the micro-tensiometer ceramic and the soil. A certain quantity of the mud soil also came to the soil surface. Then, the flexible tensiometric tube was filled with degased distilled water. Air bubbles inside the flexible tensiometric and capillary tubes were removed using a vacuum pump. The last air bubbles which occurred within the flexible capillary tubes were removed by successive pressures on degased distilled water obtained by opening and closing the rigid PVC chamber with its latex cap.

During a period of 7 to 8 days after planting, each nearly water-saturated soil, with or without maize, was dried under the day-night cyclic conditions of the culture chamber until the selected soil water suction value was reached. However, for the nearly water-saturated sandy topsoil without maize which was very difficult to dry, the time was 11 to 13 days. From that time, daily progressive irrigation was carried out manually during the plant nighttime period (daytime for the person standing by the cylinders) by adding distilled water drop by drop, with a rate of one drop of 0.018 ml micro-volume by seconde, with a solution administration set (perfupack) until the selected daily minimal soil water suction was again nearly reached (Fig. 2). The extremity of the solution administration set (the needle) was placed into a tube which was inserted three centimeter depth into the top of the soil at the beginning of the experiment (Fig. 2). The length of the tube was a little bit longer than the needle one, to prevent blocking of the needle by the soil. At the end of the plant nighttime irrigation period, the volume of added water and the last soil water suction value were recorded. The quantity of added water was determined knowing the time consumed for progressive water addition and the micro-volumetric drop rate of 0.018 ml s^{-1}. It was a function of both evaporation from the soil surface and water uptake by the maize roots. Then, the daytime drying period started. Wetting and drying cycles were also recorded both in soil water suction and in added water. The beginning of the wetting and drying cycles was considered as time zero, as a convention, whatever was the initial drying period time.

During all the plant growth period, no nutrient solution has been added in the culture pots. For growing, the maize plant therefore used first the storage of the seed and the nutrient available in the soil thereafter.

Plant and soil sampling and analysis

The delay between the last progressive irrigation during the nighttime period and the removal of the soil-filled pots with or without maize was always of 17 hours (final daytime drying period). The maize plants were harvested 11 days after sowing, that is to say that the plants were submitted to a drying period of 7 to 8 days to reach the selected soil water suction values and to 3 to 4 wetting-drying cycles thereafter. The stage of development of plants at the end of the culture was that of two to three leaves per plant, occurring just before tillering.

At that time, the final water suction value was recorded and, after removing the soil:root system from each pot, we measured the shoot biomass and the gravimetric water content of the bulk soil. Photographs of some soil:root systems from the pots with a minimum suction value of 10 kPa were also made.

Results and discussion

Soil water retention by drainage

Water retention curves (Fig. 3) showed that (i) the gravimetric water content at both nearly soil water-saturation (soil water suction of 10 kPa) and at the experimental end of these soil drainage curves (soil water suction of 60 kPa) was three to four times higher for the packed aggregates of the silty topsoil than for those of the sandy topsoil and (ii) the silty topsoil seemed to drain more easily than the sandy one, from 10 or 20 to 60 kPa soil water suction.

The first result was mainly attributed to clay micro-porosity, as has been widely reported (e. g. Baver *et al.*, 1972; Scheffer and Schachtshabel, 1976). For the silty soil, the relatively high gravimetric water content at nearly soil water saturation was due to the importance of meso and microporosities, which has been well observed by MEB and MET on thin sections and ultra-thin sections (Gomendy, 1996; Bartoli *et al.*, 1999). In contrast, for the sandy soil, the small gravimetric water content at soil water saturation was due to the predominant macro-pores (pore radii > 100 µm) occurring between the coarse sandy particles.

The second result was more difficult to interpret. However, some recent work carried out on the studied silty soil showed that its relatively easy soil water drainage was explained by its low interfacial solid:pore rugosity (fractal analysis),

its high meso-pore connectivity and its low pressure threshold value (Gomendy *et al.*, 1998). The meso-pore connectivity was defined as the surface area of the percolation networks extending without interruption from the top to the bottom of the SEM image of a soil thin section whereas the pressure threshold value was defined as the beginning of the rapid rise in the mercury injection curve, which was interpreted as a breakthrough event corresponding to the mercury invasion of the largest connected pore cluster (Thompson *et al.*, 1987). On the other hand, the fact that most sandy soils easily drained (e. g., Rawls and Brakensiek, 1985; Vereecken *et al.*, 1989; Petersen *et al.*, 1996) but not the studied one was yet unclear. It could be attributed to the hydrophobic characteristics of the studied sandy topsoil.

Finally, the coefficient of variation CV of the retained water content, which is the standard deviation:mean percentage ratio, was higher for the sandy (CV value of 2 to 5 %) than for the silty (CV value of 0.5 to 2 %) topsoil for most of the soil water suction studied (results not shown). It was attributed to a more variable spatial distribution of the retained soil water within the packed soil aggregates for the sandy than for the silty topsoil.

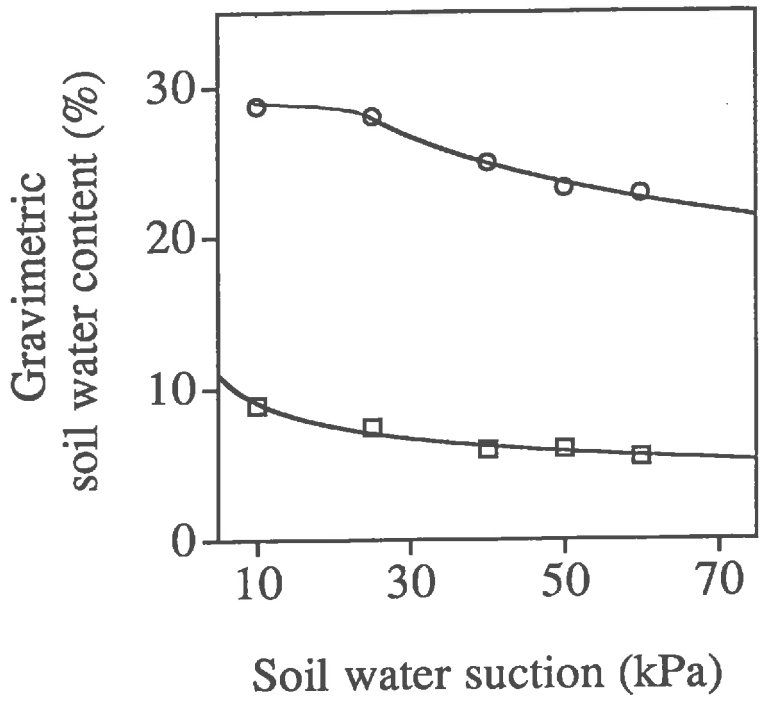

Figure II. 3. Soil water retention curves (drainage) plotted from data which were obtained under quasi-static conditions (membrane plates). Open circle and square symbols correspond to the silty and the sandy topsoil (air-dried and sieved to < 4 mm aggregates and particles), respectively.

Plant growth and root geometry

No statistically significant effect of soil water suction on maize plant growth was identified from the shoot biomass data into either the silty or the sandy topsoil (Table 2). It is not surprising because the soil was relatively wet, even at a suction value of 50 kPa. It was atributed to the fact that the soils were not totally water-saturated. Roots need at least 10 % by volume air space in the soil to survive, because they obtain oxygen from the air (Wesseling and van Wijk, 1957). However, for the silty topsoil, the shoot biomass tends to be lower at 10 kPa than at 20 and 40 kPa (Table 2) which indicated that the soil might have been too wet for good plant growth at 10 kPa. In contrast, a statistically significant effect of soil type was observed on plant growth (Table 2). It could be attributed to the hydrophobic characteristics of the nearly water-saturated sandy topsoil which was very difficult to dry during the beginning of the long initial period of soil drying. It was also attributed to the fact that no nutrient solution has been used during the culture. This should be a limiting growing factor for the sandy topsoil, poor in nutrients, but not for the silty topsoil, rich in nutrients (CEC data of Table 1).

	Silty topsoil			Sandy topsoil		
	Soil water suction (kPa)			Soil water suction (kPa)		
	10	20	40	10	20	40
Shoot Biomass (mg)	81 ± 6* a	98 ± 5* a	103 ± 6* a	79 ± 3* b	68 ± 6* b	74 ± 8* b

*Table II. 2. Shoot biomass of maize at harvested time (about 11 days). Values with different letters are significantly different at $P < 0.05$ in the Newman-Keuls test. * = standard error of mean values.*

On the other hand, although no data on root biomass were available, we qualitatively characterized the geometry of the 11 day-old maize root system as follows. By visual observations of the soil-root samples (see e. g. Fig. 4), the roots which had grown into the sandy topsoil with daily minimum water suction of 10 kPa had greater lengths and smaller diameters than their silty soil counterparts. The number of roots was also higher in the sandy than in the silty topsoil. Finally, the mean radial distance between two seminal roots of order one had been measured on the soil-root samples at a distance of 6.8 cm below the crown which nearly corresponds to the half root length. It was of 7 to 10 mm for

the silty topsoil:root system whereas it was only of 0.3 to 0.6 mm for the sandy topsoil:root system.

Jensen et *al.* (1993) had also previously shown that the distribution of maize roots was homogeneous in sandy soils, with numerous and long fine roots. This was attributed to the poor water retention properties of these soils. Similarly, Dwyer *et al.* (1988) and Veen and Boone (1990) had obtained an inverse relationship between the maximum root depth and the fractional available water measured during the growing season for each crop studied (maize, wheat, soybean and barley), which, in its turn, increased as a function of soil clay content. In this study, the observed combined increase of root diameter and decrease of root length from the sandy soil to the silty soil could also be attributed to the increase of soil strength. The silty soil had higher strength than the sandy soil (Czarnes *et al.*, 1998). Such relationships between maize root geometry and soil strength also have been reported in numerous previous studies of the maize rhizosphere (e. g., Veen and Boone, 1990; Materechera *et al.*, 1992, 1994; Bengough *et al.*, 1997).

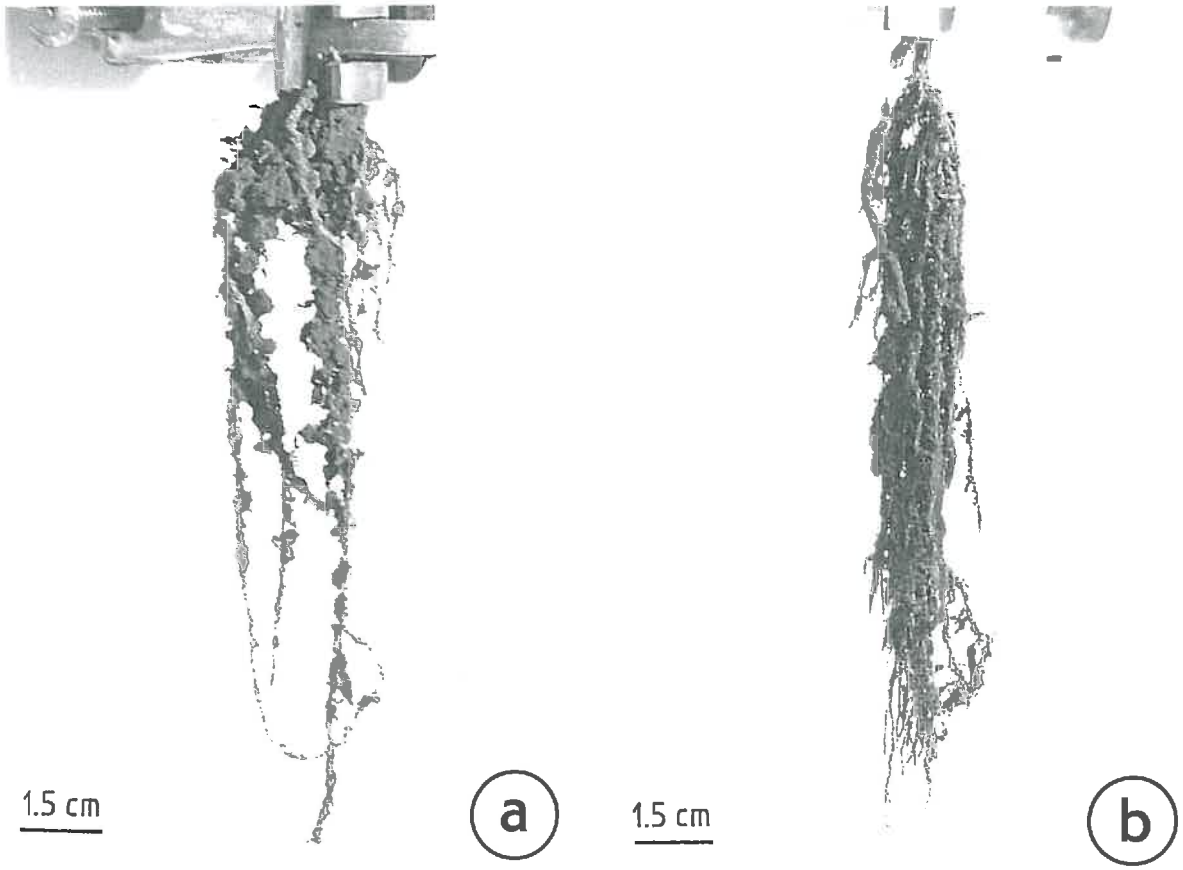

Figure II. 4. Examples of the architecture of the 11 day-old maize root system, with its root-adhering soil, for the silty topsoil (a) or the sandy topsoil (b) and a daily minimum soil water suction of 10 kPa.

Initial drying in the maize rhizosphere and in its control soil counterpart

For each soil type, with or without maize, each soil-filled pot had its own soil drying characteristics during the initial part of the experiment, which was due to both its spatial position in the growth chamber (changes of the incident light energy of the lights) and to its initial water content. Although the low, middle and high evaporative demand domains which were used for the selection of the 10 kPa, 20 kPa and both 40 and 50 kPa soil water suction treatments, respectively, were partly related to the position of the soil-filled pots in the growth chamber, their spatial distribution looked apparently random. However, further progress in recording environmental characteristics of the soil-filled pots (temperature, air moisture, incident light intensity of the lights, initial soil water content) are required.

When we used all the data (nearly 12 replicates by treatment) we can analyse the effects of both the plant and the soil on the mean soil drying because (i) the heterogeneities of the incident light energy of the lights and of the initial soil water content were then similar whatever was the treatment and (ii) the standard errors of the mean soil water suction were also relatively low (Fig. 5).

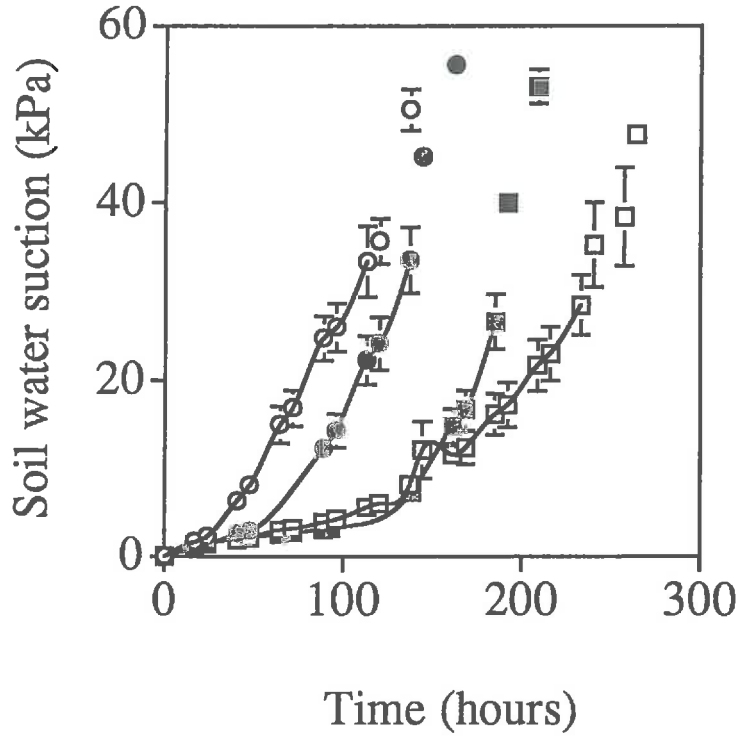

Figure II. 5. Mean soil drying under controlled 17 h daytime lighting and 7 h nighttime cycles for the maize rhizosphere (filled symbols) and its control soil counterpart (open symbols) of either the silty topsoil (circle symbols) or the sandy topsoil (square symbols). Error bars show standard errors of mean values.

The results were as follows .

First, the non-linear increase of soil water suction as a function of time was always higher for the silty than for the sandy control topsoil (Fig. 5), which was very difficult to dry. The soil drying time threshold, when soil drying went from slow to fast, was only two days for the silty control topsoil whereas it was five days for the sandy control topsoil (Fig. 5). This discrepancy could be attributed to (i) the hydrophobic characteristics of the sandy soil organic matter, (ii) the fact that aggregates and particles were more closely packed for the sandy than for the silty topsoil, with total porosities of 0.50 cm^3 cm^{-3} and 0.58 cm^3 cm^{-3}, respectively, and (iii) the relatively large decrease in the hydraulic conductivity of the sandy soil as it dries. Also, as the surface dries, the drying of the lower layers would be greatly retarded by the low conductivity of water to the surface.

Second, the drying curves of the maize rhizosphere and of the control soil were rather similar for the silty topsoil (Fig. 5). In contrast, after the soil drying time threshold, the non-linear increase of soil water suction as a function of time was statistically higher for the maize sandy rhizosphere than for the sandy control (Fig. 5). Evaporation of soil water and plant transpiration are complementary processes. Each is affected by the availability of water in the soil and by the incident energy intensity of the light. Soil evaporation is also affected both by the degree of surface exposure and by the ability of the surface soil layers to conduct water held in the deeper layers (Huck, 1984) whereas plant transpiration is affected on the one hand on the ability of the soil to supply roots with water at a certain rate, which was rather slow for the sandy topsoil, and, on the other hand, on the geometry of the root system.

Third, after the soil drying time thresholds, the drying curves of the maize rhizosphere had also rather similar shapes for both the silty and the sandy topsoil (Fig. 5). Although the soil water suction is not a measure of the water flux occurring between the maize and the soil it may be assumed that the balance between the abilities of the soil and of the root system to supply roots with water at a certain rate (Droogers *et al.*, 1997) is rather similar for both the silty and the sandy topsoil. The silty topsoil should be characterized by a good soil water retention capacity but an hypothetic bad root ability for plant water uptake, which was only based on visual observations of the root system (low number of roots and clustered root distribution pattern) (Fig. 4), and, in contrast, in the case of the sandy topsoil, a bad soil water retention capacity but an hypothetic good root ability for maize water uptake (large number of roots, small inter-root distances

and homogeneous root distribution pattern) (Fig. 4). In this study, only visual observations of the root systems were carried out and the roots filled each cylinder whatever was the soil, so no conclusions can be made about water moving differently in the silty and sandy topsoils due to different root geometry.

Controlled wetting and drying cycles in the maize rhizosphere and in its control soil counterpart

The controlled wetting and drying cycles occurred in either the maize rhizosphere or its soil control counterpart after an initial soil drying period of 7 to 9 days (11 to 13 days for the control sandy topsoil). Although few data were recorded during the wetting and drying cycles, the main results are as follows.

First, the range of soil water suction of each wetting and drying cycle was larger for the silty (5 to 12 kPa) than for the sandy (3 to 7 kPa) control topsoil (Figs. 6a and 6c). This result confirmed that which was obtained from the initial soil drying, which was faster for the silty control topsoil than for the sandy control topsoil (Fig. 5). This discrepancy again can be attributed to the hydrophobic characteristics of the organic matter in the sandy soil, to the relative high density of the packed sandy particles and aggregates and to the asssumed relatively large decrease in the hydraulic conductivity of the soil as it dries.

Second, the range of soil water suction of each wetting and drying cycle was rather similarly high for the silty and the sandy rhizosphere, and for the silty control topsoil (e. g., 15 to 30 kPa for the third wetting and drying cycle) (Figs. 6a, 6b and 6d) whereas it was rather low for the sandy control topsoil (e. g., 6 to 11 kPa for the third wetting and drying cycle) (Fig. 6c). A plant effect was then again observed for the sandy topsoil, but apparently not for the silty topsoil (Figs 5a and 6). However, plants are taking up and transpiring water in the two contrasting studied soils.

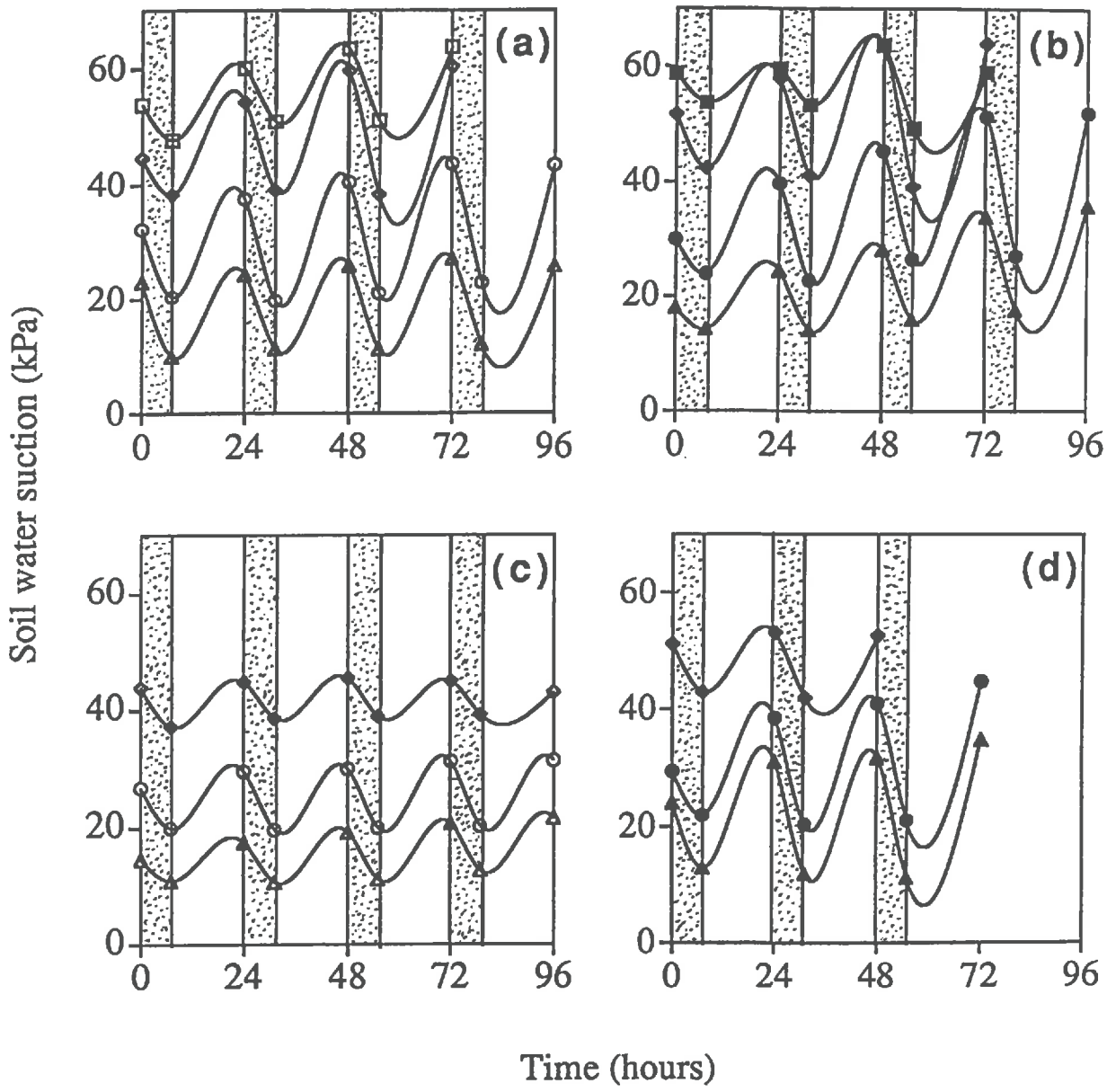

Figure II. 6. *Examples of controlled wetting and drying cycles occurring after the preliminary soil drying (Fig. 5) for the maize rhizosphere (b and d) and its control soil counterpart (a and c) of either the silty topsoil (a and b) or the sandy topsoil (c and d). The beginning of the wetting and drying cycles was considered as time zero, as a convention, whatever was the initial drying period time.*

Soil water retention in the maize rhizosphere and its control soil counterpart (end of the last soil drying cycle)

Soil water retention data (both gravimetric soil water content determined by weighting the wett soil at 105°C and soil water suction measured with the micro-tensiometers) of either the rhizosphere or its control soil counterpart (Fig. 7) were carried out at the end of the last 17 hours drying period of the wetting and drying cycles and plotted on figures 7a and 7b for the silty and the sandy topsoil, respectively. The results are as follows.

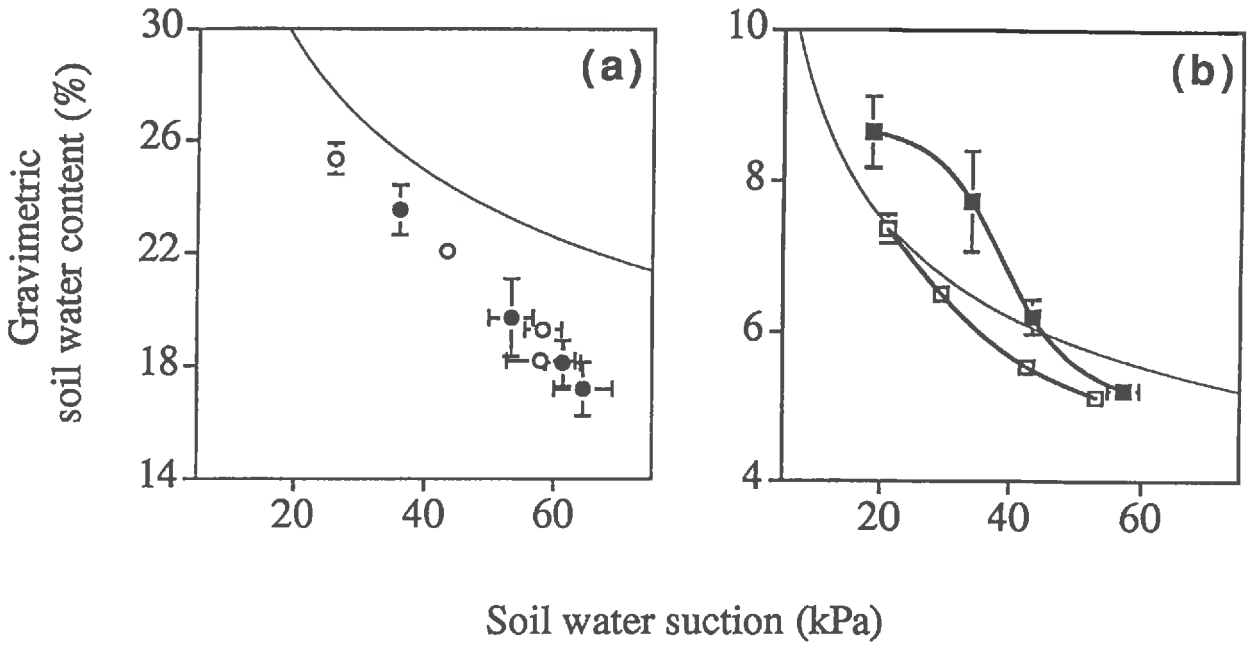

Figure II. 7. Soil water retention curves (drainage) plotted from data which were obtained under either quasi-static conditions (curves) or dynamic conditions for the maize rhizosphere (big filled symbols) and the control soil (big open symbols) for the silty topsoil (circle symbols on figure 7a) and for the sandy topsoil (square symbols on figure 7b). Error bars show standard errors of mean values.

First, soil water content was much more variable in the rhizosphere soil than in the control soil, both for the silty and for the sandy topsoil (Figs. 7a and 7b). This discrepency characterized the variability of the plant growth and of the plant transpiration rate.

Second, the two soil water retention curves of either the rhizosphere silty topsoil or the control silty topsoil under dynamic conditions are rather similar

(Fig. 7a). However, plants were taking up and transpiring water, leading to the fact that the rhizosphere silty topsoil dried much more than the control silty topsoil, as it was expected, with a higher soil water suction and, conversely, a lower soil water content in the rhizosphere than in its control soil counterpart (Fig. 7a).

Figure 7a shows that the silty topsoil water retention curves under dynamic conditions diverge, with a gradual shift to lower soil water content, from the soil water retention curve at constant pressure and quasi-equilibrium. The underlying process could be an increase of the water flow speed from the slow drainage (72 to 116 hours of soil drying) at constant pressure and no light energy intensity to fast soil drying (17 hours of final soil drying) due to a significant light energy intensity occurring during soil drying, and to the plant for the rhizosphere soil. Similarly, soil water retention curves diverge, with a gradual shift to lower soil water content, when temperature increases (e. g., Liu and Dane, 1993).

Third, in contrast, the two soil water retention curves of either the rhizosphere sandy topsoil or the control sandy topsoil under dynamic conditions are significantly different, with a shift to higher soil water suction values from the control sandy topsoil to its rhizosphere counterpart (Fig. 7b).

Soil water hysteresis was often observed when comparing the water retention curves of silty and sandy soils, plotted from water sorption (wetting) and dehydratation (drainage) (e. g., Topp, 1971; Scheffer and Schachtshabel, 1976; Richter, 1987). For a definite soil water suction value, the amount of retained soil water was higher for the drained than for the wetted soil. Such soil water hysteresis is generally attributed to the geometry of the interconnected pore network (pore throats) which can be rapidly water-filled, after a certain pressure threshold value, but, in contrast, is slowly drained therafter.

In this study, all the water retention curves were obtained by drainage which was either slow (quasi-equilibrium with the membrane plates) or fast (last controlled soil drying with the micro-tensiometers). The question therefore arises on what kind of underlying process, other than wetting and drainage, can explain the observed soil water hysteresis. Our hypothesis is that this apparent soil water hysteresis could be caused by a discrepancy between the water flow speed values of the rhizosphere sandy topsoil and those of the control sandy topsoil. Three complementary arguments are in favour of this hypothesis and are presented as follows.

The first argument is the self-consistancy of our results. In this study, we have already reported a clear plant effect on the sandy topsoil drying under dynamic conditions (Figs. 5 and 6). It was attributed to both the low amount of retained soil water, which was also difficult to be drained, and the geometry of the root system which looked by visual observation highly favourable for water uptake.

The second argument comes from the recent results obtained by Doussan and co-workers (Doussan *et al.* 1998; Doussan and Pagès, 1998) who have modelled, in a three-dimensional space, the spatial water uptake by a single maize root. They have shown that the radial gradient of soil water suction (and, conversely, of the water flow speed) was very pronounced along the maize root for maize growing into a sandy soil, whereas it was moderate for maize growing into a clayey soil.

The third argument comes from the hysteresis effects which have been reported on sandstone water retention curves (drainage) by Nguyen Tan Hoa (1978). For the same sandstone water content, the capillary pressure was higher under dynamic conditions (water flow speed of 13 cm h^{-1}) than under quasi-static ones (water flow speed of 0.6 cm h^{-1}). The author attributed this hysteresis process to a progressive decrease of the contact angle when the water flow speed increases. Another interpretation of the results of Nguyen Tan Hoa (1978) was suggested by Lenormand (1981) who claimed that numerous water-filled pores belonging to the percolation network (percolation theory) had not the time to be drained when the water flow speed was high (drying kinetics).

Further experimental research is required to evaluate our hypothesis.

Conclusion

A clear plant effect has been found for the sandy topsoil whereas it was moderate for the silty topsoil. Compared with the control sandy topsoil, the rhizosphere sandy topsoil was characterized by (i) a greater increase of soil water suction as a function of time during the preliminary soil drying (Fig. 5), (ii) a larger range of soil water suction during each controlled wetting and drying cycle (Fig. 6). This plant effect was mainly attributed to the low amount of retained soil water, which was also difficult to be drained. In contrast, the moderate plant effect

which has been found for the silty topsoil was attributed to its high amount of retained soil water and its high pore connectivity.

However, plants were taking up and transpiring water in the two contrasting soils, leading to the fact that the rhizosphere silty topsoil dried much more than the control silty topsoil, as it was expected, with a higher final soil water suction and, conversely, a lower final soil water content in the rhizosphere than in its control soil counterpart.

On the other hand, the silty rhizosphere and its control soil counterpart again had rather similar hydro-physical behaviour whereas a soil water hysteresis effect was observed between the soil water retention curves of the rhizosphere sandy topsoil and of the control sandy topsoil. This hysteresis effect could be attributed to significant slower water flow speed in the control soil as compared with the rhizosphere. Further experimental high resolution work is required to evaluate this last key hypothesis.

Acknowledgements

The authors thank Michel Bloin, Gérard Burtin and Renée Philippy, CPB-CNRS, for valuable technical assistance for the plant growth device, ultrasonication, and soil water retention curves under quasi-static conditions, respectively. Financial support from the CPB-CNRS aggregation team (3 years and six months) and the Lorraine Regional Council (9 months) for a Henri Poincaré - Nancy I grant, and a complementary grant, given to the first author, are also greatly appreciated.

References

Bartoli F, Bird N, Gomendy V and Vivier H 1999 The relationship between silty soil structures and their mercury porosimetry curve counterparts. Fractals and percolation. European Journal of Soil Science 50 (in print).

Baver L D, Gardner W H and Gardner W R 1972 Soil physics; 4th edition. John Wiley, New York, 498 p..

Bengough A G, Croser C and Pritchard J 1997 A biophysical analysis of root growth under mechanical stress. Plant and Soil 189, 155-164.

Bristow K L, Campbell G S and Calissendorf C 1984 The effects of tecture on the resistance to water movement within the rhizosphere. Soil Science Society of America Journal 48, 266-270.

Czarnes S 1994 Effet de l'inoculation de *Bacillus polymixa* sur la structure du sol dans la rhizosphere du ble. Nancy I University DEA.

Czarnes S, Dexter A R and Bartoli F 1998 Mechanics of two adherent centimetric remoulded soil balls : a preliminary examination. Soil and Tillage Research (submitted).

Doussan C, Vercambre G and Pagès L 1998 Modelling of the hydraulic architecture of root systems: an integrated approach to water absorption. 2. Distribution of axial and radial conductances in maize. Annal of Botany 81, 225-232.

Doussan C and Pagès L 1998 Absorption hydrique racinaire: sur l'ambiance hydrique de la rhizosphère et les transferts d'eau-racines. *In* Colloque Rhizosphere Aix'97, Aix-en-Provence 26-27 Novembre 1997, p.15.

Droogers P, van der Meer F B W and Bouma J 1997 Water accessibility to plant roots in different soil structures occurring in the same soil type. Plant and Soil 188, 83-91.

Dwyer L M, Stewart D W and Balchin D 1988 Rooting characteritics of corn, soybeans and barley as a function of available water and soil physical characteristics. Canadian Journal of Soil Science 68, 121-132.

Faiz S M A and Weatherley P E 1978 Further investigations into the location and magnitude of the hydraulic resistances in the soil-plant system. New Phytologist 92, 333-343.

Gardner W R 1960 Dynamic aspects of water availability to plants. Soil Science 89, 63-73.

Gomendy V 1996. Variabilités spatiale et temporelle des propriétés structurales et hydriques des horizons de surface de la couverture limoneuse du bassin versant d'Orgeval (Brie). Nancy University pHD thesis.

Gomendy V, Bartoli F, Burtin G, Doirisse M, Philippy Niquet S and Vivier H 1998 Silty topsoil structure and its dynamics : the fractal approach. Geoderma, special issue on "fractal models in Soil Science" edited by Y. Pachepsky, J. Crawford and W. Rawls (in print).

Herkelrath W N, Miller E E and Gardner W R 1977 Water uptake by plants : I. Divided root experiments. II. The root contact model. Soil Science Society of America Journal 41, 1033-1043.

Huck M G 1984. Water flux in the soil-root continuum. *In* Roots, nutrient and water influx, and plant growth. Soil Science Society of America, Crop Science Society of America, and American Society of Agronomy, 677 South Segoe Road, Madison, WI 53711 pp 47-63.

Jensen C R, Svendsen H, Andersen M N and Lösch R 1993 Use of the root contact concept, an empirical leaf conductance model and pressure-volume curves in simulating crop water relations. Plant and Soil 149, 1-26.

Klute A 1986 Water retention : laboratory methods. *In* A. Klute (ed.), Methods of Soil Analysis, part 1: Physical and Mineralogical Methods. Soil Science Society of America, Agronomy Monograph n° 9, pp 635-662.

Lafolie F, Brucker L and Tardieux F, 1991 Modelling root water potential and soil-root water transport: I. Model presentation. Soil Science Society of America Journal 55, 1203-1212.

Lenormand R 1981 Déplacements polyphasiques en milieu poreux sous l'influence des forces capillaires. Etude expérimentale et modélisation de type percolation. Toulouse Institut National Polytechnique State thesis.

Liu H H and Dane J H 1993 Reconciliation between measured and theoritical temperature effects on soil water retention curves. Soil Science Society of America journal 57, 1202-1207.

Materechera S A, Dexter A R and Alston A M 1992 Formation of aggregates by plant roots in homogenised soils. Plant and Soil 142: 69-79.

Materechera S A, Kirby J M, Alston A M and Dexter A R 1994 Modification of soil aggregation by watering regime and roots growing through beds of large aggregates. Plant and Soil 160: 57-66.

Matsumoto H, Okada K and Takahashi E 1979 Excretion products of maize roots from seedling to seed development stage. Plant and Soil 53, 17-26.

Nguyen Tan H 1978 Ecoulements non permanents dans des massifs de milieux poreux non saturés avec effets d'hystérésis. Toulouse Institut National Polytechnique State thesis.

Passioura J B 1980 The transport of water from soil to shoot in wheat seedlings. Journal of Experimental Botany 31, 331-345.

Petersen L W, Moldrup P, Jacobsen D H and Rolston D E 1996 Relations between specific area and soil physical and chemical properties. Soil Science 161, 9-21.

Philip J R 1966 Plant water relations: some physical aspects. Annual Review of Plant Physiology 17, 245-268.

Rawls W J and Brakensiek D L 1985 Prediction of soil water properties for hydrologic modeling. *In* Proceedings of the Symposium "Watershed Management in the Eighties", Denver pp 293-299.

Reicosky D C and Ritchie J T 1976 Relative importance of soil resistance and plant resistance in root water absorption. Soil Science Society of America Journal 40, 293-297.

Richter J 1987 The soil as a reactor: modeling processes in the soil. Catena, Verlag.

Scheffer F and Schachtshabel P 1976 Lehrbuch der Bodenkunde. Ferdinand Enke Verlag Stuttgart, 394 p.

Stirzaker R J and Passioura J B 1996 The water relations of the root-soil interface. Plant, Cell and Environment 19, 201-208.

Thompson A H, Katz A J and Krohn C E 1987 The microgeometry and transport properties of sedimentary rock. Advances in Physics 36, 625-694.

Topp G C 1971 Soil water hysteresis in silt loam and clay loam soils. Water Resources Research 7, 914-920.

Veen B W and Boone F R 1990 The influence of mechanical resistance and soil water on the growth of seminal roots of maize. Soil and Tillage Research 16: 219-226.

Veen B W, Van Noordwijk M, De Willigen P, Boone F R and Kooistra M J 1992 Root-soil contact of maize, as measured by a thin-section technique. III. Effects on shoot growth, nitrate and water uptake efficiency. Plant and Soil 139, 131-138.

Vereecken H, Maes J, Feysen J and Darius P 1989 Estimating the soil moisture retention characteristics from texture, bulk density, and carbon content. Soil Science 148, 389-403.

Wesseling J and van Wijk W R 1957 Soil physical conditions in relation to drain depth. *In* J N Lutin (ed.), Drainage of agricultural lands. Agronomy Monograph 7, American Society of Agronomy, Madison, Wisconsin, p. 461-504.

Wetting and drying cycles in the maize rhizosphere under controlled conditions. II. Mechanics of the root-adhering soil

S. CZARNES[a, b], *A.R. DEXTER*[b, c] *and F. BARTOLI*[a*]

[a] *Centre de Pédologie Biologique UPR 6831 du CNRS associé à l'Université Henri Poincaré - Nancy I, BP 5, 54501 Vandoeuvre-les-Nancy, France*

[b] *Silsoe Research Institute, Wrest Park, Silsoe, Bedford MK45 4HS, United Kingdom*

[c] present address: Instytut Uprawy Nawozenia i Gleboznawstwa, ul. Czartoryskich 8, 24 - 100 Pulawy, Poland

Key words: friability, maize rhizosphere, soil water suction, root-adhering soil rupture, root exudates, tensile strength,

[*] Corresponding author. Present address: Centre de Pedologie Biologique UPR 6831 du CNRS associé à l'Université Henri Poincaré - Nancy I, BP 5, 54501 Vandoeuvre-lès-Nancy, France

Tel: (33) 3 83 51 08 60 Fax: (33) 3 83 57 65 23 e-mail: bartoli@cpb.cnrs-nancy.fr

Abstract

Mechanical properties of the topsoil (sandy Podsols and silty Luvisols, FAO) adhering to maize (*Zea maiys* L.) roots and its bulk soil counterpart were studied as a function of soil texture and final soil water suction at harvest, with three soil water suction values of nearly 30, 50 and 60 kPa. Two scales of observation were also selected: the whole soil:root system and the root-adhering soil aggregates.

Three methods were used to characterize the stability of the soil:root system: mechanical shaking in air; low dispersive ultrasonication in water, with or without preliminary immersion of the soil:root system in water. Soil disruption kinetics, which were fitted with first-order kinetics equations, are analysed and discussed. For example, silty soil ultrasonication kinetics, without preliminary water-immersion, can be divided into two parts: the first faster part, which was characterized by a mean rate K value of 6.8 to 7.2 mJ^{-1}, was attributed to soil slaking whereas the second slower part, which was characterized by a mean rate K value of 1.5 to 1.6 mJ^{-1}, was attributed to the rupture of the "firmly root-adhering soil" from the roots.

A clear plant effect is reported for both aggregate tensile strength and friability, with higher aggregate strength for the root-adhering silty soil (450 to 500 kPa) than for its bulk silty soil counterpart (410 to 420 kPa), and lower friability (coeficient of variation of the aggregate strength) for the root-adhering silty soil (e. g., 67 % at a soil water suction value of 30 kPa) than for its bulk silty soil counterpart (e. g. 49 % at a soil water suction value of 30 kPa). These effects are attributed to root exudation, which was significantly higher for the driest silty topsoil than for the wetter ones.

In conclusion, the results on the mechanical properties of the silty topsoil adhering to the maize roots were attributed to both physical and biological interactions, and their dunamics, which occured in the maize rhizosphere.

Introduction

The rhizosphere is the localised volume of soil around plant roots directly influenced by the roots and their associated microorganisms (Hiltner, 1904). The main biological rhizosphere process is root exudation which has been found to be first a function of plant species (e. g., maize roots strongly exdude compare to wheat ones) and second a function of various hydric, mechanical or chemical stresses (e. g., Kraffczyk *et al.*, 1984; Lynch and Whipps, 1990). Virtually all the nutrients and water absorbed by a plant must pass through the rhizosphere, making its physical, chemical, and biological properties of crucial importance to plant growth. It may have very different properties compare to the surrounding soil because of physical stresses associated with plant growth and with enhanced cycles of drying and wetting, chemical changes caused by the exudation of the root mucilage, and enhanced biological activity caused by higher levels of nutrients.

Aggregate stability, and its dynamics, is one of these rhizosphere properties which are crucial for plant growth. The mechanical properties of the soil:root interface influences root elongation and the tensile resistance for characterizing root anchorage in the soil (e. g. Greacen *et al.*, 1968; Beck *et al.*, 1988; Ennos, 1989, 1990, 1993; Bengough *et al.*, 1997). The stability of the root-adhering soil, and its dynamics, is also a key parameter which can control interactions occurring between microorganisms, organic matter, minerals and soil solution.

To our knowledge, the first study on root-adhering soil was carried out on quartz sand sized particles adherent to soybean roots under a range of water stresses (Sprent, 1975). The mass of the root-adhering sand particles, which was measured by incineration of the root-adhering particles:root system, decreased as water content of the sand increased. In another study, the rhizosheath, which is the complex volumetric soil zone adherent to the roots, was found to be composed of soil particles and micro-aggregates, microbes, mucilaginous substances, and interwined root hairs (McCully and Canny, 1989). The diurnal soil drying should lead to a firm binding of the mucilage to the root-adhering soil, thus stabilizing it (McCully and Canny, 1989).

The notion of root-adhering soil has been further discussed by Parke *et al.* (1990) who subdivided it into the "firmly adhering soil" and the "loosely adhering soil". The amount of the "firmly adhering soil" may vary by several orders of magnitude depending on soil type, soil water content, root age, and the

vigor with which root samples are shaken to dislodge the "loosely adhering soil". Later, Watt *et al.* (1994) tried to determine how tightly the rhizosheath was bound to a maize root system. For that study, fractions of the rhizosheath were removed by three successive treatments: first, sonication; then, hot water; and finally, brushing of the roots. In their study, the rhizosheaths were larger and adhered to the roots more tightly when formed in dry soils, confirming and clarifying the pioneering work of Sprent (1975).

Few studies have been carried out on the effect of soil water regime on root-adhering soil stability and there is also conflicting evidence as to whether the rhizosheath soil can be wetter or drier than the bulk soil (Young, 1995). Our objective is to study effects of soil type and intensity of maize rhizosphere drying on the strength of the root-adhering soil from either the whole soil:root system or the separate root-adhering aggregates. Geometry and exudation of the root system will also be taken into account.

Materials and methods

Soils

Selected properties of the two topsoil samples are listed in Table 1. The sandy podzolic soil (Podsols, FAO) and the silty leached brown soil (Luvisols, FAO) were both granular and friable, with poor plastic behaviours (Czarnes *et al.*, 1998a). Details of the two studied topsoils have been reported elsewhere (Czarnes *et al.*, 1998a; Czarnes and Bartoli, 1998).

Topsoil samples	Soil types	Clay < 2 mm (%)	Atterberg limits (%)			Shear strength 10 kPa
			Liquid limit	Plastic limit	Plastic Index	
Sandy	podzolic	1.9	24.5	nm	nm	8,4
Silty	leached brown	16.4	34.4	23.4	11	15,2

nm: measure not possible

Table II. 1. Main soil characteristics

Factorial design for disruption of the root-adhering soil

A 2 * 3 * 3 factorial design with five replicates for each treatment was used (a total of 90 samples). The factors were: soil type (the silty and the sandy topsoil packed aggregates), daily minimum soil water suction value (10, 20, and 40 kPa) (Czarnes and Bartoli, 1998), method for disruption of root-adhering soil from the whole soil:root system by either (i) mechanical shaking in air or (ii) low dispersive ultrasonication in water, or (iii) immersion in water, followed by low dispersive ultrasonication in water.

Maize seedlings, culture chamber conditions and soil water characteristics

Details of the selection, growth, and sowing of maize seedlings, and of the control environment chamber conditions and rhizosphere water characteristics and dynamics have been reported in the first part of this series of papers (Czarnes and Bartoli, 1998).

Plant and soil sampling and analysis

The delay between the last progressive irrigation during the nighttime period and the removal of each soil-filled pot with its 11 day-old maize plant was always 17 hours (final daytime drying period). The stage of development of plants at the end of the culture was that of two to three leaves per plant, occurring just before tillering. At that time, we recorded the final soil water suction using STM 2030S micro-tensiometers, made by SDEC, 19 rue Edouard Vaillant, 37 000 Tours, France, as described in more details by Czarnes and Bartoli (1998). We measured the final gravimetric water content of the bulk soil by weighing the soil before and after oven-drying at 105°C. We excised the shoot for measurement of its biomass (Czarnes and Bartoli, 1998). The entire soil:root system also was removed carefully from each pot for either mechanical shaking in air or low dispersive ultrasonication in water, immediately after the harvest.

Mechanical shaking of the soil:root system

We placed the soil:root system on a mechanical shaker (Oscill 8, Bioblock), fixing the end of the non-excised stem into an appropriate arm with 4 PVC finger-pegs. Mechanical, vertical agitation was gentle with 500 oscillations min^{-1}. Each oscillation had an amplitude of 8 mm. Unstable root-adhering soil, which fell onto an aluminium sheet, was sampled during the disruption of the root-adhering soil at 0.5, 1, 2, 3, 4, and 5 minutes, and was dried at 105°C for 48 hours for weighing. Then, cumulative unstable root-adhering soil was computed, as a function of time (with, for each soil, three replicates by daily minimum soil water suction value). Each stable soil fraction was also removed by high ultrasonication, and dried at 105°C for 48 hours for weighing.

Image analysis of the soil:root system as a function of mechanical soil disruption

Photographs of some soil:root systems taken from the pots submittted to a daily minimum suction value of 10 kPa were also made during the soil disruption by mechanical shaking, at the selected times of 0, 1, 3 and 5 minutes. Then, image analysis of the soil:root system (the root-adhering soil and the roots) was carried out using a customed-made package (Centre Inter-Regional Informatique de Lorraine, Nancy, France) for determining its vertical area distribution. The results were normalized in proportions of the initial total area of the soil:root system.

Low dispersive ultrasonication of the soil:root system

For this technique, a Branson 1210 cleaning ultrasonicator was used in a 21°C constant temperature room. The rectangular tank of this was 10 cm high and 14 cm X 15 cm horizontal area. The dispersive output ultrasonic energy came from quartz micro-cells which were arranged in an array of approximately 3 cm size. The selected dispersive output energy, which was calibrated following the procedure of North (1976), was 116 J min^{-1} for an ultrasonication (US) unit time of 6 minutes. At each US unit time, the soil suspension was transferred from the ultrasonicator tank to a vial, for oven-drying and weighing. The water-empty ultrasonic tank, with the soil:root system, was immediately filled again with

distilled water for another 6 minutes of ultrasonication. Soil disruption was repeated until a nearly clear soil suspension was obtained. However, a small quantity of soil always remained firmly adherent to the roots. It was also removed by high ultrasonication, and dried at 105°C for 48 hours for weighing. Then, cumulative unstable root-adhering soil vs time curves were plotted with again, for each soil, three replicates by daily minimum soil water suction value.

High ultrasonication of the soil:root system (Determination of the total root-adhering soil)

High ultrasonication was used to get all soil off, so ratios of the amounts of soil that came off by the different mechanical treatments could be determined. The denominator was the maximum amount (soil dispersed by high ultrasonication plus what came off by the mechanical treatment). The stable root-adhering soil occurring after either mechanical shaking or low dispersive ultrasonication was so removed from the roots by ultrasonication of the stable soil:root system in 100 ml distilled water, into a 150 TU Ultrasonic Ultrasons unit, 74 Annemasse, France which was used at 21°C constant temperature room. The selected probe output energy was calibrated following the procedure of North (1976). It was of 2214 $J.min^{-1}$ (nearly 20 times higher than the selected output energy from the Branson 1210 cleaning ultrasonicator used for the low dispersive ultrasonication of the soil:root system). The soil dispersed by high ultrasonication was weighed after oven drying at 105°C for 48 hours. Then, the total root-adhering soil was computed as the sum of the unstable soil after either mechanical shaking or low dispersive ultrasonication and of its stable soil counterpart, determined by high ultrasonication.

Mathematical fitting of the unstable root-adhering soil

We used the first-order kinetics equation (see e. g., Richter and Söndgerath, 1990) as an unified framework for fitting the cumulative unstable root-adhering soil vs time curves from the data of either mechanical shaking or low dispersive ultrasonication. This simple mathematical function crosses the zero and has a physical signification, mainly by the constant rate, K, of the kinetics. The equations were as follows:

$$US_t = b*(1-exp^{-K*t}) \quad (1)$$

for the mechanichal shaking data, and

$$US_t = b*(1-exp^{-K*E}) \quad (2)$$

for the low dispersive ultrasonication data, with or without preliminary immersion of the soil:root system in water,
where US_t, in grams, is the total unstable root-adhering soil at time t, in seconds; b is a fitting parameter which described the limit of the unstable adherant soil mass; E, in Joules, is the output ultrasonic energy; and K, in s^{-1} or in J^{-1}, is the constant rate which characterized the whole kinetics.

Each experimental soil disruption curve was fitted by eye, using the Microsoft Excel package by varying up and down the two b and K parameters of the equation which described the kinetics.

For each soil disruption curve, a ln-transformation of equation (2) was used to identify the different rate parameters, K, which were the slopes of the successive linear relations occurring between $\ln(1-US_t/b)$ and the applied ultrasonic energy, E.

Root-adhering and bulk silty soil aggregates

Another set of pots was used for characterizing root-adhering soil aggregates. For each daily minimal soil water suction value of 10, 20 or 40 kPa, five plants were harvested, as described in this study and in its companion paper (Czarnes and Bartoli, 1998). Root-adhering soil aggregates were carefully separated from the roots using a paint brush and tweezers. To obtain a similar soil water suction value for each replication of each soil drying treatment, special precautions were taken as follows. We harvested five plants each day and for each harvest day, we started to separate the root-adhering soil aggregates from the roots of only one soil:root system, the others being kept in a cold chamber at 5°C to prevent soil drying. The bulk soil also was sampled to compare its characteristics with those of the root-adhering soil. Then, for each pot, the root-adhering soil and the bulk soil were placed separately in open boxes for air-drying for one week at room temperature.

Then, aggregate water and organic contents, aggregate porosity by mercury porosimetry, aggregate tensile strength, and friability were measured in both the air-dried root-adhering soil and its bulk soil counterpart.

Gravimetric soil water content was measured only on soil samples corresponding to a daily minimum soil water suction value of 20 kPa, with 5 pot replications, for either the root-adhering soil or its bulk soil counterpart. The soil samples were oven-dried for 24 hours at 105 °C before weighing.

Aggregate tensile strength, which is defined as the stress, or force per unit area, required to crush the aggregate under tension, was measured by a crushing test which has been previously described in detail by Dexter and Kroesbergen (1985) and Guérif (1988a). The use of aggregates with rather similar diameters was recommanded to minimize the effects of differences in diameter on the tensile strength (e. g., Guérif, 1988a, b; Hadas and Lennard, 1988). We therefore selected aggregates, of diameter between 2.00 and 4.76 mm, from the median gravimetric aggregate-size class, which was obtained by dry-sieving the collections of either root-adhering or bulk soil aggregates. These represented nearly 70 % of the aggregates.

For particles of incompressible material, the tensile strength Y of the particles, expressed in 10^4 N cm^{-2} (Pa), whereupon the particle cracks on a plane through the polar diameter, can be defined by:

$$Y = 0.576\ F / D^2 \qquad (3)$$

where F is the polar force at failure, in Newtons, D is the aggregate diameter, in cm, and the value of 0.576 has been used as a standard (Dexter 1988). The diameter of each individual soil aggregate was determined indirectly using its mass (Dexter and Kroesbergen, 1985), because the small size and the irregular shape of each aggregate rendered impossible a direct measurement of its diameter. Assuming that each individual soil aggregate was spherical (sphere volume = $\pi\ D^3\ /6$), and that the soil particle density was of 2.65 g cm^{-3}, leads to transformation of equation (3) into:

$$Y = 0.576\ F / \{(6/\pi\ (M/2.65 + V_p)\}^{2/3} \qquad (4)$$

where M is the mass of the studied individual aggregate, in g, and V_p is its pore volume, in $cm^3\ g^{-1}$, which was determined by mercury porosimetry.

For each studied pot, the number of subsamples was nearly 30 for either the root-adhering soil or its bulk soil counterpart, leading to 150 measurements for either the root-adhering soil or its bulk soil counterpart from each soil water suction series of 5 pot replications.

Aggregate friability was the second parameter used for characterizing the mechanical behaviour of the soil aggregates studied. Friability was defined by Utomo and Dexter (1981) as "the tendency of a mass of unconfined soil to break down and crumble under applied stress into a particular size range of small fragments". In this study, the measure of friability used was the coefficient of variation of the aggregate tensile strength (standard deviation:mean tensile strength percentage ratio), as recently recommended and discussed in detail by Watts and Dexter (1998), and Dexter and Watts (1998).

Parts of the root-adhering soil aggregates and their bulk soil aggregate counterparts, which were used for tensile strength measurements (see below), were analysed with a Carlo Erba (Series 2000) pore sizer mercury intrusion porosimeter, linked to the Macropore Unit Series 120/IBM PC computer, for determining the pore size distribution as a function of either pressure from 1.25×10^{-3} to 200 MPa or pore radii from 3.75 to 6 $\times 10^{5}$ nm. Samples were previously degassed at room temperature for 2 hours before analysis. The relative error of pore volume measurements was 5 to 15 % and 5 pot replications were analysed for either the root-adhering soil or its bulk soil counterpart.

Total carbon analysis which corresponds to organic carbon analysis (soils without carbonates) was carried out by a CHON Carbo Erba gas analyser on the crushed air-dried aggregates which were used for tensile strengh measurements. At each soil water suction value, 10 organic carbon analyses (5 pot replications and 2 subsamples by pot) were so carried out for each type of aggregate (root-adhering soil or bulk soil).

Statistics

Analyses of variance were performed using the Statview software program (version 1.03, STSC software products). The least significant difference test (LSD, Fisher test) and the Scheffe F-test were used for multiple range analyses.

Results and discussion

Soil water and shoot biomass characteristics

For each topsoil studied, the last soil drying from the three daily minimum soil water suction values had led to three different values of both gravimetric soil water content (bulk soil) and soil water suction. Soil water retention capacity was three to four times greater in the silty soil than in the sandy soil (Fig. 1a). The variability of the soil water suction was also greater for the sandy than for the silty topsoil (Fig. 1a). These data on rhizosphere water retention are consistent with those reported in detail in the companion paper of this study (Czarnes and Bartoli, 1998).

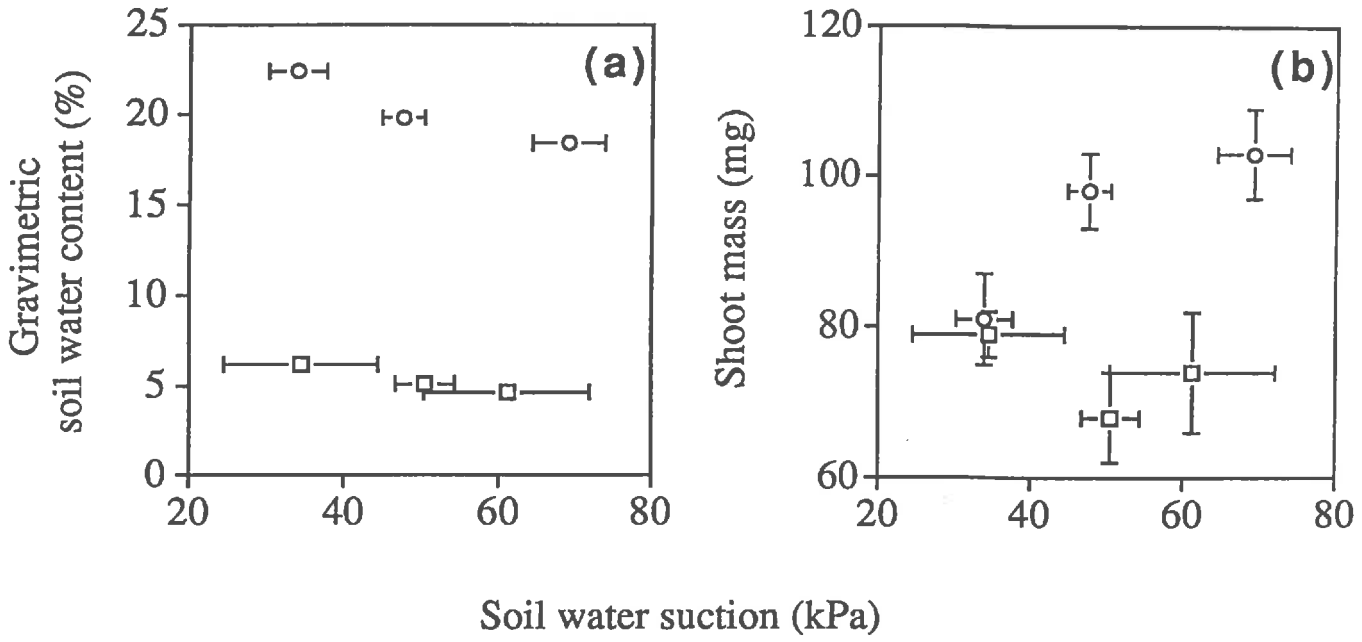

Figure II. 1. *Mean gravimetric water content (a) and mean shoot biomass (b) as a function of the final soil water suction of either silty (open circle symbols) or sandy (open square symbols) soil-filled pots with maize. Error bars show standard errors of mean values.*

Shoot biomass values were significantly smaller for maize growing into the sandy than into the silty topsoil (Fig. 1b). This discrepancy was already discussed by Czarnes and Bartoli (1998) who attributed it to (i) slow drying occurring in the sandy topsoil during the first period of the maize culture and (ii) the fact that no nutrient solution has been used during the culture, which should be a limiting growing factor for the sandy topsoil, poor in nutrients. On the other hand, no significant effect of soil water suction on the shoot biomass was observed, either for the silty or for the sandy topsoil. However, for the silty topsoil, the shoot biomass tends to be lower at 10 kPa than at 20 and 40 kPa (Fig. 1b) which indicated that the soil might have been too wet for good plant growth at 10 kPa.

Mechanical shaking of the soil:root system

The unstable:total root-adhering soil (UTRAS) was significantly nearly twice as large for the sandy than for the silty topoil (Fig. 2a). This difference was of a similar order of magnitude to that found between the shear strength values of the soils studied (Table 1; Czarnes *et al.*, 1998a). It confirmed that the soil strength characteristic varies with soil type (e. g., Davies, 1985; Young and Mullins, 1991; Watts and Dexter, 1993). This internal soil strength could be mainly attributed to resistances due to interlocking rough surfaces of compact particles (e. g., Panayiotopoulos and Mullins, 1985; Mitchell, 1993).

On the other hand, fluctuations of the UTRAS ratio as a function of the mean final soil water suction were similar for the two topsoils studied, with a minimum UTRAS ratio value at the median soil water suction of 47.6 or 50.5 kPa (Fig. 2a).

The validity of the first-order kinetics, equation (1), was confirmed for the first six cumulative amounts of unstable root-adhering soil, but not for the last two ones (Fig. 3). When the soil:root system was removed from the soil and placed on the mechanical shaker, it tended to dry rapidly which could explain why the two last cumulative data points were not fitted by equation (1). This relatively poor curve-fitting could explain why the K parameter, which describes the kinetic rate, did not statistically discriminate between the two topsoils studied (Fig. 2b) whereas the UTRAS ratio clearly did (Fig. 2a). However, we observed a tendency of an increase of the K value as a function of the mean final soil water suction, with a more pronounced soil water suction effect, still unclear, for the silty than for the sandy topsoil (Fig. 2b).

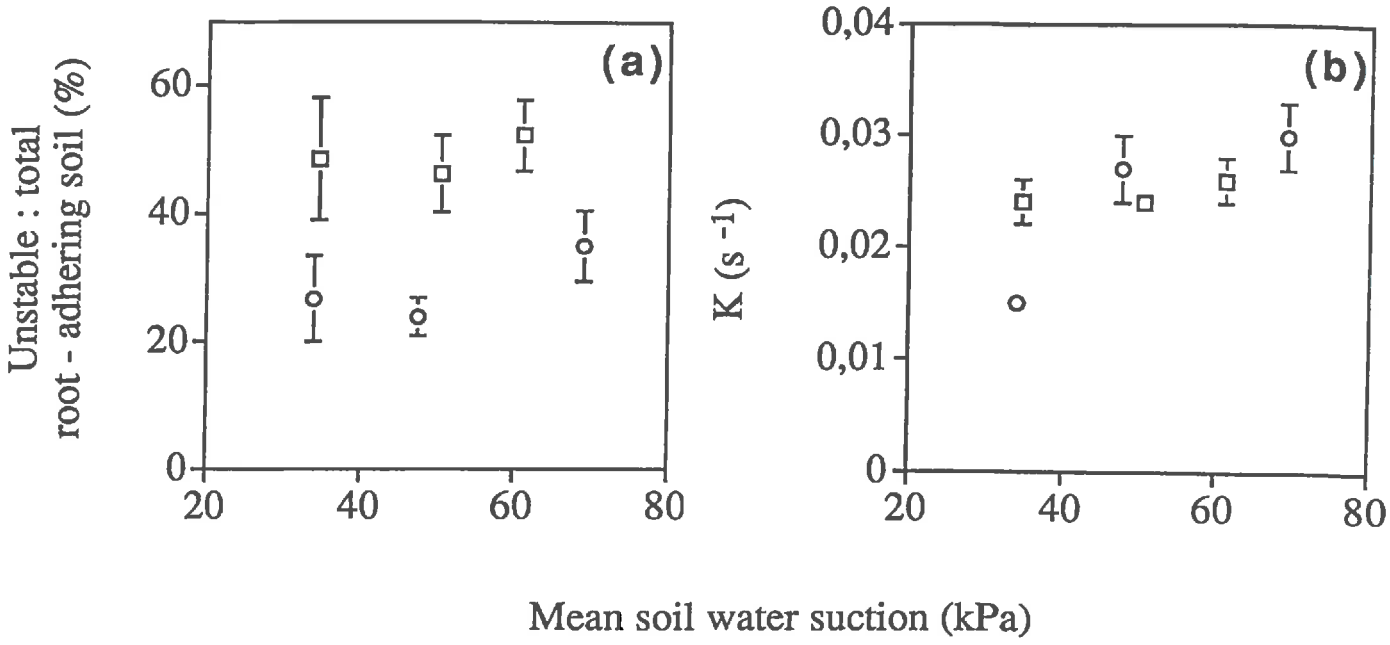

Figure II. 2. The mean unstable:total root-adhering soil ratio as a function of the final mean soil water suction (a) and the mean rate parameter, K, of the soil disruption kinetics, equation (1) as a function of the final mean soil water suction (b) during mechanical shaking of either the silty (open circle symbols) or the sandy (open square symbols) soil:root system. Error bars show standard errors of mean values.

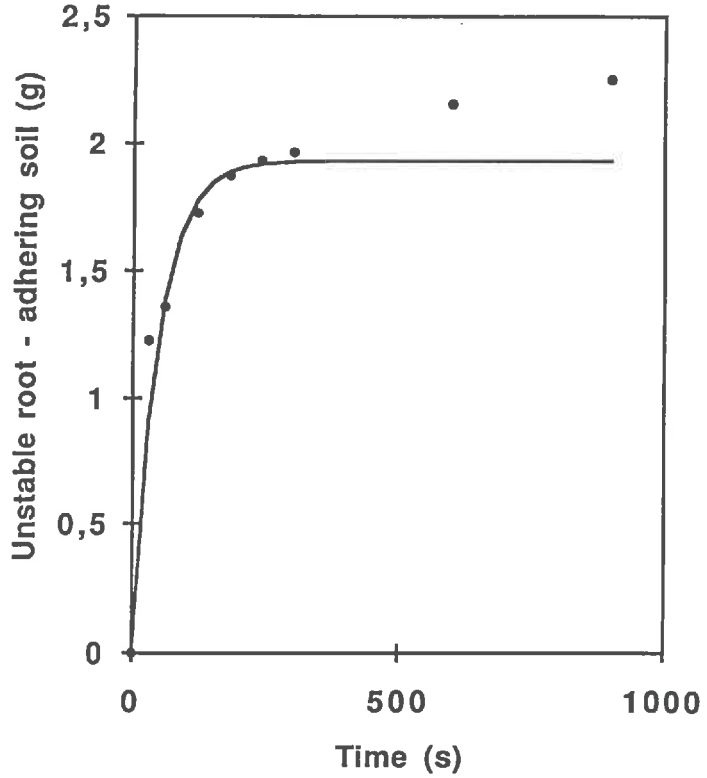

Figure 3: Example of soil disruption fitted kinetics (equation (1)) occurring during mechanical shaking of the silty soil:root system.

Image analysis of the soil:root system as a function of mechanical soil disruption

Direct soil:root interfacial rupture was not often observed whereas intra-aggregate failures frequently occurred during the mechanical shaking of the soil:root system. Image analysis of the soil:root system was attempted to characterize the spatial variability of the root-adhering disruption. The difference between the total black areas of the binary images corresponding to two successive times of the soil disruption kinetics quantified the unstable root-adhering soil between these two successive times. We did observe a positive correlation between this difference and the gravimetric amount of the unstable root-adhering soil between these two successive times (results not shown), as expected. The consistency of the results is largely due to the careful chrono-image analysis, with only slight changes of the spatial position of the roots (Fig. 4).

The normalized root and root-adhering area was a function of the distance between the outer roots. It decreased non-linearly from the crown of the root to the beginning of the apical root zone and this decrease was more pronounced for the maize root system from the silty than from the sandy topsoil (Fig. 5).

The dotted area of figure 5a or figure 5b corresponds to the amount of unstable root-adhering soil after 3 minutes of mechanical shaking. It increases from the apex to the crown of the root (Fig. 5). Then, the root apex-adhering soil was highly stable whereas the soil adherent to the other root domains was rather unstable, for both soils. Conversely, the soil adherent to the root apex was a continuous rhizosheath, whereas the soil adherent to the other root domains was formed of root-adhering aggregates (Figs. 4a and 4b). This spatial pattern was attributed to root exudates, which are produced mainly in the apical root zone (Groleau-Renaud, 1998).

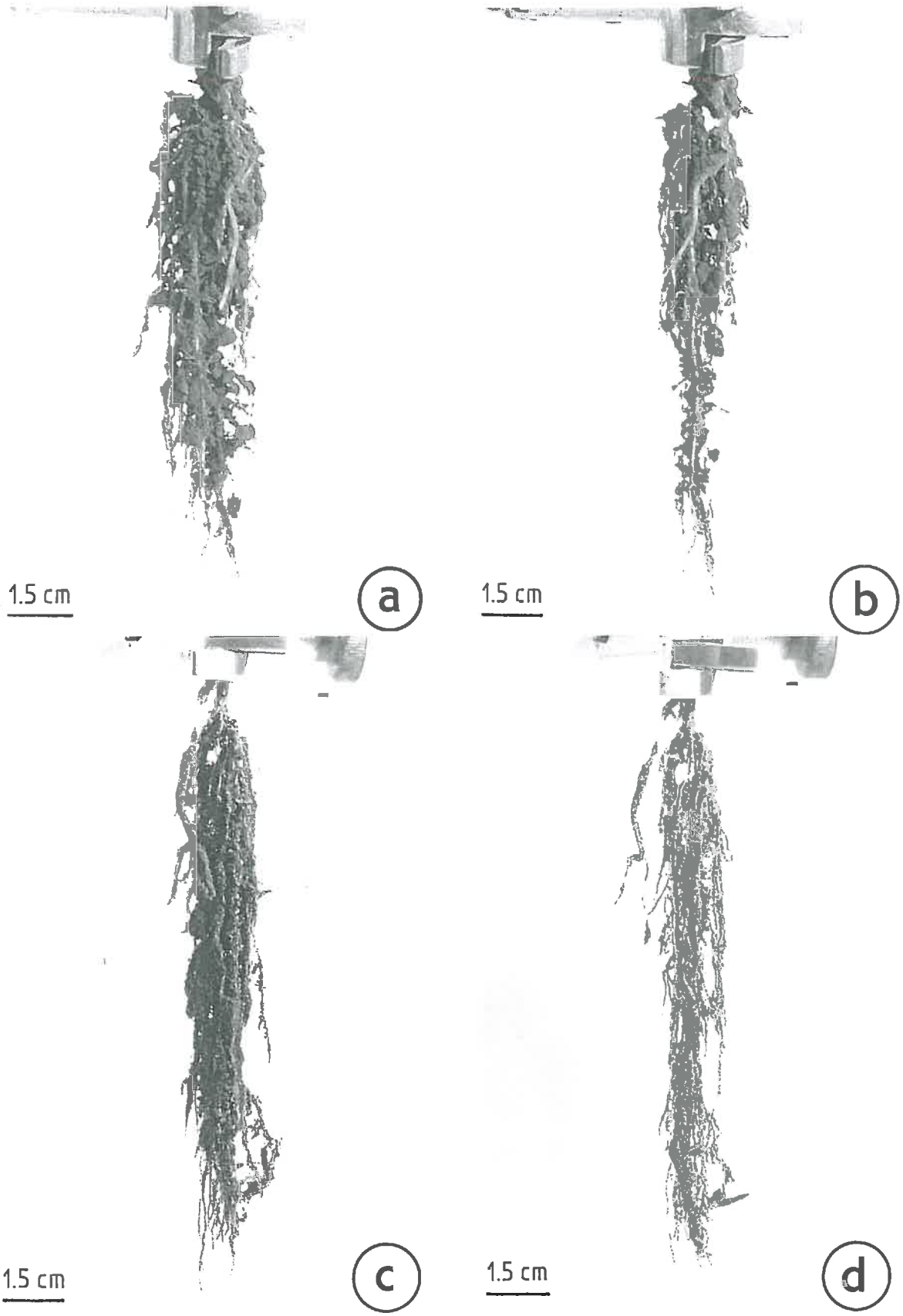

Figure II. 4. *Photographs after 0 (a and c) and 3 minutes (b and d) of mechanical shaking of the soil:root system for the silty (a and b) or the sandy (c and d) soil-filled pots with maize at a daily minimum soil water suction of 10 kPa.*

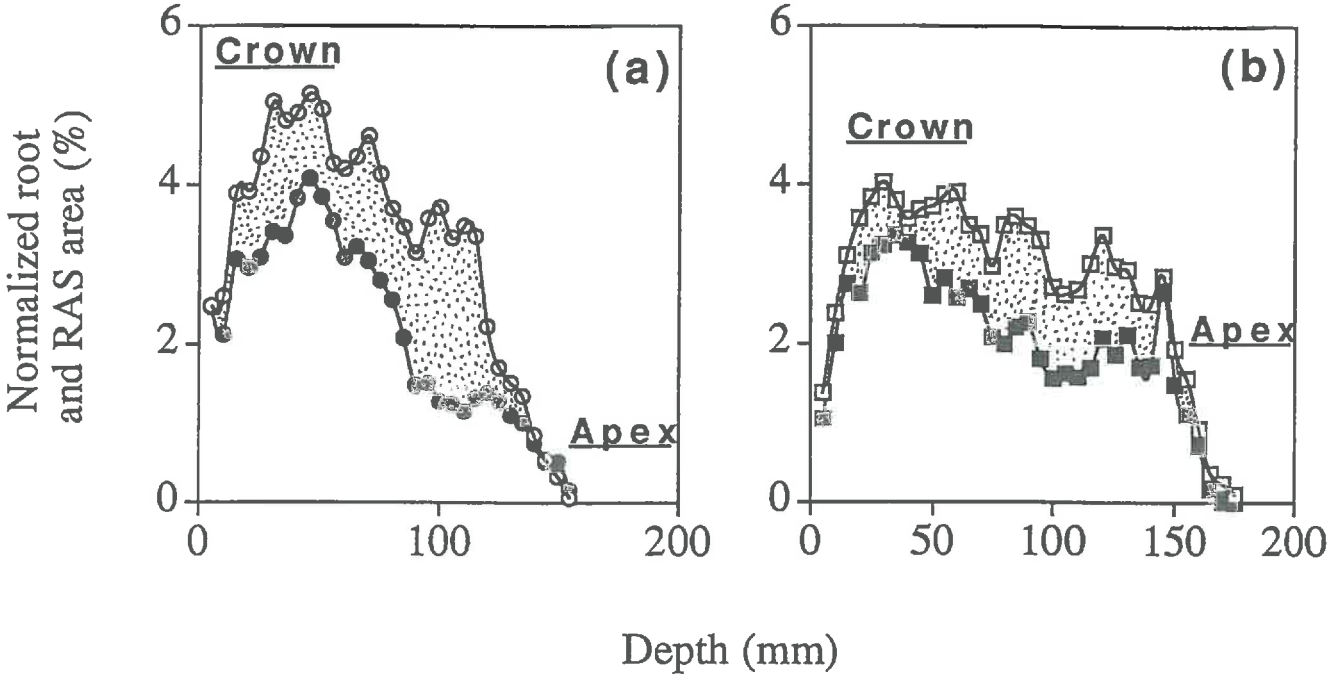

Figure II. 5. Chrono image analysis after 0 (open circle symbols) to 3 minutes (filled circle symbols) mechanical shaking, of the soil:root system for the silty (a) or the sandy (b) soil-filled pots with maize at a daily minimum soil water suction of 10 kPa. The dotted area correspond to the unstable root-adhering soil which was removed during the 3 minute period of mechanical shaking.

Low dispersive ultrasonication of the silty soil:root system

From 97 to 98 % of the root-adhering silty soil was disrupted by low dispersive ultrasonication of the soil:root system (Fig. 6a) and the validity of the ultrasonication first-order kinetics, equation (2), was confirmed for all the cumulative amounts of unstable root-adhering soil (Fig. 7a).

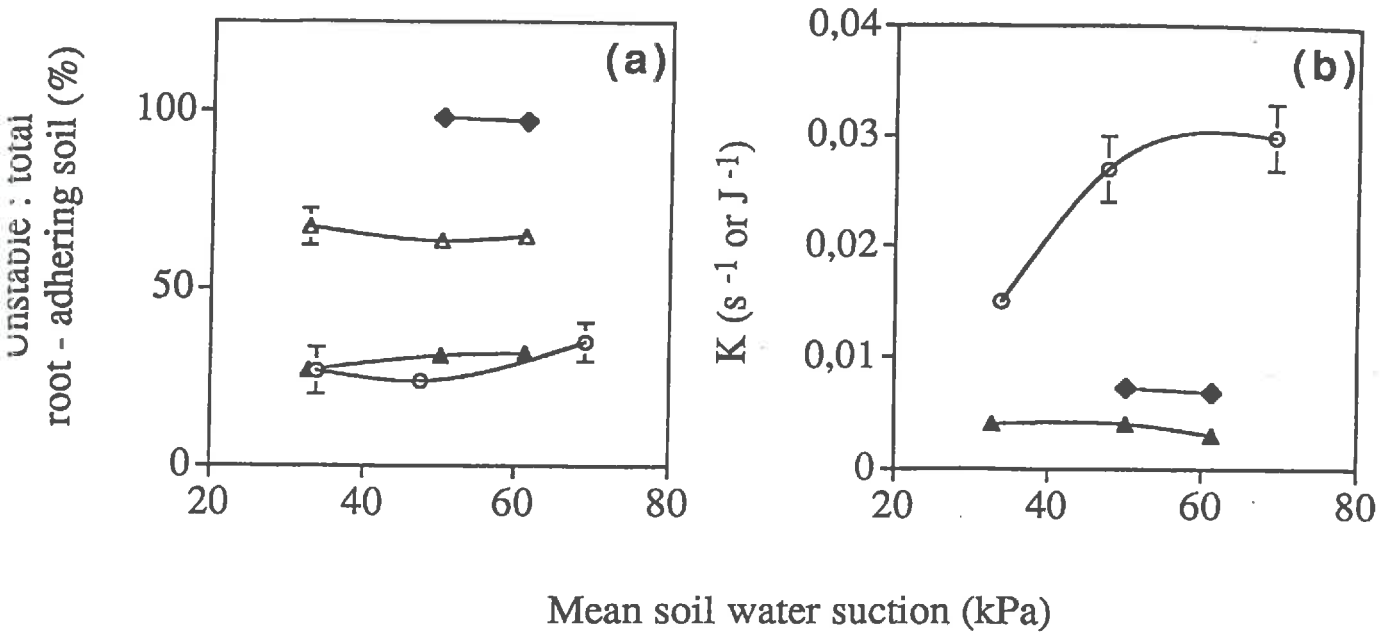

Figure II. 6. *The mean unstable:total root-adhering soil ratio as a function of the final mean soil water suction (a) and the mean rate parameter, K, of the soil disruption kinetics, equation (2) as a function of the final mean soil water suction (b) during mechanical shaking (open circle symbols), ultrasonication (filled lozenge symbols), water-immersion (open triangle symbols) followed by ultrasonication (filled triangle symbols) of the silty soil:root system. Error bars show standard errors of mean values.*

However, the ln-transformation of the equation (2) led to a decomposition of the ultrasonication kinetics into two parts: (i) a first fast period, occurring in the first 8 minutes of ultrasonication, which was characterized by a mean K value of 6.8 to 7.2 mJ^{-1} (slope of the first straight line plotted on figure 7b, with a standard error of 0.26 to 0.49 mJ^{-1}), and (ii) a second slower kinetic period thereafter, which was characterized by a mean K value of 1.5 to 1.6 mJ^{-1} (slope of the second straight line plotted on figure 7b, with a standard error of 0.05 to 0.06 mJ^{-1}).

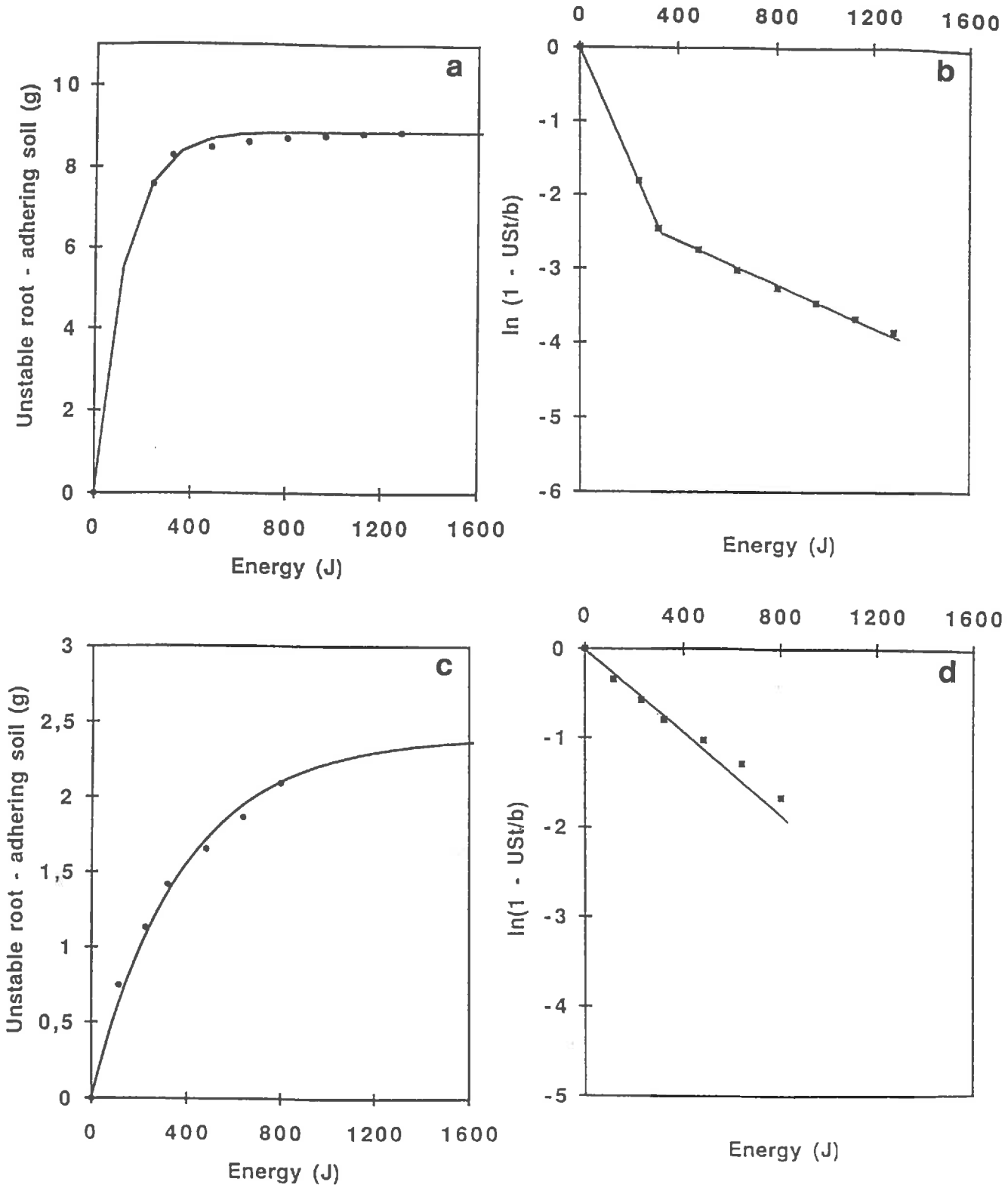

Figure II. 7. Examples of soil disruption fitted kinetics (equation (2)) (a and c), and their ln-transformed linear parts (b and c), occurring during ultrasonication of the silty soil:root system, with (c) or without (a) preliminary water-immersion. Figure b shows two embedded straight lines, whose slopes were the K and K' rate parameters of each soil disruption kinetics. Figure d shows only one straight line.

The question now arises as to the underlying mechanisms of these two time-embedded ultrasonication kinetics. Our hypothesis was that aggregate slaking, which is a key process for water-unstability of dry silty soil aggregates (entrapped air) (e. g., Concaret, 1967; Le Bissonnais, 1988; Bartoli *et al.*, 1992), would be a good candidate for understanding the first fast soil disruption kinetics. To evaluate this hypothesis we immersed each soil:root system in the water-filled ultrasonicator tank for 8 minutes, without ultrasonication. Then, the soil suspension was transferred from the ultrasonicator tank to a vial for oven-drying and weighing. Thewater-empty ultrasonic tank, with the soil:root system, was immediately filled again with distilled water for ultrasonication kinetics, as described in the materials and methods section. The results are as follows.

First, the UTRAS ratio was of 63.5 to 67.5 %, when roots were immersed in water (fig. 6a). This ratio was not affected by soil water suction. However, its standard error did decrease from 5.2 % to 1.2 % as a function of soil water suction (Fig. 6a). The UTRAS ratio value was similar to the one occurring at the end of the first fast ultrasonication kinetics, which supported our hypothesis. It was also of the same order of magnitude as the proportion of water-unstable silty soil aggregates (e. g., Le Bissonnais, 1988; Bartoli *et al.*, 1992). Immersion of the silty soil:root system in water seemed to be either more, or less, efficient for soil disruption than either mechanical shaking in air or ultrasonication in water, respectively (Fig. 6a).

Second, the proportion of the unstable root-adhering soil occurring after the ultrasonication phase was rather similar to that in the mechanical shaking data (Fig. 6a). We also observed that the UTRAS ratio, which was computed after ultrasonication of the root-adhering water-stable aggregates, tends to increase slightly as a function of soil water suction (Fig. 6a). Similarly, for the same silty topsoil, but for 3-day old maize seedlings, Czarnes *et al.* (1998b) have recently reported a slight decrease of the soil:root interfacial rupture energy as soil water suction increases, which was partly attributed to the increase of soil strength when the soil dried. The root-adhering water-stable soil could therefore be attributed to the proportions of the root-adhering soil aggregates which are still firmly adherent to the roots after the water-immersion slaking phase.

Finally, the cumulative amount of unstable root-adhering soil was better fitted by equation (2) when ultrasonisation was carried out after a preliminary water-immersion (Fig. 7c) than without (Fig. 7a). It could be attributed to a less

heterogeneous soil disruption process. Conversely, only one straight line was nearly observed on the ln-transformed graph of the kinetics equation (2), with a slope value, which is the mean K value, of 1 to 4 mJ^{-1} (Fig. 7d). One key point was that the K values were of the same order of magnitude of those characterizing the slow second part of the ultrasonication kinetics which was carried out without preliminary water-immersion of the soil:root system (Fig. 6b). This result again supports our hypothesis that the two parts of the ln-transformed kinetics curve correspond to two different physical processes: slaking for the first part, and soil:root rupture for the second one.

Root-adhering and bulk silty soil aggregates

Aggregate tensile strength was significantly higher in the root-adhering silty soil than in its bulk silty soil counterpart, except at the median soil water suction (Fig. 8a). Aggregate tensile strength of the root-adhering soil was also higher for the driest soil than for the two other wetter soils, whereas no soil water suction effect was found for the bulk soil (Fig. 8a).

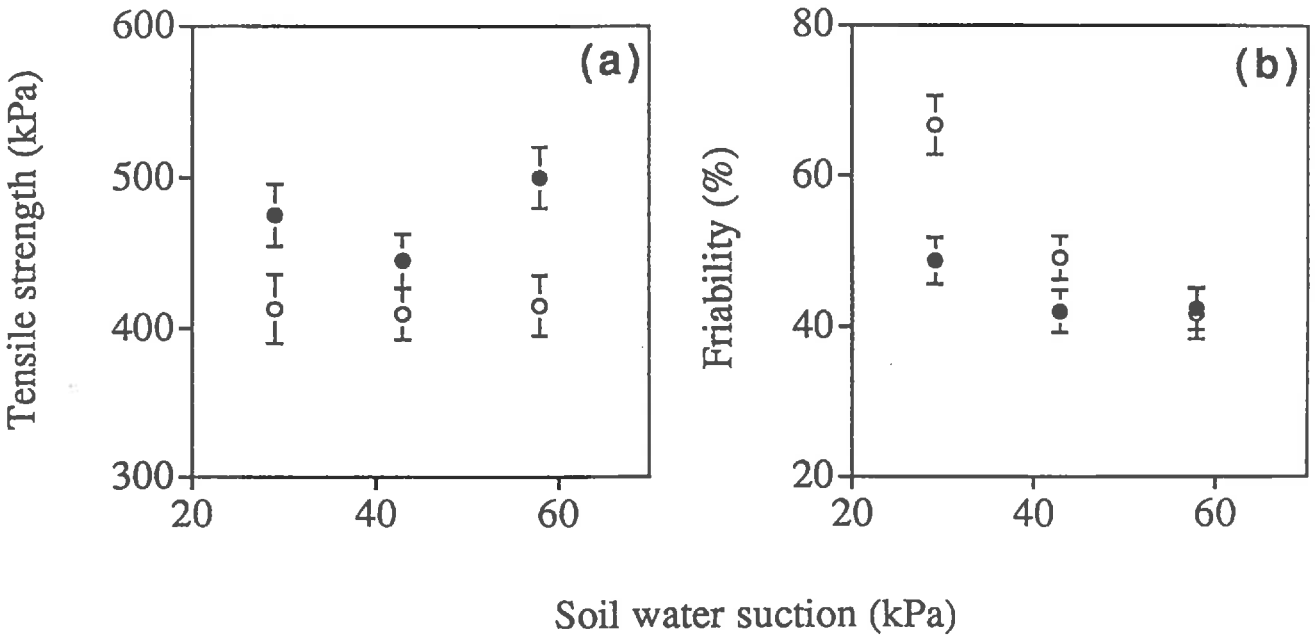

Figure II. 8. Mean aggregate tensile strength as a function of the final mean soil water suction (a) and mean friability as a function of the final mean soil water suction (b) of the root-adhering silty (filled circle symbols) or bulk silty (open circle symbols) soil. Error bars show standard errors of mean values.

Our first hypothesis was that this discrepency could be explain by a discrepency in aggregate porosity. Aa a matter of fact, aggregate porosity was negatively related to aggregate tensile strength in soils with a wide range of clay content (Dexter *et al.*, 1984a, b; Hadas, 1987a, b; Guérif, 1988b). In this study, aggregate pore volume was statistically similar for the root-adhering silty soil and for the bulk silty soil, for the three soil water suction values (Fig. 9a). It was attributed to the negligible soil shrinkage (4 % of the soil volume) which occurred when a soil cylinder of the studied topsoil was dried (Gomendy, 1996). The discrepancy occurring between aggregate tensile strength values of the root-adhering silty soil and of the bulk silty soil, therefore, cannot be attributed to a structural discrepancy between them. It leads to the hypothesis of an increase of intra-aggregate bonds by root exudates, which should be important during the 11 day-old plant growth phase (Matsumoto *et al.*, 1979).

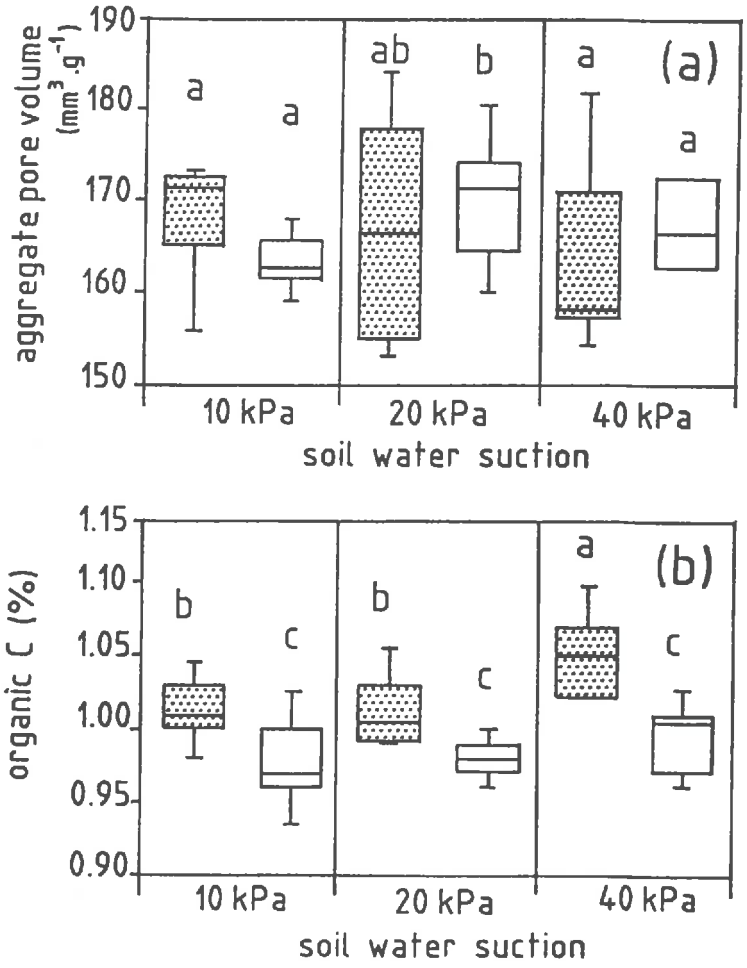

Figure II. 9. Notched box plots for aggregate mercury pore volume (a) and aggregate organic carbon content (b) of the root-adhering silty (dotted box) or bulk (open box) soil which was sampled from soil-filled pots with maize at a daily minimum soil water suction of 10, 20 and 40 kPa.

However, aggregate pore volume tends to be more variable and lower (at 20 and 40 kPa daily minimum soil water suction value) for the root-adhering soil than for its bulk soil counterpart (Fig. 9a). This can be attributed to the fact that the gravimetric soil water content was significantly lower, and more variable, for the root-adhering soil than for its bulk soil counterpart, with mean values of 18.6 % ± 0.4 % and 20.0 % ± 0.2 %, respectively, for the daily minimum soil water suction of 20 kPa (results not shown). Similarly, Horn and Dexter (1989) showed that the tensile strength of aggregates, which were adjacent to the roots, was increased by the intense and periodic drying of the soil due to plant evapotranspiration. Similar relationships between either the shear or the tensile strength and either the soil matric water potential or the soil water content have been also previously reported by Spoor and Godwin (1979), Utomo and Dexter (1981), Davies (1985), Guérif (1988b), Young and Mullins (1991) Kay and Dexter (1992), and Watts and Dexter (1993). The drying effect tends to pull the particles together, thus functioning as a cohesive force.

The validity of our hypothesis of an increase of intra-aggregate bonds by root exudates (and associated bacterial exudates) was tested using the results of organic carbon analysis of the studied aggregates. Aggregate organic carbon content was higher in the root-adhering soil than in its bulk soil counterpart, with a more pronounced difference for the driest soils (Fig. 9b). It leads to a positive but scattered relationship between aggregate tensile strength and organic carbon (Fig. 10a). Similarly, Dowdy (1975) and Chenu and Guérif (1991) previously observed an increase in tensile strength of clay as a function of adsorbed organic polymer or polysaccharide, respectively. As in this study, mechanical properties of kaolinite:polysaccharide associations were influenced by the progressive formation of interparticle polymer bonds rather than by clay fabric, which did not change significantly (Chenu and Guérif, 1991). A positive relationship between aggregate tensile strength and organic carbon also has been observed by Materechera *et al.* (1992) on rhizospheric fine sandy loam soil aggregates in soil-filled pots with a range of crops. Positive relationships between maize mucilage and aggregate water-stability have also been previously reported (e. g. Gückert, 1973; Cheshire, 1979; Morel *et al.*, 1991; Watt *et al.*, 1993).

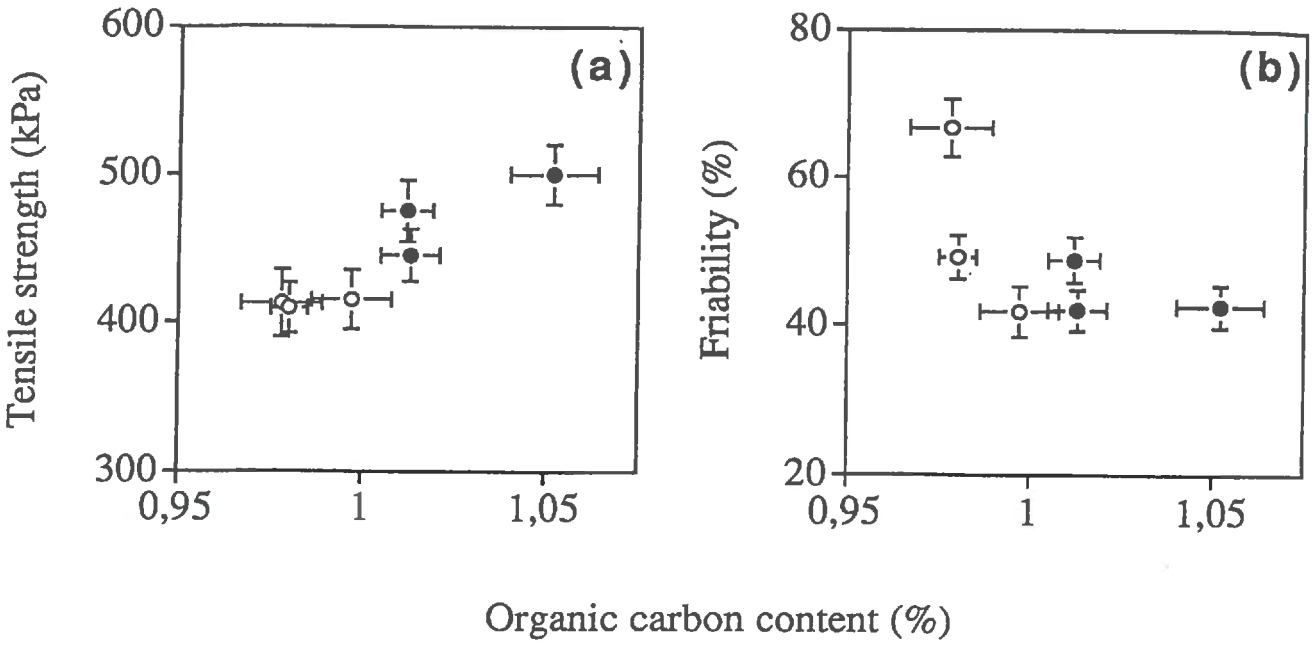

Figure II. 10. *Mean aggregate tensile strength as a function of aggregate organic carbon content (a) and mean friability as a function of aggregate organic carbon content (b) of the root-adhering silty (filled circle symbols) or bulk (open circle symbols) soil. Error bars show standard errors of mean values.*

Here, the key point is that the organic carbon content of the bulk soil is nearly constant for the three soil water suction values (Fig. 9b). It led to the interpretation that the difference between organic content of the root-adhering aggregates and that of their bulk soil aggregate counterparts can be the amount of root (and associated bacterial) exudate organic carbon, assuming that root hairs are not included in the root-adhering aggregates. This "root (and associated bacterial) exudate organic carbon" increased as soil water suction increased from 10 - 20 kPa to 40 kPa daily minimum soil water suction (Fig. 9a), explaining the significant companion increase of aggregate tensile strength (Fig. 8a). Similar effects of soil water suction on root exudation have been reported previously by Vancura and Garcia (1969) and Reid (1974) for pine (*Pinus poderosa* L.) and millet (*Panicum Miliaceum* L.) , respectively.

If we multiply this assumed amount of root (and associated bacterial) exudate organic carbon by the weight of the root-adhering soil we can obtain the asumed stock of the root (and associated bacterial) exudate organic carbon which had been produced by the maize plants during the 11 days of culture and which had not been biodegraded thereafter. It was of 2.04, 1.48 and 2.37 mg organic C

from each maize plant at daily minimum soil water suctions of 10, 20 and 40 kPa, respectively. These values of root exudate organic carbon were of the same order of magnitude that the mean amount of root exudate organic carbon recently obtained by Groleau-Renaud (1998). This author observed that 0.65 mg of root exudate organic carbon was produced during 24 hours by an 8 to 12 day-old maize plant. This plant grew under a controlled closed $^{14}CO_2$ atmosphere and the organic carbon was exuded into an hydroponic medium with randomly packed glass spheres of 1 mm diameter (Groleau-Renaud, 1998). It leads to overestimated values of root exudate organic carbon of 5.5 and 7.7 mg for 11 days, assuming a constant rate of root exudation and no biodegradation, which is not the case (Matsumoto *et al.*, 1979).

Aggregate friability decreased as soil water suction increased (Fig. 8b). This decrease was less pronounced for the root-adhering silty soil than for its bulk silty soil counterpart (Fig. 8b). Similarly, Utomo and Dexter (1981) and Causarano (1993) observed that soil friability generally increased as soil water content increased. Most soils were friable when moist and close to the plastic limit. We also know that shrinkahe and crack patterns occurred when soils have been submitted to a fast wetting period (e. g., Grant and Dexter, 1989). Friability could be an indirect measurement of the number of cracks in each volumetric unit, which should be further required for evaluating this hypothesis.

Aggregate friability was also significantly lower in the root-adhering silty soil than in its bulk silty soil counterpart, except for the driest soils (Fig. 8b). Conversely, although the relationship between aggregate friability and organic carbon content is highly scattered, we observed, for each pair of root-adhering and bulk silty soils, that aggregate friability decreased as organic carbon content increased, except for the driest soils (Fig. 10b). This decrease was also more pronounced for the wettest soil than for the drier ones (Fig. 10b). Similarly, Guérif (1988b; 1990) found that the variability of the aggregate tensile strength decreased as a function of organic carbon for a collection of aggregates from a tilled loam soil. In contrast, Watts and Dexter (1998) observed a positive correlation between aggregate friability and organic matter content for a range of cultivated temperate topsoils. In fact, Watts and Dexter also reported that aggregate porosity also increased as organic matter content increased, explaining, with a physical meaning, the positive relationship between friability and organic carbon content.

Conclusion

The main results of this study were as follows:

1- Intra-aggregate rupture was the main process occurring when the soil:root system was submitted to either mechanical shaking or water-immersion.

2- The spatial distribution of the unstable root-adhering soil after mechanical shaking showed that the continuous rhizosheath of the apical root zone was extremely stable, which was attributed to root exudates. The crown root zone with its network of outer roots also mechanically protects the root-adhering soil against disruption.

3- The "firmly root-adhering soil" (Watt et al., 1994), which was still stable after water-immersion, was nearly removed from the roots by low dispersive ultra-sonication. The kinetic rate parameter was 1 to 4 mJ^{-1}.

4- Ultrasonication kinetics, without preliminary water-immersion, was divided into two parts: the first, faster part was attributed to soil slaking, and the second, slower part was attributed to the rupture of the "firmly root-adhering soil" from the roots.

5- Aggregate tensile strength was higher for the root-adhering silty soil than for its bulk silty soil counterpart. It was related to the assumed amount of root exudates that were produced during maize growth, with a maximum under the driest soil conditions.

6- Aggregate friability decreased as a function of soil water suction, and this decrease was less pronounced for the root-adhering silty soil than for its bulk silty soil counterpart. It was attributed to both physical and biological interactions.

Acknowledgements

Financial support from the Alliance project (1995-1997) and the British Council Fellowship given to the first author for a period of 6 months (1996-1997) were greatly appreciated, allowing efficient cooperation between the Soil Science group of the Silsoe Research Institute, UK, and the Soil Aggregation team of the

Centre de Pédologie Biologique CNRS, France. The authors also thank Chritian Mustin and Vincent Rouiller, CPB - CNRS, Nancy, for valuable advices for the mathematical fitting of the curves, Sylvie Niquet, CIRIL, Nancy, for image analysis, Bernadette Gerard, CPB - CNRS, Nancy, for the organic crbon analysis and Gerard Burtin, CPB - CNRS, Nancy, for the mercury porosimetry data and the calibration of the output ultrasonic energy. Finally, the authors also thank the two anonymous reviewers for their constructive comments and suggestions on an early draft of the paper.

References

Bartoli F, Philippy R and Burtin G 1992 Poorly ordered hydrous Fe oxides, colloidal dispersion and soil aggregation. II Modifications of silty soil aggregation with Fe(III) polycations and model humic macromolecules. Journal of Soil Science 43, 59-75.

Beck D L, Darrah L L and Zuber M S 1988 Relationship of root tensile strength to vertical root pulling resistance in maize. Crop Science 28, 571-573.

Bengough A G, Croser C and Pritchard J 1997 A biophysical analysis of root growth under mechanical stress. Plant and Soil 189, 155-164.

Causarano H, 1993 Factors affecting the tensile strength of soil aggregates. Soil and Tillage Research 28, 15-25.

Chenu C and Guérif J 1991 Mechanical strength of clay minerals as influenced by an absorbed polysaccharide. Soil Sci. Am. J. 55, 1076-1080.

Cheshire M V 1979 Nature and origins of carbohydrates in soils. Academic Press, London.

Concaret J 1967 Etude des mécanismes de la destruction des agrégats de terre au contact de solutions acqueuses. Ann. Agronom. 18, 99-144.

Czarnes S and Bartoli F 1998 Wetting and drying cycles in the maize rhizosphere under controlled culture chamber conditions. I. Soil and daily minimal soil water suction effects (submitted to Plant and Soil).

Czarnes S, Dexter A R and Bartoli F 1998$_a$ Mechanics of two adherent centimetric remoulded soil balls : a preliminary examination (submitted to Soil and Tillage Research).

Czarnes S, Hiller S, Dexter A R, Hallett P D and Bartoli F 1998$_b$ Soil: root adhesion in the maize rhizosphere: the rheological approach (submitted to Plant and Soil).

Davies P 1985 Influence of organic matter content, moisture status and time after reworking on soil shear strength. Journal of Soil Science, 36, 299-306.

Dexter A R, 1988 Strength of soil aggregates and of aggregate beds. *In* Drescher J, Horn R and de Boodt M (eds.) "impact of water and external forces on soil structure" Catena Supplement No 11, 35-52.

Dexter A R and Kroesbergen B 1985 Methodologiy for determination of tensile strength of soil aggregates. J. agric. Engng Res. 32, 139-147.

Dexter A R, Kroesbergen B and Kuipers H, 1984a. Some mechanical properties of aggregates of top soils from the IJsselmeer polders. I. Undisturbed soil aggregates. Neth. J. Agric. Sci. 32, 205-214.

Dexter A R, Kroesbergen B and Kuipers H, 1984b. Some mechanical properties of aggregates of top soils from the IJsselmeer polders. II. Remoulded soil aggregates and the effect of wetting and drying cycles. Neth. J. Agric. Sci. 32, 215-227.

Dexter A R and Watts C W 1998. Tensile strength and friability. *In* Smith K A and Mullins C E (eds.) "Soil Analysis: Physical Methods", 2nd Edition, Marcell Dekker Inc., New York (in press).

Dowdy R H 1975 The effect of organic polymers and hydrous oxides on the tensile strength of clay. In: B A Stewart (editor), Soil Conditionners. Soil Sci. Soc. Am. Spec. Publ. Ser. 7, 25-33.

Ennos A R 1989 The mechanics of anchorage in seedlings of sunflower, *Helianthus annuus* L. New Phytol. 113, 185-192.

Ennos A. R 1990 The anchorage of leek seedlings: The effect of root length and soil strength. Annals of Botany 65, 409-416.

Ennos A R 1993 The anchorage mechanics of Maize, *Zea mays*. Journal of Experimental Botany 4, 147-153.

Gomendy V 1996 Variabilités spatiale et temporelle des propriétés structurales et hydriques des horizons de surface de la couverture limoneuse du bassin versant d'Orgeval (Brie). Nancy University pHD thesis.

Grant C D and Dexter A R 1989 Generation of microcracks in moulded soils by rapid wetting. Australian Journal of Soil Science 27, 169-182.

Greacen E L, Farrell D A and Cockroft B 1968 Soil Resistance of metal probes and plant roots. In Transactions of the 9th International Congress in Soil Science, pp. 769-779.

Groleau - Renaud V 1998 Contrainte mécanique et exsudation racinaire du maïs : incidence de la morphologie du système racinaire. INPL pHD thesis.

Gückert A 1973 Contribution à l'étude des polysaccharides dans les sols et leurs rôle dans les mécanismes d'agrégation: Nancy University State thesis, 124 pp.

Guérif J 1988_a Détermination de la résistance en traction des agrégats terreux: revue bibliographique et mise au point technique. Agronomie 8, 281-288.

Guérif J 1988_b Résistance en traction des agrégats terreux: influence de la texture, de la matière organique et de la teneur en eau. Agronomie 8, 379-386.

Guérif J 1990 Factor influencing compaction-induced increases in soil strength. Soil and Tillage Research 16, 167-178.

Hadas A 1987_a Dependence of "true" surface energy of soils on air entry pore size and chemical constituents. Soil Sci. Soc. Am. J. 51, 187-191.

Hadas A 1987_b Long-term tillage practice effects on soil aggregation modes and strength. Soil Sci. Soc. Am. J. 51, 191-197.

Hadas A and Lennard G 1988 Dependence of tensile strength of soil aggregates on soil constituents, density and load history. Journal of Soil Science 39, 577-586.

Hiltner L 1904 Uber neuere Erfahrungen und Probleme auf dem Gebeit der Bodenbakteriologie und unter besonder Berücksichtigung der Gründüngung und Brache. Arb. Dstch Landwrit. Ges. 98, 59-78.

Horn R and Dexter A R 1989 Dynamics of soil aggregation in an irrigated desert loess. Soil & Tillage Research 13, 253-266.

Kay B D and Dexter A R 1992 The influence of dispersive clay and wetting/drying cycles on the tensile strength of a red-brown earth. Aust. J. Soil Res. 30, 297-310.

Kraffczyk I, Trolldenier G and Beringer 1984 Soluble root exudates of maize: influence of potassium supply and rhizosphere micro-organisms. Soil Biology and Biochemistry 16, 315-322.

Le Bissonnais Y 1988 Analyse des mécanismes de la desagrégation et de la mobilisation des particules de terre sous l'action des pluies. Orléans University pHD thésis.

Lynch J M and Whipps J M 1990 Substrate flow in the rhizosphere. Plant and soil 129, 1-10

Materechera S A, Dexter A R and Alston A M 1992 Formation of aggregates by plant roots in homogenised soils. Plant and Soil 142, 69-79.

Matsumoto H, Okada K and Takahashi E 1979 Excretion products of maize roots from seedling to seed development stage. Plant and Soil 53, 17-26.

McCully M E and Canny M J 1989 Pathways and processes water and nutrient movement in roots. Plant and Soil 111, 159-170.

Mitchell J K 1993 Fundamentals of soil behavior, second edition. John Wiley & Sons, New York.

Morel J , Habib L, Plantureux S and Gückert A 1991 Influence of maize root mucilage on soil aggregate stability. Plant and Soil 136, 111-119.

North P F 1976 Towards an absolute measurement of soil structural stability using ultra-sound. J. Soil Sci. 27, 451-459.

Panayiotopoulos, K. P. and Mullins, C. E. 1985 Packing of sands. Journal of Soil Science 36, 129-139.

Parke J L, Liddell C M and Clayton 1990 Relationship between soil mass adhering to pea taproots and recovery of Pseudomonas Fluorescens from the rhizosphere. Soil Biol. Biochem. 22, 495-499.

Reid C P P 1974 Assimilation, distribution and root exudation of ^{14}C by *poderosa* pine seedling under induced water stress. Plant Physiology 54, 44-49.

Richter O and Söndgerath D 1990 Parameter Estimation in Ecology. The link between data and models. VCH, Weinheim and New York, 218 p.

Spoor G and Godwin R J 1979 Soil deformation and shear strength characteristics of some clay soils at different moisture contents. Journal of Soil Science 30, 493-498.

Sprent J I 1975 Adherence of sand particles to soybean roots under water stress. New Phytol 74, 461-463.

Utomo W.H. and Dexter A.R., 1981. Soil friability. J. Soil Sci. 32: 203-213.

Vancura V and Garcia J L 1969 Root exudates of reversibly wilted millet plants (*Panicum Miliaceum* L.) Oecol. Plant 4, 93-98.

Watt M, McCully M E and Canny M J 1994 Formation and stabilization of rhizosheaths of Zea mays L. Effect of soil water content. Plant Physiol. 106, 179-186.

Watt M, McCully M E and Jeffree C E 1993 Plant and bacterial mucilages of the maize rhizosphere: comparison of their soil binding properties and histochemistry in a model system. Plant and Soil 151, 151-165.

Watts C W and Dexter A R 1993 A hand-held instrument for the in situ measurement of soil shear strength in the puddled layer of paddy fields. J. agric. Engng Res. 54, 329-337.

Watts C W and Dexter A R 1998 Soil friability: theory, measurement and the effects of managelent and organic carbon content. European Journal of Soil Science Science 49, 73-84.

Young I M 1995 Variation in moisture contents between bulk soil ands the rhizosheath of wheat (*Triticum aestivum* L. cv. Wembley). New Physiologist 130, 135-139.

Young I M and Mullins C E 1991 Factors affecting the strength of undisturbed cores from soils with low structural stability. Journal of Soil Science 42, 205-217.

CHAPITRE III

ADHESION SOL:RACINES DANS LA RHIZOSPHERE DU MAÏS: L'APPROCHE RHEOLOGIQUE

Ce chapitre comprend un article soumis à la revue Plant and Soil.

Czarnes S., Hiller S.,Dexter A.R., Hallett P.D. and Bartoli F. Soil:root adhesion in the maize rhizosphere: the rheological approach

ADHESION SOL:RACINES DANS LA RHIZOSPHERE DU MAÏS: L'APPROCHE RHEOLOGIQUE

Présentation et objectifs de l'étude sur l'adhésion sol:racines dans la rhizosphère du maïs par l'approche rhéologique

Nous avons pu observer, qu'une agitation mécanique, ou une immersion dans l'eau, du système sol limoneux:racines permettait de casser et de récupérer 30 à 60% des agrégats adhérents, respectivement (chapitre II). Le sol adhérent stable, après immersion dans l'eau, a pu être séparé des racines par ultrasonication modérée. L'energie de séparation sol:racines apparaît donc être plus élevée que l'energie de rupture intra-agrégat.

Aussi est ce la raison pour laquelle une approche rhéologique de l'adhésion sol:racines a été entreprise en utilisant cette fois-ci de toutes petites racines de maïs, agées de 4 jours, ainsi qu'un dispositif spécifique de croissance racinaire par adhésion sur une surface plane de sol, de façon à mieux maitriser les paramètres biologiques et physiques intervenant dans le système. Pour cette étude, des observations morphologiques de l'interface sol:racines ont été couplées à des mesures d'energie de rupture de cette interface.

L'analyse de ces résultats expérimentaux va nous permettre d'identifier les différents paramètres de contrôle de l'adhésion sol:racines afin de formuler, puis de valider, une théorie de l'adhésion sol:racines.

Soil:root adhesion in the maize rhizosphere: the rheological approach

S. CZARNES[a, b], S. HILLER[a], A.R. DEXTER[a, c], P. D. HALLETT[a, d] and F. BARTOLI[b]*

[a] *Silsoe Research Institute, Wrest Park, Silsoe, Bedford MK45 4HS, United Kingdom*

[b] *Centre de Pedologie Biologique UPR 6831 du CNRS associé à l'Université Henri Poincaré - Nancy I, BP 5, 54501 Vandoeuvre-lès-Nancy, France*

[c] *present address: Instytut Uprawy Nawozenia i Gleboznawstwa, ul. Czartoryskich 8, 24 - 100 Pulawy, Poland*

[d] *present permanent address: Scottish Crop Research Institute, Invergowrie, Dundee DD2 5DA, United Kingdom*

Key words: maize, matric water potential, rhizosphere, soil:root adhesion, soil:root contact surface area, soil surface properties.

* Corresponding author. Present address: Centre de Pédologie Biologique UPR 6831 du CNRS associé à l'Université Henri Poincaré - Nancy I, BP 5, 54501 Vandoeuvre-lès-Nancy, France

Tel: (33) 3 83 51 08 60 Fax: (33) 3 83 57 65 23 e-mail: czarnes@cpb.cnrs-nancy.fr

Résumé

L'adhésion d'une racine de 4 jours à une surface de sol remanié a été étudiée en fonction de la texture du sol et de son potentiel hydrique. Un dispositif de croissance racinaire à la surface du sol a été mis au point afin d'effectuer des mesures de force de rupture interfaciale sol:racine en fonction du déplacement de la racine par rapport à la surface du sol.

Une théorie de l'adhésion sol:racine, à signification physique, a été formulée et validée à l'aide de ces mesures de force de séparation sol:racine. L'énergie de rupture interfaciale qui permet de séparer la racine du sol est fonction de la surface spécifique du sol et de la surface de contact sol:racine, estimée à partir la longueur racinaire totale. Les interactions biologiques et physiques contribuant à cette adhésion sol:racine ont pu être identifiées et discutées.

Abstract

Adhesion of the seedling maize root to soil has been studied as a function of both soil texture and water matric potential. A device for growing root on soil surface was designed and was used to produce roots which adhered to the soil. A soil:root peeling test was developed to quantify root:soil adhesion. The results have been analysed through a combination of rheological and video chrono analysis.

A soil:root adhesion theory, of real physical significance, has been formulated and subsequently validated using peeling test data. The soil:root interfacial rupture energy was controlled mainly by a product of microscopic soil specific surface area and root length, which in its turn controlled the macroscopic contact surface area between the root and the soil. Biological and physical interactions contributing to soil:root adhesion were also analysed and discussed.

Introduction

The rhizosphere is the localised volume of soil around plant roots directly influenced by the root activity and their associated microorganisms (Hiltner, 1904). Virtually all the nutrients and water absorbed by a plant must pass through the rhizosphere, and through the soil:root interface thereafter making the physical, chemical, and biological properties of this zone important to plant growth.

Some studies focused on the rhizosphere have indirectly shown that the geometrical and hydraulic properties of the soil:root interface can be key parameters for plant growth, especially during intensive soil drying.

In the field, Barataud *et al.* (1995) have observed a loss of total hydraulic conductivity of a soil:tree system under drought conditions whereby the metabolism of the trees seemed to remain unaffected. These authors have used an analytical model to explain these results by an increase of the soil:root resistance. They have also demonstrated that this resistance becomes the limiting factor when the volumetric soil water content decreases below a threshold value. Other experimental studies have shown that the sum of the resistances in the plant and the soil was too small to account for the fall in water pressure between the leaf xylem and the soil, especially when plants were growing in sandy soils, which were prone to dry rapidly. A resistance at the soil:root interface, caused possibly by poor contact between the roots and the soil, has been proposed by Veen *et al.*, (1992) to account for this discrepancy.

The mechanical properties of the soil:root interface influence root elongation and the tensile resistance for characterizing root anchorage in the soil (e. g. Greacen *et al.*, 1968; Beck *et al.*, 1988; Ennos, 1989, 1990, 1993; Bengough *et al.*, 1997). Soil:root contact has been also characterized using minirhizotron and thin section techniques (Gijsman *et al.*, 1991; van Noordwijk *et al.*, 1992; Kooistra *et al.*, 1992; Veen *et al.*, 1992) whereas, to our knowledge, no study has been carried out on the adhesion of roots to soil.

Our study has two aims. First, we characterize, for maize seedlings, the soil:root interfacial pulling resistance as a function of soil texture and matric water potential. Second, we develop a soil:root adhesion theory by relating the soil:root interfacial rupture energy to the contact surface area between the roots

and the soil, the soil:root interfacial adhesion energy and the dissipation energy occurring during the rupture of the soil:root interface.

Materials and methods

Soil sampling and characteristics

Selected properties of the three topsoil samples are listed in Table 1. The Bordeaux topsoil belongs to the podzolic soils of the Landes area (South-Western France) which are developed from Miocene and quaternary sandy marine and alluvial materials. The soil had been under pine forest for one century and under maize for 4 years. It was kindly supplied by D. Plenet, INRA Bordeaux. The Orgeval topsoil belongs to the silty leached brown soils of the Parisian Basin which have developed from quaternary silty eolian materials and have been under intensive wheat agriculture for the past 40 years. The La Bouzule topsoil belongs to a loam leached brown soil of Eastern France which have developed from eolian quaternary silty materials and which have been under intensive wheat and maize agriculture for the last 20 years.

The three soils have very different clay contents (Table 1) and from herein the Bordeaux, Orgeval, and La Bouzoule topsoils will be referred to as sandy, silty and clayey respectively. Both Atterberg limits and shear strength values increased as a function of clay content (Czarnes *et al.*, 1998), as did the CEC values and, more significantly, the BET surface area values, which were computed from nitrogen adsorption data (Table 1). The clay fraction of the sandy topsoil was composed mainly of smectites and kaolinite, with traces of illite and quartz. Those of the silty or the clayey topsoil were composed of 35 % or 45 % of < 0.1 µm smectites and some illite-smectite interstratified clays, respectively, whereas their coarse 0.1 to 2 µm sub-fractions were composed of illite, vermiculite and kaolinite whose proportions are similar, and of traces of quartz. Organo-mineral clay fractions were also poor in organic carbon (OC), for the long-term cultivated silty and clayey topsoils, with OC values of 3.5 % and 2.3 %, respectively, whereas they were rich for the short-term cultivated sandy topsoil, with an OC value of 27.6 %. Conversely, organic matter of the clay fraction was rich both in nitrogen and in oxygenated functional groups for the silty and the clayey topsoils, whereas it was

polyaromatic and rich in aliphatic functional groups for the sandy one (C/N ratio and IR spectroscopy data, not shown).

Finally, calcium was the dominant exchangeable cation (70 to 95 %) of the studied topsoils which were also free of calcium carbonates, leading to pH values of soil suspensions in water of 6.8 to 7.0, except for the sandy organic topsoil which was relatively acid (pH value of 5.6).

Topsoil samples	Soil types	Particle-size distribution (%)					BET Specific surface area (m2/g)	pH $_{H2O}$	0.5 M NH_4Cl CEC (mg/100g)	Organic carbon content (%)
		coarse sand >200 µm	fine sand 50-200 µm	coarse silt 20-50 µm	fine silt 2-20 µm	clay < 2 µm				
Bordeaux	podzolic	85.7	8.1	0.9	3.6	1.9	0.3	5.6	6.8	1.7
Orgeval	silty leached brown	1.3	2.7	44.6	29.8	16.4	13.6	6.8	20.5	0.8
Bouzule	loam leached brown	11.5	4.2	19.6	27.3	33.1	40.8	7.0	29.0	1.8

Table III. 1. *Main soil characteristics*

Mechanics for two adherent remoulded silty topsoil balls

Two adherent remoulded silty topsoil balls, of diameter 30 mm and porosity 0.37 cm^3 cm^{-3}, were continuously pressed together until their flat interfaces reached about half the initial diameter (0.47). The compression axial force was recorded as a function of the axial compression displacement. Details of this experimental method have been reported elsewhere (Czarnes *et al.*, 1998).

A complementary set of experiments was designed and carried out for this study in order to characterize soil:soil adhesion. First, as above, the axial compression force was measured as a function of the soil:soil displacement. Then, this pair of adherent, flattened, remoulded silty topsoil balls was pulled apart, recording the decrease of compression force to zero, and the subsequent increase in tensile force, as a function of axial displacement. A composite graph of tensile force versus displacement was then constructed, in which three areas were evident, corresponding to (i) the plastic part of the compression stress (cohesive resistance), which was always dominant, (ii) the elastic part of the compression stress, and (iii) the soil:soil adhesion energy, which was always very small (Fig. 5).

Remoulded topsoils used for the soil:root peeling test

Each topsoil was air-dried and sieved to < 4 mm diameter. It was mixed gently by hand, in a plastic bag, with the appropriate amount of distilled water in order to obtain the desired water content which was determined from the water retention curve (drainage). At a suction value of 10 kPa, the gravimetric water contents were 9, 28 and 31 % for the sandy, silty and clayey topsoils, respectively. For the silty topsoil, two other suction values of 50 kPa and 100 kPa, were also selected and had gravimetric water contents of 23 and 18 %, respectively.

Each remoulded topsoil sample was kept in its plastic bag at about 10 °C for 4 to 7 days in order to facilitate equilibration and homogeneisation of water in the soil. Then, the remoulded topsoil was packed gently into a PVC cylinder of 64 mm internal diameter and 42 mm internal height which was close at the bottom. This resulted in a soil volume of 60 cm^3. The mean porosity value was of 0.37 $cm^3\ cm^{-3}$ for both the silty and clayey remoulded topsoils whereas it was 0.50 $cm^3\ cm^{-3}$ for the sandy one, assuming particle density value of 2.65 g cm^{-3}. During soil packing, the topsoil surface was also prepared to be as smooth as possible in order to have the best soil:root contact.

Seedling selection

The maize seeds which were used for this study belong to the *Zea mays cultivar DEA*. They were submitted to an antifungal treatment by Pioneer France Maïs, Toulouse, France, which kindly supplied us with the seeds. Batches of seeds were germinated on filter papers in Petri dishes for about three days. A limited number of seedlings which were selected were characterized by very similar radicle features. They were flat and straight, their weigths were close to 0.40 g and their lengths were in the range 14 to 20 mm.

Seedling growth on soil surfaces

Each selected 3-days-old seedling was transferred onto the surface of the remoulded topsoil, which partly filled the PVC cylinder. Special precautions were then taken as follows. First, a short length of strong plastic fishing line, with a high Young's Modulus, was attached to the seedling adjacent to the seed. By this means, the seed, and then the root of the seedling, could be progressively separated from the soil during the soil:root peeling test (Fig. 1).

Secondly, in order to reduce the seed:soil adhesion, a small piece of non-porous and flexible latex membrane was placed on the area of the topsoil where the seed was to be placed (Fig. 1). Thirdly, the seedling was placed on the topsoil surface next to one side of the cylinder, to make possible the growth of the root as far as the opposite side. Root elongation was limited by the horizontal size of the cylinder which resulted in a maximum possible root length of 55 mm, the seed length being about 5 mm. Fourthly, a circular latex membrane of diameter similar to the internal diameter of the cylinder, was placed on top of the seedling (Fig. 1). Fifthly, the cylinder was closed by placing a circular porous and deformable polystyrene cap, of diameter of 64 mm and height 25 mm, on the top of the membrane, followed by a PVC cap especially adapted to the cylinder (Fig. 1). Finally, the closed cylinder was rotated through 90 ° to orientate the root into the vertical position required for natural geotropic growth which occurred for one day in darkness at 25 °C (Fig. 1).

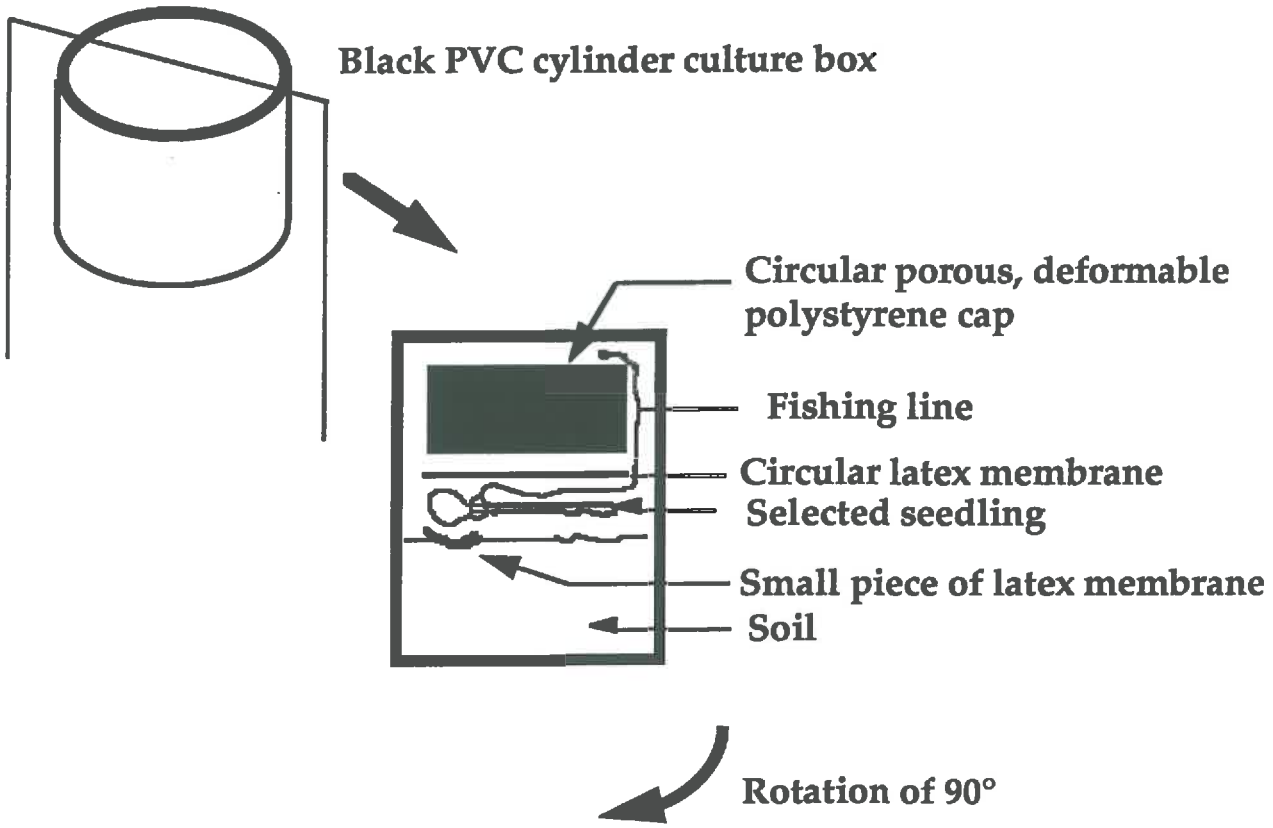

Figure III. 1. Special root growth design

Root uniaxial tensile test

This test measures the stress required to break a root in tension. It required special modification to conventional methods since the roots of young plants are not sufficiently fibrous or strong to be clamped. The two ends of a piece of root of 20 mm length were glued onto little rods which were clamped. The root sample was placed vertically, with one extremity fixed and the other one moving by the verticaly displacement of the loading-frame cross-head, controlled by motor-driven screws. The root was stretched at a rate 0.5 mm min^{-1}. The tensile force in the specimen was continuously measured by an electronic load cell (2N) until rupture occurred. The extension was also electronically monitored up to the point of root fracture. Force:extention or stress:strain curves, normalized with reference to the root dimensions, were subsequently plotted. The secant elastic modulus of the roots was finally calculated.

Root tensile cycling test: is root stretching elastic?

A straight line result from the unidirectional tensile stress:strain test points to the possibility of elastic mechanical behaviour, but this is not necessarily the case. For this reason, a complementary study of the behaviour of roots submitted to repetitive cyclic loading tests was carried out.

Using the tensile test machine, cycling was carried out between a lower limit of 0.001 N each time, and an upper limit set to increase incrementally by 0.1 mm on each cycle until root failure (or a total displacement of 1 mm).

This test allows the loading and unloading curves to be compared. The strain energy absorbed by the stretched specimen is equal to the externally-produced work. This is determined directly, either in Joules from the area under the force:extension curve, or per unit volume (in J m^{-3}) from the area under the stress:strain curve. The energy recovered in elastic recoil is the area under the unloading curve, and the energy lost by viscous damping is the area between the two curves (the hysteresis loop). The ratio of the energy lost to the strain energy absorbed (mechanical hysteresis), and the ratio of the strain energy recovered to the total energy input (resilience) which is a measure of the elastic efficiency of the material, can both be calculated (Vincent, 1992; Niklas, 1992).

Root bending test

In the soil:root peeling test, described below, the geometry is complex. Parts of root are in tension, parts are in bending and some energy is stored in the root:soil adhesion. It is therefore useful to know how much energy is needed to stretch a root and to bend a root. Also, whether much energy is lost due to hysteresis. In this way, it should be possible to understand the partitioning of energy in the soil:root peeling test. In this root bending test, the root sample was placed horizontally, attached at its tip by some glue to an horizontal support, and the seed side of the root was pulled up by the vertical displacement of the cross-head of the universal test machine at the rate of 5 mm min^{-1}.

Soil:root peeling test

Twenty four hours after being transferred, the seedlings were submitted to a peeling test using a universal test machine (Type DN 10, Davenport-Nene with v. 6.4 control software) fitted with a 2N load cell (see Fig. 2_a).

The free end of a length of fishing-line which was attached to the root adjacent to the seed, was attached to a piece of wood 70 cm in length (Fig. 2_b), which was in turn attached to the load cell.

A constant speed of 5 mm min^{-1} was used and the force F required to pull apart the soil and the root was recorded on a chart to give a pulling force:displacement curve. The soil:root interfacial rupture energy, W_{ru}, was caracterised by the following relation:

$$W_{ru} = F/b\,(1 - \cos\theta) \qquad (1)$$

where F/b is the soil:root peel force per unit width, termed the soil:root peel energy or peel strength and θ is the soil:root peel angle, which is here assumed to be negligible, leading to an equality of the soil:root interfacial rupture energy and the experimentally-determined soil:root peel energy.

In order to better understand the different mechanical processes occurring during the soil:root peeling test, a video camera with a macro objective was used, located above the cylinder (Fig. 2_b) and connected to a video recorder system.

To assist in the interpretation of soil:root peeling test results, experiments were also carried out on various model systems using an identical test geometry. One such experiment utilised a strip of flexible polycarbonate film (in place of a root), attached to a horizontal metal support (in place of the soil surface) using 'Postit' paper adhesive. The film was selected on account of its Young's modulus, and preliminary tensile and bending tests dictated the strip width and thickness which most closely simulated the mechanical behaviour of a maize seedling root. This model system was very similar in scale to the soil:root system. A larger-scale model system comprised a 300 mm plastic ruler, attached along its length to a horizontal support by means of 'Velcro' tape. Both of the above systems were used in simple tensile peeling tests, as well as for cyclic tests between zero and progressively larger incremental displacements.

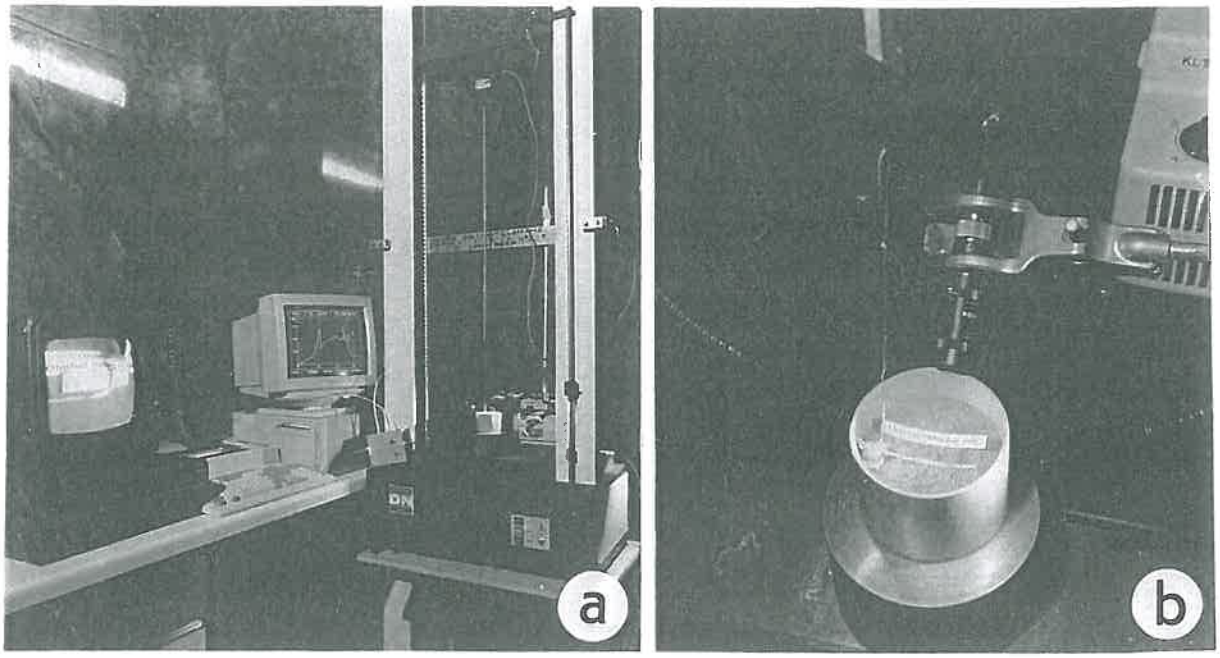

Figure III. 2. Equipment used in the soil:root peeling test.
(a) general overview of the apparatus showing the Davenport-Nene machine and its associated computer and video-camera systems.
(b) A PVC sample cylinder showing a root adhered to the soil under the micro-camera and the fishing line used to separate the root from the soil.

Root morphology

Microscopic observations of the seedlings were carried out at the end of the soil:root peeling test. The roots were examined before and after sonication under water for one minute in order to remove the soil adherent to the root without breaking the root hairs. The roots, which were unstained, were mounted in distilled water and observed with dark-field optics with an Olympus microscope. Micrographs were recorded on a Kodak 160 T film. The lengths of the roots were also measured with vernier calipers. The diameters of the roots which had grown on the remoulded water-saturated silty topsoil were also determined at three different points along the primary root, from the seed to the root tip.

Results and discussion

Root growth

Table 2 summarises the data on both final root length and root growth length, which were determined when the soil:root rupture experiments were successful. First, it may be observed that, for the three remoulded topsoils, the number of root samples increased as a function of soil clay content. This is partly attributable to the fact that the difficulty of obtaining soil:root rupture measurements greatly increased as an inverse function of clay content. Few measurements were obtainable using the sandy topsoil.

For studying the effect of soil texture on root growth, very similar initial root lengths and nearly water-saturated remoulded topsoils (water suction value of 10 kPa) were selected. In this way, it was observed that the mean final root length was higher for the clayey (45.69 mm) and sandy (46.57 mm) soils, than for the silty soil (39.36 mm) (Table 2).

The mean root growth length was found to fluctuate as a function of soil water status. For the remoulded silty topsoil, it was significantly lower for the wet soil (suction value of 50 kPa) than for the water-saturated or drained soils (suction values of 10 and 100 kPa, respectively) (Table 2).

topsoil	clayey		silty		sandy
water suction	10 kPa	10 kPa	50 kPa	100 kPa	10 kPa
Final root length (mm)	45.69 ± 0.70 **	39.36 ± 2.45 **	36.76 ± 1.23 **	42.6 ± 0.73 **	46.57 ± 1.52 **
Growth root length (mm)	29.32 ± 0.54 **	24.47 ± 1.86 ** b	19.78 ± 0.64 ** a	23.63 ± 0.74 ** b	27.01 ± 1.46 **
	n=61	n=10	n=12	n=12	n=4

*Table III. 2. Final root length and root growth length characteristics after root growth onto the soil surface. Values with different letters are significantly different at $p < 0.05$ in the Newman-Keuls test. ** = standard errors of mean values, respectively. n = number of root samples.*

Root morphology

Seedling roots grown on Petri dishes under moist air were characterized by a woolly appearance (Fig. 3_a) which is attributable to a high root hair density on the root surface. Similar root surface morphology has been previously described e. g. by Cormack (1949) who reported, as others, a positive relationship between air moisture and root-hair production. Although at this stage of initial development, the primary roots were very small with lengths of 15 to 20 mm, two root zones were identified: the apical root domain, without root-hairs, and the root hair domain, up to the seed. A progressive increase of the root hair length from the end of the apical root domain to the seed was also observed. This is consistent with the commonly accepted picture of the acropetal development of root hairs, the first appearing very close to the root apex (Cormack, 1949).

Leaving the seedlings more than three days in the Petri dishes, or leaving the roots growing one day on the soil for the soil:root rupture experiments, leads to more spatial segmentation of the root surface, which could then be subdivided into three zones: an apical root domain, without root hairs, a central root hair domain and a basal root domain, without root hairs, located near the seed (Fig. 4). These three root domains have been previously described by Jaunin and Hofer (1986) for the primary roots of maize cultivated under humid atmospheric conditions. These authors also reported positive correlations between the length

of the root hair domain, L_{rhd}, the maximum length of the root hairs (determined in the basal region of the root hair domain), L_r, and the elongation rate of the primary root. From video photos, it was found that the length of the root hair domain, L_{rhd}, was about half the total length of the primary root, L_r, irrespective of the topsoil (Fig. 4).

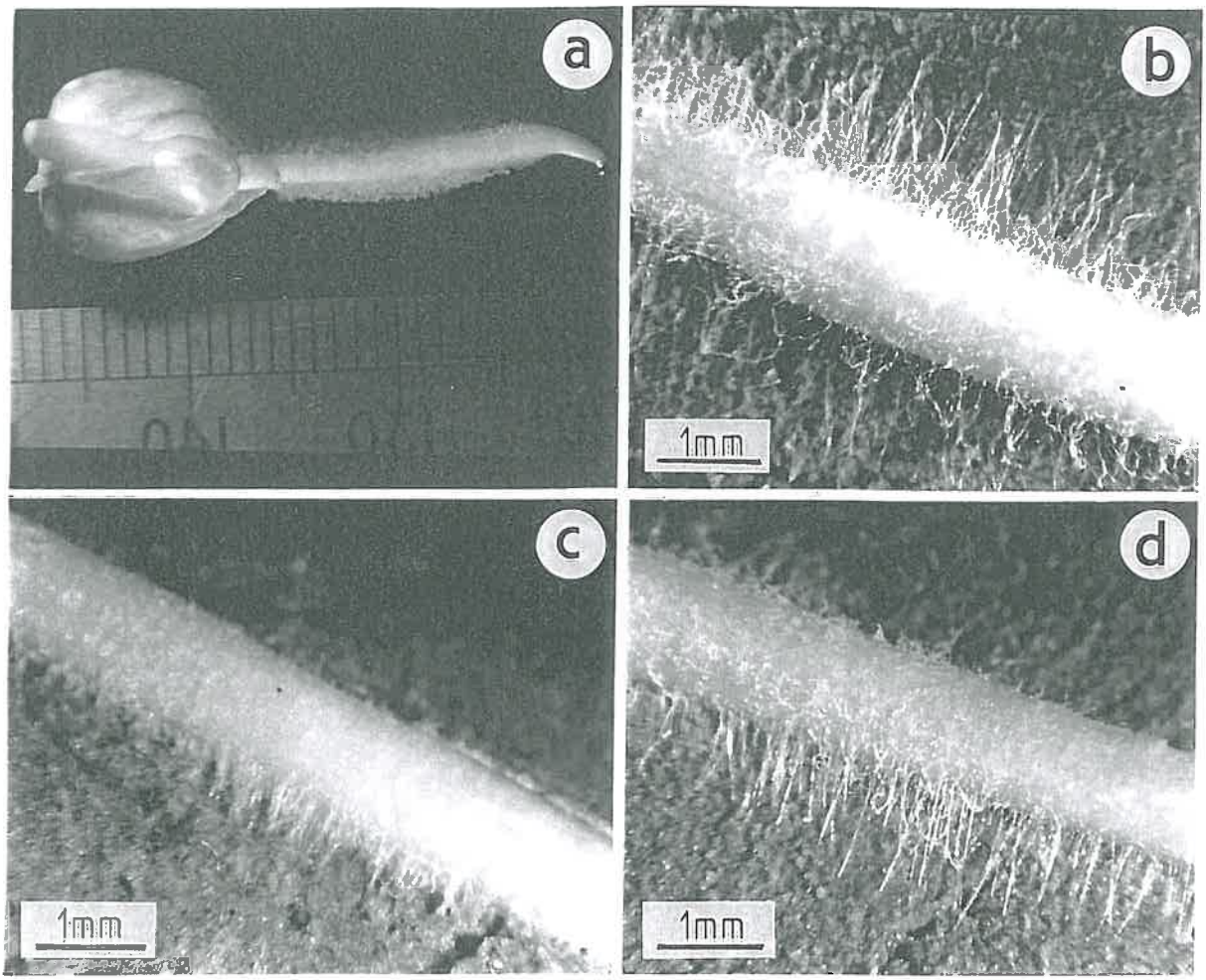

Figure III. 3. Morphological examination of a seedling root from a Petri dish under moisture air (a), from the La Bouzoule (clayey) soil at a water suction of 10 kPa (b), and from Orgeval (silty) soil at water suctions of 10 kPa and 100 kPa (c and d).

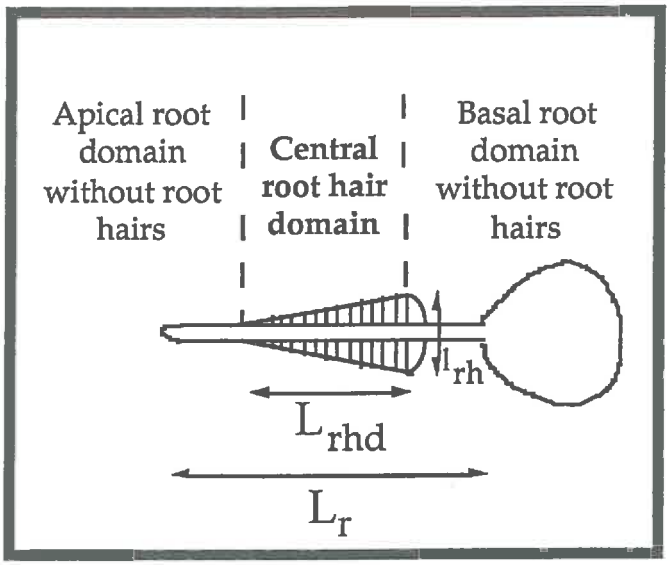

Figure III. 4. The three root zones on the maize seedling.

Root hairs increase the surface area of the root and hence the volume of the rhizosphere, leading to a better root uptake of both water and nutrients (Barley, 1970; Ewens and Leigh, 1985; Misra *et al.*, 1988). Ennos (1989) has also reported that root hairs could also play a role for anchorage of young roots in soil, root exudation and maintenance of contact between the root and the soil. For this reason it was decided to assess the maximum length of root hairs as a function of soil type and water status.

Although no clear difference in root hair production was observed for the nearly water-saturated remoulded topsoils (suction value of 10 kPa), there was some indication of an increase of maximum root hair length as a function of clay content (Figs. $3_{b, c, d}$). Similarly, Meisner and Karnok (1991) showed that peanut root hair production varied as a function of soil type.

We also observed that soil water status had a greater effect on root-hair production than soil type, such that the drier the soil, the higher the root hair length. A similar conclusion was previously reported by Reid and Bowen (1977), who observed that the volume of soil occupied by root hairs, per unit root length, was three times higher for a dry soil than for an equivalent water-saturated soil. Mackay and Barber (1987) have also shown that soil moisture is the key factor regulating root hair growth.

Root uniaxial tensile test

Among the mechanical tests carried out on plant tissues, tensile tests are the simplest to both perform and interpret. They give informations on the stiffness of the sample tested. In the model of root growth in tilled soil developed by Dexter (1978) and Dexter and Hewitt (1978), knowledge of the mean and spatial variability of the root diameter was required as well as that of the linear or non-linear elastic response of the root to applied tensile stress.

In our study, the root diameter had a consistent value of approximately 1.1 mm along the root length, irrespective of the soil type on which the seedling was grown. The seedling roots were relatively cylindrical with a constant uniform circular cross-section, validating the main assumption used in calculating the elasticity. Various other authors have previously shown that root tensile strength increases as a function of root diameter (Fincher *et al.*, 1985; Beck *et al.*, 1988).

In this study, the stress:strain curves were sigmoidal (results not shown), as previously reported by Whiteley and Dexter (1981), indicating that some plastic deformation occurred, possibly the result of cell wall rupture. The value of the secant elastic modulus was 39.82 MPa ± 3.66 MPa, a reflection of the very low rigidity of the root.

Root cyclic tensile tests

Root cyclic tensile tests confirmed the non-linearity of the root stress:strain behaviour. When an ideal linear elastic material is loaded and unloaded, the loading and unloading portions of the stress-strain curve should be superposed. This was not the case for the root tested in this study. The force:displacement diagram of the root showed hysteresis when the force level dropped to nearly zero (0.001 N) and the root was reloaded (results not shown). The root showed a linear elastic response during the initiation of each of the loading episodes. The plastic deformation resulting from the loading-unloading cycles was observed as permanent displacement when the force level was dropped to zero. The area within the hysteresis loop was a measure of the energy consumed by the root during loading i.e. the amount of energy internally dissipated during the loading-unloading cycles. In the cyclic tensile tests, the area of the hysteresis loop

was not very large. The dissipation energy was found to be insignificant compared to the reversible elastic strain energy absorbed by the stretched root.

Root bending test

During the peeling test, the root was also bent, hence a comparison of the energy stored in bending with the soil:root interfacial rupture energy was deemed of value. The typical bending energy of the root, per unit length, was found to be very small, with a value of 1.15 10^{-6} J mm^{-1} (results not shown). These roots were not yet strengthened because they were very young (3-4 days). In contrast, Ennos (1993) has previously shown that, in the mature maize root system, roots are strengthened near the base by a heavy lignified exodermis, which makes them rigid in bending. All the results in this study would certainly have been completely different with older maize roots. Thus, in mechanical studies such as these, it is impossible to extrapolate the results from maize seedlings to the mature maize root system.

Because of the constant root diameter, it was assumed that the root reacted to mechanical tests similarly at any point along its length. As the elasticity of the cell wall material and the cell turgor pressure are determining parameters in these tests, bending tests were carried out on roots, growing either on a Petri dish, or on a remoulded topsoil surface (sandy topsoil with a water suction of 10 kPa), with an addition of water 5 or 10 minutes before the test. The value of the bending energy was found to be 5 10^{-5} J, irrespective of the treatment.

This lead to the conclusion that the environment had no effect on the bending properties of the roots tested.

Mechanics for two adherent remoulded silty topsoil balls

We first observed an increase, as a function of the suction value, of the compression stress computed from the flattening test. More details of these results have recently been reported elsewhere (Czarnes *et al.*, 1998). Similar relationships between the shear strength, and either the matric water potential or the water content, have been previously reported e.g. by Davies (1985), Young and Mullins (1991), Watts and Dexter (1993) and Tengbeh (1993). The drying effect tends to pull the soil particles together, resulting in a cohesive force.

In this study, we also demonstrated that the elastic part of the compression stress was relatively small. The soil:soil adhesion interfacial energy was also very small, and decreased as a function of the suction value, leading to a negative relationship between the soil:soil adhesion interfacial energy and its plastic energy counterpart (Fig. 5). This result is very important to the development of a soil:root adhesion theory.

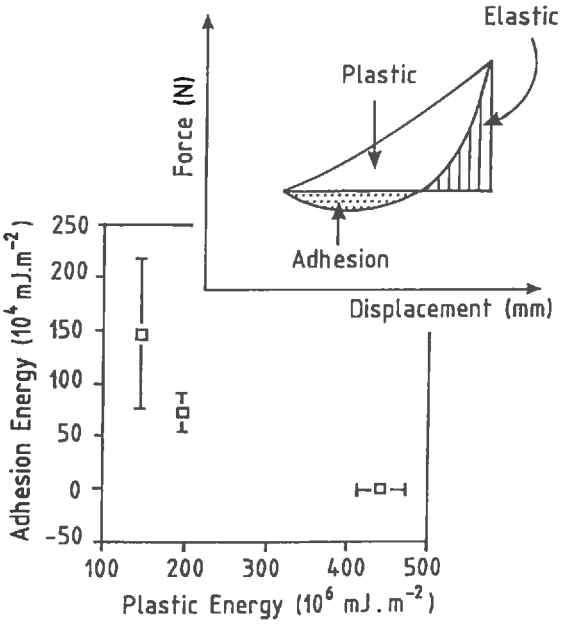

Figure III. 5. *Relationship between the soil:soil adhesion energy and the plastic energy obtained and calculated from the experiment of pushing together and pulling apart two adherent remoulded balls of silty topsoil. An example of the synthesis of the force:displacement curves is added in the top right-hand corner.*

Combined rheological and video chrono-analysis of the soil:root peeling test

Although a membrane was placed between the seed itself and the soil, the soil:seed interface sometimes contributed to the tensile load, with a narrow and high specific peak at the beginning of the force:displacement curve (Fig. $6_{a,b}$), although similar peaks were not observed for other soil:root peeling test experiments (Fig. $6_{c,d}$). Thanks to the video camera system, it was quite allowed easy separation of the peak due to the seed and the broad shoulder due to the root.

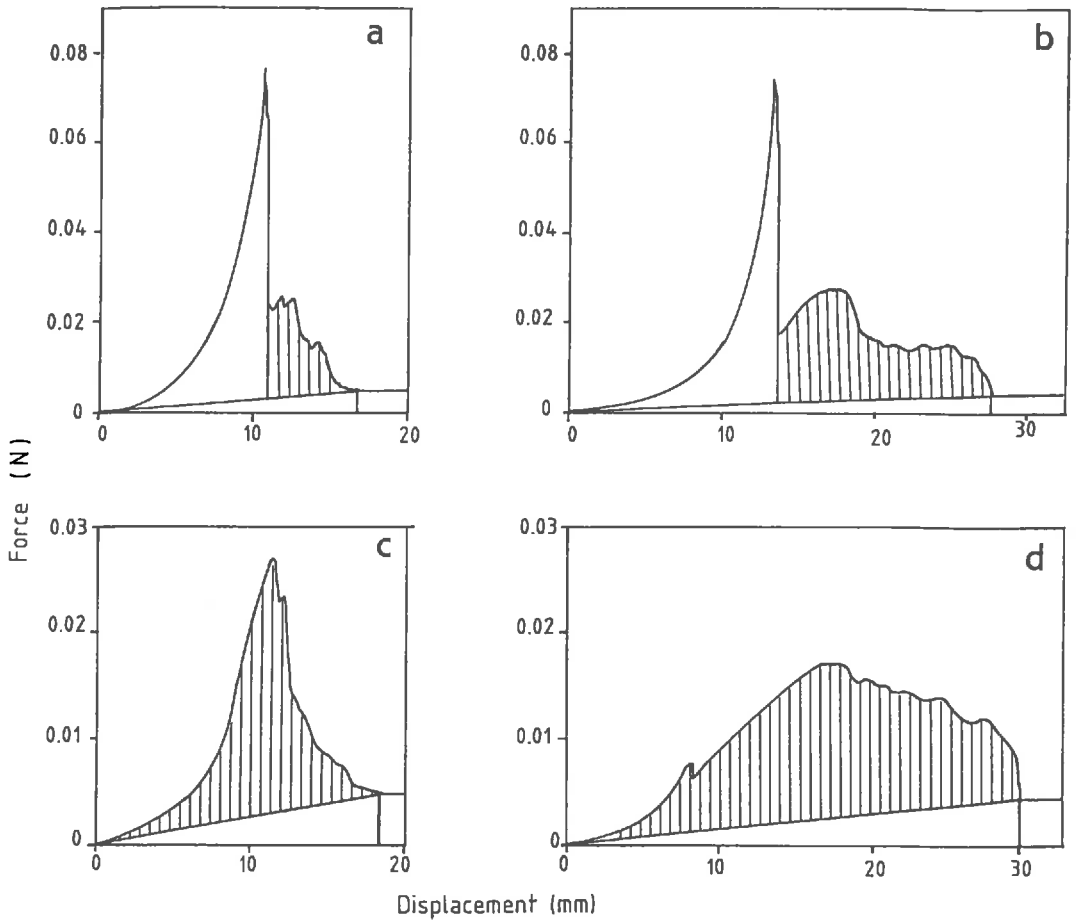

Figure III. 6. Example of pulling force:displacement curves carried out during the silty topsoil:root peeling test: with (a and b) or without (c and d) the peak which is attributed to the soil:seed interfacial rupture, using either short (a and c) or long (b and d) roots. The spread shoulder on the pulling force:displacement curves is attributed to the soil:root interfacial rupture.

For normalization, the soil:root interfacial rupture energy (surface area of the specific shoulder on the tensile force:displacement curve) was divided by the final length of the root to give the interfacial rupture energy per unit length, W_{ru}. For the same suction value of 10 kPa, the W_{ru} value strongly increased as a function of soil clay content. It was of 0.038 10^{-6} J mm^{-1} root length, 5.28 10^{-6} J mm^{-1} root length and 11.45 10^{-6} J mm^{-1} root length for the sandy (1.9 % clay), the silty (16.4 % clay) and the clayey (33.1 % clay) remoulded topsoils, respectively (Fig. 8). The more granular and coarse the remoulded topsoil, the less the tensile resistance of the soil:root interface. Conversely, the root bending increased as a function of soil clay content. The higher the soil:root adhesion, the

more bent the root. For the same suction value of 10 kPa, the angle between the bending root and the soil was 5 to 10 ° for the remoulded sandy topsoil (Fig. 7_a), 30 to 40 ° for the remoulded silty topsoil (Fig. 7_b) and 70 to 90° for the remoulded clayey topsoil (Fig. 7_c). The high clayey soil:root adhesion explains why roots pulled from the clayey topsoil sometimes started to divide in two from the beginning of the root hair domain, one part being firmly adherent to the soil, the other pulling free from the soil, as far as the apical root domain.

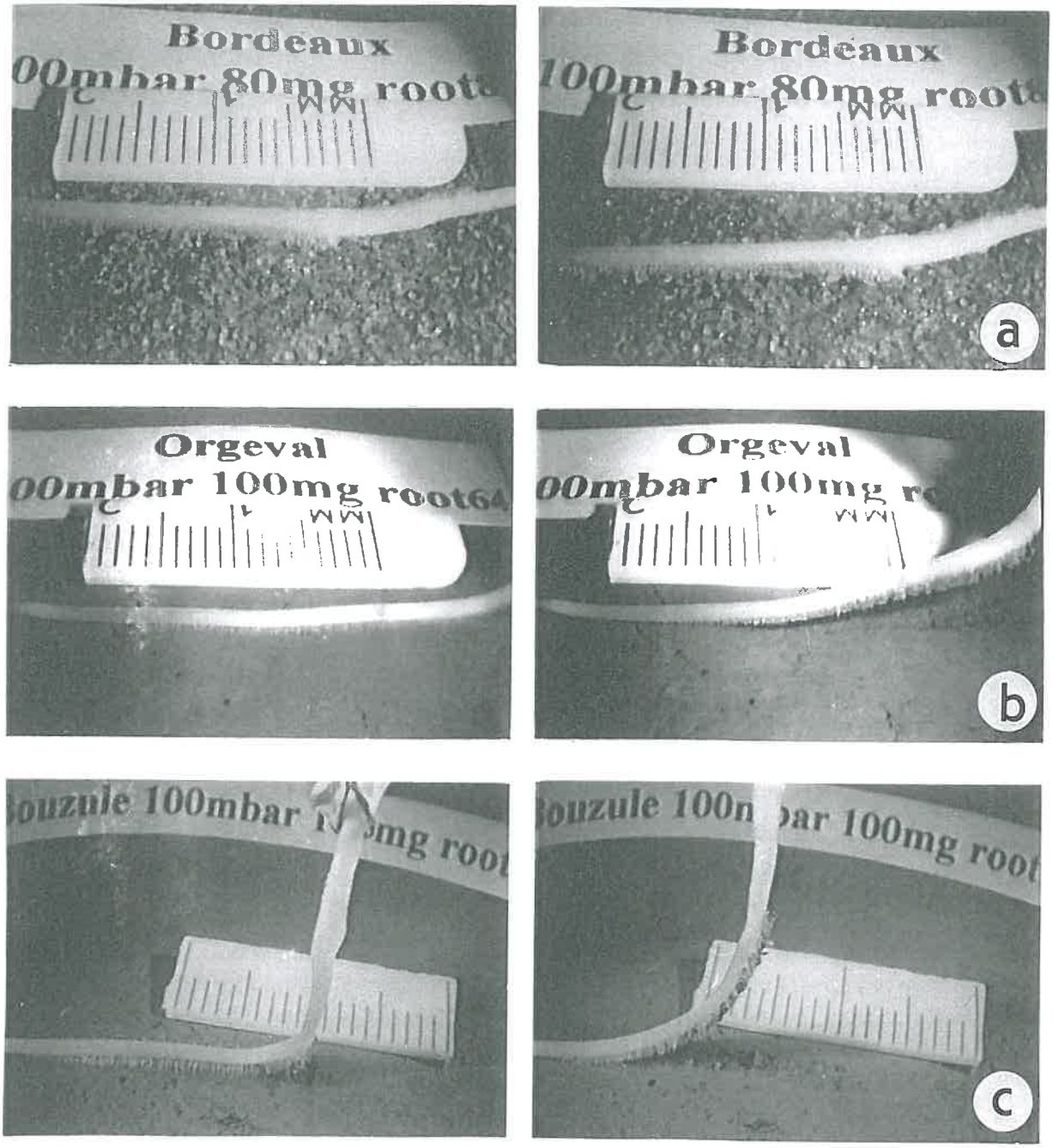

Figure III. 7. Chronosequence of photographs reproduced from the video film for the *remoulded sandy (a), silty (b) and clayey (c) topsoils at the beginning and at the end of the soil:root peeling test.*

The length of the root, L_r, was also a key parameter determining soil:root interfacial rupture energy. The shoulder on the tensile force:displacement curve was simple for a short root (Fig. $6_{a, c}$) but more complex and diffuse for a long root (Fig. $6_{b, d}$). In addition, the position of the shoulder shifted to higher displacement values, e. g. for the remoulded silty topsoil, from a displacement value of 12 mm for a short root, to that of 17 mm for a long root (Fig. 6).

By contrast, the effect of water suction on the W_{ru} value was very moderate for the silty soil (Fig. 8). It was 5.28 ± 0.67 10^{-6} J mm^{-1} root length; 4.23 ± 0.27 10^{-6} J mm^{-1} root length and 3.18 ± 0.22 10^{-6} J mm^{-1} root length when the silty topsoil was prepared at water suction of 10 kPa, 50 kPa and 100 kPa, respectively (Fig. 8).

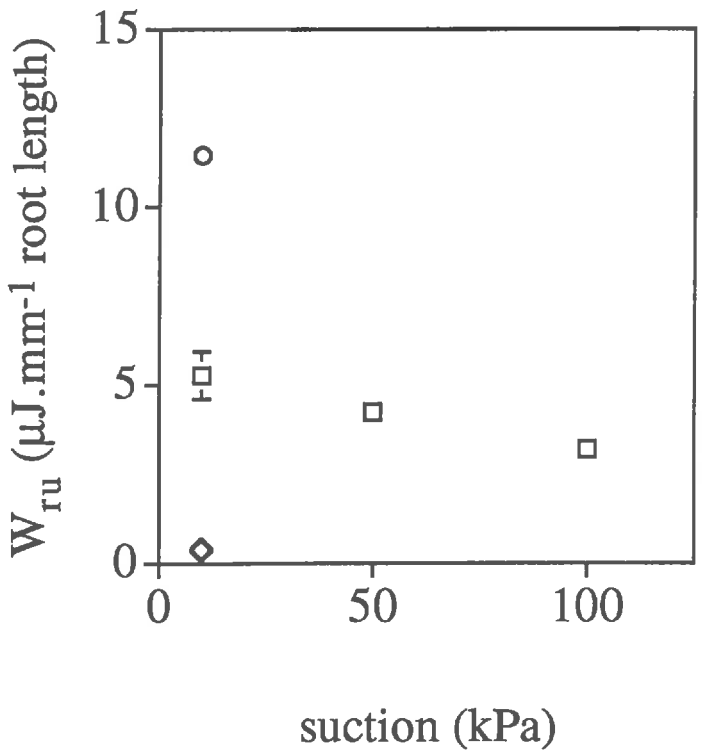

Figure III. 8. Relationship between the mean soil:root interfacial rupture energy in *root length units, W_{ru}/L_r, and its standard deviation, and the soil water suction for the remoulded sandy (open lozenge), silty (open square) and clayey (open circle) topsoils.*

The question now arises as to the nature of the specific geometrical characteristics responsible for the shape of the more or less complex shoulder on the tensile force:displacement curve, linked to the rupture of the soil:root interface.

First, it was observed that the root hair domain was the main root domain which adhered to the soil and, as mentioned above, that its length was half of the total root length. This could therefore explain the shift of the specific shoulder on the tensile force:displacement curve to higher displacement values. Secondly, as reported above, the length of the root hairs decreased, from the side of the root hair domain adjacent to the seed, to its end. This could therefore partly explain the elongation of certain soil:root interfacial rupture shoulders on the tensile force:displacement curves.

Peeling tests were also carried out on the mentioned model soil:root analogue systems, in which the artificial root was known to be homogeneous along its length. Since the horizontal adhesive supports used had uniform surface properties, a perfectly constant adhesion along the material:support interface was to be expected. Instead of such constant adhesion, curves similar to those of the soil:root peeling tests (Fig. 6) were obtained (results not shown). This suggests that the spatial heterogeneity of the root hair distribution along the root is probably not the only parameter responsible for the elongated shoulder on the tensile force:displacement curve. In the model cases, rupture of the interface between the non-biological solid film and the adhesive planar substrate appears to have been a progressive process, dependent on the changing geometry of the interface as the peeling test advanced. A similar mechanism is likely to operate in the soil:root peeling test.

Geometry of the soil:root rupture surface

After the soil:root peeling test, the root surface appeared relatively free of soil, apart from the root hair domain, which was characterized by a semi-conical soil-filled volume delimited by the ends of the root hairs (Fig. 7). A matching semi-conical indentation was observed on the soil surface (Fig. 7). The surface area, $S_{s:r}$, of the soil:root rupture surface (the semi-conical indentation) corresponds to a triangle with the length of the root hair domain, L_{rhd}, equal to half of the total root length, L_r, as its height, and a proportion of the maximum

length of the root hairs, l_{rh}, as its width (the maximum depth of the semi-conical indentation) (Fig. 4.):

$$S_{s:r} \alpha L_r l_{rh} \quad (2)$$

where the symbol α denotes the proportionality.

Both the depth of the semi-conical indentation, and the value of its semi-conical soil-filled volume counterpart, increased as a function of soil clay content (Fig. 7). This was attributed to the observed increase, as a function of soil clay content, of both soil plasticity (significant relation) and maximum root hair length (tenuous relationship). For the wet and drained remoulded silty topsoils, which were prepared at water suctions of 50 kPa and 100 kPa, respectively, the relationship between the semi-conical indentation and the soil-filled volume adhering to the root was more complicated. However, the depth of the semi-conical indentation decreased as a function of the suction, which was again attributed to a decrease of soil plasticity, and an increase of soil cohesion.

Soil:root adhesion theory: the rheological approach

First, because adhesion is not a pure reversible process, it may be assumed that the tensile energy, W_{ru}, for disrupting the soil:root interface equals the sum of the soil:root reversible adhesion energy, W_{adh}, and the energy, W_d, which was dissipated during the plastic (non-elastic) strains of either or both deformable adherents:

$$W_{ru} = W_{adh} + W_d \quad (3)$$

where W_{ru}, W_{adh} and W_d are expressed in energy units, e. g. in mJ.

It was demonstrated above that the dissipation energy could be neglected for the root strain, but not for the soil plastic strain. It was also shown above that the soil:soil adhesion energy decreased as a function of the plastic fraction of the soil cohesion energy (Fig. 5).

Similarly, Schultz and Carre (1985) have discussed in their review that, for a non-biological system composed of two adherent materials: a plastic epoxy resin and a rigid aluminium substrate, with the same contact interfacial surface area, the W_{adh} and W_d values were interdependant parameters, leading to the following proportionality:

$$W_{ru} \alpha W_{adh} W_d \quad (4)$$

where W_d is the dissipation energy factor, function of the nature of the polymer, the pulling speed, v, and the temperature, θ.

In our study, both the rate of displacement and the temperature were constant parameters in all the soil:root peeling tests, whereas the macroscopic contact surface area between the root and the soil, $S_{s:r}$, (equation (2)) and the dissipation energy, W_d, related to soil plasticity, were not. It is therefore necessary to take into account both $S_{s:r}$ and W_d for modelling the rupture of the soil:root interface, as in the following relationship:

$$W_{ru} \alpha W_{adh} S_{s:r} W_d \qquad (5)$$

Alternatively, the reversible soil:root adhesion energy could be expressed as a function of two parameters: the BET microscopic surface area, S_{BET}, of the soil, and the reversible soil:root adhesion energy per unit microscopic surface area, $W_{adh/SBET}$, difficult to determinate:

$$W_{adh} \alpha S_{BET} W_{adh/SBET} \qquad (6)$$

with W_{adh} in mJ, S_{BET} in $m^2\ g^{-1}$ and $W_{adh/SBET}$ in mJ m^{-2}.

Combining equations (2), (5) and (6) leads to the following equation:

$$W_{ru} \alpha L_r\ l_{rh}\ S_{BET}\ W_{adh/SBET}\ W_d \qquad (7)$$

We will now try to validate this soil:root adhesion theory by studying the possible impacts on the soil:root interfacial rupture energy, W_{ru}, of: (i) the macroscopic contact surface area between the root and the soil, indirectly measured by the total root length, L_r, (ii) the soil microscopic specific surface area, S_{BET}, and (iii) the plastic dissipation energy, W_d.

Validation of the soil:root adhesion theory

First, for each soil, the effect of the root length, L_r, on the soil:root interfacial rupture energy, W_{ru}., was analysed. Assuming that samples of the same remoulded topsoil prepared at a suction value of 10 kPa, and the corresponding roots, were characterized by the same l_{rh}, S_{BET}, W_{adh}/S_{BET} and W_d values leads to a simplification of equation (7) as follows:

$$W_{ru} \alpha L_r \qquad (8)$$

Although the W_{ru}:L_r relation was scattered in the plots of the remoulded clayey topsoil:root peeling tests, and 30 % of the data for the remoulded silty topsoil was not directly controlled by a W_{ru}:L_r relation, and that not enough data was collected for the remoulded sandy topsoil, positive linear relationships between the W_{ru} value and the root length (Fig. 9) were nevertheless observed,

with significant statistical validity for both the clayey topsoil data and 70 % of the silty topsoil data. From equations (2) and (5), the positive effect of the root length on the W_{ru} value (Fig. 7) clearly reflected the effect of the macroscopic root:soil contact surface area on the value of W_{ru}. In addition, fig. 9 showed a bimodal distribution of W_{ru} values for the remoulded clayey topsoil, with one set of data characterized by small values of both W_{ru} and L_r, and a second set characterized by high values of both W_{ru} and L_r.

Equation (8) was validated, but the W_{ru}:L_r linear regression lines did not cross the origin of the W_{ru}:L_r graph, as required by equation (8), but they crossed the abscissa at a mean value of 20 mm root length, yielding:

$$W_{ru} = a(L_r - 20) \qquad (9)$$

If the soil:root interfacial rupture energy is normalised with reference to unit length, it yields the following linear statistical relationship:

$$W_{ru}/L_r = a\,(1 - 20/L_r) \qquad (10)$$

Equations (9) and (10) suggests that 20 mm of the root length do not participate to the soil:root adhesion process. however, the biological and physical significance of this result is not yet clear.

Furthemore, equation (7) was validated because the slope value, a, of the W_{ru}:(L_r - 20) straight regression line, increased linearly as a function of the soil specific surface area (Fig. 10). The a value was 23.40 $\mu J\ mm^{-1}$ root length, 7.75 $\mu J\ mm^{-1}$ root length and 0.61 $\mu J\ mm^{-1}$ root length for the clayey, the silty and the sandy remoulded topsoils, respectively. In this study the S_{BET} value was clearly the most important physical parameter for soil:root adhesion modelling (equation (5)) because of its very large range from 0.3 $m^2\ g^{-1}$ (sandy topsoil) to 40.8 $m^2\ g^{-1}$ (clayey topsoil) (Table 1), the ratio of the maximum to the minimum values being 136. In contrast, the equivalent ratios were 1.7 and less than 2 for the root length and the maximum length of the root hairs, respectively, leading, from equation (2), to a corresponding ratio of nearly 4 for the macroscopic contact surface area between the root and the soil.

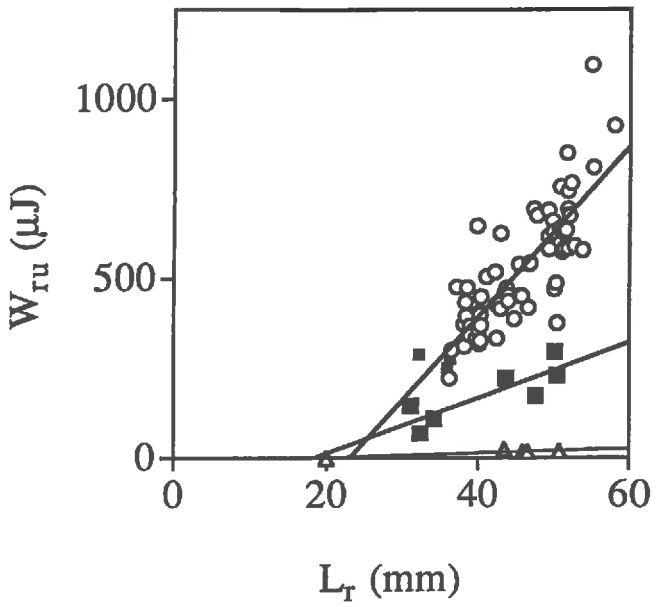

Figure III. 9. *Relationship between soil:root interfacial rupture energy, W_{ru}, and the final root length , L_r for the remoulded sandy (open triangle), silty (filled square) and clayey (open circle) topsoils.*

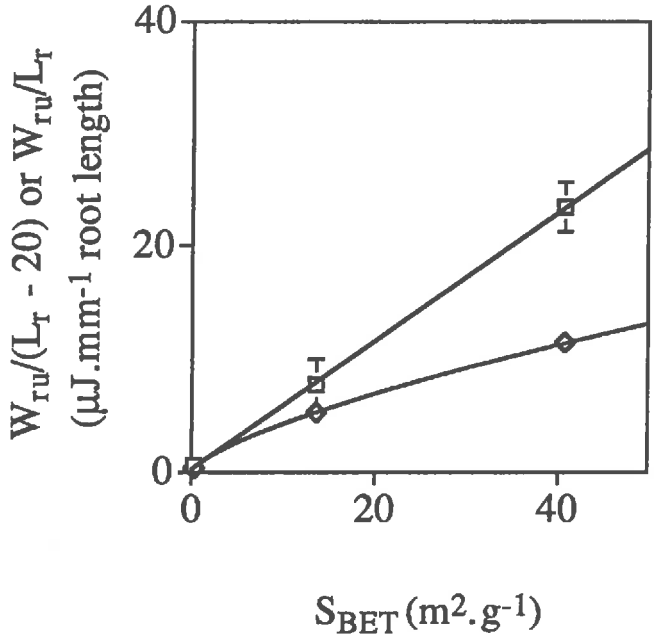

Figure III. 10. *Relationship between either the slope value, a, of the W_{ru}:(L_r - 20) straight regression line (see Fig. 9), and its standard deviation (open square) or the mean W_{ru}/L_r value, and its standard deviation (open lozenge) and the soil specific surface area, S_{BET}, for the three studied topsoil:maize root systems. Equations of the fitted curves were:*
$a = 0.565\ S_{BET} + 0.292$ and $W_{ru}/L_r = 0.868\ S_{BET}^{0.694}$ (both $r = 1.000$, $p < 0.01$).

If the mean W_{ru}/L_r value computed from all the W_{ru}/L_r data (Fig. 8) is plotted it as a function of soil surface area, the relationship appears to be non-linear, and the discrepancy between this curve and the mentioned straigth regression line can be explain by equation (10), as follows. The mean L_r values which correspond to root growth on nearly water-saturated remoulded topsoils were of 46.6 mm, 39.4 mm and 45.7 mm for the sandy, the silty and the clayey topsoils, respectively (Table 2). This leads to equivalent $(1 - 20/L_r)$ values of 0.57, 0.49 and 0.56, respectively. This explains both (i) why the W_{ru}/L_r value was nearly half the $W_{ru}:L_r$ slope value (Fig. 10), and (ii) why the $W_{ru}:L_r$ curve was not a straight regression line, because the $(1 - 20/L_r)$ value was lower for the remoulded silty topsoil, than for the sandy and clayey topsoils. If root growth had been constant, the relationship should have been linear. Here, its non-linearity suggested that interactions occured between root growth and soil:root interfacial rupture energy.

In any case, the relationship between the $W_{ru}:(L_r - 20)$ slope and the corresponding soil surface area (Fig. 10) has a strong physical meaning. First, specific surface area is the main characteristic of the soil surface properties, as mentioned above in the soil:root adhesion theory section. Furthermore, it is also a good indicator of the soil clay micro-rugosity (e. g. van Damme, 1995), which strongly increases the contact surface area between the root and the soil. Our soil:root adhesion theory and its preliminary validation suggest that soil:root adhesion is a multiscale physical process, with (a) two intrinsic contact areas between the root and the soil: the macroscopic (that of the semi-conical indentation at the end of the soil:root peeling test), and the microscopic (the soil specific surface area), and (b) two complementary intrinsic soil rugosity factors: the macroscopic (a function of soil porosity) and the microscopic (a function of soil specific surface area). Macroscopic root rugosity due to root hairs may also play an important role.

In much less complex systems, Fuller and Tabor (1975) have shown that the decrease of the micro-rugosity of a hard smooth flat surface of Perspex greatly decreases the interfacial rupture energy between a smooth rubber sphere and that Perspex surface.

Finally, it was shown above that suction only had a very moderate effect on the W_{ru} value in the silty topsoil:root peeling test (Fig. 6). The specific parameters which could be involved here are the width of the indentation and

the plastic energy. It was reported above that the maximum root-hair length and the soil cohesion increased as a function of the suction, whereas the soil plastic strain decreased. The dissipation energy should be proportional to soil strength. These two factors due to biological and physical interactions may possibly act antagonistically, leading to the observed moderate effect of water suction on the W_{ru} value.

Conclusion

This study was aimed at improving our understanding of the nature of the soil:root interface zone, which is the main interfacial resistance for water transport from the soil to the plant. The experimental work focussed on soil:root adhesion for the maize seedling. A device for stimulating root growth and adhesion on a soil surface was designed. The soil:root peeling test method has been analysed by a combination of rheological and timed video analysis. Using these methods, the effects of root length, soil texture and matric water potential on soil:root interfacial rupture energy, were investigated. The main results were:

1- A heterogeneous distribution of the root hair zone along the root has been observed, with a central root hair domain firmly adhering to the soil surface. The length of this central domain is equivalent to the sum of the lengths of the surrounding basal and apical root domains, which were devoid of root hairs. The root hair length also increased (i) from the basal side to the apical side of the root hair domain and (ii) as a function of clay content and soil drying.

2- During the peeling test, parts of the root are in tension, parts are in bending, and some energy was stored as root:soil adhesion. The mechanical properties of the seedling root with a constant diameter were a low rigidity, in conjunction with a small degree of root-bending. This resulted in a low stored energy of bending, which was negligible compared to the soil:root adhesion energy.

3- The mechanical properties (plasticity, elasticity and adhesion) of two adherent spheres of soil demonstrated an increase in soil:soil plastic interfacial energy, and a decrease in soil:soil adhesion interfacial energy, as a function of suction. Adhesion and dissipation energies were related, the interdependency being described in a soil:root adhesion theory.

4- Thanks to a video-camera system, it was possible to interpret the complex and variable force:displacement curves on which extensive shoulders have been attributed to soil:root interfacial rupture. The shapes and the positions of these shoulders were related to the semi-conical geometry of the soil:root rupture surface, which was dependent upon total root length.

5- A soil:root adhesion theory, with strict physical meaning, has been formulated and validated with data from soil:root peeling tests. The soil:root interfacial rupture energy was mainly controlled by the product of the microscopic soil specific surface area and the root length, which in turn controlled the macroscopic contact surface area between the root and the soil.

To go further, it will be interesting to use a similar rheological approach on older maize seedlings with roots of different ages, and with a root system. The initial aim would be to study the specific effect of root exudation on soil:root interfacial rupture energy for a selected wet soil. Matsumoto et al. (1979) have reported that the production of maize root exudates was highest at the young seedling stage (11-days-old), and strongly decreased as a function of root growth thereafter. A range of seedlings of different ages would thus be required.

A further goal of such a physical approach should be to integrate it with multidisciplinary research into the combined effects of both root exudation and rhizosphere water retention on water, nutrient and pathogen transport from the soil to the plant.

Acknowledgements

Financial support from the Alliance project (1995-1997) and the British Council Fellowship given to the first author for a period of 6 months (1996-1997) were greatly appreciated, allowing efficient cooperation between the Soil Science group of the Silsoe Research Institute, UK, and the Soil Aggregation team of the Centre de Pédologie Biologique CNRS, France.

References

Barataud F, Moyne C, Bréda N and Granier A 1995 Soil water dynamics in an oak stand. II. A model of the soil-root network compared with experimental data. Plant and Soil 172, 29-43.

Barley D 1970 The configuration of the root system in relation to nutrient uptake. Advances in Agronomy 22, 159-201.

Beck D L, Darrah L L and Zuber M S 1988 Relationship of root tensile strength to vertical root pulling resistance in maize. Crop Science 28, 571-573.

Bengough A G, Croser C and Pritchard J 1997 A biophysical analysis of root growth under mechanical stress. Plant and Soil 189, 155-164.

Cormack R G H 1949 The development of root hairs in Angiosperms. The Botanical Review XV, 583-611.

Czarnes S, Dexter A R and Bartoli F 1998 Mechanics of two adherent centimetric remoulded soil balls : a preliminary examination. Soil Tillage Research (in preparation).

Davies P 1985 Influence of organic matter content, moisture status and time after reworking on soil shear strength. Journal of Soil Science 102, 59-63.

Dexter A R 1978 A stochastic model for the growth of roots in tilled soil. Journal of Soil Science 29, 102-116.

Dexter A R and Hewitt J S 1978 The deflection of plant roots. J. Agric. Engng Res. 23, 17-22

Ennos A R 1989 The mechanics of anchorage in seedlings of sunflower, *Helianthus annuus* L. New Phytol. 113, 185-192.

Ennos A. R 1990 The anchorage of leek seedlings: The effect of root length and soil strength. Annals of Botany 65, 409-416.

Ennos A R 1993 The anchorage mechanics of Maize, *Zea mays*. Journal of Experimental Botany 4, 147-153.

Ewens M and Leigh R A 1985 The effect of nutrient solution composition on the length of root hairs of wheat (*Triticum aestivum L.*). Journal of Experimental Botany 36, 713-724.

Fincher R R, Darrah L L and Zuber M S 1985 Root development in maize as measured by vertical pulling resistance. Maydica 30, 383-394.

Fuller K. N. G. and Tabor, D., 1975. The effect of surface roughness on the adhesion of elastic solids. Proc. R. Soc. Lond. A 345, 327-342.

Gijsman A J, Flopris J, van Noordwijk M and Brouwer G 1991 An inflatable minirhizotron system for root observations with improved soil/tube contact. Plant and Soil 134, 261-269.

Greacen E L, Farrell D A and Cockroft B 1968 Soil resistance to metal probes and plant roots. Transactions of the 9th International Congress of Soil Science, Adelaide, Australia volume I, 769-779.

Hiltner L 1904 Uber neuere Erfahrungen und Probleme auf dem Gebeit der Bodenbakteriologie und unter besonder Berücksichtigung der Gründüngung und Brache. Arb. Dstch Landwrit. Ges. 98, 59-78.

Jaunin F and Hofer R M 1986 Root hair formation and elongation of primary maize root. Physiologia Plantarum 68, 653-656.

Kooistra M J, Scoonderbeek D, Boone F R, Veen B W and van Noordwijk, M 1992 Root-sol contact of maize, as measured by a thin-section technique. II. Effects of soil compaction. Plant and Soil 139, 119-129.

Mackay A D and Barber S A 1987 Effect of wetting and drying of a soil on root hair growth of maize roots. Plant and Soil 104, 291-293.

Meisner C A and Karnok K J 1991 Root hair occurence and variation with environment. Agron. J. 83, 814-818.

Misra R K, Alston A M and Dexter A R 1988 Role of root hairs in phosphorus depletion from a macrostructured soil. Plant and Soil, 107, 11-18.

Niklas K J 1992 Plant biomechanics: an engineering approach to plant form and function. John Wiley & Sons, New York.

Reid C P P and Bowen G D 1979 Effect of soil moisture on V/A mycorrhiza formation and root development in *Medicago*. In Harley J L (ed.) "the soil-root interface" New phytologist, London, 211-220.

Schultz J and Carre A 1985 Prévision de l'adhésion d'aluminium traité à l'aide de méthodes de mouillabilité. Surfaces 178, 30-36.

Tengbeh G T 1993 The effect of grass roots on shear strength variations with moisture content. Soil Technology 6, 287-295.

van Damme H 1995 Scale invariance and hydric behaviour of soils and clays. Comptes Rendus à l'Académie des Sciences, Paris, 320, Series II a, 665-681.

van Noordwijk M, Kooistra M J, Boone F R, Veen B W and Scoonderbeek, D 1992 Root-sol contact of maize, as measured by a thin-section technique. I. Validity of the method. Plant and Soil 139, 109-118.

Veen B W, van Noordwijk M, De Willigen P, Boone F R and Kooistra M J 1992 Root-sol contact of maize, as measured by a thin-section technique. III. Effects on shoot growth, nitrate and water uptake efficiency. Plant and Soil 139, 131-138.

Vincent J F V 1992 Biomechanics - materials: a practical approach. Oxford University Press, New York.

Watts C W and Dexter A R 1993 A hand-held instrument for the in situ measurement of soil shear strength in the puddled layer of paddy fields. J. agric. Engng Res. 54, 329-337.

Whiteley G M and Dexter A R 1981 Elastic response of the roots of field crops. Physiologia Plantarum 51, 407-417.

Young I M and Mullins C E 1991 Factors affecting the strength of undisturbed cores from soils with low structural stability. Journal of Soil Science 42, 205-217.

CONCLUSION GENERALE

CONCLUSION GENERALE

Notre travail de thèse à permis d'étudier les interactions physiques et biologiques, et leurs dynamiques, existant entre les racines de maïs et le sol, milieu poreux et réserve en eau et en éléments nutritifs.

Trois grands types de résultats ont été obtenus.

1- Les cinétiques de séchage d'un sol sableux organique et hydrophobe soumis à un rayonnement lumineux intense sont nettement plus marquées dans la rhizosphère que dans le sol témoin sans plante. De même, nous avons mis en évidence, dans le cas du sol sableux, un phénomène d'hystérésis des courbes de rétention d'eau, obtenu sous conditions dynamiques, lorsque l'on passe du sol témoin à la rhizosphère (figure 1).

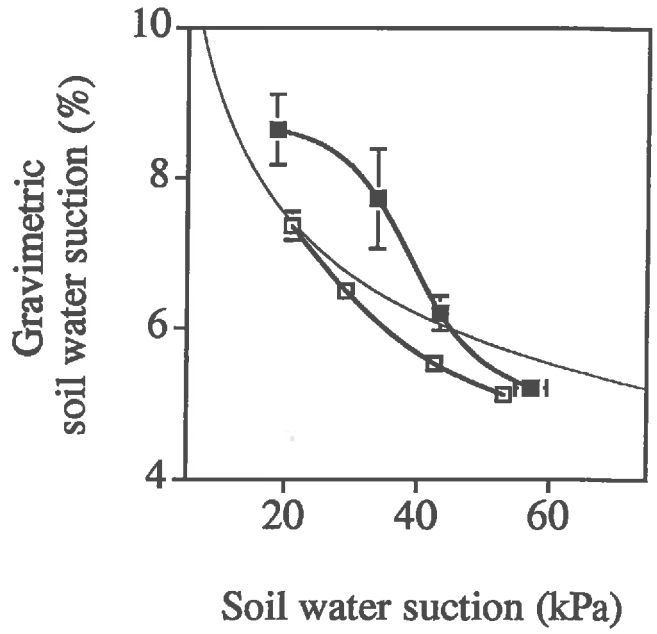

Figure 1. *Courbe de rétention d'eau du sol sableux réalisée à partir de conditions quasi-statiques (courbe sans symboles) ou de conditions dynamiques (symboles "carrés") pour la rhizosphère de maïs (symboles "carrés pleins") et le sol témoin (symboles "carrés vides").*

Ceci serait attribuable à des différences très significatives de flux d'eau qu'il faudrait, à l'avenir, mesurer.

A l'opposé, l'effet rhizosphère paraît moins marqué dans le cas du sol limoneux.

Cette différence de mode d'absorption de l'eau par la plante a été attribuée à deux facteurs interdépendants: le stock d'eau - celui du sol sableux étant beaucoup plus limité que celui du sol limoneux - et à l'architecture du système racinaire (figure 2).

L'architecture du système racinaire est ouverte, avec des racines relativement épaisses et courtes lorsque le maïs a poussé sur le sol limoneux, alors, qu'à l'opposé, elle est ramassée et homogène, avec de nombreuses racines fines lorsque le maïs a poussé sur le sol sableux, ce qui est favorable à l'absorption de l'eau par la plante.

2- La caractérisation des propriétés mécaniques du sol adhérant aux racines a révélé que celles-ci étaient complexes.

C'est ainsi que, dans le cas du sol limoneux, le sol adhérent a pu être subdivisé en deux classes d'agrégats:

- des agrégats peu stables, pouvant être assez facilement détachés des racines, par rupture intra-agrégats, à l'aide d'agitation mécanique du système sol adhérent:racines. L'immersion dans l'eau du système sol adhérent:racines accélère ce processus de rupture.

- des agrégats fermement adhérant aux racines que l'on ne peut détacher des racines que par ultrasonication du système sol adhérent:racines, préalablement immergé dans de l'eau. La zone apicale racinaire s'est avérée être un domaine privilégié pour cette catégorie d'agrégats qui s'associent alors en un manchon continu de sol très stable autour des racines (figure 3).

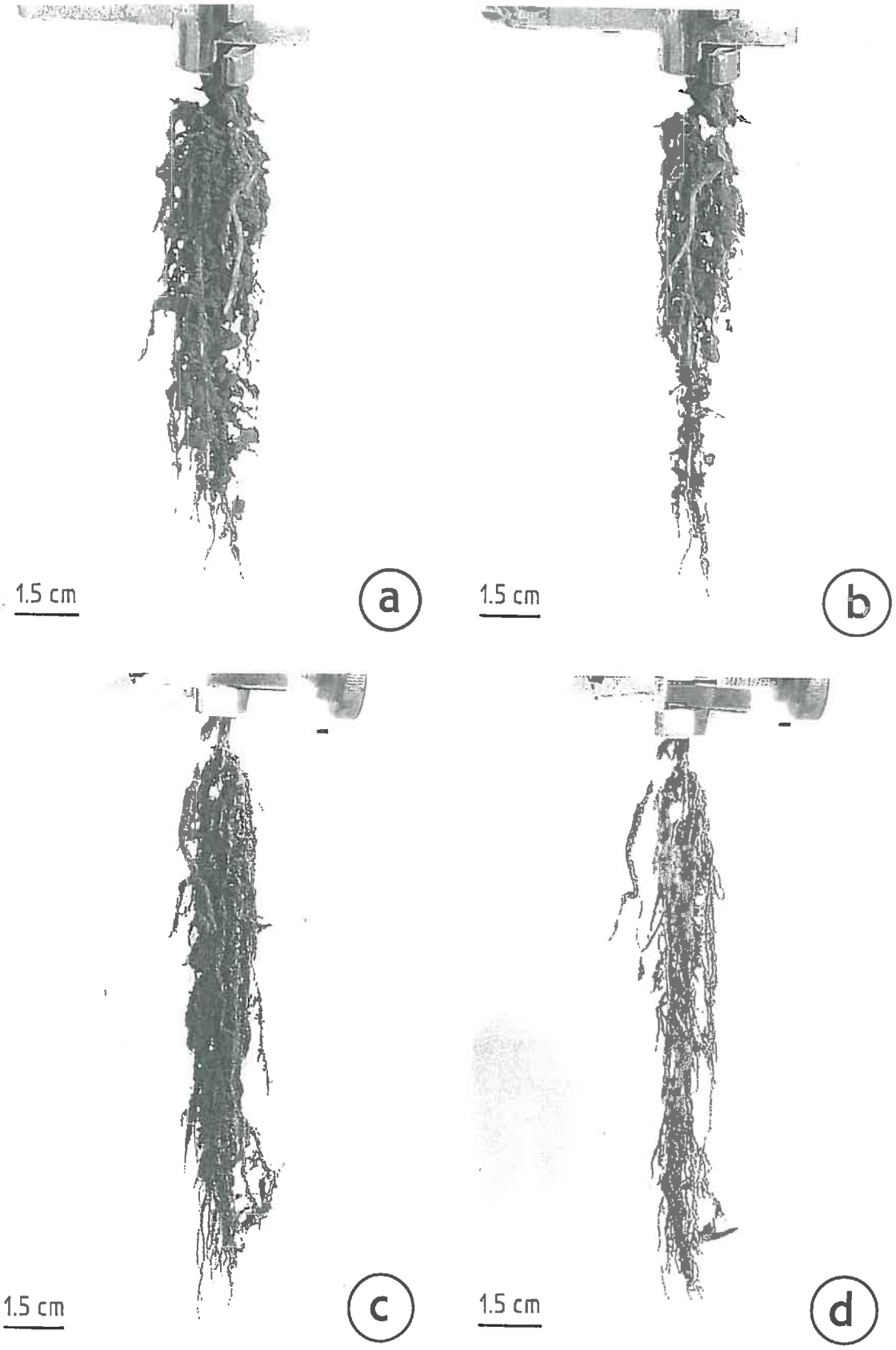

Figure 2. Photographies, prises après 0 (a and c) et 3 minutes (b and d) d'agitation mécanique du système sol:racines pour la culture du maïs avec le sol limoneux (a et b) ou le sol sableux (c et d) sous des conditions dynamiques, à une valeur de succion journalière minimale de 10 kPa.

De façon plus précise, nous avons pu démontrer que la cohésion des agrégats adhérant aux racines était beaucoup plus élevée que celle des agrégats de sol non soumis à l'influence du système racinaire, et que cela était dûe à l'exsudation racinaire et microbienne et à la présence des poils racinaires (figure 3).

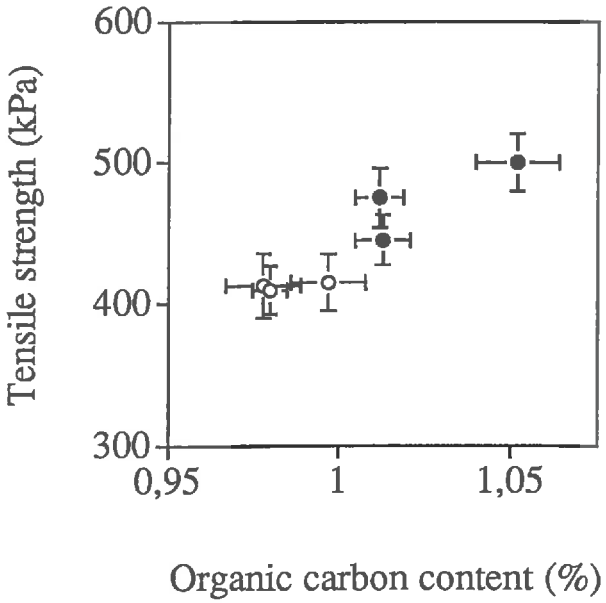

Figure 3. Evolution de la résistance en traction des agrégats limoneux de sol adhérant ("cercles pleins") et non adhérant aux racines ("cercles vides") en fonction de la teneur en carbone organique.

3- L'étude rhéologique de l'adhésion sol:racines a debouché sur une théorie, que nous avons pu valider. La surface spécifique du sol et la surface de contact sol:racines, indirectement mesurée par la longueur racinaire, sont les deux principaux paramètres de contrôle de l'energie de séparation sol:racines (figures 4 et 5)

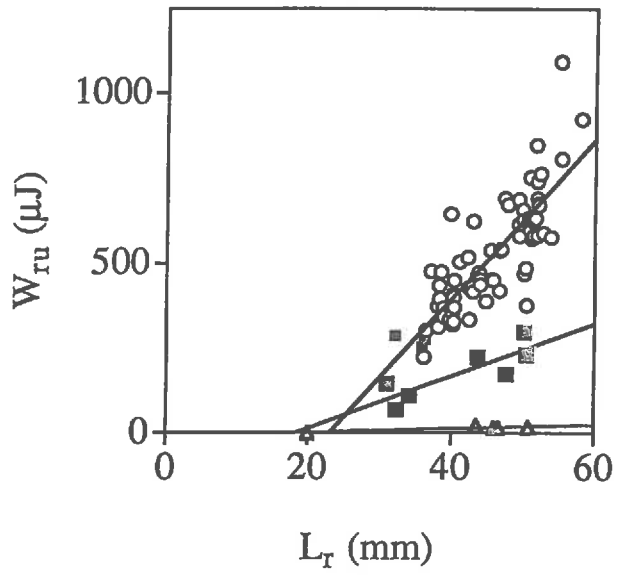

Figure 4. Relation entre l'energie de séparation sol:racine, W_{ru}, et la longueur finale racinaire, L_r, pour le sol remanié sableux ("triangles vide"), limoneux ("carrés plein") et argileux ("cercles vide").

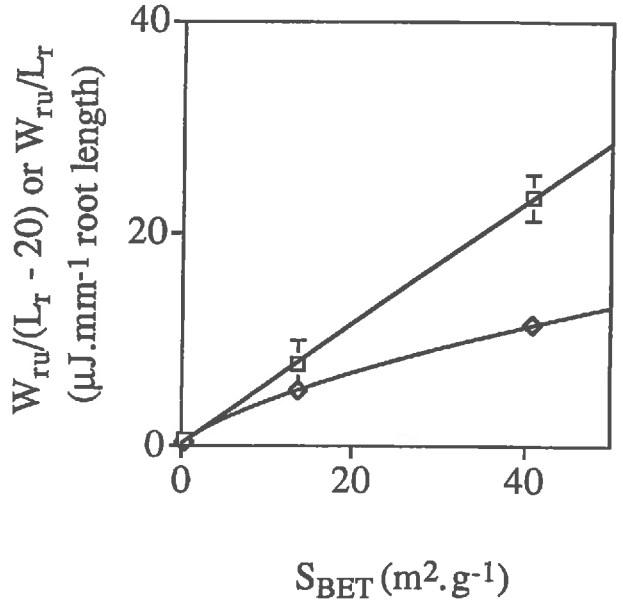

Figure 5. Relation entre la pente, a, de la droite de régression W_{ru}:(L_r - 20) (figure 4) ("carrés vides"), ou la moyenne W_{ru}/L_r ("losanges vides"), et la surface spécifique du sol, S_{BET}, pour les trois sytèmes sol:maïs étudiés.
Les équations des courbes ajustées sont les suivantes:
$a = 0.565\ S_{BET} + 0.292$ et $W_{ru}/L_r = 0.868\ S_{BET}^{0.694}$ (avec $r = 1.000$, $p < 0.01$)

Enfin, l'effet du séchage sur cette energie de séparation sol:racines s'est avérée être modéré, du fait de l'extraordinaire compensation biologique de la plante qui produit d'autant plus de poils adsorbants, s'ancrant dans le sol, que le sol est sec (figure 6).

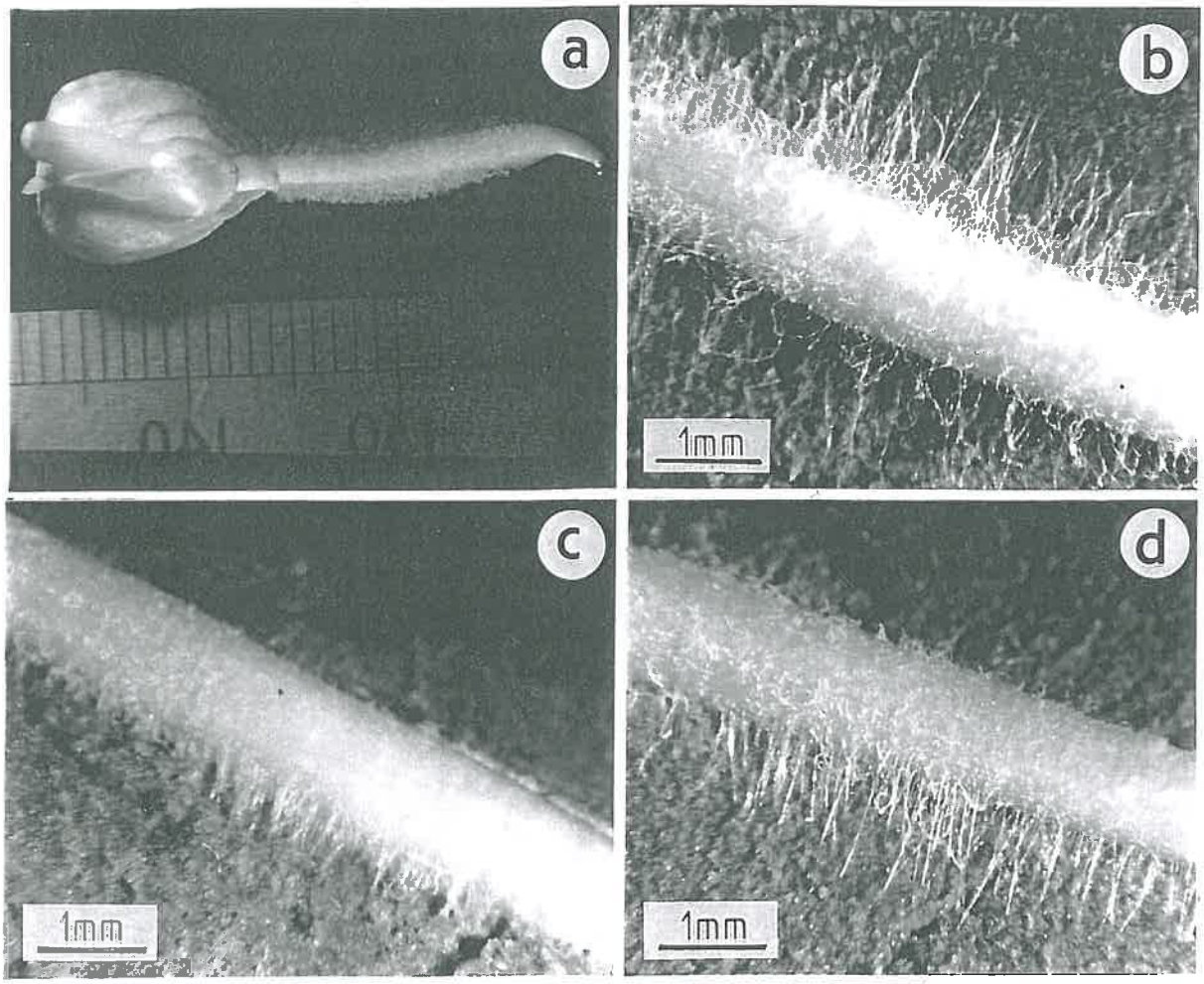

Figure 6. Examen morphologique de petites racines de maïs cultivées dans des boîtes de Petri (a) , sur la surface du sol argileux (La Bouzule) saturé à une suction de 10 kPa (b), et sur la surface du sol limoneux (Orgeval) saturé et drainé aux succions de 10 et 100 kPa (c et d).

PERSPECTIVES DE RECHERCHE POST-DOCTORALE

PERSPECTIVES DE RECHERCHE POST-DOCTORALES

Influence spatiale de la dynamique de la rhizosphère sur les propriétés physiques du sol: modèles expérimentaux

Introduction

Au cours de mon travail de thèse, j'ai pu identifier et étudier la dynamique de l'eau dans la rhizosphère du maïs, les interactions fortes existant entre le type de sol et l'architecture du système racinaire, ainsi que les modes d'impact de l'action combinée du séchage et de l'exsudation racinaire sur les propriétés mécaniques du sol adhérant aux racines de maïs.

Mais il ne m'a pas été possible de séparer l'influence respective, sur l'agrégation du sol, du séchage induit par la transpiration et de l'exsudation racinaire, du fait de la complexité de ces interactions. C'est la raison pour laquelle j'aimerais analyser l'effet séparé, ou combiné, de ces deux processus biophysiques et biologiques sur les propriétés physiques du sol rhizosphérique. J'utiliserai pour cela un système expérimental modèle qui vient d'être conçu, lors de discussions conjointes, par l'Unité de recherche Soil-Plant Dynamics du Scottish Crop Research Institute. Ce dispositif expérimental sera construit et utilisé lors de mon séjour post-doctoral à Dundee, si la bourse Lavoisier m'est accordée.

Mes objectifs de recherche post-doctorale seront ainsi de mesurer l'influence de la succion générée par les racines et le potentiel foliaire, la quantité et la qualité de l'exsudation racinaire, ainsi que l'effet des cycles de séchage et d'humectation sur les propriétés hydrauliques et mécaniques de la rhizosphère. Nous testerons l'hypothèse selon laquelle cette exsudation racinaire joue un rôle majeur vis-à-vis des propriétés structurales, hydriques et mécaniques du sol

rhizosphérique. Pour cela, nous utiliserons un système expérimental modèle qui nous permettra de simuler les effets du sèchage ou/et de l'exsudation racinaire sur les propriétés du sol, en fonction de sa distance à l'analogue expérimental de la racine (Fig. 1). Les résultats ainsi obtenus seront finalement comparés à d'autres qui seront alors issus d'un modèle expérimental plus complexe pour lequel des racines réelles pourront croître sur une surface plane.

Approche expérimentale proposée (projet de bourse Lavoisier d'un an au Scottish Crop Research Institute, Dundee)

La figure 1 illustre l'idée du système expérimental modèle que nous développerons au cours de ce projet. Les flux d'eau seront contrôlés par un réservoir à hauteur contrôlée et l'analogue de l'exsudat racinaire sera ajouté au système à l'aide d'une seringue. Le séchage pourra également être simulé par envoi d'air chaud dans la céramique. Le sol, préalablement caractérisé, sera placé au dessus de la céramique, parallélipédique. Des microtensiomètres et des équipements TDR seront disposés à différentes distances de ce système racinaire analogue afin de pouvoir caractériser la dynamique spatiale et temporelle des propriétés hydriques du sol. De petites ouvertures permettront également l'insertion de micropénétromètres afin de mesurer les différences de propriétés mécaniques induites. Grâce à ce modèle, nous pourrons contrôler le gradient de pression hydrique à l'interface sol:racine, la quantité, la nature chimique et la concentration du mucilage analogue, ainsi que les propriétés biologiques et physiques du sol. Le mucilage de maïs contient jusqu'à 30% d'acide uronique (Kraffczyk *et al.*, 1984). Nous utiliserons donc, à différentes concentrations, l'acide polygalacturonique, comme mucilage analogue.

Figure 1-Model Root System

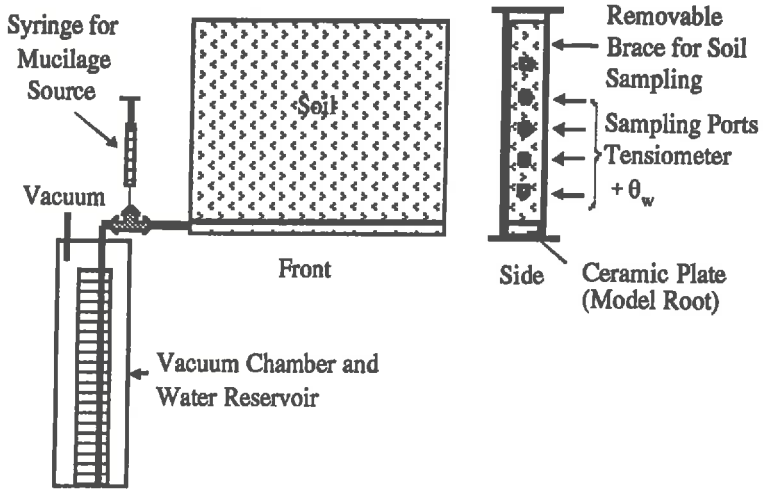

La construction du modèle (figure 1) sera effectuée pendant les trois premiers mois de mon séjour. Cette période servira aussi à tester les techniques de mesure des changements de propriétés du sol à des distances selectives de l'interface sol:racine grâce aux équipements disponibles au Scottish Crop Research Institute: pénétromètres pour mesurer les propriétés mécaniques, microtensiomètres et psychromètres pour déterminer le potentiel matriciel et TDR pour mesurer la teneur en eau volumique. D'autres équipements, permettant une résolution plus fine, pourront être disponibles tels que: rayonnements Gamma (Université d'Aberdeen) et imagerie RMN (Université de Londres). A la fin de chaque expérience, un échantillon de sol sera prélevé de facon à déterminer la teneur en eau du sol, le potentiel hydrique, les caractéristiques de rétention d'eau, la micro-structure par porosimétrie mercure, la stabilité des agrégats, les changements de propriétés chimiques (carbone organique) ainsi que la distribution du mucilage analogue. Certains échantillons pourront être imprégnés afin de réaliser des blocs et des lames minces de sols en vue de l'étude directe, par analyse d'image, de la macro- et de la micro-structure du sol.

L'expérimentation commençera par l'utilisation de mélanges artificiels sable fin - argile (2 mois). Ceci sera suivi par l'étude, d'un sol naturel homogénéisé (tamisé et mélangé) puis d'un sol intact avec sa structure d'origine (4 mois). Enfin, nous remplacerons la céramique par des racines naturelles dont la croissance vers le sol sera limitée par une membrane de diamètre de pore de 60 µm (3 mois).

Référence

Kraffczyk I., Trolldenier G. and Beringer, 1984. Soluble root exudates of maize: influence of potassium supply and rhizosphere micro-organisms. *Soil Biology and Biochemistry* **16**, 315-322.

REFERENCES BIBLIOGRAPHIQUES

REFERENCES BIBLIOGRAPHIQUES

A

Amellal N, Burtin G, Bartoli F and Heulin T 1998_a Colonisation of wheat roots by an EPS-producing *Pantoea agglomerans* strain and its effect on rhizosphere soil aggregation. Appl. Environ. Microbiol. (accepted).

Amellal N, Bartoli F, Villemin G., Talouizte A and Heulin T 1998_b Effect of inoculation of EPS-producing *Pantoea agglomerans* on wheat rhizosphere aggregation. (submited to Plant and Soil).

Amellal, 1996 Rôle des bactéries productrices d'exopolysaccharides dans la rhizosphère du blé dur. Université de Nancy, thèse.

Attou F 1996 Etude expérimentale d'assemblages squelette-argile. Apport à la compréhension du comportement physique des sols. Université d'Orléans, thèse.

B

Barataud F, Moyne C, Bréda N et Granier A 1995 Soil water dynamics in an oak stand. II. A model of the soil-root network compared with experimental data. Plant and Soil 172, 29-43.

Barley D 1970 The configuration of the root system in relation to nutrient uptake. Advances in Agronomy 22, 159-201.

Bartoli F, Bird N, Gomendy V and Vivier H 1998 The relationship between silty soil structures and their mercury porosimetry curve counterparts. Fractals and percolation. European Journal of Soil Science (accepted).

Bartoli F, Burtin G and Guerif J 1992 Influence of organic matter on aggregation in Oxisols rich in gibbsite or in goethite. II. Clay dispersion, aggregate strength and water-stability. Geoderma 54, 259-274.

Bartoli F, Burtin G and Herbillon A 1991. Disaggregation and clay dispersion of Oxisols: Na resin, a recommended methodology. Geoderma 49, 301-317.

Bartoli F, Burtin G, Royer J J, Gury M, Gomendy V, Philippy R, Leviandier T and Gaffrej R 1995 Spatial variability of topsoil characteristics within one silty soil type. Effects on clay migration. Geoderma 68, 279-300.

Bartoli F, Philippy R and Burtin G 1992 Poorly ordered hydrous Fe oxides, colloidal dispersion and soil aggregation. II. Modification of silty soil aggregation with Fe(III) polycations and model humic macromolecules. Journal of Soil Science 43, 59-75.

Baver L D, Gardner W H and Gardner W R 1972 Soil physics; 4th edition. John Wiley, New York, 498 p..

Beck D L, Darrah L L and Zuber M S 1988 Relationship of root tensile strength to vertical root pulling resistance in maize. Crop Science 28, 571-573.

Bengough A G, Croser C and Pritchard J 1997 A biophysical analysis of root growth under mechanical stress. Plant and Soil 189, 155-164.

Bristow K L, Campbell G S and Calissendorf C 1984 The effects of tecture on the resistance to water movement within the rhizosphere. Soil Science Society of America Journal 48, 266-270.

Bruand A, Cousin I, Nicoullaud B, Duval O and Bégon J C 1996 Backscattered Electron Scanning Image of Soil Porosity for Analyzing Soil Compaction around Roots. Soil Sci. Soc. Am. J. 60, 895-901

Bruce R R and Luxmoore R J 1986 Water retention : field methods. In : Methods of Soil Analysis. Part I. Physical and Mineralogical Methods. Agronomy Monograph n°9 (2nd edition). American Society of Agronomy - Soil Science Society of America, Madison, pp. 663-686.

BS1377 1975 Methods of Test for Soils for Civil Engineering Purposes. British Standards Institution, London.

C

Cailloux M 1972 Metabolism and the absorption of water by root hairs. Canadian Journal of Botany 50, 557-573.

Causarano H 1993 Factors affecting the tensile strength of soil aggregates. Soil and Tillage Research 28, 15-25.

Chaboud A 1983 Isolation, purification and chemical composition of root cap slime. Plant and Soil 73, 395-402.

Chapman S J and Lynch J M 1985 Polysaccharide synthesis by capsular microorganisms in coculture with cellulytic fungi on straw and stabilization of soil agregates. Biol. Fert. Soils 1, 161-166.

Chenu C 1993 Clay- or sand-polysaccharide associations as models for the interface between micro-organisms and soil-water related properties and micro-structure. Geoderma 56, 143-156.

Chenu C and Guérif J 1991 Mechanical strength of clay minerals as influenced by an absorbed polysaccharide. Soil Sci. Soc. Am. J. 55, 1076-1080.

Chenu C, Pons C H and Robert M 1987 Interaction of kaolinite and montmorillonite with neutral polysaccharides. In L.G. Schultz, H. van Olphen and F.A. Mumpton, (Editors), Proceedings of international Clay Conference, Denver, 1985. The Clay Minerals Society, Biomington, pp 375-381.

Cheshire M V 1979 Nature andd origins of carbohydrates in soils. Academic Press, London.

Chrétien J 1986 Rôle du squelette dans l'organisation des sols. Université de Dijon, thèse d'état.

Clothier B E and Green S R 1997 Roots: The big movers of water and chemical in soil. Soil Science 162, 534-543.

Concaret J 1967 Etude des mécanismes de la destruction des agrégats de terre au contact de solutions acqueuses. Ann. Agronom. 18, 99-144.

Cormack R G H 1949 The development of root hairs in Angiosperms. The Botanical Review XV, 583-611.

Czarnes S 1994 Effet de l'inoculation de *Bacillus polymixa* sur la structure du sol dans la rhizosphère du blé. Université de Nancy I, DEA.

Czarnes S and Bartoli F 1998 Wetting and drying cycles in the maize rhizosphere under controlled conditions. I. Soil and daily minimum soil water suction effects (submitted to Plant and Soil).

Czarnes S, Dexter A R and Bartoli F 1998_a Mechanics of two adherent centimetric remoulded soil balls : a preliminary examination (submitted to Soil and Tillage Research).

Czarnes S, Hiller S, Dexter A R, Hallett P D and Bartoli F 1998_b Soil:root adhesion in the maize rhizosphere: the rheological approach (submitted to Plant and Soil).

D

Davies P 1985 Influence of organic matter content, moisture status and time after reworking on soil shear strength. Journal of Soil Science 36, 299-306.

Dexter A R 1978 A stochastic model for the growth of roots in tilled soil. Journal of Soil Science 29, 102-116.

Dexter A R 1987 Compression of soil around roots. Plant and Soil 97, 401-406.

Dexter A R, 1988 Strength of soil aggregates and of aggregate beds. In Drescher J, Horn R and de Boodt M (eds.) "impact of water and external forces on soil structure" Catena Supplement No 11, 35-52.

Dexter A R and Hewitt J S 1978 The deflection of plant roots. J. Agric. Engng Res. 23, 17-22.

Dexter A R and Kroesbergen B 1985 Methodologiy for determination of tensile strength of soil aggregates. J. agric. Engng Res. 32, 139-147.

Dexter A R, Kroesbergen B and Kuipers H 1984a Some mechanical properties of aggregates of top soils from the IJsselmeer polders. 1. Undisturbed soil aggregates. Netherlands Journal of Agricultural Science, 32, 205-214.

Dexter A R, Kroesbergen B and Kuipers H 1984b Some mechanical properties of aggregates of top soils from the IJsselmeer polders. 2. Remoulded soil aggregates and the effects of wetting and drying cycles. Netherlands Journal of Agricultural Science 32, 215-227.

Dexter A R and Watts C W 1998. Tensile strength and friability. *In* Smith K A and Mullins C E (eds.) "Soil Analysis: Physical Methods", 2nd Edition, Marcell Dekker Inc., New York (in press).

Dexter A R 1991 Amelioration of soil by natural processes. Soil &Tillage Research, 20, 87-100.

Dorioz J M et Robert M 1987 Aspects microscopiques des relations entre les microorganismes ou végétaux et les orgiles : conséquences sur les microorganisations et la microstructuration des sols. In N. Fedoroff, L.M. Bresson and M.A. Courty (Editors), Soil Micromorphology. Pro VIIth Int. Work. Meet. Soil Micromorphology. AFES, Plaisir, pp 353-362. janvier

Dorioz J M , Robert M and Chenu C 1993 The role of roots, fungi and bacteria on clay particle organization. An experimental approach. Geoderma 56, 179-194.

Doussan C and Pages L 1998 Absorption hydrique racinaire: sur l'ambiance hydrique de la rhizosphère et les transferts d'eau-racines. *In* Colloque Rhizosphere Aix'97, Aix-en-Provence 26-27 Novembre 1997, p.15.

Doussan C, Pagès L and Vercambre G 1998 Modelling of the hydraulic architecture of root systems: An integrated approach to water absorption. 1. Model description. Annals of Botany 81, 213-223.

Doussan C, Vercambre G and Pagès L 1998 Modelling of the hydraulic architecture of root systems: an integrated approach to water absorption. 2. Distribution of axial and radial conductances in maize. Annals of Botany 81, 225-232.

Dowdy R H 1975 The effect of organic polymers and hydrous oxides on the tensile strength of clay. In: B A Stewart (editor), Soil Conditionners. Soil Sci. Soc. Am. Spec. Publ. Ser. 7, 25-33.

Droogers P, van der Meer F B W and Bouma J 1997 Water accessibility to plant roots in different soil structures occuring in the same soil type. Plant and Soil 188, 83-91.

Dwyer L M, Stewart D W and Balchin D 1988 Rooting characteritics of corn, soybeans and barley as a function of available water and soil physical characteristics. Canadian Journal of Soil Science 68, 121-132.

Dufaufour Ph 1977 Pédologie T1, Masson, Paris, 477p.

E

Ennos A R 1989 The mechanics of anchorage in seedlings of sunflower, *Helianthus annuus* L. New Phytol. 113, 185-192.

Ennos A R 1990 The anchorage of leek seedlings: The effect of root length and soil strength. Annals of Botany 65, 409-416.

Ennos A R 1993 The anchorage mechanics of Maize, *Zea mays*. Journal of Experimental Botany 4, 147-153.

Ewens M and Leigh R A 1985 The effect of nutrient solution composition on the length of root hairs of wheat (*Triticum aestivum L.*). Journal of Experimental Botany 36, 713-724.

F

Faiz S M A and Weatherley P E 1978 Further investigations into the location and magnitude of the hydraulic resistances in the soil-plant system. New Phytologist 92, 333-343.

Fiès J C and Bruand A 1990 Textural porosity analysis of a silty clay soil using pore volum balance estimation, mercury porosimetry and quantified backscattered electron scanning image (BESI). Geoderma 47, 209-219.

Fincher R R, Darrah L L and Zuber M S 1985 Root development in maize as measured by vertical pulling resistance. Maydica 30, 383-394.

Finney J L 1970 Random packings and the structure of simple liquids: 1. The geometry of random close packing. Proceedings of the Royal Society, A319, 479-493.

Foster R C 1982 The fine structure of epidermal cell mucilages of roots. New phytol. 91: 727-740.

Fuller K N G and Tabor D 1975 The effect of surface roughness on the adhesion of elastic solids. Proc. R. Soc. Lond. A 345, 327-342.

Furness R R and King, S. J. 1978 Soils in North Yorkshire IV. Soil Survey Record n° 56. Harpenden.

G

Gardner W R 1960 Dynamic apects of water availability to plants. Soil Science 89, 63-73.

Gijsman A J, Flopris J, van Noordwijk M and Brouwer G 1991 An inflatable minirhizotron system for root observations with improved soil/tube contact. Plant and Soil 134, 261-269.

Gomendy V 1996 Variabilités spatiale et temporelle des propriétés structurales et hydriques des horizons de surface de la couverture limoneuse du bassin versant d'Orgeval (Brie). Université de Nancy I, thèse.

Gomendy V, Bartoli F, Burtin G, Doirisse M, Philippy Niquet S and Vivier H 1998 Silty topsoil structure and its dynamics : the fractal approach. Geoderma, special issue on "fractal models in Soil Science" edited by Y. Pachepsky, J. Crawford and W. Rawls (accepted).

Gouzou L, Burtin G, Pillipy R, Bartoli F and Heulin T 1993 Effect of inoculation with Bacillus polymyxa on soil aggregation in the wheat rhizosphere : preliminary examination. Geoderma 56, 479-491.

Gouzou L. 1992 Devenir d'une population bactérienne inoculé dans la rhizosphère du blé et ses effets sur la plante : Cas de Bacillus polymyxa. Thèse de l'Université de Nancy .

Grant C D and dexter A R 1989 Generation of microcracks in moulded soils by rapid wetting. Australian Journal of Soil Science 27, 169-182.

Greacen E L, Farrell D A and Cockroft B 1968 Soil Resistance of metal probes and plant roots. In Transactions of the 9th International Congress in Soil Science, pp. 769-779.

Greaves M P et Darbyshire J F 1972 The ultrastructure of the mucilaginous layer on plant roots. Soil Biol. Biochem. 4, 443-449.

Gregg S J and Singh K S W 1967 Microaggregates in soils. Journal of Soil Science 18, 64-73.

Gregory P J, Palta J A and Batts G R 1997 Root systems and root:mass ratio - carbon allocation under current and projected atmospheric conditions in arable crops. Plant and Soil 187, 221-228.

Groleau - Renaud V 1998 Contrainte mécanique et exsudation racinaire du maïs : incidence de la morphologie du système racinaire. Thèse de l'INPL de Nancy .

Gückert A 1973 Contribution à l'étude des polysaccharides dans les sols et leurs rôle dans les mécanismes d'agrégation: Thèse Doct. d'Etat, Univ. Nancy, France 124 pp.

Gückert A, Beisch H et Reisinger O 1975 Interface sol - racine - I Etude au microscope électronique des relations mucigel - argile - microorganismes. Soil Biol. Bioch. 7, 241-250.

Guérif J 1988$_a$ Détermination de la résistance en traction des agrégats terreux: revue bibliographique et mise au point technique. Agronomie 8, 281-288.

Guérif J 1988$_b$ Résistance en traction des agrégats terreux: influence de la texture, de la matière organique et de la teneur en eau. Agronomie 8, 379-386.

Guérif J 1990 Factor influencing compaction-induced increases in soil strength. Soil & Tillage Research 16, 167-178.

H

Hadas A 1978 a Dependence of "true" surface energy of soils on air entry pore size and chemical constituents. Soil Sci. Soc. Am. J. 51, 187-191.

Hadas A 1978 b Long-term tillage practice effects on soil aggregation modes and strength. Soil Sci. Soc. Am. J. 51, 191-197.

Hadas A and Lennard G 1988 Dependence of tensile strength of soil aggregates on soil constituants, density and load history. Journal of Soil Science 39, 577-586.

Hartge, K. H. 1994 Soil structure, its development and its implications for properties and processes in soils - a synopsis based on recent research in Germany. Z. Pflanzenernähr. Bodenk. 157, 159-164.

Haynes R J and Francis G S 1993 Changes in microbial biomass C, soil carbohydrate composition and aggregate stability induced by growth of selected crop and forage species under field conditions. Journal of Soil Science 44, 665-675.

Herkelrath W N, Miller E E and Gardner W R 1977 Water uptake by plants: I. Divided root experiments. II. The root contact model. Soil Science Society of America Journal 41, 1033-1043.

Hiltner L 1904 Uber neuere Erfahrungen und Probleme auf dem Gebeit der Bodenbakteriologie und unter besonder Berücksichtigung der Gründüngung und Brache. Arb. Dstch Landwrit. Ges. 98, 59-78.

Horn R and Dexter A R 1989 Dynamics of soil aggregation in an irrigated desert loess. Soil & Tillage Research 13, 253-266.

Horn, R., Taubner, H., Wuttke, M. & Baumgartl, T. 1994. Soil physical properties related to soil structure. Soil & Tillage Research 30, 187-216.

Huck M G 1984. Water flux in the soil-root continuum. *In* Roots, nutrient and water influx, and plant growth. Soil Science Society of America, Crop Science Society of America, and American Society of Agronomy, 677 South Segoe Road, Madison, WI 53711 pp 47-63.

I J

Jaillard B, Ruiz L and Arvieu J C 1996 pH mapping gel using color indicator videodensitometry. Plant and Soil 183, 85-95.

Jaunin F and Hofer R M 1986 Root hair formation and elongation of primary maize root. Physiologia Plantarum 68, 653-656.

Jensen C R, Svendsen H, Andersen M N and Lösch R 1993 Use of the root contact concept, an empirical leaf conductance model and pressure-volume curves in simulating crop water relations. Plant and Soil 149, 1-26.

Jones H, Tomos A D, Leigh R A and Wyn Jones R G 1983 Water-relation parameters of epidermal and cortical cells in the primary root of *Triticum aestivum* L. Planta 158, 230-236.

K

Kay B D and Dexter A R 1992 The influence of dispersive clay and wetting/drying cycles on the tensile strength of a red-brown earth. Aust. J. Soil Res. 30, 297-310.

Klute A 1986 Water retention : laboratory methods. *In* A Klute (ed.) Methods of Soil Analysis, part 1: Physical and Mineralogical Methods. Soil Science Society of America, Agronomy Monograph n° 9, pp 635-662

Kooistra M J, Scoonderbeek D, Boone F R, Veen B W and van Noordwijk, M 1992 Root-sol contact of maize, as measured by a thin-section technique. II. Effects of soil compaction. Plant and Soil 139, 119-129.

Kraffczyk I, Trolldenier G and Beringer 1984 Soluble root exudates of maize: influence of potassium supply and rhizosphere micro-organisms. Soil Biology and Biochemistry 16, 315-322.

L

Lafolie F, Brucker L and Tardieux F 1991 Modelling root water potential and soil-root water transport: I. Model presentation. Soil Science Society of America Journal 55, 1203-1212.

Le Bissonnais Y 1988 Analyse des mécanismes de la desagrégation et de la mobilisation des particules de terre sous l'action des pluies. Orléans University pHD thésis.

Lenormand R 1981 Déplacements polyphasiques en milieu poreux sous l'influence des forces capillaires. Etude expérimentale et modélisation de type percolation. Toulouse Institut National Polytechnique State thesis.

Liu H H and Dane J H 1993 Reconciliation between measured and theoritical temperature effects on soil water retention curves. Soil Science Society of America journal 57, 1202-1207.

Lynch J M and Whipps J M 1990 Substrate flow in the rhizosphere. Plant and soil 129, 1-10

M

Mackay A D and Barber S A 1984 Comparison of root and root hairs growth in solution and soil culture. Journal of plant nutrition 7, 1745-1757.

Mackay A D and Barber S A 1987 Effect of wetting and drying of a soil on root hair growth of maize roots. Plant and Soil 104, 291-293.

Mackay A D.and Barber S A 1985 Effect of soil moisture and phosphate level on root hair growth of corn roots. Plant and Soil, 86, 321-331.
Materechera S A, Dexter A R and Alston A M 1992 Formation of aggregates by plant roots in homogenised soils. Plant and Soil 142, 69-79.

Materechera S A, Kirby J M, Alston A M and Dexter A R 1994 Modification of soil aggregation by watering regime and roots growing through beds of large aggregates. Plant and Soil 160, 57-66.

Matsumoto H, Okada K and Takahashi E 1979 Excretion products of maize roots from seedling to seed development stage. Plant and Soil 53, 17-26.

Mc Cully M E and Canny M J 1989 Pathways and processes water and nutrient movement in roots. Plant and Soil 111: 159-170.

Meisner C A and Karnok K J 1991 Root hair occurence and variation with environment. Agron. J. 83, 814-818.

Misra R K, Alston A M and Dexter A R 1988 Role of root hairs in phosphorus depletion from a macrostructured soil. Plant and Soil, 107, 11-18.

Misra R K, Dexter A R and Alston A M 1986 Penetration of soil aggregates of finite size II. Plant roots. Plant and Soil 94, 59-85.

Mitchell J K 1993 Fundamentals of soil behavior, second edition. John Wiley and Sons, New York.

Monnier G, Stengel P and Fiès J C 1973 Une méthode de mesure de la densité apparente de petits agglomérats terreux. Application à l'analyse des systèmes de porosité du sol. Annales agronomiques, 24, 533-545.

Morel J , Habib L, Plantureux S and Guckert A 1991 Influence of maize root mucilage on soil aggregate stability. Plant and Soil 136, 111-119.

Mullins C E and Panayiotopoulos K P 1984 The strength of unsaturated mixture of sand and kaolin and the concept of effective stress. Journal of Soil Sciences, 35, 459-468.

N

Nguyen Tan H 1978 Ecoulements non permanents dans des massifs de milieux poreux non saturés avec effts d'hystérésis Toulouse Institut National Polytechnique State thesis.

Niklas K J 1992 Plant biomechanics: an engineering approach to plant form and function. John Wiley & Sons, New York.

North P F 1976 Towards an absolute measurement of soil structural stability using ultra-sound. J. Soil Sci. 27, 451-459.

O

Oades J M 1978 Mucilages at the root surface. J. Soil Sci. 29, 1-16.

Oades J M 1989 An introduction to organic matter in mineral soils. In Minerals in Soil environents (eds. J.B. Dixon et S.B. Weed), Soil Science Society of America Book, Serie n°1, Madisen, pp. 89-160.

Oades J M 1993 The role of biology in the formation, stabilization and degradation of soil structure. Geoderma 56, 377-400.

P Q

Pagès L et Pellerin S 1994 Evaluation of parameters describing the root system architecture of field grown maize plants (Zea mays L.). II Density, length and branching of first order lateral roots. Plant and Soil 164, 169-176.

Panayiotopoulos, K. P. and Mullins, C. E. 1985 Packing of sands. Journal of Soil Science, 36, 129-139.

Parke J L, Liddell C M and Clayton 1990 Relationship between soil mass adhering to pea taproots and recovery of Pseudomonas Fluorescens from the rhizosphere. Soil Biol. Biochem. 22, 495-499.

Passioura J B 1980 The transport of water from soil to shoot in wheat seedlings. Journal of Experimental Botany 31, 331-345.

Petersen L W, Moldrup P, Jacobsen D H and Rolston D E 1996 Relations between specific area and soil physical and chemical properties. Soil Science 161, 9-21.

Philip J R 1966 Plant water relations: some physical aspects. Annual Review of Plant Physiology 17, 245-268.

R

Rawls W J and Brakensiek D L 1985 Prediction of soil water properties for hydrologic modeling. *In* Proceedings of the Symposium "Watershed Management in the Eighties", Denver pp 293-299.

Reeve, M. J. 1978 Soils in Northamptonshire 1. Soil Survey Record n° 54. Harpenden.

Reicosky D C and Richie J T 1976 Relative importance of soil resistance and plante resistance in root water absorption. Soil Science Society of America Journal 40, 293-297.

Reid C P P and Bowen G D 1979 Effect of soil moisture on V/A mycorrhiza formation and root development in *Medicago*. In Harley J L (ed.) "the soil-root interface" New phytologist, London, 211-220.

Reid C P P 1974 Assimilation, distribution and root exudation of 14C by poderosa pine seedling under induced water stress. Plant Physiology 54, 44-49.

Richter J 1987 The soil as a reactor: modeling processes in the soil. Catena, Verlag.

Richter O and Söndgerath D 1990 Parameter Estimation in Ecology. The link between data and models. VCH, Weinheim and New York, 218 p.

Rouiller J, Burtin G and Souchier B 1972 La dispersion des sols dans l'analyse granulométrique, méthode utilisant les résines échangeuses d'ions. Bull ENSAIA Nancy, XIV, Fasc. II, 193-205.

Rouiller J, Brethes A, Burtin G and Guillet B 1984 Fractionnement des argiles par iltracentrifugation en continu: Evolution des illites en milieu podzolique. Sci. Géol. Bull. 37, 319-331.

Rovira A.D. and Davey C.B. 1974 Biology of the rhizosphere. *In* The Plant Root and Its Environment (E.W. Carson, ED.). pp. 153-204. University Press of Virginia, Charlottesville.

S

Sachs J. 1882 Vorlesungen über Plantzenphysiologie. Englemann, Leipzig.

Scheffer F and Schachtshabel P 1976 Lehrbuch der Bodenkunde. Ferdinand Enke Verlag Stuttgart, 394 p.

Schultz J and Carre A 1985 Prévision de l'adhésion d'aluminium traité à l'aide de méthodes de mouillabilité. Surfaces 178, 30-36.

Smith C W, Hadas A, Dan J and Koyumdjisky H 1985 Shrinkage and Atterberg limits in relation to other properties of principal soil types in Israel. Geoderma 35, 47-65.

Smith W O, Foote P D and Busang P F 1929 Packing of homogeneous spheres. Physical Review 34, 1271-1274.

Sowers G F 1965 Consistency. In: Methods of Soil Analysis (eds. C.A. Black, D.D. Evans, J.L. White, L.E. Ensminger & F.E. Clark) Agronomy 9, pp 391-399, American Society of Agronomy, Madison.

Spoor G and Godwin R J 1979 Soil deformation and shear strength characteristics of some clay soils at different moisture contents. Journal of Soil Science, 30, 493-498.

Sprent J I 1975 Adherence of sand particles to soybean roots under water stress. New Phytol 74, 461-463.

Stirzaker R J and Passioura J B 1996 The water relations of the root-soil interface. Plant, Cell and Environment 19, 201-208.

T

Taylor H M and Klepper B 1978 The role of rooting characteristics in the supply of water to plants. Adv. Agron. 30, 99-128.

Tengbeh G T 1993 The effect of grass roots on shear strength variations with moisture content. Soil Technology 6, 287-295.

Tisdall J M and Oades J M 1979 Stabilization of soil aggregates by root systems of rye-grass. Aust. J. Soil Research. 17, 429-441.

Topp G C 1971 Soil water hysteresis in silt loam and clay loam soils. Water Resources Research 7, 914-920.

Tri B H 1968 Dynamique de la granulation du sol sous prairie. Ann. Agron. 19, 415-439.

Tripodi M A, Puri V M, Manbeck H B and Messing G L 1992 Constitutive Models for cohesive particulate materials. J. agric. Engng Res., 53, 1-21.

U V

Utomo W H and Dexter A R 1981 Soil friability. J. Soil Sci. 32, 203-213.

van Brackel J 1975 Pore space models for transport phenomena in porous media. Powder Technology 11, 205-236.

van Damme H 1995 Scale invariance and hydric behaviour of soils and clays. Comptes Rendus à l'Académie des Sciences, Paris, 320, Series II a, 665-681.

Vancura V and Garcia J L 1969 Root exudates of reversibly wilted millet plants (*Panicum Miliaceum* L.) Oecol. Plant 4, 93-98.
Van Noordwijk M, Kooistra M J, Boone F R, veen B W and Schoonderbeek D 1992 Root-soil contact of maize, as meadured by a thin-section technique. I. Validity of the method. Plant and Soil 139, 109-118.

Van Noordwick M, Schoonderbeek D and Kooistra M J 1993 Root-soil contact of field-grown winter wheat. Géoderma 56, 277-286.

Veen B W and Boone F R 1990 The influence of mechanical resistance and soil water on the growth of seminal roots of maize. Soil 1 Tillage Research 16, 219-226.

Veen B W, Van Noodwijk M, De Willigen P, Boone F R and Kooistra M J 1992 Root-soil contact of maize, as measured by a thin-section technique. III. Effets on shoot growth, nitrate and water uptake efficiency. Plant and Soil 139, 131-138.

Vereecken H, Maes J, Feysen J and Darius P, 1989 Estimating the soil moisture retention characteristics from texture, bulk density, and carbon content. Soil Science 148, 389-403.

Villemin G et Toutain F 1987 Méthode de fixation d'échantillons organo-minéraux de sols pour la microscopie electronique à transmission. In Soil Micromorphology. (Eds. Fedoroff N., Bresson L.M. et Courty M.A), pp 43-48.

Vincent J F V 1992 Biomechanics - materials: a practical approach. Oxford University Press, New York.

W

Walter C, Schvartz C, Claudot B, Bouedo T and Aurousseau P 1997 Synthèse nationale des analyses de terre réalisées entre 1990 et 1994. Etude et Gestion des Sols, 4, 205-219.

Watt M, McCully M E and Canny M J 1994 Formation and stabilization of rhizosheaths of Zea mays L. Effect of soil water content. Plant Physiol. 106, 179-186.

Watt M, McCully M E and Jeffree C E 1993 Plant and bacterial mucilages of the maize rhizosphere: comparison of their soil binding properties and histochemistry in a model system. Plant and Soil 151: 151-165.

Watts C W and Dexter A R 1993 A hand-held instrument for the in situ measurement of soil shear strength in the puddled layer of paddy fields. J. agric. Engng Res. 54, 329-337.

Watts C W and Dexter A R 1998 Soil friability: theory, measurement and the effects of managelent and organic carbon content. European Journal of Soil Science Science 49, 73-84.

Wesseling J and van Wijk W R 1957 Soil physical conditions in relation to drain depth. In: J N Lutin (ed.), Drainage of agricultural lands. Agronomy Monograph 7, American Society of Agronomy, Madison, Wisconsin, p. 461-504.

Whiteley G M and Dexter A R 1981 Elastic response of the roots of field crops. Physiologia Plantarum 51, 407-417.

X Y Z

Young I M 1997 Variation in moisture contents between bulk soil ands the rhizosheath of wheat (*Triticum aestivum* L. cv. Wembley). New Physiologist 130, 135-139.

Young I M and Mullins C E 1991 Factors affecting the strength of undisturbed cores from soils with low structural stability. Journal of Soil Science 42, 205-217.

Zwiggelaar R, Bull C R, Mooney M J and Czarnes S 1997 The detection of "soft" materials by selective energy Xray transmission imaging and computer tomography. J. agric. Engng Res. 66, 203-212.

ANNEXES

UNIVERSITÉ HENRI POINCARÉ NANCY 1

Attribution du label

DOCTORAT EUROPÉEN

Il s'agit d'un "Label" décerné en sus du Doctorat délivré dans chaque établissement lorsque les 4 conditions (non qualitatives) suivantes sont remplies :

1) L'autorisation de soutenance est accordée au vu de rapports rédigés par au moins deux professeurs appartenant à deux établissements d'Enseignement Supérieur de deux Etats européens autres que celui dans lequel le doctorat est soutenu.

2) Un membre au moins du jury doit appartenir à un établissement d'Enseignement Supérieur d'un Etat européen autre que celui dans lequel le doctorat est soutenu.

3) Une partie de la soutenance doit être effectuée dans une langue nationale européenne autre que la (ou les) langue(s) nationale(s) du pays où est soutenu le doctorat.

4) Ce doctorat devra avoir été préparé, en partie, lors d'un séjour d'au moins un trimestre dans une autre pays européen.

Ce label est attribué par le Service de la Recherche et des Etudes doctorales (SRED) Présidence de l'Université, après la soutenance, et sur demande du candidat.

UNIVERSITÉ HENRI POINCARÉ . NANCY 1
SRED
24-30, rue Lionnois B.P.3069 54013 Nancy cedex
Tél : 83 85..48.00 Fax : 83 85.48.48
Adresse électronique : malo @presnl.u-nancy.fr

Université HENRI POINCARÉ NANCY 1

LABEL "DOCTORAT EUROPEEN"

Je soussigné Jean Pierre FINANCE, Président de l'Université Henri Poincaré Nancy 1 certifie que **Madame Sonia CZARNES** a rempli toutes les conditions requises pour l'attribution du label **"Doctorat Européen"** lors de la préparation de sa thèse et de l'obtention de son diplôme de doctorat de l'Université Henri Poincaré Nancy 1 dans le cadre de l'Ecole doctorale Biologie et Santé

Sujet de la thèse :
Adhésion sol : racines et biophysique de la rhizosphère de maïs.

Pour copie certifiée conforme
à l'original qui a été présenté.

NANCY, le - 7 SEP. 1998

VILLE DE NANCY

Pour le Maire,
Le Fonctionnaire Municipal délégué

Le Directeur de recherche était Monsieur François BARTOLI.

Les rapports ont été rédigés par :

- Monsieur le Professeur Peter J. GREGORY, The University of Reading – Royaume Uni
- Monsieur le Professeur E. FROSSARD, Eidgenössische Technische Hochschule Zürich - Suisse

Le jury était composé de

- Monsieur le Professeur Jean DEXHEIMER
- Monsieur le Professeur Anthony Roger DEXTER (membre étranger)
- Monsieur le Professeur François BARTOLI
- Madame le Professeur Claire CHENU
- Monsieur le Professeur Benoît JAILLARD

Cette thèse a été soutenue en français et partiellement en anglais le 1er juillet 1998.

Le stage à l'étranger s'est déroulé durant 9 mois sous la direction du professeur A. R. DEXTER au Silsoe Research Institute, Royaume Uni.

DOCTOR
COMMUNITATIS
EUROPEAE

Fait à Nancy le 2 septembre 1998

Le Président de l'Université
Henri Poincaré Nancy 1,

UNIVERSITÉ HENRI POINCARÉ NANCY 1 LE PRESIDENT

Jean Pierre FINANCE

24-30, rue Lionnois B.P. 3069 54013 Nancy cedex - Tél. 03 83 85 48 00 - Fax 03 83 85 48 48
Adresse électronique : _____ @uhp.u-nancy.fr